A MORPHOMETRIC ANALYSIS OF HOMININ TEETH ATTRIBUTED TO DIFFERENT SPECIES OF *AUSTRALOPITHECUS, PARANTHROPUS* AND *HOMO*

Susan J Dykes

Evolutionary Studies Institute, University of the Witwatersrand
Student number: 763068

Supervisor: Professor J Francis Thackeray
Co-Supervisor: Dr Bernhard Zipfel

A dissertation submitted to the Faculty of Science, University of the Witwatersrand, in fulfilment of the requirements for the degree of Master of Science

Johannesburg, October 29, 2014

DECLARATION
I declare that this dissertation is my own, unaided work. It is being submitted for the Degree of Master of Science in the University of the Witwatersrand, Johannesburg. It has not been submitted before for any degree or examination in any other University.

SUSAN J DYKES
OCTOBER 29, 2014

_____

Table of Contents

LIST OF FIGURES 7
LIST OF TABLES 11
DEDICATION 13
ACKNOWLEDGMENTS 14
ABSTRACT 17
CHAPTER ONE – BACKGROUND, AIM, PRIOR WORK. 19
1.1 Background to the current study 19
1.2 Aim of the project 21
1.3 Prior work : taxonomy and species variability 24
1.4 Quantification of morphological variation 29
1.5 Some features of the study that differentiate it from other similar studies 32
1.6 Scope of the study, primary objectives and working hypotheses 38
1.6.1 Scope of the study - limitations 38
1.6.1.1 Access to specimens 38
1.6.1.2 Inclusion of original photographs of all holotypes (or proxies) – selection of M_1 as common molar to all holotypes 38
1.6.1.3 Limitations of mandibular molars with respect to cranial comparisons 39
1.6.1.4 Selection of a limited array of analytical methods to confirm results 40
1.6.1.5 Exploratory nature of the study, leading to future research 40
1.6.2 Primary aims of the study, approaches used to achieve these aims 41
1.6.3 Working hypotheses 42
CHAPTER TWO – BACKGROUND TO THE MORPHOMETRIC STUDY: DIAGNOSTIC MORPHOLOGY OF SURFACE ENAMEL FEATURES OF LOWER FIRST MOLARS OF AFRICAN PLIO-PLEISTOCENE HOMININ SPECIMENS 43
2.1 Background: morphological taxonomic diagnostics of lower first molars requiring to be “landmarked”. 43
2.2 General tooth morphology of African Plio-Pleistocene fossil hominins 43
2.3 Diagnostic morphology of lower first molars of African Plio-Pleistocene fossil hominins 44
2.3.1 *Australopithecus afarensis* 45
2.3.2 *Australopithecus africanus* 47
2.3.3 *Homo habilis; Homo rudolfensis* 49
2.3.4 *Homo erectus (Homo ergaster)* 50
2.3.5 *Paranthropus boisei; Paranthropus robustus* 51

2.3.6 Summary: diagnostic features distinguishing African Plio-Pleistocene hominin fossil lower first molars 54
2.4 Morphology into morphometrics; landmarking for species recognition 56
CHAPTER THREE – MATERIALS AND METHODS 60
3.1 Rationale for the choice of skeletal element (lower first molars) 60
3.2 Materials 63
3.2.1 Extant species 63
3.2.1.1 Modern Humans (MH, *Homo sapiens*) 63
3.2.1.2 Gorillas (*Gorilla gorilla gorilla*), Chimpanzees (*Pan troglodytes schweinfurthii*) and Bonobos (*Pan paniscus*) 68
3.2.2 Fossils 70
3.2.2.1 A note on antimeres 70
3.2.2.2 Final selection of fossil hominin first mandibular molars 74
3.3 Data collection – 2D photography 77
3.3.1 Rationale for sampling by means of two-dimensional photography 77
3.3.2 Data collection: photographic protocols and methodology 78
3.3.2.1 Equipment and photographic protocols 78
3.3.2.2 Parallax error avoidance 78
3.3.2.3 Errors of tilt 79
3.4 Landmark placement optimisation ("Landmark Model") 84
3.4.1 The importance of optimising landmark placements 84
3.4.2 Prelude to landmarking – image processing 85
3.4.3 Observer error for the placement of the central MD:BL intersection reference point (Landmark #1) 87
3.4.4 A note on linear diameter (MD and BL) measurements: "corrected" and "uncorrected" MD diameters 89
3.5 Digitisation of data – landmarking methodology and the selection of a landmark model to maximise digitisation of diagnostic traits 93
3.6 Methods - analyses 109
3.6.1 Analytical methods used for the study 111
3.6.1.1 Generalised Procrustes Analysis (GPA) 111
3.6.1.2 Principal Components Analysis (PCA or PC) 112
3.6.1.3 General tooth dimension analysis 115
3.6.1.4 Discriminant Function Analysis (DFA or DF) 116
3.6.1.5 A "log se_m" regression analysis combined with a correlation analysis . 118
3.6.2 Summary – analyses carried out 128

CHAPTER FOUR – RESULTS 130
4.1 Introduction 130
4.2 Phase I – Testing of "inputs" – landmark model tests to ascertain the importance of scaling in the analyses 131
4.2.1 Extant species – Test for species differentiation with and without scaling using a principal components analysis 132
4.2.2 Prior expectations from shape-only analyses vs. size-and-shape analyses 132
4.2.3 Results of the shape-only and size-and-shape analyses 134
4.2.4 Fossil hominin species – application of parameters identified in extant species analysis to test for fossil species differentiation using PCA 138
4.2.5 Implications of (Phase I) "inputs" tests for the remainder of the study (testing of "outputs", Phase II) 142
4.3 Phase II – testing of "outputs" – additional analyses carried out on the specimens 142
4.3.1 Linear Dimension analyses 142
4.3.1.1 Modern humans (*Homo sapiens)*: 142
4.3.1.2 Extant primate species: 146
4.3.1.3 Fossil molars: 151
4.3.2 Principal components analyses based on Procrustes form space 157
4.3.2.1 Extant species 157
4.3.2.2 Fossil species 158
4.3.3 Procrustes distance matrix between fossil species 170
4.3.4 Results obtained from the discriminant function analysis and probability predictions for groupings of fossils. 174
4.3.4.1 Extant species 174
4.3.4.2 Fossil specimens 175
4.3.5 Results of Log se_m on radial measurements of landmarks 178
4.3.5.1 Four extant species 178
4.3.5.2 African Plio-Pleistocene fossil hominin species 187
4.3.5.3 Potential anomalies – log se_m analysis 196
4.4 Summary tables of results of analyses 198
CHAPTER FIVE – DISCUSSION 202
5.1 Extant primate species 202
5.2 Fossil species 205
5.2.1 *Australopithecus afarensis* 205

5.2.2 *Australopithecus africanus* 217
5.2.3 *Homo erectus* 220
5.2.4 *Homo habilis; Homo rudolfensis* 225
5.2.5 *Paranthropus boisei; Paranthropus robustus* 227
5.3 Discussion of potential anomalous specimens 234
5.4 Re-working of the PCA analysis with the exclusion of the six main anomalies 237
5.5 Re-working of the log se_m analysis with the exclusion of the six main anomalies 240
5.6 Antimeres 242
5.7 Link between dental morphology and diet 242
CHAPTER SIX – CONCLUSIONS 245
6.1 Review of the aims of the project 245
6.1.1 Quantification of species variability and the existence of clear boundaries between species 246
6.1.2 Diagnostic features of lower first molars; development of a landmark model 247
6.1.3 Confirmation of results using additional analytical methods 248
6.1.4 Trends over time and geographical distance 248
6.1.5 Evidence of sexual dimorphism – patterns identified: extant and fossil species 249
6.1.6 Range of variability observed within species in the fossil record; identification of cases of unexpectedly little variation or higher than expected variability 250
6.2 Potential anomalies detected 253
6.3 Limitations of this study and opportunities for further research. 257
6.4 Final conclusions 259
APPENDICES 278
Appendix 1 Reference size data for fossil hominin mandibular first molars 278
Average mesiodistal and buccolingual diameters of *Australopithecus afarensis* lower first molar specimens 278
Mesiodistal and buccolingual diameters of *Australopithecus africanus* M_1 specimens 278
Mesiodistal and buccolingual diameters of *Homo habilis* and *Homo rudolfensis* M_1 specimens 278
Mesiodistal and buccolingual diameters of *Homo erectus* M_1 specimens 278

Mesiodistal and buccolingual diameters of *Paranthropus robustus* and *boisei* M_1 specimens 280
Appendix 2 Photographic protocols 281
Appendix 3 Principal Components Analyses: output data 283
Appendix 4 Procrustes Distance Matrix – 36 fossil specimens 285
Appendix 5 Log se_m matrices for four extant species 286
Appendix 6 Log se_m matrix for fossil specimens 36 x 36 log se_m pairwise comparisons 288

LIST OF FIGURES

Figure	Description	Page
2.1	Diagrams of a hominin lower left permanent first molar showing cusp names and the position of the C_6	44
2.2	Examples of *Australopithecus afarensis* M_1 morphology	45
2.3	*Australopithecus afarensis* - AL 266-1 R (mirrored)	47
2.4	Examples of *Australopithecus africanus* M_1 morphology	47
2.5	*Australopithecus africanus* – MLD 2 L.	48
2.6	Examples of *Homo habilis and Homo rudolfensis* M_1 morphology	49
2.7	*Homo habilis* – OH 7 L.	50
2.8	Examples of *Homo ergaster/erectus* M_1 morphology	50
2.9	*Homo erectus (ergaster)* – KNM-ER 992 L.	51
2.10a	Examples of *Paranthropus (robustus* and *boisei*) M_1 morphology	52
2.10b	*Paranthropus robustus* and *boisei* – SKW 5 (R) (mirrored) and Peninj 1 (L).	53
2.11	Visual summary of overall size and width variation between M_1s of specimens allocated to various species of Plio-Pleistocene fossil hominins	55
2.12	Visual summary of the main cusp arrangement variations between M_1s of specimens allocated to various species of Plio-Pleistocene fossil hominins	55
3.1	Antimeres of AL266-1 (scaled images)	73
3.2	Landmark distances from the centre of 11 views of a pristine tooth at varying degrees of tilt compared to the same calculation for a different tooth entirely.	81
3.3	2D snapshots of 3D unworn tooth images for the calculation of tilt error bars.	83
3.4	Calculation of the angle of tilt for existing 2D photographs	84

3.5	Placement of a “bounding box” and a fan overlay on images	86
3.6	Observer error test for placement of central landmark	87
3.7	Test for inter-and intra-observer error in locating the central landmark at the mesiodistal-buccolingual diameter intersection	88
3.8	Diagram to show how the buccolingual and the mesiodistal (corrected and uncorrected) diameters are calculated	91
3.9	Measurement of the “maximum” buccolingual diameter and the “uncorrected” mesiodistal diameter of the molars; calculation of the centre of the tooth at the intersection of the midpoints of both diameters	92
3.10	Landmark model: 5 anatomical (Type I) landmarks plus 44 Type III/pseudo/constructed landmarks	101
3.11	Landmarks 1-5: centre, overall size and relative width	102
3.12	Landmarks 6-29: perimeter shape	103
3.13	Landmarks 30-49: inner and outer cusp arrangement,cusp orientation	104
3.14	Image to show cusp midline differences for differently oriented cusps	105
3.15	Example of Procrustes wireframe overlays	111
3.16a	Illustrative plot of a regression of 48 pairwise measurements between two antimeres from the same specimen	120
3.16b	Illustrative plot of a regression of 48 pairwise measurements between two molars of different specimens from the same species	120
3.16c	Illustrative plot of a regression of 48 pairwise measurements between two morphologically distinct molars of different species	121
3.17	A statistical definition of a species (based on cranial data)	122
3.18	Illustrative frequency diagram for log se_m values for intra-species comparisons of cranial measurements, compared to inter- species comparisons	124
3.19	Illustrative examples of x-on-y and y-on x pairwise comparisons for a) conspecific, almost identically-sized specimens and b) differently-shaped and differently-sized specimens from different species	126

4.1	Typical shapes of modern human, gorilla, chimpanzee and bonobo mandibular first molars	133
4.2	Procrustes shape space analysis of lower first molars of four extant species	134
4.3	Procrustes form space analysis of lower first molars of four extant species	135
4.4	PCA results for 4 extant species: PC1 correlated to centroid size	136
4.5	"Undifferentiated" Procrustes form space principal components analysis of lower first molars of African Plio-Pleistocene lower first molars attributed to seven species	140
4.6	"Colour-coded" Procrustes form space principal components analysis of lower first molars of African Plio-Pleistocene lower first molars from seven presumed species	141
4.7	Graph of mesiodistal and buccolingual diameters for mandibular first molars of modern human males and females	145
4.8	Graph showing the mesiodistal:buccolingual measurements of mandibular first molars of four extant primates	147
4.9	Mesiodistal and buccolingual measurements for M_1s of 36 fossil specimens, taken from occlusal photograph views	152
4.10	M_1 MD:BL ratios plotted against time for 36 fossil samples	155
4.11	Principal Components graph for sample of lower first molars of four extant primate species	157
4.12	Principal Components graph (colour-coded data points) for fossil M_1 sample of lower first molars	164
4.13	Principal Components graph (fossil M_1 sample) with bonobo sample as a species outgroup	165
4.14	Principal Components graph (fossil M_1 sample) with chimpanzee sample as a species outgroup	166
4.15	Principal Components graph (fossil M_1 sample) with gorilla sample as a species outgroup	167
4.16	Principal Components graph (fossil M_1 sample) with modern human sample as a species outgroup	168

4.17	Principal Components graph (fossil M_1 sample) with four extant species outgroups	169
4.18	Frequency distributions of average log se_m values for intra-specific pairwise comparisons lower first molars of gorilla, chimpanzee, bonobo and modern *Homo sapiens*	179
4.19	Frequency distributions of average log se_m values for inter-specific pairwise comparisons of lower first molars of gorilla, chimpanzee, bonobo and modern *Homo sapiens*, shown in order of shape similarity	184
5.1	M_1 of AL 288-1 ("Lucy") compared with other specimens from *A. afarensis* (AL 266-1 and LH 4), bonobos, chimpanzees, *Homo erectus* and a modern human	209
5.2	Comparison between the M_1 of LH 2 (*Australopithecus afarensis)* with other *A. afarensis* specimens and with the holotype of *Australopithecus africanus*	211
5.3	M_1 of Sts52b pictured with a) Taung 1 and MLD 2 (both *Australopithecus africanus)* and with AL266-1 (L) and KNM-ER 806c, the two closest specimens to it on the PC chart, Figure 4.12	218
5.4	M_1 of Taung 1, with a visible sixth cusp, compared with similarly-sized *Paranthropus* specimens	219
5.5	M_1 of KNM-ER 806c (L), showing the sixth and seventh cusps	221
5.6	M_1 of KNM-ER 806c compared to a) other *Homo erectus* specimens, b) *Australopithecus africanus* specimens and c) KNM-ER 15930 *(Paranthropus boisei)* and OH 16 (*Homo habilis)*	223
5.7	Close PCA grouping of four M_1 molars each from different species	226
5.8	M_1 of OH 7 (*Homo habilis* holotype*)* compared to other specimens	227
5.9	PCA grouping of "robust" *Paranthropus* M_1 specimens	230
5.10	Principal components grouping of smaller *Paranthropus* M_1 specimens	231
5.11	Principal Components Analysis of 36 fossil M_1 specimens showing six anomalous specimens	237
5.12	Principal Components Analysis of fossil M_1 specimens showing well-defined species groupings after exclusion of 6 anomalous specimens	238
5.13	Schematic colour-coded graph relating to time.	239

LIST OF TABLES

Table	Description	Page
1.1	Summary of primary aims, with approaches applied to achieve the aims	41
2.1	Summary of observed morphology of lower first molars of holotypes or typical specimens from presumed fossil species	54
3.1	Materials: Modern human specimens (*Homo sapiens)* included in the study	67
3.2	Materials: African ape specimens included in the comparative study	69
3.3	Fossil lower first molar specimens included in the comparative study	75
3.4	Percentage errors for x and y coordinates recorded during the inter- and intra-observer error test for locating the central landmark for teeth	88
3.5	Descriptive summary of landmark placements	107
3.6	Sensitivity test to establish the number of PC score inputs to include in a discriminant function analysis	118
3.7	Illustrative log se_m matrix showing paired x-on-y and y-on-x values for pairwise comparisons (intra-specific and inter-specific)	124
3.8	Expectations for pairwise comparisons between two specimens of similar size and morphology (likely to be "conspecific")	127
3.9	Expectations for pairwise comparisons between two specimens of different size and morphology (unlikely to be "conspecific")	127
3.10	Summary table of analyses	129
4.1	Measurements from lower first molars of modern *Homo sapiens*	144
4.2	Mesiodistal and buccolingual diameter comparisons for modern human female and male left and right lower first molars.	146
4.3	Descriptive statistics: Modern *Homo sapiens* sample	146
4.4	Summary table of area and width data for extant species	150
4.5	Procrustes distance matrix: *Australopithecus afarensis*	170
4.6	Procrustes distance matrix: *Australopithecus africanus*	171

4.7	Procrustes distance matrix: *Homo erectus*	171
4.8	Procrustes distance matrix: *Homo habilis* and *Homo rudolfensis*	171
4.9	Procrustes distance matrix: *Paranthropus boisei*	172
4.10	Procrustes distance matrix: *Paranthropus robustus*	172
4.11	Procrustes distance matrix: *Paranthropus boisei* and *robustus* together	173
4.12a	Discriminant function analysis results - extant species	176
4.12b	Discriminant function analysis results - fossil specimens	177
4.13	Summary of average log se_m values for conspecific pairwise comparisons of gorilla, chimpanzee, bonobo and modern *Homo sapiens*	179
4.14	Summary of differentials (delta values) between pairs of log se_m values for comparisons of conspecific pairs of gorilla, chimpanzee, bonobo and modern *Homo sapiens*	180
4.15	Summary of average log se_m values for inter-specific pairs of gorilla, chimpanzee, bonobo and modern *Homo sapiens*	182
4.16	Summary of log se_m delta values for inter-specific pairs of gorilla, chimpanzee, bonobo and modern *Homo sapiens*	185
4.17	Summary of results from log se_m analyses: extant species	187
4.18	Average intra-species log se_m values for fossil M_1 specimens as currently classified	188
4.19	Average intra-species delta values for fossil M_1 specimens as currently classified	189
4.20	Log se_m matrix - *Australopithecus afarensis*	190
4.21	Log se_m matrix - *Australopithecus africanus*	192
4.22	Log se_m matrix - *Homo erectus*	193
4.23	Log se_m matrix - *Homo habilis* and *Homo rudolfensis*	194
4.24	Log se_m matrix - *Paranthropus boisei* and *Paranthropus robustus*	194

4.25	Average log se_m values for M_1s of *Paranthropus* specimens compared to specimens from other species groups and to specimens within the *Paranthropus* group	196
4.26	Species grouping patterns detected by each type of analysis	199
4.27	Specimens identified as potential anomalies by each type of analysis	201
5.1	Log se_m mean and standard deviation values – comparisons obtained from different studies	241
6.1	Summary table of assessment of range of variability of fossil species	251

DEDICATION

I dedicate this study to my husband, Dennis, for the unerring support he has given me.

ACKNOWLEDGMENTS

I am deeply grateful to Bernhard Zipfel for support, encouragement and advice as my co-supervisor and for assisting me with access to fossils housed at the University of the Witwatersrand.

To the Director and staff of the Ditsong National Museum of Natural History in Pretoria, I owe sincere thanks, and in particular to Stephany Potze and Lazarus Kgasi for assistance in accessing the fossil specimens housed at the museum.

I would like to express heartfelt gratitude to the Directors and collections managers of the Kenya National Museum in Nairobi (and in particular, Ms Emma Mbua, Ms Mary Muungu and Ms Rose Nyaboke); the National Museums of Dar es Salaam in Tanzania (specifically Ms Eliwasa E. Maro, Mr Mawazo Ramadhani and Dr Amandus P. Kweka); as well as the National Museum in Arusha, Tanzania (particularly Mr Jackson Njau).

Thanks go to Emmanuel Gilissen for his assistance and for access to primate specimens housed at the National Museum for Central Africa in Tervuren, Belgium and to Brendon Billings for all his help in enabling access to modern human specimens in the Raymond Dart collection at the Medical School of the University of the Witwatersrand.

Very special thanks are due to Professor José Braga, Jean Dumoncel and Amélie Beaudet, for providing access to 3D images of teeth, as well as for valuable advice, training and assistance with Amira software.

Many of the faculty and staff at the Evolutionary Studies Institute at the University of the Witwatersrand have contributed ideas, advice and tuition, without which this dissertation would not have been possible. For statistical and geometric morphometric training, as well as useful advice, I am extremely grateful to Dr Kristian Carlson and to Dr Tea Jashashvili. Other scholars, including Dr Christine Steininger, Dr Jonah Choinière and Eddie Odes have supported my efforts and offered advice and direction along the way. Professor Marion Bamford has provided invaluable help with administrative matters and ideas for taking the project further. Evelyn Ho and Sarah Sejake have been indispensable in their assistance with travel arrangements, expense claims and other clerical tasks.

Financial support for this project has been obtained from the National Research Foundation through Professor J. Francis Thackeray, supplementing my own personal contributions.

To Professor Thackeray I owe a sincere debt of gratitude. Not only has he provided invaluable direction and advice as my senior supervisor for the project, as well as the great majority of the funding for trips to Europe and to East Africa to collect original data, but his huge enthusiasm and unfaltering support towards this project have ensured that this has been one of the most rewarding experiences I have ever undertaken. I am truly thankful.

To my son Richard, who, upon learning that I had laboriously calculated the first 2780 pairwise regressions for my log se_m calculations individually, wrote (with little help from me) a complicated programme that enabled me to produce additional matrices of tens of thousands of se_m and delta values automatically at the click of an "I regress!" button (which action then initiated a pop-up that instructed me to go away and make a cup of coffee while I waited for the programme to execute itself).

Lastly, to my husband for his unswerving encouragement, financial backing and assistance with proof-reading of the final dissertation, and to my family generally, who all encouraged me, supported me in many ways and who have shared the excitement as well as the pressure-filled moments, thank-you.

ABSTRACT

Teeth are the most common element in the fossil record and play a critical role in taxonomic assessments. Size, relative width and cusp arrangements on enamel crown surfaces are used to help assess relationships between specimens. In this exploratory study, a model is developed for the placement of landmarks on images of lower first molars to maximise key information from crown surfaces of molars of African Plio-Pleistocene hominin fossils representing species of *Australopithecus, Paranthropus* and *Homo*. Lower first molar data of four extant species (*Pan paniscus, Pan troglodytes, Gorilla* and *Homo sapiens*) are visualised in a principal components analysis to detect whether landmark placements are adequate to identify species groupings and overlaps and patterns indicative of sexual dimorphism. The role of size as a differentiator between extant species is visualised using Procrustes Form Space as the basis for the analysis. A series of analyses, including linear diameter plots, Procrustes averaging, principal components analyses, discriminant function analyses and log se_m (based on regression analyses) are used to test whether species groupings agree with currently accepted taxonomic classifications of thirty-six African Plio-Pleistocene hominin lower first molars. Specimens in the sample that consistently fail to group with current species designations are flagged as "anomalous". Six specimens are identified as anomalous and these are ultimately removed from the analyses. The resultant principal components plot of the fossil specimens appears to show distinctions between currently accepted species groups. The statistical regression analyses (log se_m) confirm the results from the geometric morphometric analyses, and are associated with an average log se_m value of -1.61 for conspecific pairwise comparisons. The log se_m value of -1.61 has been proposed by Thackeray (2007a) as an approximation of a biological species

constant (T), based on pairwise comparisons of modern vertebrate taxa, using cranial data. The anomalies confirm the hypothesis that certain specimens from the sample may have been misclassified, and that certain species groups as currently defined may comprise more than one morphotype.

CHAPTER ONE – BACKGROUND, AIM, PRIOR WORK.

1.1 Background to the current study

Teeth are the most commonly found element in the hominin[1] fossil record, due to their composition and their resistance to taphonomic modification. Classification of fossil finds consisting only of teeth and their associated mandibular and maxillary remains is often problematic, particularly if the new discovery includes features that are considered to be outside of the normal range of variability for the dentition of previously defined species.

When dealing with issues of "classification" (and, by extension, potential "misclassification") of specimens in the fossil record, the main question arises as to how within-species and between-species variability is quantified and delineated. The question of what defines a species and how much variability is to be considered normal within any one species is a subject of some debate, even for extant species (Mayr 1970; Paterson 1985; De Queiroz 2007; Kimbel & Martin 1993), so when specimens in the fossil record require classifying into discrete species, there is considerable challenge to be met (Aiello et al. 2000). This study is exploratory and aims to investigate the possibility of identifying and quantifying diagnostic features that relate to variability of lower first molars, building on research that aims to distinguish the molars of one presumed species from another in the African Plio-Pleistocene hominin fossil record (e. g. Aiello & Dean 1990; Hillson 1996; Wood & Abbott 1983; Wood et al. 1983; Wood & Uytterschaut 1987). Using a suite of analytical methodologies, an exploratory attempt will be made in this study to quantify variability in differentially worn and damaged molars, with a view to

[1] "Hominin" refers to modern humans and extinct species considered to be most closely related to modern humans; "hominid" is an informal name usually given to hominin species plus species belonging to the genera *Pan, Gorilla* and *Pongo* (Chimpanzees, bonobos, gorillas and orang-utans) (Wood, 2011).

obtaining an indication of within-species variability, based on patterns observed on molars from extant primate species, in addition to assessing variation between species.

According to Gómez-Robles et al. (2008) (in reference to fossil hominin dentition), "The morphological differences among *Paranthropus, Australopithecus,* and African early *Homo [...]* are small". Other researchers argue that taxonomic differentiation within specimens currently attributed to a single species such as *Australopithecus africanus* or Early Pleistocene *Homo* can be differentiated yet further into additional species (Clarke 2012; Leakey et al. 2012). Researchers debate as to how many species are recognisable in the Plio-Pleistocene hominin record, with hypotheses ranging from one single lineage evolving over time and geographical space (Wolpoff 1971; Henneberg & Thackeray 1995; Henneberg & de Miguel 2004; Van Arsdale & Wolpoff 2013), to a tendency to consider the number of species in the palaeoanthropological record to have been underestimated (Tattersall 1986).

The question of species overlap or distinct resolution between species is further complicated by the issue of whether specimens from different geographical areas should be likely to be of the same species (Grine et al. 2012; Lordkipanidze et al. 2013). Leakey et al. recently (2012) published a description of two new specimens found in Kenya, consisting of a near-complete mandible (KNM-ER 60000) and a mandibular fragment (KNM-ER 62003), but comparisons were not made with fossil materials from Southern Africa, despite some specimens attributed to early Pleistocene *Homo* being located there (see, for example, Hughes & Tobias 1977). Other recent comparisons, involving elements such as cranial and maxillary bones and brain endocasts have rendered results suggesting that more research needs to be undertaken to investigate conspecificity

between certain Southern African and East African specimens (Thackeray 2003; Thackeray & Odes 2013; Thackeray et al. 2005; Navsa et al., 1998). In view of the fact that during the Plio-Pleistocene period, some species of fauna and flora existed in both East Africa and Southern Africa (Grine, Jacobs, et al. 2012), that sister species of *Paranthropus,* as well as specimens attributed to *Homo habilis* (e.g. W.H. Kimbel & Rak, 1993) and possibly *Australopithecus africanus* (see, for instance, Crevecoeur et al., 2014) have been identified in both locations, a conscious effort has been made to include personally-captured images from specimens, including holotypes, from both areas (for instance, to include both *Paranthropus boisei* and *Paranthropus robustus*), ideally from the original fossils rather than from casts.

1.2 Aim of the project

Within the context of the debate concerning how little or how much variability exists within a single species and whether boundaries between species are well-defined, the aim of this project was to carry out morphometric analyses of molar crown morphology using images of the dentition (lower first molars) of modern primates (*Homo sapiens, Pan* and *Gorilla*) as well as African Plio-Pleistocene hominin fossil teeth in order to establish whether diagnostic features of mandibular first molars that are traditionally used by morphologists to distinguish between fossil species can be successfully quantified and analysed, to the point where species groupings are defined sufficiently well by the analyses used, so that assessments can be made as to whether certain fossil teeth currently attributed to particular species of *Australopithecus, Paranthropus* or *Homo* are correctly assigned, or are instead attributable to different taxa. Species grouping patterns, boundaries and/or overlaps and anomalous specimens (those failing

to group with their currently assigned taxa) are analysed and conclusions are drawn as to whether classifications of individual lower first molars from specimens in the Plio-Pleistocene hominin fossil record are reasonable, and as to whether species groupings themselves should be further investigated due to potentially excessive variability or large overlaps observed between specimens attributed to different species.

To achieve this aim, the descriptive or "*qualitative"* approach of the traditional morphologist needs to be converted into some form of numerical or "*quantitative"* "distance data" between specimens, by applying numerical techniques that optimise the potential for classifying individual specimens into their respective species groups. These quantitative techniques will first be applied to mandibular first molars of extant species, to obtain benchmark distance data and grouping patterns for known, distinct species. Thereafter, the fossil specimens will be compared against each other and against the results for the extant species. This study will therefore attempt to answer the following questions:

- Can a species be defined numerically: in terms of lower first molars, how much variability is to be expected within a species and do clear boundaries exist between species?
- What are the traditionally accepted diagnostic features of lower first molars that distinguish the various species groups in the fossil record? How can these diagnostic features best be represented by landmark placements on images of these teeth, so that each feature is correctly emphasised for purposes of analysis?
- Can the application of various morphometric techniques and other numerically-based methodologies confirm or falsify the results obtained?

- Is it possible to assess trends over time and/or geographical distance in hominin tooth morphology?
- Is it possible to discern the influences on molar tooth size and/or shape of sexual dimorphism in extant species, and can this be applied to analyses of tooth morphology variation in the fossil record?
- Based on morphometric studies of size and shape variation in molars of extant species, are the currently accepted ranges of variability within taxonomic groupings of hominin fossils reasonable? Are there particular species groups that display a significant amount of variability between specimens in the group, or is there unexpectedly little variation between hominin species in the Plio-Pleistocene period?

Ultimately, by applying numerous different analytical techniques, any specimens that appear to be misclassified into their currently accepted species groups should regularly recur as anomalous specimens. These anomalies will allow for assessments to be made as to whether the specimens in question group better with another species entirely, whether the differences in size or shape could be due to sexual dimorphism or other factors, or whether the species to which they are currently attributed contains distinct morphotypes that might imply (or confirm) the existence of a second species within that particular group.

1.3 Prior work : taxonomy and species variability

As soon as a new fossil specimen is discovered, the immediate question will always revolve around the identification of the specimen, and whether it can be assigned to a pre-existing taxon or whether this discovery heralds the introduction of a new species. Morphological, morphometric, cladistic and even genetic data (where recoverable) will help in the assessment of how to assign the specimen to genera and to species. Nevertheless, the process of establishing where the boundaries lie between genera, species and sub-species is difficult even in the case of extant taxa where soft tissues and behaviour (including reproductive behaviour) can be examined. The "biological species concept", introduced by Mayr (1942; 1970) identified the process whereby sexually reproductive communities become isolated from other communities, thereby forming a new species. The concept of the biological species concept was expanded upon with the introduction of the idea of the Recognition Concept (Paterson 1985), whereby a system of specific mate-recognition is also factored in to the idea of defining a species. For fossil species of the African Plio-Pleistocene, in the absence of genetic data and of possible clues as to where genetic boundaries lay and where hybridisation may have occurred, our only clues when diagnosing skeletal elements like teeth with a view to classifying these into species (or with a view to identifying individual specimens that might be classified incorrectly) are the features that distinguish such specimens by their phenotypic differences, which involves quantifying variability within and between suspected reproductive communities in the fossil record, and comparing this variability to analogous extant species (Kimbel 1991).

However, species have different degrees of morphological variability; on the one hand there are overlaps between species when measuring specific bone or dental elements, and in some morphological traits of these elements there is a substantial or even complete overlap (Tattersall & Schwartz 2009; Tattersall 1986). On the other hand, there is a balance that needs to be found between the expected variation with a species, (and sometimes this involves admitting that there is "much variation" (Darwin 1869)), and the interpretation that such are the phenotypic differences between specimens that they are recognisably distinct, "fully separated species" (Hublin, 2014). As already discussed, great debate surrounds the concept of species and species delimitation (de Queiroz, 2007, Kimbel and Martin, 1993) and in particular (once a temporal dimension has been added to the concept of biological species (Simpson 1961)), how palaeoanthropological species can, in light of this, themselves be delimited (Hublin, 2014). It is therefore not surprising that a great deal of divergence in opinion exists when it comes to taxonomic allocations in the context of palaeontology.

In this respect, a recent study has raised questions about the possible range of within-species variability that can be found within one single fossil assemblage (Lordkipanidze et al. 2013). Such is the variability that exists in the crania, the mandibles and the post-cranial remains on this single site, that at first glance, there is a rush to judgement to declare the existence of multiple species represented in the fossil assemblage at Dmanisi (Georgia) (e. g., Schwartz, 2000). However, on closer inspection, all the specimens found at the site come from one single geological member and it is hard to believe that several different species of *Homo erectus* might be occupying the same space at the same period of time. Many researchers accept that the remains come from one single palaeodeme at the site (S. H. Lee 2005; Lordkipanidze et al. 2007; Rightmire

et al. 2008; Martinón-Torres et al. 2008; Van Arsdale and Wolpoff 2012; Lordkipanidze et al. 2013).

The extreme variability between specimens witnessed at Dmanisi has a counterpart in the African Plio-Pleistocene fossil hominin record. Specimens attributed to *Australopithecus afarensis* vary from one extreme (the tiny, narrow, chimp-like teeth of AL 288-1, set in a gracile V-shaped mandible) to another (very square-shaped teeth in a robust, U-shaped mandible, typical of the holotype (LH 4 from Laetoli in Tanzania) and other specimens found at Hadar in Ethiopia). Again, at first glance, such are the vast differences in shape and size between the two morphotypes that it is hard to conceive of them belonging to a single species, yet the assemblage at Dmanisi would urge caution before rushing to judgement.

When degrees of variation within a single presumed species in the fossil record rivals or exceeds even the most extreme cases of observed variability for extant species, questions should be raised as to the potential causes of the phenomenon. In the case of Dmanisi, for instance, age differences and ontology could be a factor (Van Arsdale & Lordkipanidze 2012), or some sort of extreme sexual dimorphism (Wood et al. 1991). Questions of sexual dimorphism are pertinent to the issue of intra-species variability in the case of many extant primate and fossil species (Brace 1972; Richmond & Jungers 1995; Lockwood 1999; Thackeray 1999; Lockwood et al. 2000; Reno et al. 2003; Lee 2005; Thackeray 2007b). Within extant primate species, sexual dimorphism accounts for most of the variance within species groups. Craniofacial elements, for example, and especially facial and neurocranial elements, are more subject to size and shape differences than other elements (O'Higgins & Dryden 1993). All great apes and humans

are subject to differences in scale between males and females, but craniofacial shape differences appear to be more marked in *Gorilla* and *Pongo* than in other extant primate species (*ibid*. p. 193).

If great variability can exist between species, to what extent can we assume that fossil species as they are currently defined are correctly delineated? Could *Australopithecus, Paranthropus* and early Pleistocene *Homo* possibly all be subsumed into one single species? If not all of the specimens attributed to these three genera, then could certain of the specimens be misclassified due to indistinct boundaries between the groups, resulting from extreme intra-species variability? Those who argue for less species rather than more, even if they do not subscribe to a single lineage theory, might point to the similarities in facial and dental morphology between some early Pleistocene *Homo* (with very small-bodied postcranial remains attributed to *Homo habilis* and *Homo rudolfensis*) and smaller *Paranthropus* specimens. According to researchers such as Wood and Collard (1999), it is not until the larger-bodied erect *Homo* species (*Homo ergaster, Homo erectus* and later *Homo* species) that the genus *Homo* should properly be attributed, since these early specimens are perceived to be little advanced over the Australopithecines (Wood 1996; Wood & Collard 1999). Wood and Collard (*ibid*, p.68) group *Homo habilis* and *Homo rudolfensis* cladistically with *Paranthropus robustus, Paranthropus boisei* and *Paranthropus aethiopicus,* and made the recommendation that these two early *Homo species* should be attributed to the genus *Australopithecus* (*ibid.,* p. 70). A comparison between certain specimens of "Early *Homo"* and *Paranthropus robustus* is borne out by other authors (Thackeray 1999; Thackeray & L'Abbé 2005). When Leakey, Tobias and Napier first published on *Homo habilis* (Leakey et al. 1964) attention was drawn by Phillip Tobias to OH16, the dentition of which is large, and

which he stated would fall within the range of the Australopithecines (which included the robust Australopithecines). This kind of observation was also made by Thackeray (2003) who calculated probabilities of conspecificity between "Early Homo" and specimens of *Australopithecus.* Sexual dimorphism may account for apparent differences in cranial features between specimens of *Paranthropus.* One of the features of many *Paranthropus* specimens is a gorilla-like sagittal crest, which allows for stronger temporalis muscle attachments for the larger jaws and masticatory function, and is most typically found in males of the species. Morphologically, the differences between the cranium of OH 5 (the holotype of *Paranthropus boisei*) and that of KNM-ER 732 (another *boisei* specimen from East Africa) are very marked at first glance (OH 5 having a pronounced sagittal crest, while in KNM-ER732 it is absent). Considering similar differences in crania among modern gorillas (Silverman et al. 2001), it is not hard to picture OH 5 being a male of the species and KNM-ER 732 being a female, and to accept that they are assigned to the same species. Yet in South Africa, SK 48 (with a sagittal crest) and SK 847 (probably without a sagittal crest) are usually attributed to different species – indeed, different genera – (*Paranthropus robustus* and *Homo* respectively) (Thackeray 1999).

Variability in crania does not always match variability in dentition. According to Wood et al. (1991), when it comes specifically to mandibular dentition, sexual dimorphism is determined primarily by canine variables as well as comparative buccolingual measurements in molars. This finding is borne out by studies of modern molar crown dimensions in which it has been found that female lower first molars are on average more narrow than male lower first molars (Thackeray et al. 2005). However, when it comes to taxonomic assessments, crown length (indicative of the overall size of the

tooth) and variability in individual shape features are more diagnostic in terms of taxonomic categorisations for molar teeth (Wood et al. 1991). Cusp arrangements, coupled with fissure patterns found on the crown surfaces of molars are routinely used to differentiate between species in the fossil record (Hillson 1996; Aiello & Dean 1990; Wood & Abbott 1983; Wood et al. 1983). A description of the individual diagnostic features of mandibular first molars in the context of the fossil species examined in this study is given in Chapter Two.

1.4 Quantification of morphological variation

Translating differences in molar crown width, length and cusp-fissure patterns into numeric data, and combining this quantitative information to provide a graphical or statistical analysis that equates to the results obtained by traditional morphologists in their qualitative assessment of taxonomic groupings of fossil molars, is the responsibility of the morphometrician. Various methodologies are routinely employed in the biological sciences, applying different mathematical methodologies, including:

- Linear methods: straightforward graphical representations of mesiodistal and buccolingual diameters (Moggi-Cecchi et al. 2010; Benazzi et al. 2011; Leakey et al. 2012) and the ratios between them.
- Statistical methodologies of comparing shape differences using pairwise analyses, such as Log $se_{m,}$ (Log-transformed Standard Error of the Slope) (Thackeray et al. 1997; Braun et al. 2004; Thackeray & Odes 2013); GATD (size-corrected average taxonomic distance), DIM (geometric mean ratios), SEEB (standard error of the slope) and ATD (average taxonomic distance) (Aiello et al. 2000; Richmond & Jungers 1995); STET (standard error test) (Wolpoff & Lee

2001); and S_{LR} (standard deviation of logged ratios) (Gordon & Wood 2013); other methods include analyses of coefficients of variation (e.g. Moggi-Cecchi, 2003), randomisation analyses (e. g. C.A. Lockwood, Jungers, & Kimbel, 1996) and other multivariate analyses.

- Geometric morphometric shape analyses, distance matrix shape analyses and further statistical techniques based on these. Methods include those based on landmark-based Procrustes superimposition, such as generalised Procrustes analysis (GPA) (Rohlf & Slice 1990) and Procrustes distance analyses (Zelditch et al. 2004; Dryden & Mardia, 1998). Geometric morphometrics is considered to be a "powerful multivariate statistical technique" to analyse spatial distributions of landmarks and to quantify shape similarities (Hublin 2014). Other tests for shape analysis include Euclidean distance matrix analysis (EDMA-I (Lele & Richtsmeier 1991) and EDMA-II (Lele & Cole 1995)) using multidimensional scaling to analyse inter-landmark distances. Analyses thereafter include (but are not limited to) thin plate spline (TPS) (Bookstein 1991), principal components analysis (PCA) (Bookstein 1991), canonical variates analysis (CVA) (Albrecht 1980) and discriminant function analysis (DFA or DA) (Fisher 1936; Poulsen & French 2013; Stockburger 2013).

It is not within the scope of this exploratory study to employ all of these methodologies to test both the robustness of the "inputs" (the correct placing of landmarks onto the specimens to be able to quantify diagnostic traits on molars to differentiate between species) and the strength of the "outputs" (the results from the analyses employed). A selection of these methodologies has thus been made to test the landmark model (Phase I: testing of "inputs") and to confirm the results (Phase II: testing of "outputs"). A

principal components analysis based on Procrustes matrix inputs was used primarily to obtain a visualisation of potential species grouping patterns and anomalies, and to test for the role of size in species differentiation. Other methodologies (such as a discriminant function analysis and a log se_m analysis) were chosen to see if they confirmed these preliminary findings.

A large part of this study (Chapter Three; 3.5) is dedicated to the development of a "Landmark Model". Most of the above-mentioned analyses are based on the placement of homologous or "matching" landmarks on 2D or 3D images of each of the objects being compared for size and shape differences (Bookstein, 1991; Zelditch et al., 2004, Dryden & Mardia, 1998). These landmarks are usually based on biological points that are homologous between the shapes being analysed (Dryden & Mardia, 1998; Zelditch et al., 2004). In the case of images of molar teeth in two dimensions, cusp boundaries and peaks, fissures, fovea, tooth perimeters and other anatomical features can be used for landmark purposes, as well as mathematically-calculated landmarks (for instance, the geometric centre of the tooth, mathematically-calculated maximal diameters, or centre-points between two other landmarks, etc.). In any landmark-based analysis, the number of homologous landmarks must be equal for all of the images being compared. This means that all anatomical landmarks used must ideally be identifiable on every single one of the specimens used for any particular study and all mathematically-calculated landmarks must be repeatable for all specimens. In the case of analyses of images of molar teeth, particularly those from the fossil record, wear and damage rule out the use of some of the landmarks that might be identifiable on pristine teeth (such as the peaks of cusps, or the fovea found on the teeth), so a mixture of anatomically-sited ("biological" or Type I) landmarks and mathematically-calculated ("pseudo",

"constructed" or Type III) landmarks is used for this study (Dryden & Mardia, 1998; Bookstein, 1997).

1.5 Some features of the study that differentiate it from other similar studies

While several studies have been conducted on fossil teeth based on occlusal morphology (Wood & Abbott 1983; Wood et al. 1983; Martinón-Torres et al., 2006; Gómez-Robles et al., 2007, 2008, 2012, 2013), the materials and/or the methods used in these previous studies differ from those being used in the present study. This study, in particular, includes the following:

- **Unique landmark placement model optimising information from worn molars and including size, perimeter shape and full cusp description including direction of cusps:** an experimental landmark model was developed, using five "anatomical" landmarks, the remainder being primarily "pseudo" or "constructed" landmarks (Dryden & Mardia, 1998, pages 3-6; see 3.5 below) which are geometrically calculated landmarks that can be independent of anatomical structures on the tooth itself. Included in the sample are some teeth that are effectively "blank canvasses" except for the perimeter edge which preserves the intersections of the five cusps. Using just the overall length, relative width and spatial "weighting" of the tooth (larger or smaller talonid relative to the geometric centre of the tooth) as well as the direction, length and width of each cusp, geometry can be employed to optimise what might seem at first glance to be sparse information from differentially worn and damaged occlusal crown enamel surfaces. Landmarks are divided into three polygon groups (external (dimensions); peripheral (shape); inner (cusp arrangement)) to

provide a calculated balance in the analysis to areas of taxonomic diagnostic assessment normally considered by morphologists when differentiating between molars from fossil specimens (see Aiello & Dean, 1990; Hillson, 1996 and Wood & Abbott 1983; Wood *et al,* 1983 for general descriptions). Provision has been made for the landmarking of a) mesiodistal-buccolingual diameters (relative size together with relative width of the molar); b) general perimeter shape; c) the presence of a sixth cusp or "tuberculum sextum"; and d) the internal cusp arrangement including the width of the individual cusps, relative length of the individual cusps and direction of the individual cusps from the mesiodistal-buccolingual diameter intersection at the centre of the tooth. This differs from the work done by Wood & Abbott (1983) and Wood et al. (1983), in that their work concentrated on overall morphology of the crown and a morphometric analysis of cusp *areas*. The value of landmarking the width, length and direction of each cusp is that a) cusps that have wide arcs along the perimeter edge of the molar, but that are fairly "shallow" in terms of their general projection (perimeter distance) from the centre of the tooth might have the same surface area as cusps that are very narrow along the perimeter edge but which project well out from the centre of the tooth, so this is a way to differentiate between "wide, shallow cusps" and "narrow, long cusps" that might have the same area but are spatially distinct; and b) each cusp can be evaluated in terms of its general direction from the centre of the crown: for example, is the hypoconid very buccally-oriented, or is it angled more distally? Cusp direction can be as diagnostic between species as cusp size (see below, Chapter Two). The landmarking and digitisation of these parameters allows the basic geometry of

these features to be included in the analyses even if the features themselves are absent due to wear or damage;

- **Focus on Plio-Pleistocene molars, and use of original data rather than casts:** researchers such as Gómez-Robles et al. (2007, 2008, 2012, 2013) and Martinón-Torres et al. (2006) have published articles on Geometric Morphometric analyses of the post-canine dentition of hominins, but this study differs in that a) the focus of this study is on African Plio-Pleistocene hominins, rather than primarily on Lower Pleistocene hominins (designated primarily as *Homo heidelbergensis* and *Homo neandertalensis*) and b) original photographs of the bulk of the Plio-Pleistocene specimens in the study have been taken from personal visits to collections in Nairobi, Dar es Salaam, Pretoria and Johannesburg, rather than using casts for these specimens as the cited researchers have done. Additionally, although Aida Gómez-Robles has mentioned (in personal correspondence) that a study of lower first molars is in progress, this has not yet been published. My own study focuses on lower first molars.
- **Unique test for the angle of tilt in occlusal photography:** this study utilises a similar photographic and image-processing methodology to that used by Gómez-Robles et al. and Martinón-Torres et al. in their various studies of post-canine teeth (*ibid.*). However, in this present study, a novel technique has been employed to calculate the error of levelling of the teeth to ensure that the teeth are directly orthogonal to the lens above them (and that the images produced are therefore true occlusal images of the teeth). By splicing three individual shots of a single specimen (taken on different days) into a 3D image of the same tooth (kindly supplied by Professor José Braga in Toulouse), differences in levelling

along 3 axes in space can be calculated and compared, to test for significant observer error during the photograph capturing process. This test is explained in more detail in 3.3.2.3. below.

- **Inclusion of extant species to test for variability in known species' lower first molar occlusal crown morphology:** the study seeks to test some aspects of species variability and to assess whether or not these can be quantified statistically and probabilistically. The study differs from the occlusal crown image-based dental studies mentioned above, in that the question of species variability is tested in a preliminary way using specimens selected from a sample of occlusal images of lower first molars of extant species. Original images of specimens of gorilla, chimpanzees, bonobos and modern *Homo sapiens* were captured in Tervuren, Belgium and in Johannesburg, South Africa for inclusion in the study for comparative purposes where possible. This is not the first study to include both extant ape species and fossil hominins for shape analyses. However, most studies that include both extant and fossil comparisons concentrate on cranial comparisons (e.g., Wood et al. 1991; Thackeray & Prat, 2009; Lordkipadnidze et al. 2013, Gordon & Wood, 2013). Those that compare dental features often concentrate on non-metric traits (e.g., Bailey & Wood 2007; Irish & Guatelli-Steinberg 2003; Guatelli-Steinberg & Irish 2005) or enamel thickness (e.g., Rabenold & Pearson 2011) or some other feature such as microwear (e.g., Grine et al. 2006) or diet and dental topography (e.g. Ungar 2004). Skinner et al. (2008a; 2008b) and Braga et al. (2010) have studied mandibular molars to examine taxonomic parameters that allow for discrimination between known species (extant species), comparing the findings to fossil hominins. The main dental elements used in those studies are molar

teeth as in this study, but in those cases, the focus is on the enamel-dentine junction (EDJ). This present study focuses on crown outer enamel surfaces and seeks to maximise the amount of information that can be gleaned from the crown itself, using a minimum number of anatomical features (those common to both worn and unworn teeth), in an attempt to be able to discriminate adequately between species even when teeth are worn. Although one of the stated advantages of using the EJD rather than the outer enamel surfaces (OES) is that the EDJ in moderately worn teeth remains pristine, the problem remains that many gorilla teeth, bonobo teeth, and more importantly, fossil teeth (including some holotypes or mandibular proxies for holotypes) are more than moderately worn. Once the enamel has worn through to the EDJ surface, the EDJ then disappears and that specimen becomes unusable for an EDJ study or it reduces the information available for such. In the case of this present study, the only disqualifying factor for a badly worn tooth to be included is in instances where the points at which the individual cusp arcs meet at the perimeter of the tooth are absent. Even severely worn teeth can be used provided that those junctions are visible at the perimeter. This study is therefore able to include some teeth that are badly worn. Thus, not only has the study included some specimens of extant species that would sometimes be excluded from studies, but some important specimens such as Peninj 1, which is a proxy for the holotype of *Paranthropus boisei*, have also been able to be included.

- **Use of numerous analytical methodologies to test robustness of initial results:** the study juxtaposes various analytical methodologies that investigate shape (and shape-size) comparisons from quite different approaches. A similar approach has been taken by Valeria Bernal (Bernal 2007), wherein geometric

morphometric techniques are compared to more traditional analyses. This study, based on lower first molars, uses some different methodologies. One of these is the "Log se_m" regression-based probability approach, pioneered by Professor F. Thackeray (Thackeray et al. 1997; Thackeray 1997; Braun et al. 2004; Thackeray 2005; 2007a; Thackeray & Odes 2013), to determine the probability of pairs of individuals being conspecific. By first subjecting the data to geometric morphometric analyses and a principal components analysis (based on a Procrustes "form-space" analysis (Mitteroecker et al. 2004) – see 4.2.3), followed by a discriminant function analysis, a framework exists to determine, *a priori*, whether species groupings can be discriminated visually and statistically, and whether the likelihood of misclassifications exists for any of the individual specimens studied. Thereafter, the application of the Log se_m method would provide a different, independently-based approach to confirm or falsify these results. In doing so, the Log se_m methodology itself might also be able to be confirmed by methodologies more widely used at present by researchers (geometric morphometric methods and statistical analyses such as principal components analyses), and if the results largely concur, this would confirm the methodology's usefulness in contributing a probabilistic approach to the examination of the "mathematical species concept" (bearing in mind the fact that the species concept itself is a subject of great discussion (Hublin 2014); see also Kimbel & Martin 1993; De Queiroz 2007).

1.6 Scope of the study, primary objectives and working hypotheses

1.6.1 Scope of the study - limitations

1.6.1.1 Access to specimens

In order to compare teeth from several presumed species of African Plio-Pleistocene hominin fossil teeth, uniformity of "inputs" to the analyses was paramount: occlusal images of specimens of lower first molars to a similar scale and format were required. To ensure such, original data was personally collected using identical photographic protocols on each occasion from several museums and collections in South Africa, Tanzania and Kenya. Additional data were collected for extant species from Belgium and South Africa. Access to specimens was limited in certain cases due to limitations imposed by permits (Nairobi), availability of personnel to allow access (Arusha) and due to limited numbers of usable, well-identified specimens in the collection itself (Nairobi, Dar es Salaam; Tervuren: *Pan paniscus,* notably). Numerous specimens were photographed, but even with digital enhancement, many were too damaged to include in the analyses.

1.6.1.2 Inclusion of original photographs of all holotypes (or proxies) – selection of M_1 as common molar to all holotypes

A large part of the study involved the development of a landmark placement model for the shape analyses conducted on the teeth. Since all six molar types in the upper and lower dental arcades would require potentially different landmark placement sites for their analysis, thus requiring separate analyses for each tooth type, the most prevalent type of molar tooth was chosen for the study. Lower first molars were not only the

most common molar tooth found present in the specimens photographed around the world, but all the mandibles ***representing holotype specimens*** from fossil species that were able to be included for study (all from original photographs) contained at least one lower first molar. (See 3.1 below for additional discussion on the rationale for limiting the study to lower first molars).

1.6.1.3 Limitations of mandibular molars with respect to cranial comparisons

It is recognised that a selected sample of lower first molars from the African Plio-Pleistocene fossil record will not provide enough information to be able to test hypotheses unequivocally, regarding inter- and intra-species variability. However, since holotypes or proxies for holotypes for all seven fossil species included in the study were able to be photographed from the original specimens, the remaining specimens in the study can certainly be compared to the holotype and to other specimens in the same species groups, so that in certain cases, anomalies (specimens that fail to group with the holotype or with others in the species group that do group in the same general area as the holotype) can be identified and highlighted for further examination. It is not within the scope of this study to include equivalent extant and fossil cranial metrics for comparative purposes. In the case of the extant species, ranges of shape and size variability in the crania of certain species do not necessarily predict what the range of shape and size variability of lower first molars would be for that same species. For the fossil analyses, many of the specimens used for this study consist only of mandibular remains, with no full cranial data available for comparison with these specific individuals.

1.6.1.4 Selection of a limited array of analytical methods to confirm results

Rather than conduct one single type of analysis on the specimens included in the study, it was decided to select a number of analytical techniques in order to test as independently as possible the robustness of the results: species groupings and overlaps that might become apparent; anomalous specimens, failing to group with their presumed species. It is stressed that this study is exploratory in nature, with small sample sizes. Due to this limitation and to considerations of length of the dissertation, each analysis tended to be carried out at a fairly basic level and additional in-depth statistical tests were not able to be considered in each instance. However, despite these limitations, the data were sufficient to confirm basic patterns of variability within extant species, and from these, the fossil sample could be assessed for species variability and potential anomalies.

1.6.1.5 Exploratory nature of the study, leading to future research

This study may be viewed as being exploratory in nature. Future research can be conducted on other molar types (e.g. maxillary molars), using other analytical techniques again (such as Euclidian distance matrix-based analyses) to compare the results obtained via the methodologies applied here. In doing so, additional specimens of extant species' molars and those of the African Plio-Pleistocene hominin fossil record (including OH 5, the holotype for *Paranthropus boisei,* which has maxillary but not mandibular dentition) can be included in the study to reinforce the conclusions made. In future studies, and once sample sizes of both extant and fossil specimens can be increased, additional statistical tests should be carried out on each of the analyses conducted to add robustness to the results.

1.6.2 Primary aims of the study, approaches used to achieve these aims

The primary aims of the study as discussed in 1.2 above together with some of the specific approaches used to address these are summarised in Table 1.1:

Table 1.1 Summary of primary aims, with approaches applied to achieve the aims.

Aim	Solution
Identification of diagnostic features of lower first molars	Comparative study conducted on fossil lower first molars based on personal observation and on literature review
Recognition of the most significant diagnostic features of lower first molars *quantitatively* based on landmark placements so that each feature is correctly emphasised for purposes of the analysis	Consideration of different models of landmark placements to emphasise each diagnostic trait. Testing of the final model chosen to distinguish between known biological species (extant species); application of the same model and the same analyses to fossil molars; comparison of patterns of results between extant species and fossil species. Further testing of the model using different analytical methodologies to confirm results from the other methodologies.
Grouping of species numerically in terms of variability within and between species	Landmark model to be optimised by applying "shape only" and "shape and size" analyses to provide the best resolution between species groupings; statistical probabilistic methods to be applied to determine probabilities of conspecificity.
Application of additional morphometric techniques to test whether there is harmony between their results	Apply not one but several analytical techniques and compare the results. Repeated confirmations of trends and of anomalies would add robustness to the results.
Assessment of any identifiable trends over time and/or geographical distance in hominin tooth morphology	Analyse shape data and size-shape data to see if trends appear over time and over geographical distance.
Detection of sexual dimorphism in the molars of extant species and comparison of these patterns in the molars of fossil species	Analyse linear and size-shape data to see if similar trends appear in both extant species and fossil species.
Correctness of the classifications of certain fossil molars from specimens currently attributed to particular species	Within the limitations of the particular specimens included in the study, check for anomalous specimens that fail repeatedly to group with their presumed species group, no matter which methodology is applied to the data
Reasonability of ranges of variability within taxonomic groupings of hominin fossils	Acknowledging that this study analyses only lower first molars, compare the ranges of variability observed within and between extant species to inform an analysis of the expected ranges of variability seen within and between the presumed species groups from the African Plio-Pleistocene period

1.6.3 Working hypotheses

The working hypotheses to be tested were as follows:

- **HSQ**: "Status Quo Hypothesis": all African Plio-Pleistocene first molar specimens discovered to date, including holotypes, are correctly classified into their current taxa;
- **H0**: The observed degree of variability in first molar shape and size within extant species is so narrow in range that when the same parameters are applied to samples of African Plio-Pleistocene fossil hominin dental specimens discovered to date, the latter should be recognisable as discrete species;
- **H1**: At least some of the African Plio-Pleistocene specimens currently attributed to certain species of *Homo, Paranthropus* or *Australopithecus* may have been misclassified.;
- **H2**: The observed degree of variability in first molar shape and size within extant species is so wide in range that when the same parameters are applied to specimens attributed to currently-accepted species groups in the African Plio-Pleistocene period, this would result in all species of that period being subsumed into one species;
- **H3**: There are no clear boundaries between species.

CHAPTER TWO – BACKGROUND TO THE MORPHOMETRIC STUDY: DIAGNOSTIC MORPHOLOGY OF SURFACE ENAMEL FEATURES OF LOWER FIRST MOLARS OF AFRICAN PLIO-PLEISTOCENE HOMININ SPECIMENS

2.1 Background: morphological taxonomic diagnostics of lower first molars requiring to be "landmarked".

In order to develop a landmark model that adequately "translates" qualitative, taxonomically diagnostic features of molars into numeric values for use in statistical analyses, it is first necessary to establish which main features of crown surface morphology most influence taxonomic assessments made by morphologists. For this reason, it is of value to discuss general lower first molar morphology and in particular, specific features that distinguish one Plio-Pleistocene fossil hominin species from another, since these are the very traits that need to be identified by the landmarks to be used in the study. The descriptions presented below are based on literature cited, and are supplemented by personal observations made from the photographic images captured for this present study (examples shown in each section).

2.2 General tooth morphology of African Plio-Pleistocene fossil hominins

Lower first molars in all hominins are generally five-cusped, with, in a few cases (notably *Paranthropus*) a sixth cusp, the C_6 or "tuberculum sextum" (Aiello & Dean 1990; Hillson 1996; Wood et al. 1983; Braga & Thackeray 2003). Figure 2.1 illustrates this.

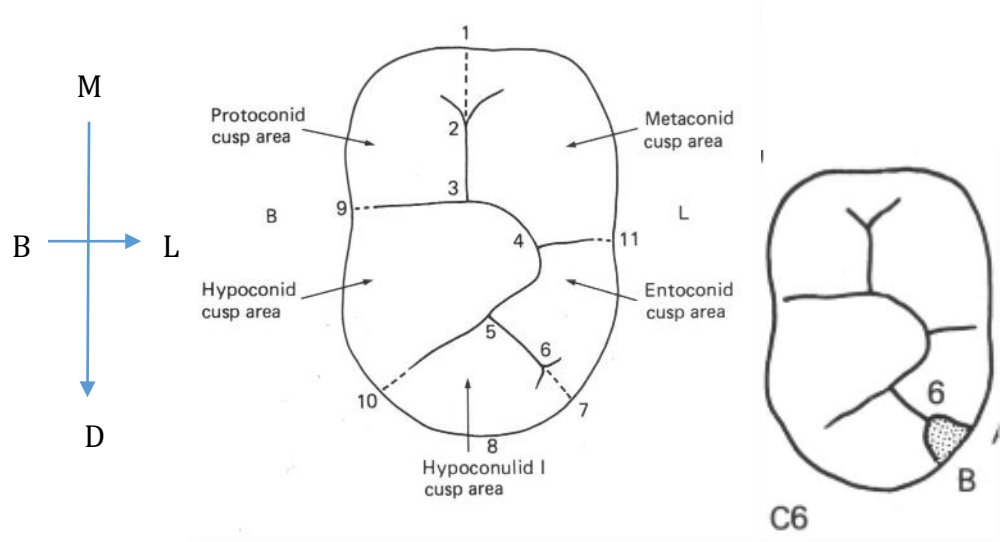

Figure 2.1. Diagrams of a hominin lower left permanent first molar showing cusp names and the position of the C_6
From Wood et al. (1983), diagram on left also reproduced in Aiello & Dean, (1990)
M=Mesial margin; B=Buccal; D=Distal; L: Lingual.

The five cusps are named as follows: the metaconid (mesiolingual cusp); the entoconid (the distolingual); the protoconid (the mesiobuccal cusp); the hypoconid (the distobuccal cusp); and the hypoconulid (the distal cusp). The C_6, if present, would be located between the entoconid and the hypoconulid, towards the distal margin of the tooth.

The mesial margin of the tooth will be reasonably straight in shape, or even concave; the distal margin will tend to be more rounded.

2.3 Diagnostic morphology of lower first molars of African Plio-Pleistocene fossil hominins

Set out below are the distinguishing features generally cited by morphologists (*ibid.*) in the context of lower first molars of hominin fossil species in the Plio-Pleistocene period. Photographic examples of the occlusal views of chosen specimens from each species group in the study have been added to the descriptions for purposes of illustration and

for clarification of personal observations made. Reference size data (mesiodistal and buccolingual diameters) are provided for each species group in Appendix 1.

2.3.1 *Australopithecus afarensis*

Holotype: LH 4, Laetoli, Tanzania. Examples: see Figures 2.2 and 2.3

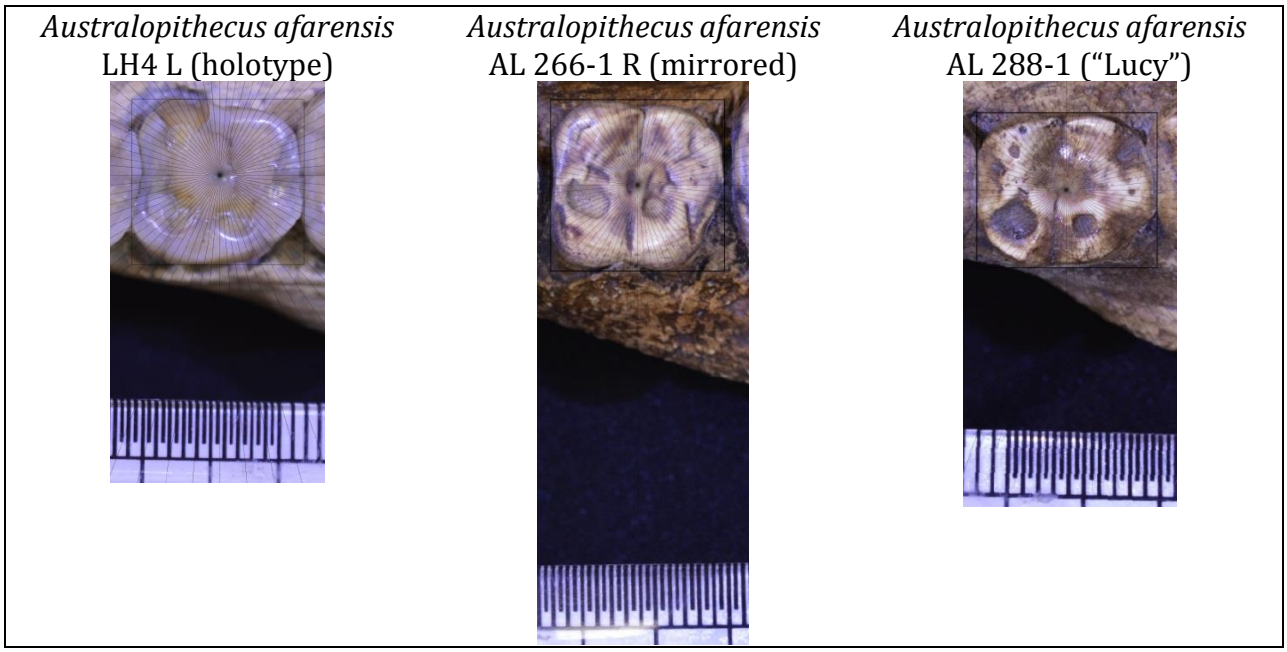

Figure 2.2. Examples of *Australopithecus afarensis* M_1 morphology

There is a considerable range of tooth-shape variability between specimens attributed to the *Australopithecus afarensis* group, as there is with other skeletal elements of this species (see 5.2.1 for a discussion). The holotype is LH 4, a mandible from the Laetoli area of Tanzania.

Australopithecus afarensis lower molars are generally smaller mesiodistally than *Australopithecus africanus* lower molars, which in turn are smaller than those of *Paranthropus* (Aiello & Dean, 1990; Hillson, 1996; Human Origins Database (humanoriginsdatabase.org, Wood & Gordon); Kimbel et al. 2004; figures given in

Appendix 1 of this study). *A. afarensis* molars are similar in mesiodistal size to *Homo* molars, but tend to be wider buccolingually (Aiello & Dean 1990:154). Personal observations : as can be seen from the above photographs, there appear to be at least two morphotypes represented in the M_1 sample from Hadar in Ethiopia – the very wide molars that resemble the holotype and a narrow molar that is more *Homo*-like in overall width and length but more chimpanzee-like in appearance. These differences reflect the discussion that has been ongoing since the first discoveries of these fossils in the 1970s, as to whether or not these differences (not just in molars, but in other cranial and skeletal elements) are far greater than would be expected for a single species of hominin or whether all the specimens can be allocated to a single species, the larger molars belonging to presumed males and the more delicate teeth to the presumed females of the species. (See, for example, Leonard & Hegmon 1987; Ferguson 1989; Schmid 1989; Leonard 1991; Richmond & Jungers 1995; Lockwood et al. 1996; Reno et al. 2003; Gordon et al. 2008; Kimbel & Delezene 2009; Reno et al. 2010).

The holotype (from Laetoli in Tanzania) is LH 4. In terms of its lower first molar, it is typified by a very prominent metaconid and, to a lesser extent, entoconid, and this is similar to many of the specimens from the Hadar region of Ethiopia (Afar localities). The protoconid and hypoconid are almost directly opposite the metaconid and entoconid respectively, giving the tooth a very square appearance, accentuated by the fact that the MD:BL ratio for the majority of M_1s attributed to this species is in the region of 1.0 (LH 4: M_1 (R) – MD diameter : 14.0; BL diameter : 13.9 (White 1977)).

Figure 2.3. ***Australopithecus afarensis*** **- AL 266-1 R (mirrored).** **Similar in occlusal morphology to the holotype, LH4, AL 266-1 (Rm) is pictured here as the cusps are more easily differentiated from the photographic images.**

2.3.2 *Australopithecus africanus*

Holotype: Taung 1 (U.W. 1-1), University of the Witwatersrand, South Africa

Examples: see Figures 2.4 and 2.5

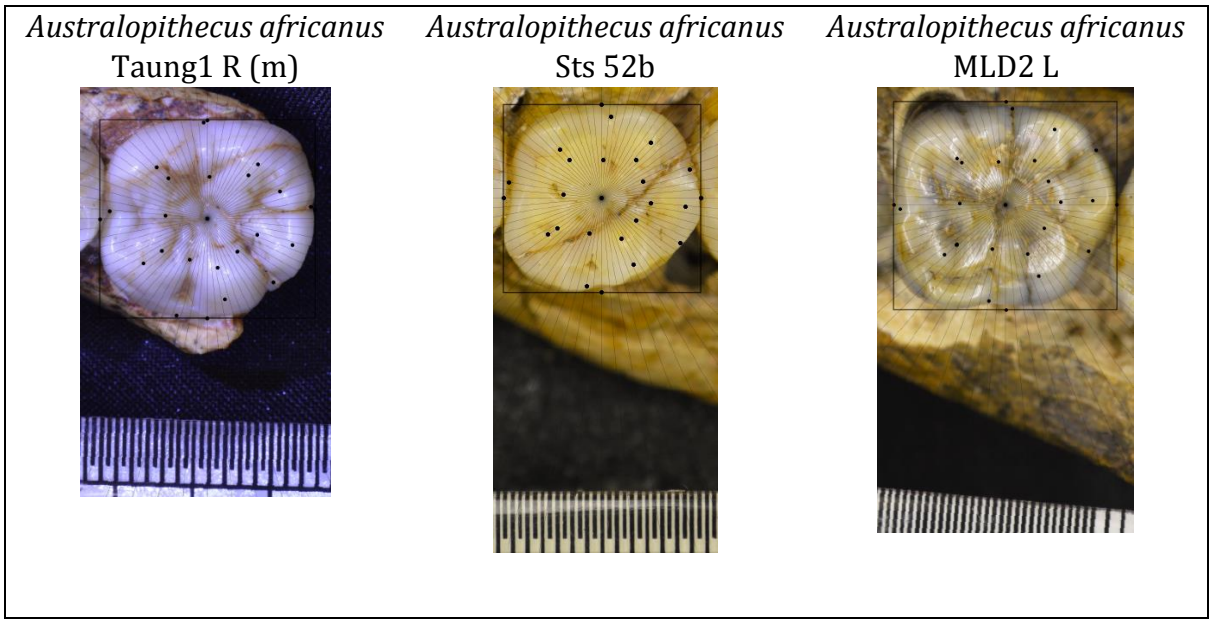

Figure 2.4 Examples of *Australopithecus africanus* M_1 morphology

Although Taung 1 is the holotype for *Australopithecus africanus*, MLD 2 is perhaps more typical of the species, as it has a well-defined "cingulum" or "protostylid", a

characteristic, shelf-like area that often runs along the edge of the protoconid and sometimes the hypoconid of this species (Aiello & Dean, 1990; Hillson, 1996, etc.). There are, however, wide variations in the occurrences of the protostylid (Hlusko 2004). *Australopithecus africanus* first lower molars are generally larger than *Australopithecus afarensis* M_1 molars (Human Origins Database – figures reproduced in Appendix 1) but their buccolingual diameter tends to be smaller by comparison to their mesiodistal diameter on average, so they tend to be less "square" than *Australopithecus afarensis* first lower molars. Observations: these teeth generally have very square metaconids and buccodistally-oriented hypoconids, with hypoconulids located centrally to buccocentrally on the distal margin. The entoconid extends distally, so that it is not directly opposite the hypoconid, and the buccolingual groove is more diagonally oriented than is the case for *Australopithecus afarensis.* Taung 1 is unusual in that the M_1 has a sixth cusp, which is usually only present on lower first molars of *Paranthropus* and which is considered to be a diagnostic feature of *Paranthropus* M_1 teeth (Aiello & Dean 1990; Wood et al. 1983; Braga et al. 2003).

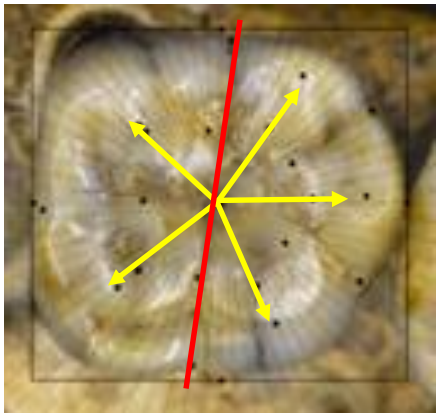

Figure2.5– *Australopithecus africanus* – MLD 2 L.

2.3.3 *Homo habilis; Homo rudolfensis*

Holotype, *Homo habilis:* OH 7, National Museum, Dar es Salaam, Tanzania.

Holotype, *Homo rudolfensis:* KNM-ER 1470 (cranium/maxilla), National Museum, Nairobi, Kenya. Examples: see Figures 2.6 and 2.7

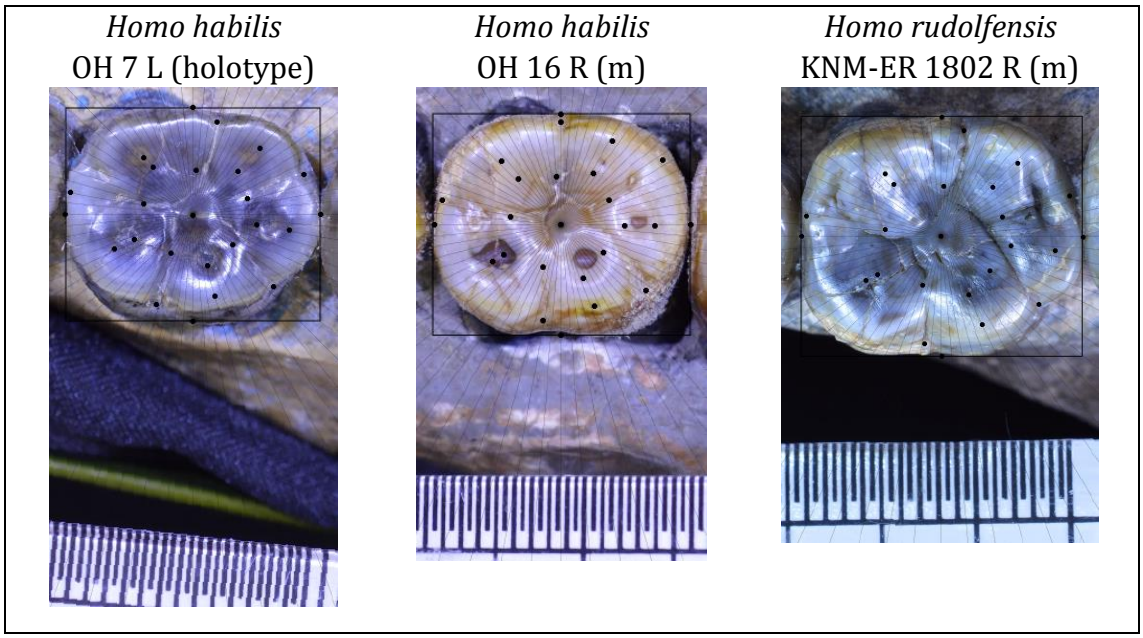

Figure 2.6 Examples of *Homo habilis and Homo rudolfensis* M_1 morphology

These mandibular first molars generally have the lowest relative mesiodistal:buccolingual ratios of early Pleistocene hominin lower first molars (Human Origins Database). An exception to this might be OH 16, which is not quite as narrow and approaches *Australopithecus africanus* in size (Leakey et al. 1964). The mesiodistal diameters are greater than those of later *Homo* species and of *Australopithecus afarensis.* They are therefore recognised as very long and narrow teeth (Aiello & Dean, 1990; Hillson, 1996, etc.). Observations: using the holotype of *Homo habilis* as an example, it can be observed that these molars have wide, shallow metaconids with the longest relative cusp arc along the perimeter edge mesiodistally of all the teeth examined (see comparative illustration, Figure 2.12 below), small protoconids, relatively small entoconids and buccodistally-oriented hypoconids with almost

centrally-distal hypoconulids. Due to the large metaconid and small protoconid, the mesial cusps are more noticeably skewed, relative to the tooth axes, (obtuse buccolingual groove angle) unlike the almost perfectly direct midline split between mesial and distal cusps as observed in *Australopithecus afarensis*.

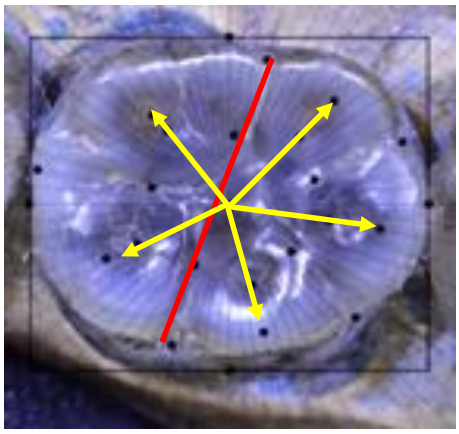

Figure 2.7– *Homo habilis* – OH 7 L.

2.3.4 *Homo erectus (Homo ergaster)*

Holotype, *Homo ergaster* (African *Homo erectus)*: KNM-ER 992, National Museum, Nairobi, Kenya. Examples: see Figures 2.8 and 2.9.

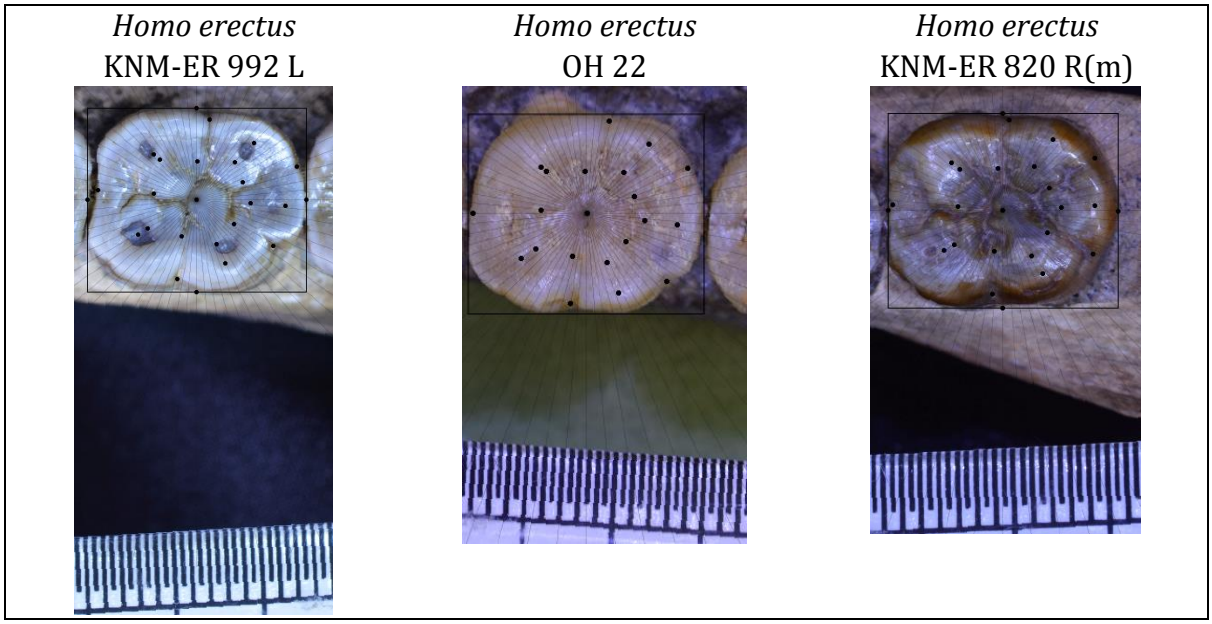

Figure 2.8 Examples of *Homo ergaster/erectus* M_1 morphology

These lower molars are characterised by being very small and narrow (Human Origins Database, figures reproduced in Appendix 1). Observations: the longest cusp along the mesiodistal axis is the metaconid, leaving the entoconid to be extremely small. The hypoconulid tends to be centrally located on the distal margin.

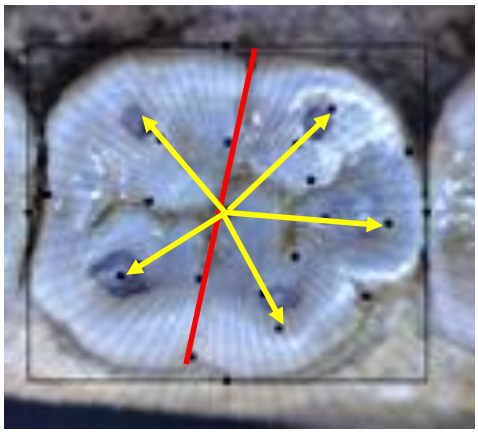

Figure 2.9 ***Homo erectus (ergaster)*** **– KNM-ER 992 L.**

2.3.5 *Paranthropus boisei; Paranthropus robustus*

Holotype (*Paranthropus boisei*): OH 5, (Cranium/maxilla) National Museum, Dar es Salaam, Tanzania;

Holotype proxy *(Paranthropus boisei)* (mandibular): Peninj 1, National Museum, Dar es Salaam, Tanzania;

Holotype *(Paranthropus robustus*): TM1517, Ditsong National Museum, Pretoria, South Africa.

Examples: see Figures 2.10a and 2.10b.

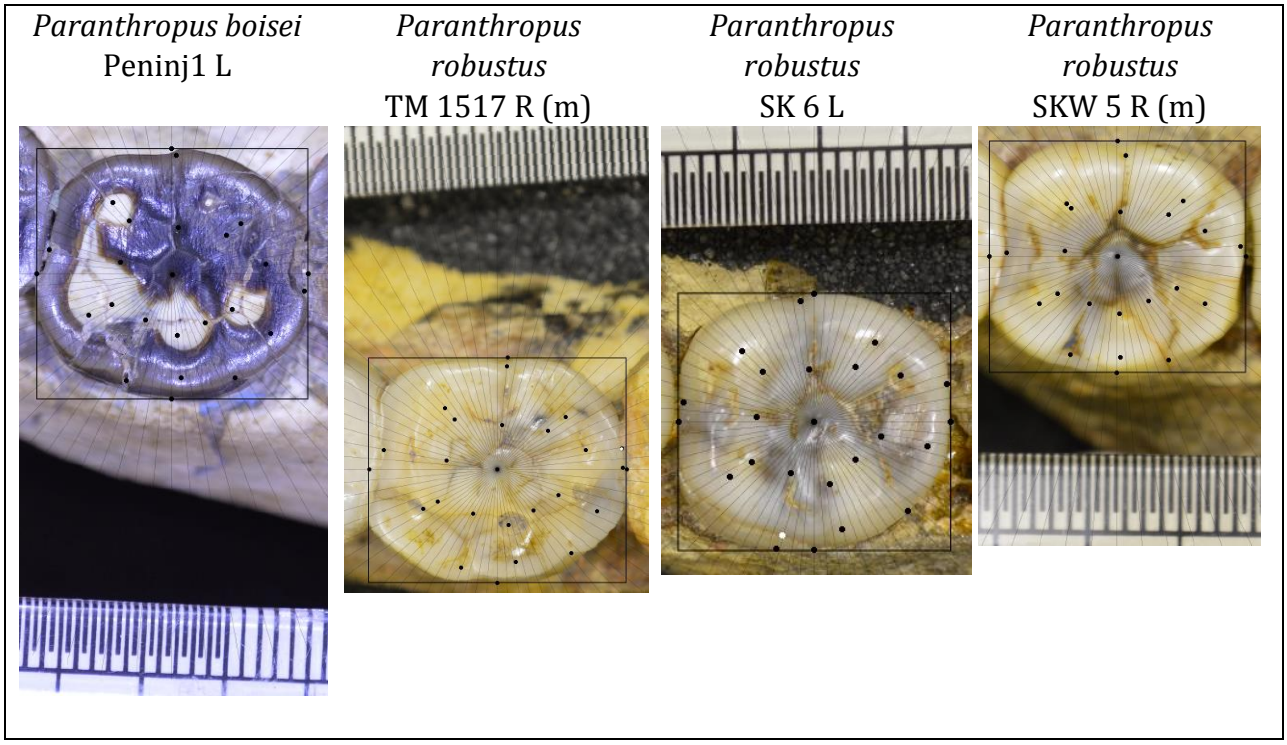

Figure 2.10a Examples of *Paranthropus (robustus* and *boisei*) M_1 morphology

Paranthropus lower first molars have a number of diagnostic features that morphologists consider to be important for their taxonomic classification (Aiello & Dean 1990; Hillson, 1996; Wood et al., 1983). Firstly, their size is a major distinguishing feature, particularly in relation to their anterior teeth, which are small: this is the opposite condition to that found in *Australopithecus afarensis,* where anterior teeth are large and post-canine teeth are small (Aiello & Dean 1990:155). On average, *Paranthropus boisei* and *robustus* molars are larger than those of other species in the hominin fossil record, although the range in size variation is considerable (Silverman et al. 2001; Grine 2007; Grine et al. 2012). Secondly, the distal cusps (hypoconulid and entoconid) tend to be large in *Paranthropus* and the mesial cusps (metaconid and protoconid) small by comparison (Wood et al. 1983, Suwa et al., 1994). Also of note in lower first molars is the almost invariable presence of a C_6, which may be related to the fact that the talonid (the distal area of the tooth) is enlarged (*ibid.,* as well as Suwa et al.

1994; Skinner et al. 2008). Observations: The large hypoconulid (cited by Wood et al., 1983, Suwa et al, 1994) extends well into the buccal perimeter edge, causing the hypoconid to be narrower and more directly centrally buccally-oriented than distobuccally oriented as in the case of *Australopithecus africanus.* The mesial cusps are cumulatively smaller in area than the distal cusps, in contrast to those of *Australopithecus africanus* (see summary illustration below in Figure 2.12)

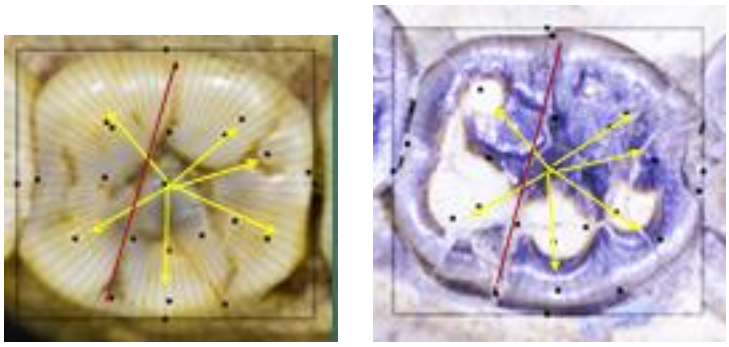

Figure 2.10b *Paranthropus robustus* and *boisei* – SKW 5 (R) (mirrored) and Peninj 1 (L).

2.3.6 Summary: diagnostic features distinguishing African Plio-Pleistocene hominin fossil lower first molars (Table 2.1)

Table 2.1 Summary of observed morphology of lower first molars of holotypes or typical specimens from presumed fossil species:

Species	Holotype	Relative size/length	Relative width	Cusp pattern
A. afarensis	LH 4	MD diameter smaller than *A. africanus* and *Paranthropus spp.*	Most specimens used for the study are almost square. Relatively the widest teeth in the sample.	Almost orthogonally arranged metaconid with protoconid and entoconid with hypoconid, with a very small hypoconulid. Anterior/mesial cusps larger than posterior/distal cusps, with the metaconid being extremely exaggerated on the lingual side. Talonid: whole tooth proportion – almost equal. Fissure demarcating the two anterior cusps: almost parallel to the BL axis, almost central, as is the fissure from the distal midpoint to the hypoconulid, these two fissures forming an almost upright cross (+) between the main cusps.
A. africanus	Taung 1	"Medium" sized tooth in relation to *Paranthropus spp.* (larger) and *A. afarensis* (relatively smaller)	"Medium" width as compared to *A. afarensis* (much squarer) and *Homo habilis* (very narrow by comparison)	Talonid smaller than the anterior part of the tooth. The fissure demarcating the two anterior cusps is slightly angled as the metaconid is larger than the protoconid. Hypoconid oriented bucco-distally.
H. habilis; (and H. rudolfensis)	OH 7 KNM-ER 1470 (no lower molars)	"Medium" in length, by comparison to *H. erectus* (significantly smaller teeth) and *P. boisei* (much larger)	Very narrow	Very large metaconid with relatively smaller protoconid, so that the angle of the fissure between the anterior cusps and the talonid is very obtuse in relation to the mesiodistal axis. Hypoconulid more distally oriented.
H. erectus/ ergaster	KNM-ER 992	Very small teeth.	Very narrow teeth.	Metaconid larger than hypoconid, with fissure crossing the MD axis at an angle. Hypoconulid distally oriented.
P. robustus/ P. boisei	TM 1517; OH 5 (proxy = Peninj 1)	Ranging from large to extremely large.	Reasonably wide teeth (medium to wide)	Metaconid and protoconid generally small, so that the talonid occupies the major part of the tooth. Larger hypoconulid than in most other specimens in the study, occupying some of the buccal perimeter edge. Hypoconid almost directly buccally oriented. Presence of a sixth cusp.

These differences can be visualised in the following two images (Figures 2.11, 2.12):

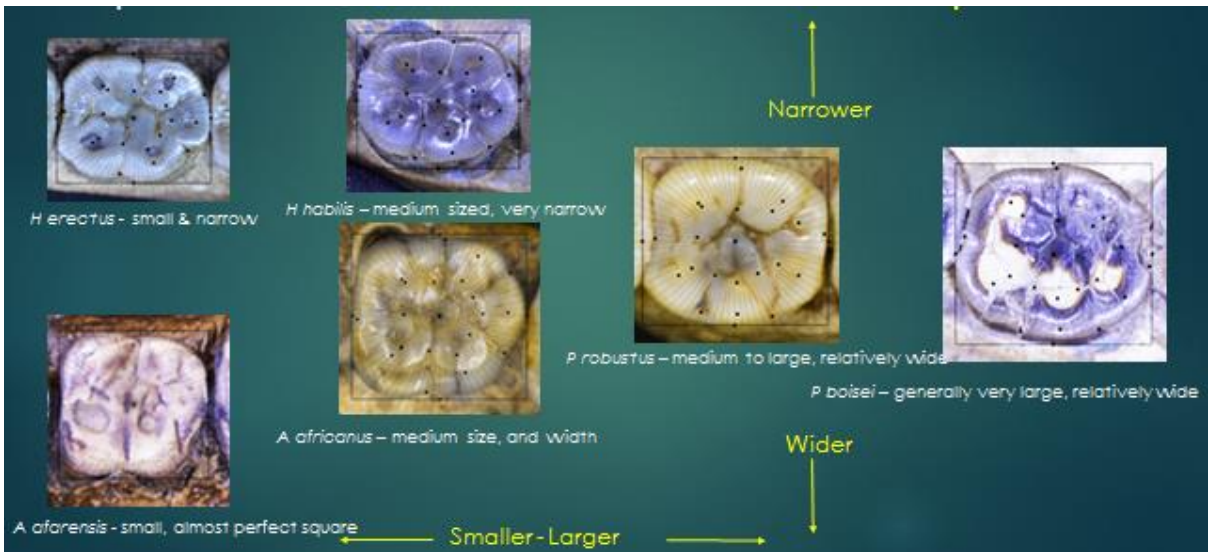

Figure 2.11 Visual summary of overall size and width variation between M_1s of specimens allocated to various species of Plio-Pleistocene fossil hominins (*A. afarensis : small and square; A. africanus: relatively longer mesiodistally, thus relatively narrower than A. afarensis; P. robustus and P. boisei: the largest teeth in the sample, relatively narrow (sometimes narrower than A. africanus); H. habilis: medium in length but very narrow compared to other specimens; H. erectus: the smallest teeth in the sample, very narrow*).

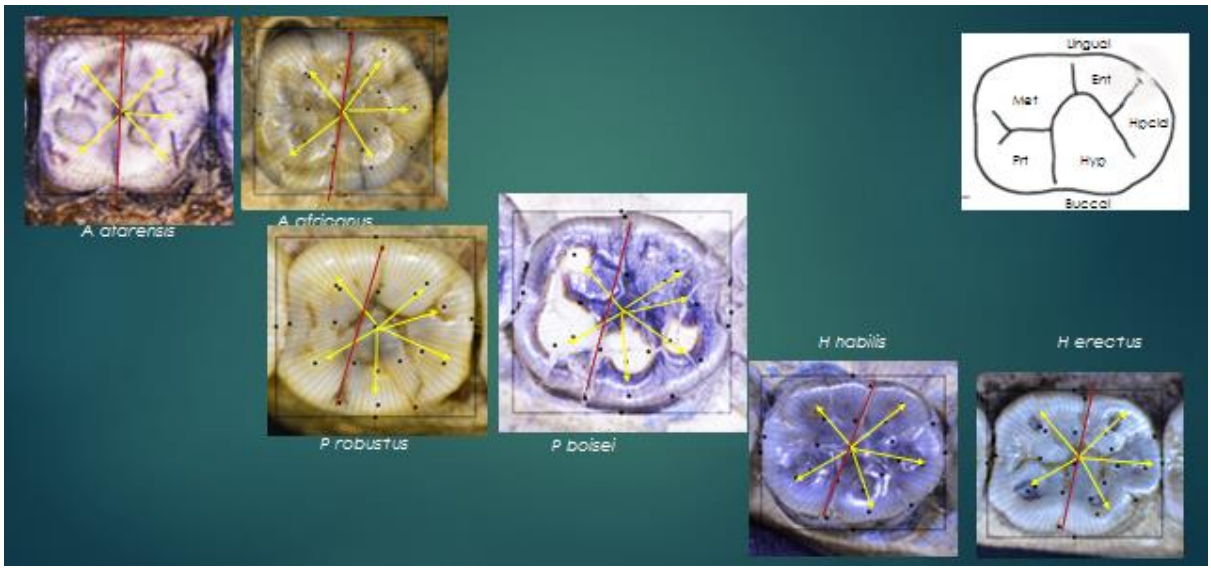

Figure 2.12 Visual summary of the main cusp arrangement variations between M_1s of specimens allocated to various species of Plio-Pleistocene fossil hominins (*A. afarensis: BL groove almost perpendicular to MD axis, protruding metaconid; A. africanus: relatively large mesial cusps with BL groove at a slight angle. Protostylid may be present; P. robustus and P. boisei: large talonid, enlarged hypoconulid, reaching to buccal margin. Hypoconid central-buccally-oriented. Sixth cusp present; H. habilis: wide metaconid with very steep BL groove angle; H. erectus: balanced cusps, distally facing hypoconulid. Fairly steep BL groove angle*).

All of these features are taken into consideration to inform the choice of landmark placements and the optimisation of the landmark model developed as part of this present study.

2.4 Morphology into morphometrics; landmarking for species recognition

Whilst a study of lower first molars of a selected sample of African Plio-Pleistocene teeth may not be expected to resolve any of the challenges facing palaeoanthropologists concerned with the issue of species and species concepts as discussed in 1.3 above, it is possible to draw some conclusions in respect of taxonomy from these teeth. If the currently cited diagnostic features that distinguish first molars of different fossil hominin species from the African Plio-Pleistocene are accepted, by comparing two lower first molars together, it should be possible to distinguish the molar of one currently-accepted species from the molar of another, if those diagnostic features are present. For example, it is possible to distinguish a molar from, for example, SK 6, an individual attributed to *Paranthropus robustus,* from that of KNM-ER 992, an individual attributed to *Homo ergaster* (*Homo erectus*) (see photographs of these specimens above in Figures 2.8 and 2.9): the size ranges for both species do not overlap, and the cusp arrangements are significantly distinct from each other. It is also possible to distinguish a difference between the lower first molar of OH 7 (the holotype of *Homo habilis)* and LH 4 (the holotype of *Australopithecus afarensis*): in this case the great width ("squareness") of LH 4 contrasts with the significant narrowness of OH 7, as well as the extreme difference in the angle of the buccolingual groove (almost perpendicular to the mesiodistal axis in the case of LH 4 and at a very steep angle in the case of OH 7). Although at times it is difficult to be specific as to what a specimen "is", and whether

fossil species designations themselves are valid or not, it is often possible when comparing between individual specimens to say what a specimen "is not". Researchers would, however, be in no doubt as to the fact that these are specimens from different species, even if cranial and/or post-cranial remains for specimens attributed to these species were not available for study. If this kind of distinction can be quantified so that these significant phenotypic differences can be visualised graphically and so that the specimens can be statistically and visually separated using classification techniques, not only will the diagnostic traits of these teeth be useful for adding further quantitative information to the datasets that already exist, particularly those of cranial elements, but also there might be instances where individual specimens produce anomalous results in terms of their currently accepted species allocation, and these individuals can be highlighted for further study.

Since many of the palaeoanthropological discoveries to date have consisted of fragments of mandibles or maxillae or isolated teeth (including lower first molars), it is not illogical to address the question of phenotype diagnostics, based on occlusal crown morphometric data aimed at determining which particular features and metrics of lower first molars contribute towards the taxonomical analysis of these remains, based on our current understanding of fossil species. The diagnostic traits of the teeth being studied ultimately provide the rationale for the next phase of the study: the landmarking of these traits to capture all the major features that add necessary information to the morphometric study.

However, even if a landmark placement model can be found that leads to the ability to differentiate between fossil species as they are designated at present, there is no

guarantee that these fossil species delineations are in any way comparable to "biological species" (see, for example, De Queiroz 2007; Wright 1940; Mayr 1942; (Dobzhansky 1950), the only examples of which are extant species. By also subjecting these metrical data *a priori* to testing on extant species, patterns of variation within known genetic species might be seen to be repeated in the fossil record.

If shape analyses and "shape-and-size" analyses based on the landmark experiments result in a "landmark model" that adequately produces visual and statistical representations of boundaries and/or overlaps between "known" (extant) species, by applying the same protocols to the fossil specimens, if any anomalous specimens are identified that fail to group with their presumed species (or in a group close to the holotype for their presumed species), these can be scrutinised in more detail. Further statistical analytical methodologies can also be applied to the data to confirm or falsify the anomalous results, with the expectation that if specimens by and large consistently group together generally as they would be predicted to do (into their presumed species groups) and that if certain specimens consistently fail to group together with their predicted groups, no matter which of the chosen analyses is employed, even if it remains difficult to draw firm conclusions about species boundaries and the reasons for the failure of certain specimens to group with their currently accepted species groupings, a certain degree of confidence can at least be placed on the "inputs" – the landmark model (the placement of the landmarks).

What should also become possible from the testing of the landmark model on the extant species alone is whether patterns can be perceived regarding *shape* differences within and between individual species, *size* differences within and between individual species

and *shape-and-size* differences together within an individual species. Sexual dimorphism is often cited as an explanation for very wide variability between specimens within individual species (see 1.3 above). If it can be established whether this sexual dimorphism is manifested in extant species as a *size* difference or as a *size-and-shape* difference in highly dimorphic species (such as gorillas), it might inform the way species groupings are perceived for the fossil species (for instance, the way that teeth group for gorillas on a principal components plot might provide some information as to how to assess the principal components output for groupings for the fossil species). If two teeth are distinct both in size and in shape, does this necessarily imply (as in the case of SK 6 and KNM-ER 992 as discussed above) that they are from a different species, or could one single species encompass such vastly different traits?

It is therefore vital that the "inputs" to all the analyses (the choice of placement of the landmarks used in the analyses) provide enough information to be able to assess the "outputs" (the charts, tables and statistical results from the analyses) in light of the above. Chapters Three and Four of this study therefore place a great deal of emphasis on both the inputs and the outputs.

CHAPTER THREE – MATERIALS AND METHODS

3.1 Rationale for the choice of skeletal element (lower first molars)

Teeth are the most abundant skeletal element in the hominin fossil record. While bone is subject to many taphonomic processes due to its organic composition, tooth enamel tends to be very well preserved due to its hardness.

Teeth are also ideal for study because they do not change in size from infancy to adulthood, so size variations due to ontogeny alone, that might add complexity to the interpretation of shape analyses in other skeletal elements (and which therefore tend to be "scaled out" of analyses so that shape alone can be assessed), are ruled out; in the case of teeth, size can actually be used diagnostically to differentiate between certain species. Indeed, as one researcher puts it, "When allometric effects are factored out, chimpanzee and bonobo molars are not morphometrically distinguishable" (Singleton et al. 2011). Thus, permanent teeth are unique in that no allowance needs to be made for ontological scaling, and **shape *and* size** can be factored into the analysis to assist with an appreciation of variability within and between species.

Other skeletal elements available for comparison are cranial and postcranial remains. In the latter instance, the Plio-Pleistocene specimen collection for postcranial remains is relatively rare, so there is not a great deal of material that can be directly compared in a quantitative way: geometric morphometric tests ideally require the placement of an exactly equal number of anatomical landmarks in homologous spots on each bone element for the analysis to be possible. Whenever one anatomical landmark site is absent from any single one of the bones being studied, this often rules out the

possibility of including that particular landmark site in all the other bones being compared, which is extremely problematic when the sample is small to begin with. Allowance can be made in many cases for missing landmarks, usually by imputing their position, but when the sample is already sparse and damage or fragmentation is in different locations between specimens, even with allowances made, the available specimens render significantly fewer homologous landmark points than do collections of skeletal elements with more specimens available. Craniodental comparisons are therefore currently a preferred target for providing adequate samples for comparative studies which aim to distinguish measurable characteristics that could be diagnostic between species.

With respect to cranial remains, a great deal of attention has already been placed on these (Braun et al. 2004; Lockwood 1999; Lockwood & Tobias 2002; Smith & Grine 2008; Lordkipanidze et al. 2013) and it is hoped that this present study, which focuses on dental elements, will add new information to supplement the cranial data to provide further quantitative data to test hypotheses of species variability and other related questions. Teeth, by themselves, do not provide the basis for alpha taxonomy. However, if a landmarking model is developed to provide a quantitative dataset for the size and shape of the crown as well as the comparative cusp arrangements that can be diagnostic between different species, if successful, it can be used diagnostically to bolster a conclusion made on the basis of studies from the remainder of the skeletal elements or from other evidence.

As explained in 1.6.1.3 above, one of the reasons for limiting the scope of the study to encompass lower first molars of African Plio-Pleistocene hominins (and therefore the

size of the comparative sample of extant primate species) is that most of the fossil specimens selected for the study, including several of the holotypes ("type specimens") of the fossil species included for analysis had at least their lower first molars present but many did not have second molars present. Since the holotypes represent each species as a whole, in the absence of the complete set of specimens available from the fossil record to represent each species being studied, the holotype can at least act as a guide for comparisons of specimens selected for the study, to ascertain whether these do group together around the holotype of the species in a shape and/or size-and-shape analysis. The lower first molar was the best represented molar to serve for a preliminary, exploratory comparative study. Priority was given to specimens that had left and right antimeres present, to gauge the extent to which lower first molars might differ at the intra-specimen level, thus providing additional information when comparing specimens within presumed species and between presumed species.

In light of the exploratory nature of this study, the sample sizes and the choice of lower first molars were deemed to be adequate, a) to test the diagnostic balance of information forming the basis of the inputs into the landmark model experiments; b) to assess the usefulness of the analytical methods employed for the study and c) to go some way towards testing the hypotheses of the study (with the caveat that lower first molars, by themselves, do not determine taxonomic assessments).

Despite the limitations of the sample size, in the case of the particular teeth forming part of the study, it should be possible to identify individual cases, should such exist, that repeatedly fail to group with their currently allocated species groups (or at the very least, fail to group with the holotypes for their currently allocated species groups) and

to ask questions about species variability, sexual dimorphism, and whether any of these individual specimens might be identified for further study.

3.2 Materials

3.2.1 Extant species

3.2.1.1 Modern Humans (MH, *Homo sapiens*)

Photographs were taken of the occlusal views of the left and right sides of the mandibles of nineteen female and nineteen male cadaver specimens from the Raymond A. Dart Collection of Human Skeletons at the University of the Witwatersrand, Johannesburg, South Africa.

Specimens were selected randomly on the following basis:

- Dentition to be as complete as possible so that antimeres would be present
- Dentition to be as unworn as possible
- Dentition with all post-canine dentition erupted to be selected if available*
- Equal numbers of males and females per population group
- Ages of the paired males and females to be closely matched if possible
- As many population groups as possible to be chosen to represent a certain level of diversity, mainly limited to groups that are present in sub-Saharan Africa today**.

* Although only first molars were selected for the study, a full dental arcade is advisable in order to be optimally reassured as to the orientation of the mesiodistal axis of the

dental arcade and as to whether the first molar is well-aligned within the arcade. In the case of this particular study, where teeth are required to be centred mathematically using the mesiodistal-buccolingual diameter intersection (in the absence of anatomically homologous structures visible on all of the teeth in the study due to differential wear and damage between specimens), it is absolutely vital that no significant errors are made when aligning the mesiodistal axis during image processing. The central reference point for the placement of perimeter landmarks depends on the repeatability of locating the intersection between the two diameters, so the presence of all post-canine teeth, if available, assists with the alignment procedures and will render the study itself repeatable and testable.

**The scope of this study did not allow for original data collection (i.e. occlusal photography) to be conducted worldwide for all populations of modern *Homo sapiens*, to include megadonts (for instance, from Australia) and population groups with very small molars (such as those from Egypt and the Near East) which should reflect the whole range of human lower first molar diversity (Harris & Lease 2005; Larsen 1995; Scott & Turner 1997), although a European sample was included to represent some of the smallest teeth worldwide. However, much of the extremely high range of variability in human dentition is considered to have occurred only recently (particularly in the last 100000 years, escalating as a result of the migration of modern humans around the world and more recently, since the Neolithic period and the introduction of farming and cooking (Brace 1979; Brace et al. 1987; Brace et al. 1993; Pinhasi et al. 2008; Emes et al. 2011), which is accompanied by recent accelerations in genetic adaptive mutations (Dempsey & Townsend 2001; Hawks et al. 2007; Williamson et al. 2007; Gómez-Robles et al. 2013)). Just how much of this variability in modern human dentition should be

included in the study, since it is intended to be used in comparisons with geographically limited species known to have utilised only certain types of primitive dietary sources (C_3 and/or C_4 vegetation in the cases of African Plio-Pleistocene fossil hominins and similar food sources selectively in the cases of gorillas, chimpanzees and bonobos, whose populations are relatively small and limited geographically compared with those of modern humans, and whose diets do not contain modern starches and grains or processed foods – see, for example, Wolpoff 1973; Teaford & Ungar 2000; Ungar 2004; Grine et al. 2006; Estebaranz et al. 2009; Rabenold & Pearson 2011; Cerling et al. 2011; Lee-Thorp 2011; Grine et al. 2012; Spoonheimer 2013) is a very complex issue; unfortunately it is not possible to do this subject justice, except peripherally, within the scope of this study. Even the limited number of specimens included in this study show extreme variability (the European molars were included as representative of some of the smallest molars in the world (Kieser 1990) and the largest of the sub-Saharan molars sampled for the study were included to represent diversity, albeit on a local level (many sub-Saharan African populations falling into the "megadont" category, according to Brace et al. (1993: page 18)), thus even in analyses that utilised a sub-set of the final 38 specimens selected, individuals were able to be selected to represent the smallest, largest, narrowest and widest teeth sampled, to reflect diversity).

Most of the specimens that had been selected at random from the catalogue list were edentulous or had very damaged or missing teeth. In many cases, both a male and a female with usable dentition (unworn or undamaged enough to be able to distinguish the five cusp intersections along the perimeter of the occlusal view of the crown enamel) could not be found for some specific population groups. Other population groups had plentiful specimens with good dentition and in certain cases, two or more

males and two or more females were chosen from these. The final selection of the 38 specimens selected for the study are set out in Table 3.1:

Table 3.1 Materials: Modern human specimens (*Homo sapiens)* included in the study

Catalogue Number Dart Collection	Population group (as stated in the catalogue)	Male or Female	Age at death
Females:			
A2179	European	F	19
A863	Xhosa (S. Africa)	F	20
A935	Rolong (Botswana)	F	20
A381	Zulu (S. Africa)	F	29
A1319	Zulu (S. Africa)	F	20
A4035	"South African Negro"	F	22
A1263	Sotho (S. Africa)	F	18
A900	Swazi (S. Africa or Swaziland)	F	26
A263	Shangaan (S. Africa)	F	30
A1903	Venda (S. Africa)	F	24
A1954	Ndebele (S. Africa)	F	30
A1483	Tswana (S. Africa or Botswana)	F	19
A3319	Mixed ("Coloured")	F	33
A3607	Mixed ("Coloured")	F	40
A84	Amafengu (S. Africa)	F	38
A3894	Not Stated ("Black" S. African)	F	35
A3469	Mixed ("Coloured")	F	25
A27	San ("Bushman" – S. Africa)	F	N/A
A320	San ("Bushman" – S. Africa)	F	N/A
Males:			
A3109	European	M	15
A973	Xhosa (S. Africa)	M	18
A1860	Rolong (Botswana)	M	22
A3360	Zulu (S. Africa)	M	47
A3770	Zulu (S. Africa)	M	23
A4037	"South African Negro"	M	24
A691	Sotho (S. Africa)	M	18
A1570	Swazi (S. Africa or Swaziland)	M	32
A924	Shangaan (S. Africa)	M	30
A821	Venda (S. Africa)	M	25
A927	Ndebele (S. Africa)	M	37
A1264	Tswana (S. Africa or Botswana)	M	23
A2093	Mixed ("Coloured")	M	23
A3421	Mixed ("Coloured")	M	60
A861	Amafengu (S. Africa)	M	34
A3906	Not Stated ("Black" S. African)	M	40
A3386	Mixed ("Coloured")	M	34
A173	San ("Bushman" – S. Africa)	M	N/A
A28	San ("Bushman" – S. Africa)	M	N/A

All genders, ages and population group data are presumed to have been recorded correctly in the collection, as they have been taken from cadavers rather than "in situ" skeleton remains. Population groups were recorded, until the 1990s, from the Death Certificate of the cadavers, but from then onwards, these were not recorded, other than to stipulate "White" or "S.A.N." ("South African Negro" or "Black" South African) (Dayal et al. 2009).

3.2.1.2 Gorillas (*Gorilla gorilla gorilla*), Chimpanzees (*Pan troglodytes schweinfurthii*) and Bonobos (*Pan paniscus*)

Photographs were taken of the occlusal views of specimens of gorillas, chimpanzees and bonobos from the collection held in the Royal Museum for Central Africa, Tervuren, Belgium.

Specimens were selected randomly on the following basis:

- Dentition to be as complete as possible so that antimeres would be present
- Dentition to be as unworn as possible
- Dentition with all three molars erupted to be selected as far as possible (for the same reasons as discussed in paragraph 2.3.1.1 above)
- The gender of each specimen needed to be specified

A large number of specimens was photographed.

However, due to imbalances between males and females (particularly in the gorilla collection) and to the preponderance of badly damaged and worn first molars (particularly in the cases of gorillas and bonobos), the useable sample was eventually

very limited for the comparative study, as a result of which, ten specimens (providing twenty mandibular first molars for each species as all selected specimens had both antimeres present) of *Gorilla gorilla gorilla, Pan troglodytes schweinfurthii* and *Pan paniscus* were chosen. These are listed in Table 3.2.

Table 3.2 Materials: African ape specimens included in the comparative study

Species	RMCA (Tervuren) Catalogue number	Gender
Gorilla gorilla gorilla	7732M15	F
Gorilla gorilla gorilla	7732M8	F
Gorilla gorilla gorilla	7732M5	M
Gorilla gorilla gorilla	7318M3	F
Gorilla gorilla gorilla	7732M7	M
Gorilla gorilla gorilla	7732M6	M
Gorilla gorilla gorilla	7732M3	F
Gorilla gorilla gorilla	7732M2	M
Gorilla gorilla gorilla	7732M1	M
Gorilla gorilla gorilla	7556M2	F
Pan troglodytes schweinfurthii	91060M422	F
Pan troglodytes schweinfurthii	91060M414	M
Pan troglodytes schweinfurthii	91060M410	F
Pan troglodytes schweinfurthii	91060M406	F
Pan troglodytes schweinfurthii	83006M37	F
Pan troglodytes schweinfurthii	83006M32	F
Pan troglodytes schweinfurthii	83006M22	M
Pan troglodytes schweinfurthii	83006M21	M
Pan troglodytes schweinfurthii	83006M17	M
Pan troglodytes schweinfurthii	83006M15	M
Pan paniscus	84036M11	F
Pan paniscus	84036M03	M
Pan paniscus	29055	F
Pan paniscus	29053	M
Pan paniscus	29050	M
Pan paniscus	29027	F
Pan paniscus	29028	M
Pan paniscus	29026	F
Pan paniscus	13021	F
Pan paniscus	11354	M

In light of the preliminary nature of this study, this sample is adequate to provide information upon which to judge general trends of size and shape between species; as the scope of the project is enlarged in future (see 6.3), additional specimens from other collections might be added to increase the sample sizes, thus to confirm these initial findings.

3.2.2 Fossils

Photographs of original Plio-Pleistocene fossil dental specimens in collections housed in Johannesburg, Pretoria, Dar es Salaam and Nairobi were taken, and where original specimens were not available for certain species (namely, *Australopithecus afarensis*), photographs of casts were obtained. It was important that all images used in the study were captured in the same way, using the same equipment and protocols, so that accurate and uniform comparisons could be made. The sample size was limited to specimens in good condition to which access was granted. Further specimens are known to exist, but not all of these were made available during visits to collections around the world.

For the purposes of this study, specimens were chosen that had relatively undamaged lower first molars. Priority was given to holotypes and to specimens with left and right antimeres present.

3.2.2.1 A note on antimeres

There are a number of reasons for retaining antimeres, rather than opting to include either a right or a left molar for each specimen. Technical considerations included the

fact that as with all studies involving fossil specimens, sample size is limited, particularly for certain species. In this particular study, specimens with all five cusp arcs evident (or inferable, often confirmed from antimeres) were included, and some specimens for which photographs were obtained (e.g. in Kenya or Tanzania) had to be excluded due to damage in key locations on the crown enamel. This left some species groups in the study with such a small sample size that a decision to increase "*n*", even at the expense of possibly duplicating some of the phenotypic variability, was preferable to leaving out the antimere completely. Since antimeric differences are quite variable (some antimeres are almost identical, others are extremely different in size and shape when assessed in the occlusal view), not all antimeres represent close duplications of phenotypic variability.

Other rationales also held sway. A second technical reason was that those specimens for which only one lower first molar was present were not consistently left- or right-sided. If no regular pattern in size variation were to be expected between left and right antimeres, a random selection of either antimere for study in cases where both antimeres were present might be justified. However, it was felt that such an assumption could not necessarily be made until put to the test. Based on discussions with Dr Donald J Barnes (M. Dent; B.D.S, Dentistry), former lecturer at the University of the Witwatersrand Dental School, prosthodontists are familiar with the tendency in modern *Homo sapiens* for left antimeres to be generally smaller than right antimeres (Kieser 1990) (possibly due to laterality: the tendency in modern *Homo sapiens* to be predominantly right-handed). It would therefore be suspected that lower right first molars in the modern *Homo sapiens* sample of the study, (and therefore potentially in

fossil sample as well), will tend to be relatively wider ("squarer") than lower left first molars. It was decided to see if the fossil sample followed a similar pattern.

Another reason for including antimeres was to test the landmark model and the analyses used, to see if either one of two differently-shaped antimeres (such as the ones depicted below) might find themselves grouped with other species. Antimeres may often have different occlusal outlines or relative size differences (longer/narrower) but from observation, they do not seem to have completely different cusp patterns, such that they would be grouped into different species based on cusp pattern arrangement as well as shape differences. This "out of group" confusion might occur in studies based purely on MD:BL ratios alone, but even if differential interstitial wear between antimeres might add to MD:BL ratio variability, once the number of measurements per tooth increases, as landmarks are strategically added and cusp arrangements are taken into consideration as well as overall size and relative width of the tooth, the nuances of each species' diagnostic crown morphology ought to rule out the possibility of one antimere being classified into one species and the other into another species, provided that the landmark model is capturing these diagnostic features correctly. As more sophisticated shape analyses (or "size-and-shape" analyses) are carried out, the assumption would be that either both antimeres (if present) will appear to be "misclassified", or neither will. The use of different methodologies further to these shape/size-and-shape analyses (such as a discriminant function analysis based on several principal components axes) should also confirm or falsify this result.

To take an example, in the case of AL 266-1, the left and the right antimeres are differently proportioned, based on the occlusal views of the teeth as they are aligned in

the dental arch (alignment additionally verified by the position of the distal fovea, the buccolingual groove angle (equal for both antimeres) and the rectilinear arrangement of the perimeters of the buccal cusps, parallel to the mesiodistal axis) as shown in Figure 3.1:

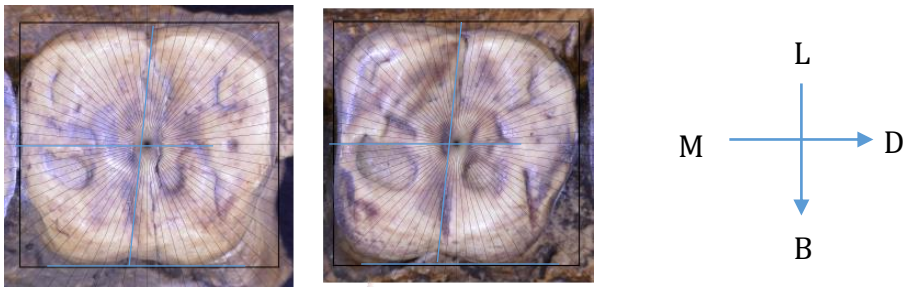

Figure 3.1: Antimeres of AL266-1 (scaled images) **AL 266-1 (L) is pictured to the left; AL 266-1 (Rm) is pictured to the right. The perimeter shapes of the teeth are visibly different in the occlusal view but the cusp arrangements are similar.**

With almost identical (maximum) buccolingual diameters, the (uncorrected) mesiodistal diameters (see 3.4.4 for a definition of these diameters) are, however, very different in the occlusal crown view, with the left tooth being longer along the mesiodistal axis than the right tooth. Differential wear (not only interstitial but on the surface and margins of the crown) is one factor in this instance, but from the occlusal view, the left antimere appears fundamentally differently-shaped from the right. The left tooth appears wider along the lingual margin than along the buccal margin (forming a "heart" shape), whereas the right antimere appears wider medially than distally, with the very pronounced metaconid that is characteristic of the species, typified by LH 4, the holotype. Nevertheless, although these teeth might not be expected to group right next to each other on a shape-size analysis (the left antimere will be *relatively* narrower but larger in area than the right tooth, which is almost square in aspect), both teeth retain diagnostic features of the *Australopithecus afarensis* species (see 2.3.1). For instance, the angle between the two mesial cusps and the talonid (the distal portion of the crown) is the same for both teeth (almost perpendicular to the mesiodistal axis, which, as discussed, is a

distinguishing feature of the species). Although they will not be expected to group directly together on linear and shape analyses (being different in computed crown area and in overall perimeter shape), it is expected that they would still group together broadly as members of the same species group due to the similarity of their cusp arrangements and overall morphology. If they do not, the adequacy of the landmark model and/or the analyses conducted should be brought into question. If they still group together in analyses taking all nuances of shape as well as size into consideration (particularly on a discriminant function analysis based on several principal components axes), they can be considered to represent part of the range of variability of tooth shape and size for the group as a whole.

3.2.2.2 Final selection of fossil hominin first mandibular molars

The final selection consisted of 36 fossil first mandibular molars from seven taxa as set out in Table 3.3 below:

Table 3.3 Fossil lower first molar specimens included in the comparative study

Specimen number	Side	Marker used	Current taxonomic designation	Location	Comments	Geological Paper **	Geological Age (Ma) (latest est.)	Reference for date
AL 145-35	L	♦	*A. afarensis*	Univ. Wits cast collection	Cast	1	3.35	(Grine et al. 2006)
AL 128-23	R	♦	*A. afarensis*	Univ. Wits cast collection	Cast	1	3.25	(Grine et al. 2006)
AL 266-1	L	♦	*A. afarensis*	Univ. Wits cast collection	Cast	1	3.2	(Grine et al. 2006)
AL 266-1	R	♦	*A. afarensis*	Univ. Wits cast collection	Cast	1	3.2	(Grine et al. 2006)
AL 288-1	R	♦	*A. afarensis*	Univ. Wits cast collection	Cast	2	3.18	(Grine et al. 2006)
AL 333-W60	L	♦	*A. afarensis*	Univ. Wits cast collection	Cast	3	3.2	(Grine et al. 2006)
LH 2	R	♦	*A. afarensis*	National Museums of Kenya, Nairobi, (cast)	Cast	4,5	3.77	(Wood 2011)
LH 4	L	♦	*A. afarensis*	National Museum, Dar es Salaam	Holotype – original	4,5	3.77	(Wood 2011)
LH 4	R	♦	*A. afarensis*	National Museum, Dar es Salaam	Holotype – original	4,5	3.77	(Wood 2011)
MLD 2	L	▲	*A. africanus*	Univ. Witwatersrand Medical School	Original	6	2.8	(Wood 2011)
MLD 2	R	▲	*A. africanus*	Univ. Witwatersrand Medical School	Original	6	2.8	(Wood 2011)
Sts 52b	R	▲	*A. africanus*	Ditsong National Museum, Pretoria	Original	7	2.3	(Pickering & Kramers 2010)
Taung 1 (U.W. 1-1)	L	▲	*A. africanus*	Univ. Witwatersrand Medical School	Holotype – original	8	2.7	(Wood 2011)
Taung 1 (U.W. 1-1)	R	▲	*A. africanus*	Univ. Witwatersrand Medical School	Holotype – original	8	2.7	(Wood 2011)
OH 22	R	●	*H. erectus*	National Museum, Dar es Salaam	Original	9	0.875	(Wood 2011)
KNM-ER 806c	L	●	*H. erectus*	National Museums of Kenya, Nairobi	Original	10	1.49	(Wood 1991)
KNM-ER 820	L	●	*H. erectus*	National Museums of Kenya, Nairobi	Original	10	1.6	(Wood 1991)
KNM-ER 820	R	●	*H. erectus*	National Museums of Kenya, Nairobi	Original	10	1.6	(Wood 1991)
KNM-ER 992	L	●	*H. erectus*	National Museums of Kenya, Nairobi	Holotype –*Homo ergaster (African Homo erectus*)* original	11	1.49	(Groves & Mazak 1975); (Wood 1991)

KNM-ER 992	R	●	*H. erectus*	National Museums of Kenya, Nairobi	Holotype –*Homo ergaster (African Homo erectus*)* original	11	1.49	(Groves & Mazak 1975); (Wood 1991)
OH 7	L	●	*H. habilis*	National Museum, Dar es Salaam	Holotype – original	12,13	1.84	(Wood 2011)
OH 7	R	●	*H. habilis*	National Museum, Dar es Salaam	Holotype – original	12,13	1.84	(Wood 2011)
OH 16	R	●	*H. habilis*	National Museum, Dar es Salaam	Original	14	1.74	(Wood 2011)
KNM-ER 1802	L	●	*H. rudolfensis*	National Museums of Kenya, Nairobi	Original	15	1.89	(Wood 1991)
KNM-ER 1802	R	●	*H. rudolfensis*	National Museums of Kenya, Nairobi	Original	15	1.89	(Wood 1991)
KNM-ER 15930	L	■	*P. boisei*	National Museums of Kenya, Nairobi	Original	16	1.78	(Wood 1991)
Peninj 1	L	■	*P. boisei*	National Museum, Dar es Salaam	Mandibular proxy for holotype (OH5)	17	1.4	(Wood 2011)
Peninj 1	R	■	*P. boisei*	National Museum, Dar es Salaam	Mandibular proxy for holotype (OH5)	17	1.4	(Wood 2011)
SK 6	L	■	*P. robustus*	Ditsong National Museum, Pretoria	Original	18	1.75	(Wood 2011)
SK 6	R	■	*P. robustus*	Ditsong National Museum, Pretoria	Original	18	1.75	(Wood 2011)
SK 23	L	■	*P. robustus*	Ditsong National Museum, Pretoria	Original	18	1.75	(Wood 2011)
SK 23	R	■	*P. robustus*	Ditsong National Museum, Pretoria	Original	18	1.75	(Wood 2011)
SK 63	L	■	*P. robustus*	Ditsong National Museum, Pretoria	Original	19	1.75	(Wood 2011)
SK 63	R	■	*P. robustus*	Ditsong National Museum, Pretoria	Original	19	1.75	(Wood 2011)
SKW 5	R	■	*P. robustus*	Ditsong National Museum, Pretoria	Original	20	1.75	(Wood 2011)
TM 1517	R	■	*P. robustus*	Ditsong National Museum, Pretoria	Holotype – original	21	1.75	(Wood 2011)

* Homo ergaster is the African Homo erectus.

**Geological Papers:

1) (White & Johanson 1982)
2) (Johanson & Taieb 1976)
3) (Kimbel et al. 1982)
4) (Leakey et al. 1976)
5) (White 1977)
6) (Dart 1948)
7) (Broom et al. 1950)
8) (Dart 1925)
9) (Rightmire 1980)
10) (Leakey 1972)
11) (Leakey & Wood 1973)
12) (Leakey 1960)
13) (Leakey 1961)

14) (Leakey et al. 1964)
15) (Day et al. 1976)
16) (Leakey & Walker 1988)
17) (Tobias 1965)
18) (Broom & Robinson 1952)
19) (Robinson 1956)
20) (Grine & Daegling 1993)
21) (Broom 1938)

3.3 Data collection – 2D photography

3.3.1 Rationale for sampling by means of two-dimensional photography

A method of data collection needed to be chosen that would satisfy the following criteria:

- non-invasive, non-destructive data collection;

- ability to capture data from as many specimens as possible in any one collection, within the shortest time frame, ideally at the site where the collection is housed for ease of accessibility;

- reasonably inexpensive data collection method;

- ability to collect data uniformly using a standardised methodology that can be repeated from collection to collection.

Two-dimensional photography of the occlusal views of molars satisfied all of these criteria. Whilst other methods may be more technologically advanced, photography remains an extremely useful data collection method in cases where the maximisation of sample sizes (such as in the fossil record) is important. Three-dimensional micro-CT scanning and similar techniques are clearly more up-to-date, information-rich methods, but these may require individual samples to be transported away from the museums or facilities that house the collections, and procedures may have to be followed that

involve sometimes lengthy applications, permit procedures, processing times and often increased costs for each individual molar being processed. Photography remains one of the most accessible methods of data-collection worldwide.

3.3.2 Data collection: photographic protocols and methodology

Strict protocols were followed for the collection of occlusal dental photographs at each collection site, to ensure uniformity of data and minimisation of errors due to artefacts from the photographic process itself.

3.3.2.1 Equipment and photographic protocols

All photographs were taken using a Nikon D3200 digital SLR 24-megapixel camera with a Nikkor 18-55mm lens. This camera has a live view screen for ease of focusing when mounted on a tripod. The camera and a tripod were purchased from personal funds, specifically for this project. An adjustable scale bar that allowed for easy mounting at the level of the crown surface at any angle (x, y or z planes) was designed and built for the project. For detailed uniform photographic protocols followed for each shot, please refer to Appendix 2.

3.3.2.2 Parallax error avoidance

In order to avoid parallax errors, the tooth being photographed was centred in the frame of the photograph at sufficient distance so as not to allow any of the area of focus (the tooth or the scale bar) to be near the edges of the photograph (Busch 2006: 343-344). The scale bar was positioned as close to the tooth as possible in the same plane as

the crown surface, with both the tooth and the scale bar aligned with the mesiodistal axis (where possible). If the crown surface was positioned at approximately 12cm beneath the lens, at full zoom (equivalent to a 55mm lens), a medium to large tooth (e.g. *Paranthropus* or female *Gorilla*) would take up the central $1/25^{th}$ of the frame of the photograph. Since a 55mm lens does not produce any wide angle (fish-eye) effect, and given the high definition of the photographs (24 megapixels), the crown surface of the tooth would receive the optimal focus of the shot and would therefore lend itself well to cropping and enlarging at a later stage in the process.

3.3.2.3 Errors of tilt

Whilst parallax errors could be effectively ruled out as a result of the equipment used and the distance between lens and subject in the shots taken, the horizontal alignment of each tooth might be subject to observer error. Various methods can be used to ensure that the cervical plane of the crown is kept horizontal: a spirit level across the dental arch crown surface can be used in cases where teeth are all in an even plane, with crown surfaces parallel to the cervical plane. These cases are rare, however, because tooth wear is rarely along a horizontal plane, particularly along the buccolingual axis. Even if a spirit level small enough to place on each tooth individually could be found, it would still not help in the levelling of the tooth due to this differential wear. Another way to level the cervical plane of the tooth would be to immerse the tooth in sand that had itself been levelled, so that the cervical plane lies at the surface of the sand. However, when photographing very delicate fossil specimens, there is a very real danger of damaging the tooth, the dental arch or the cranial remains of a specimen during the process of immersing the specimen in sand or when trying to adjust the

specimen to make it level. To avoid damaging delicate specimens, a mount was ideally pre-prepared, using a cast of the specimen, embedded in a very malleable foam material (protected by a plastic film to avoid residues from the foam being left on the specimen). This kind of pre-preparation allowed for good pre-levelling of the cast's occlusal surface and served to protect the actual specimen during handling. However, casts were not always available and such precautions and preparations were not always possible.

Ultimately, levelling along the mesiodistal axis can in principle be ensured by using a spirit level held or propped up in line with the cervical plane, but in practice, levelling across the buccolingual axis is more effectively achieved by careful alignment by eye from above the tooth through the viewfinder or via the live screen of the camera of both side walls of the tooth, so that they equally match each other for tilt.

In view of the potential for observer error of tilt (particularly buccolingually), it was decided to apply 3D imaging software to quantify this potential error. Coefficients of correlation between pairwise sets of landmark distances on a single 3D tooth image, tilted at regular intervals using Amira software with 2D snapshots taken at increasing degrees of tilt buccolingually were calculated. A particularly pristine (unworn) tooth was chosen for this exercise (in which case any change of tilt would be further exaggerated by parallax errors due to the slope of the cusp peaks, so this would be equivalent to the "worst case scenario" for tilt error bars), and the same landmark arrangements were measured at 2 degree tilt intervals from -10˚to +10˚, with each set of data being compared to the 0˚ (fully horizontal) untilted view. These 10 sets of correlation measurements were then compared to measurements taken from the same arrangement of landmark placements situated on a different tooth completely. The

results, presented in Figure 3.2, showed that tilt does not affect the outputs of a shape analysis very significantly at angles of tilt up to 4 degrees either way. When an unworn tooth is tilted at + 2 degrees or at – 2 degrees, the correlation coefficient of both sets of data against the horizontal was 0.99, indicating a strong correlation between the outputs at this degree of tilt against the horizontal. The correlation coefficient was still above 0.95 at the +/- 4˚ tilt level).

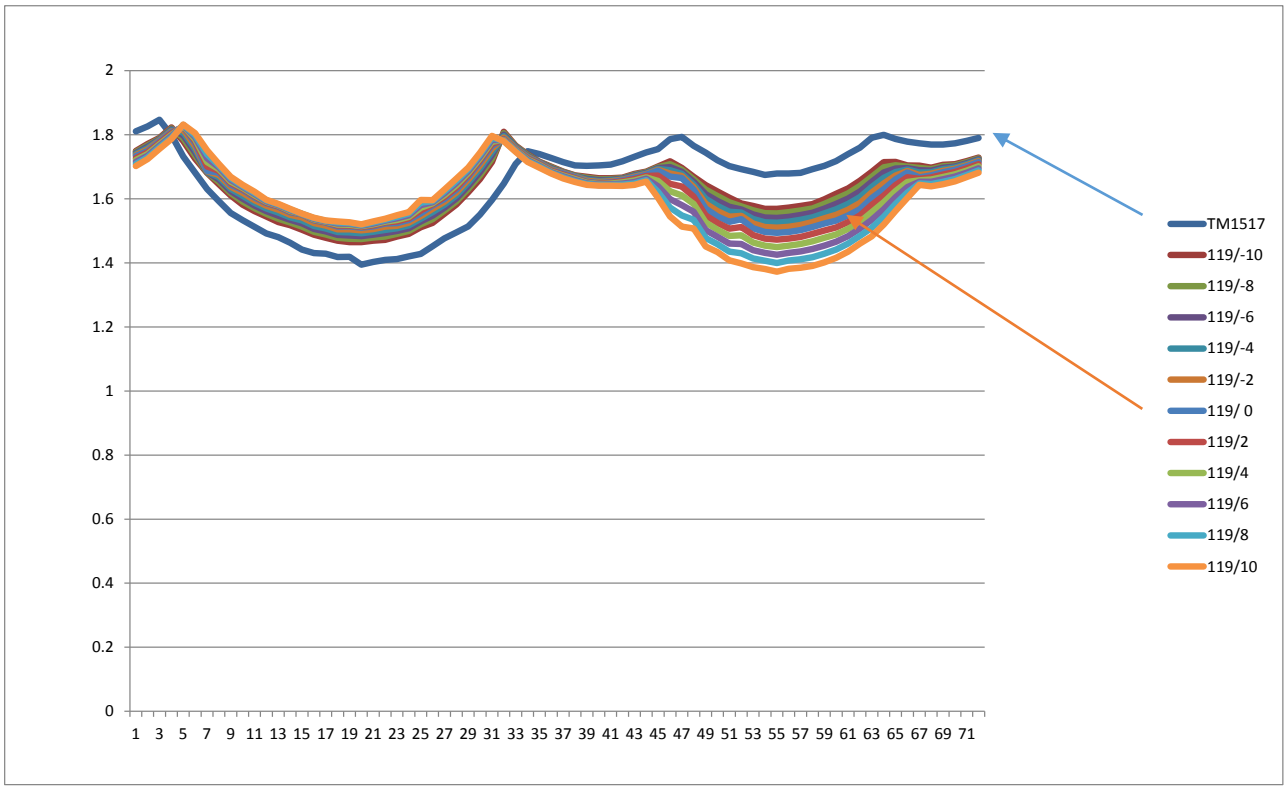

Figure 3.2 Landmark distances from the centre of 11 views of a pristine tooth at varying degrees of tilt compared to the same calculation for a different tooth entirely.

In this figure, "119" represents a 6 year-old human tooth from a collection of 3D tooth scans held at Toulouse University (with zero degrees of tilt being represented by the cobalt blue line right in the centre of the 119 series), and "TM1517" – the dark blue line with the very distinct contour, is a fossil tooth. Note that for the "119" series, the tan-coloured and the maroon-coloured lines (-2 degrees and +2 degrees respectively) on either side of the cobalt line (0 degrees) are highly correlated to the cobalt 0 degree line, so that up to 2 degrees of tilt would render very similar measurements in any statistical or geometric morphometric analysis. The dark blue line represented by tooth TM1517 at zero degrees of tilt is highly uncorrelated to the cobalt line (tooth 119 at zero degrees), the contour of its respective landmarks following a very distinct pattern.

(Acknowledgements: Professor José Braga – University of Toulouse, for access to the 3D images and to Jean Dumoncel – University of Toulouse, for training on the Amira software utilised in this exercise.)

To estimate a possible "normal" degree of observer error that might be incurred by the same observer in levelling teeth successively on separate occasions, three different 2D photographs of the same tooth (the M_1 of the holotype of *Paranthropus robustus,* TM 1517) were then embedded into the 3D image of the same tooth using Amira 3D imaging software, and their angles of tilt were compared. There was virtually no difference (0.014˚ along the x-axis, 0.107˚ along the y-axis and 0.098˚along the z-axis) between angle of tilt of two of the shots, both taken from directly above the tooth on two separate occasions, and there was a tilt of less than 2˚ in each direction in the case of a shot focussed on the adjacent tooth (i.e., when the focus was necessarily not directed toward that particular tooth). The coefficient of correlation (R^2) for pairwise landmark measurements in the same tooth at a 2˚ tilt (against the level) was 0.99. Thus it can be reasonably assumed that provided that due care and attention has been taken in levelling each tooth before taking the photograph, measurement errors caused by tilt will in all likelihood be limited to less than 1% and would certainly be very unlikely to be as much as 5% (equivalent to more than 4˚ of tilt in either direction, which would seem improbable, since already at 4˚, the sidewall tilt is clearly visible from above, and is easily avoidable). In a worn tooth (as in the case of the majority of the fossil teeth analysed) these potential tilt error bars will be lower, since the flatter the surface, the smaller the additional parallax error as the tooth is tilted (landmarks on a flat surface remain more equidistant from each other as the tooth is tilted, whereas landmarks on steep cusp surfaces move differentially apart as the tooth is tilted).

The following figures (Figure 3.3 and Figure 3.4) illustrate the process used to calculate error bars, using Amira 3D software:

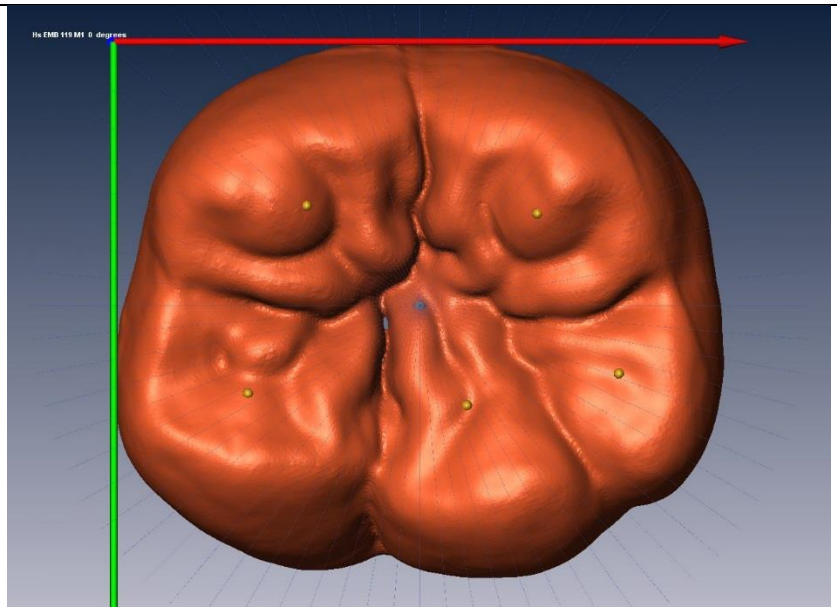

Zero degrees from horizontal – side wall (buccolingual) slopes observably even

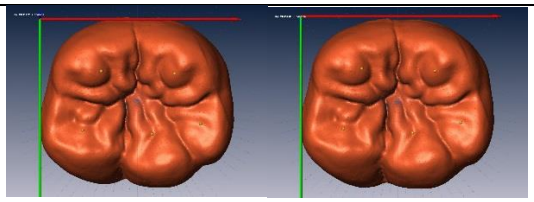

+/- 2˚- acceptable tilt (1% error each way vs. the horizontal, on an unworn tooth)

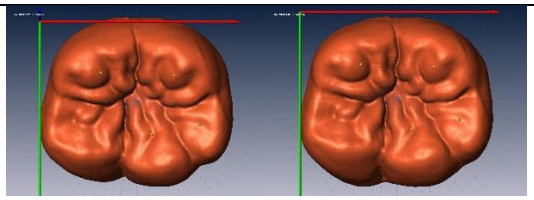

+/- 4˚ - visible, avoidable tilt (<5% error vs. the horizontal, on an unworn tooth)

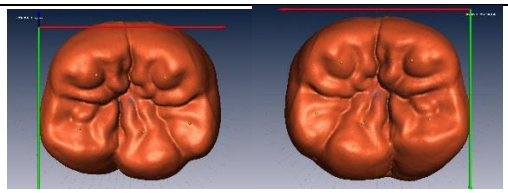

+/- 6˚- unacceptable, fully avoidable tilt

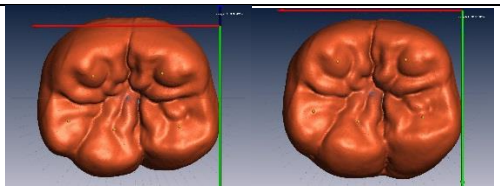

+/- 8˚- very unacceptable, fully avoidable tilt

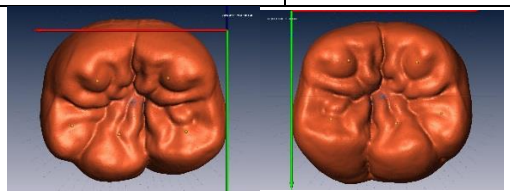

+/- 10˚- extremely unacceptable, fully avoidable tilt

Figure 3.3 2D snapshots of 3D unworn tooth images for the calculation of tilt error bars.

Figure 3.4 illustrates how, by using 3D software, it is possible to calculate tilt differences between various existing 2D photographs.

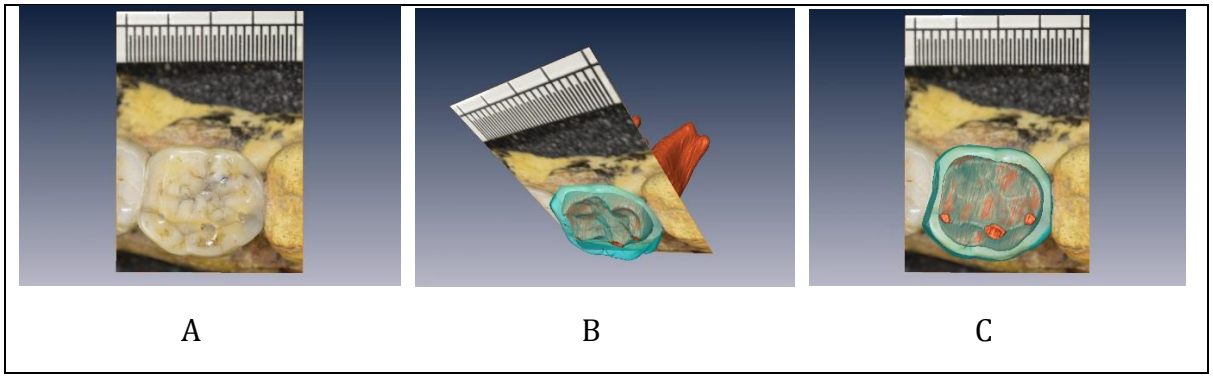

Figure 3.4 Calculation of the angle of tilt for existing 2D photographs. Using Amira 3D imaging software, three similar 2D photographs (including the photograph figuring in A above) taken on separate occasions (two from directly vertically above the tooth and one from directly above the adjacent tooth) were individually inserted into slices of the 3D image of the same tooth (B – enamel in blue, dentine in red), so that the 3D image was perfectly superimposed over the 2D perimeter (C). The angle of tilt of the 3D image was then calculated for each image and compared for differences.

3.4 Landmark placement optimisation ("Landmark Model")

3.4.1 The importance of optimising landmark placements

This study seeks to compare African Plio-Pleistocene fossil hominin molars, to try to establish whether, based on crown enamel morphology alone, species groups can be distinguished using geometric morphometric and statistical techniques, and whether anomalous specimens exist within the sample analysed that fail to group with the holotypes for their presumed species.

All analyses rely on the quality of both inputs and outputs for meaningful results to be obtained. In the case of the inputs, this study places a large emphasis on an optimal landmark placement arrangement (the "landmark model"), whereby the main diagnostic features of hominin lower first molars can be identified by the landmarks and whereby the number of landmarks chosen for each feature will be in an optimal

balance with other features; in sum, will be able to maximise the information in a correctly-weighted manner for the analyses to interpret.

Bearing in mind that fossil molars are generally very worn and often damaged, with very little in the way of anatomically homologous marker points (such as cusp peaks or fovea) on the surface of many of the specimens, a model needed to be designed to amplify the information available about the tooth from a limited number of anatomical landmark features.

3.4.2 Prelude to landmarking – image processing

For the study of mandibular first molars, all images of right mandibles were mirrored and rotated until they were oriented in the same way as the images of the left mandibles (mesial margin of the M_1 to the left of the image, distal margin to the right, lingual side at the top of the image and buccal side to the bottom of the image).

All images were then rotated using Adobe Illustrator and a large, high definition screen purposely purchased for this study to ensure accuracy, so that the mesiodistal axis of each M_1 was oriented exactly horizontally in the image (to assist with the alignment of the mesiodistal axis, which is critical to the calculation of the location of the MD:BL intersection reference point on each tooth, a horizontal line was overlain in a separate "layer" over the dental arch in the image in Adobe Illustrator (the image, centred on the M1 being rotated until the alignment was exactly horizontal in the frame of the image) and this horizontal line was then subsequently deleted or hidden from the final

.PNG/JPG file produced). A rectangle was then superimposed over the image as a kind of "bounding box" to create a boundary for the mesial, distal, buccal and lingual maximal extents. This rectangle then serves the dual purpose of providing mesiodistal and buccolingual measurements for the teeth, based on the visible occlusal outline, and of calculating the MD:BL intersection at the centre of the tooth, which, in the absence on all of the specimens of a recognisable homologous landmark such as a central fovea, would form the repeatable, centrally located point from which the "pseudo-landmarks" or "constructed landmarks" (Type III landmarks) would radiate evenly around the perimeter edge of the tooth. The next step in the process was to overlay a fan image with lines radiating from the MD:BL intersection reference point. This was achieved in Adobe Illustrator (Figure 3.5), using the software's inbuilt guide to locate the centre of the "bounding box", but other software or methodologies can be used.

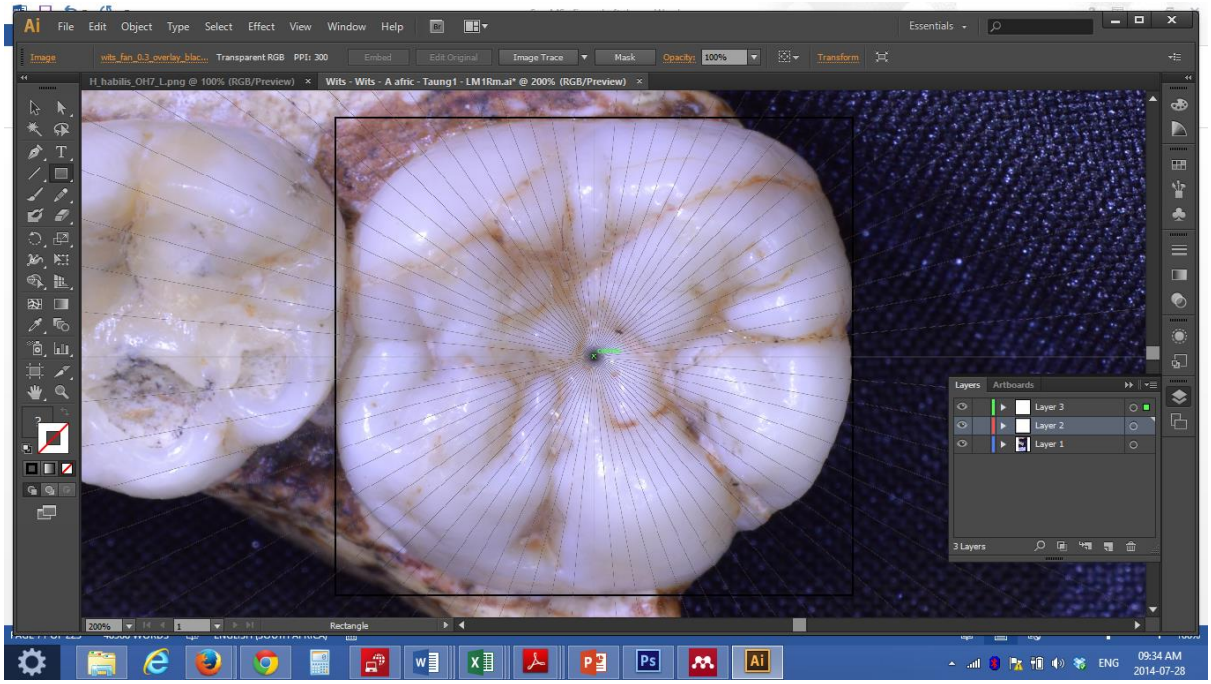

Figure 3.5 Placement of a "bounding box" and a fan overlay on images

3.4.3 Observer error for the placement of the central MD:BL intersection reference point (Landmark #1)

Due to the importance of the placement of the central landmark (the MD-BL intersection point), an inter- and intra-observer test was carried out to ascertain the accuracy of locating the central point of the teeth. One tooth was selected at random from each of the four extant species groups and a further tooth from the fossil sample. For each of the five teeth, two observers used Adobe Illustrator as described above to construct a "bounding box" around each tooth, equivalent to the (maximum) buccolingual and the (uncorrected) mesiodistal diameters as observed from the occlusal crown image. The centre point of the bounding box (equivalent to the MD:BL intersection) was then noted in terms of its x and y coordinates in mm on the image (the "centre" of the bounding box being automatically located by the software as shown in Figure 3.6):

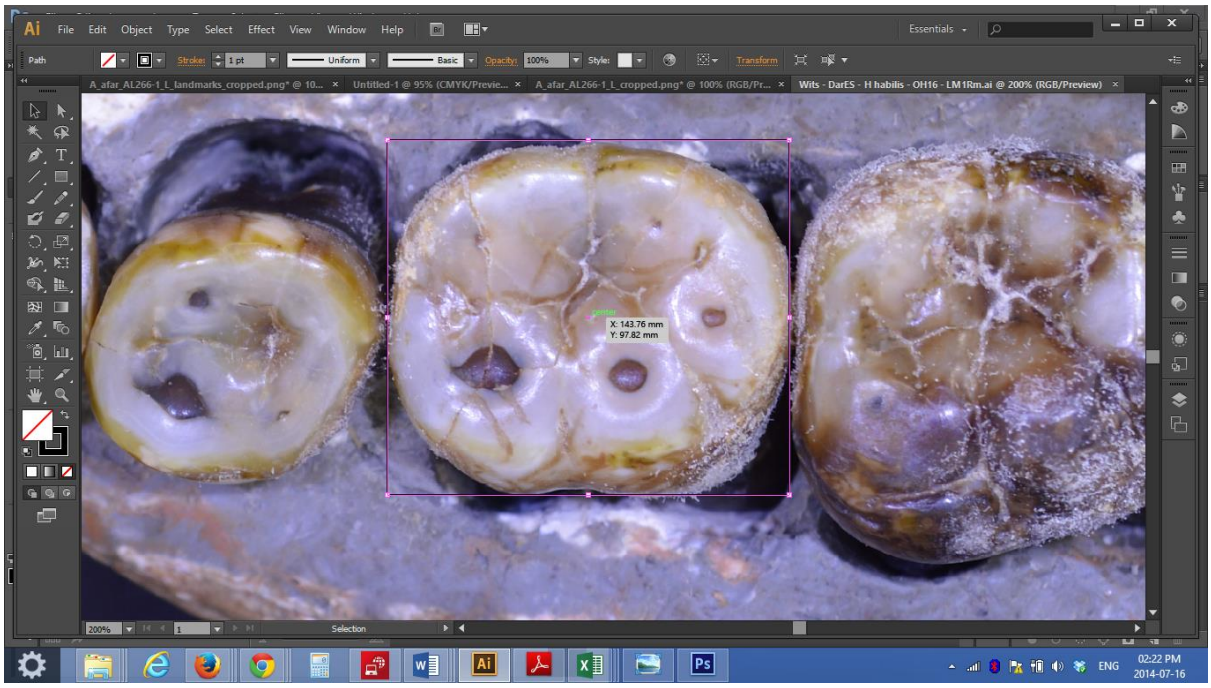

Figure 3.6 Observer error test for placement of central landmark. **Images are rotated until the mesiodistal axis is horizontal to the screen, a bounding box is placed around the tooth perimeter and the centre x and y coordinates of the bounding box are noted by two observers each on five separate occasions for five teeth.**

This process was repeated on five different occasions for each of the five teeth by both observers. The resultant 50 x and y coordinates (10 per specimen) were then plotted

on a graph and the average difference from the minimum x and y value in each instance was calculated. The results are presented in Figure 3.7 and Table 3.4 below.

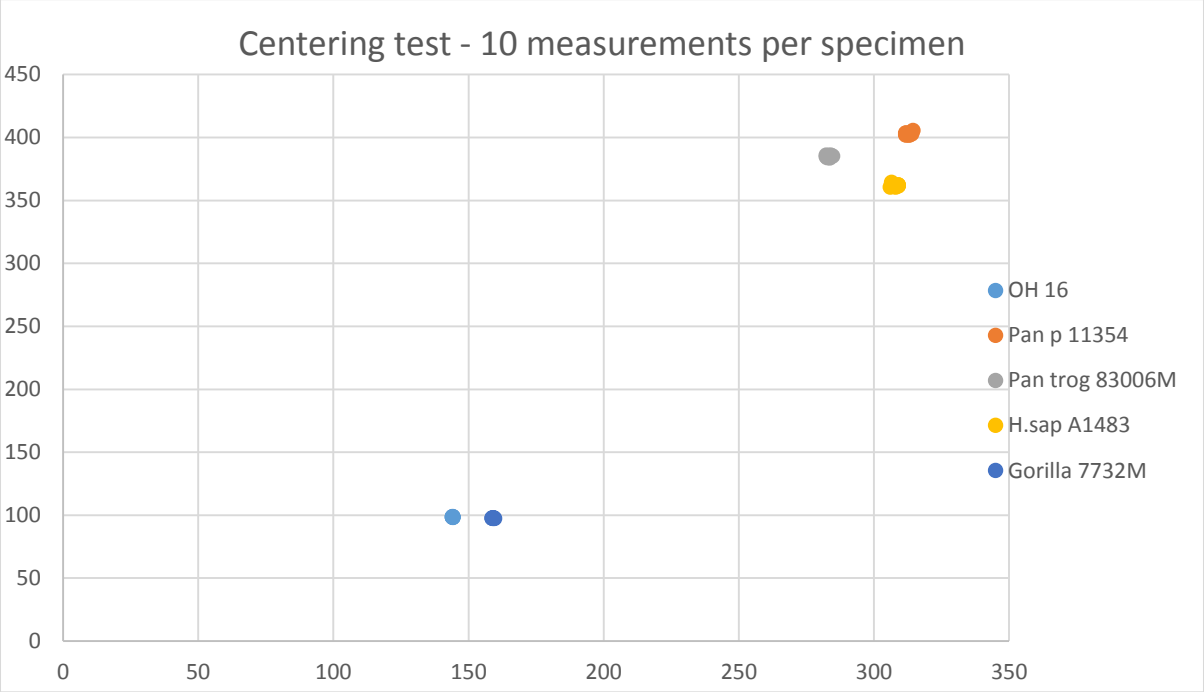

Figure 3.7 Test for inter-and intra-observer error in locating the central landmark at the mesiodistal-buccolingual diameter intersection. **Five x,y coordinates measured at different intervals by two observers for each tooth are plotted to show the variability in centring each tooth**

Table 3.4 Percentage errors for x and y coordinates recorded during the inter- and intra-observer error test for locating the central landmark for teeth.

Specimen	Average difference from minimum x coordinate	Average difference from minimum y coordinate
OH 16	0.066%	0.326%
Pan paniscus 11354	0.281%	0.311%
Pan trog. 83006M17	0.320%	0.364%
Homo sapiens A1483	0.588%	0.388%
Gorilla gor. 7732M	0.219%	0.189%
Average error	0.295%	0.316%

The average error in centring the first landmark was thus well below 1% in each case. The average centring error overall was approximately 0.3% in both the x and the y directions, which is considered to be an acceptable error.

3.4.4 A note on linear diameter (MD and BL) measurements: "corrected" and "uncorrected" MD diameters

Since tooth length and width (and the ratio between them) are key parameters utilised by morphometricians when classifying and comparing teeth (e.g. Moggi-Cecchi et al. 2010; Benazzi et al. 2011; Leakey et al. 2012), two analyses based on these measurements are included in this study. Both diameters also figure in the geometric morphometric and statistical analyses, with landmarks assigned to them in addition to the landmarks around the perimeter of the tooth, as described above.

However, there are several methods for calculating these diameters used by different authors (Moorrees & Reed 1954; Tobias 1967; Brace 1979; Wood & Abbott 1983; Wood 1991). It is important for the purposes of this study to choose definitions for the diameters that are not only acceptable according to norms used by palaeoanthropologists today, but which would be appropriate for use with occlusal photographs of teeth.

For the past few decades, linear measurements on teeth have normally been calculated according to the protocols championed by Bernard Wood (Wood and Abbott 1983; Wood 1991).

Buccolingual diameter:

The buccolingual diameter is measured at ninety degrees to the mesiodistal axis (the mesiodistal axis is an imaginary line drawn through the middle of the tooth along the dental arch to describe its length – or in the case of misaligned or isolated teeth, the line which best describes the midline of the tooth along its length (Wood, 1991)). The buccolingual diameter is taken at the point where the tooth reaches its maximum width – usually not the midline itself across the tooth.

Mesiodistal diameter:

The mesiodistal diameter can be read in several ways, so that there is a certain amount of confusion in the literature with different authors preferring different methods. However, for the past three decades or so, attempts have been made to formalise a standard methodology for defining, measuring and recording this parameter, so that comparisons of teeth described by different authors can be accurately made. Wood and Abbott (1983) made provision for a "*corrected MD diameter*" and an *"uncorrected MD diameter*". The "uncorrected" diameter calculates the maximum length of the tooth as measured parallel to the mesiodistal axis, based on the shape of the tooth as it is actually observed. Again, this may not be the measurement along the exact midline of the tooth along the axis itself unless the tooth is pristine with no flattened or worn interstitial boundaries that might have affected the tooth shape over time, as a cusp that protrudes mesially or distally may often add length to the tooth. The "corrected" diameter measurement involves the researcher inferring what the outline of the tooth would look like if there were no interstitial wear or narrowing caused by the tooth or teeth adjacent to it. The diameter is thus "inflated" by the observer to infer additional

enamel that might have been lost due to pressure from adjacent teeth. The diagram below illustrates these two measurements (Figure 3.8).

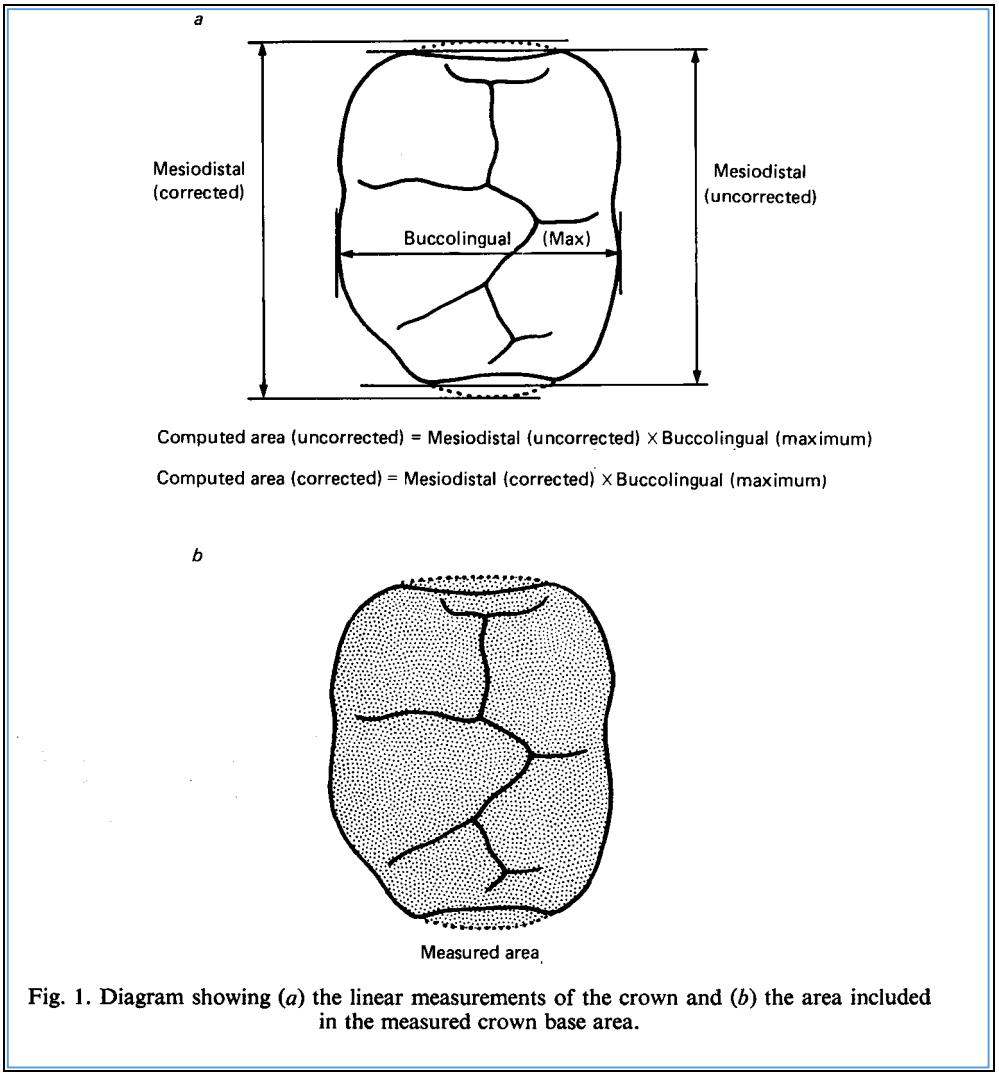

Figure 3.8 Diagram to show how the buccolingual and the mesiodistal (corrected and uncorrected) diameters are calculated. From Wood and Abbott (1983), page 202.

For the purposes of this study, the uncorrected mesiodistal diameter has been chosen. The reason for this is that wherever it is possible to avoid making subjective inferences affecting the final analysis of tooth shape and size, the safer option (observed data rather than inferred data) should be chosen whenever a researcher is working alone. (In studies where there are two or more researchers working together on the data, it is possible for multiple observers to cross-check their inferred measurements against each other and calculate average measurement errors, but this is not possible when

conducting independent research by a single person). In terms of repeatability of the research, and particularly the repeatability of landmark placements (notably landmark #1), this method also has the advantage of ruling out observer bias for future analyses. Further to this, the calculation of the central reference point landmark for analyses of the teeth can be based upon firmly observable buccolingual and mesiodistal diameters rather than inferred diameters, and the "bounding box" that is used in the image processing to define the maximal extents of the mesial and distal points of the tooth, and the buccal and lingual points of the tooth corresponds exactly to the "uncorrected" mesiodistal diameter and the "maximum" buccolingual diameter respectively. This bounding box effectively mimics the blades of callipers oriented mesiodistally to measure the maximum buccolingual diameter and buccolingually to measure the maximum visible diameter along the mesiodistal axis, as shown in Figure 3.9.

Figure 3.9 Measurement of the "maximum" buccolingual diameter and the "uncorrected" mesiodistal diameter of the molars; calculation of the centre of the tooth at the intersection of the midpoints of both diameters. (This example: SKW5 Right lower M1 – mirror-imaged).

3.5 Digitisation of data – landmarking methodology and the selection of a landmark model to maximise digitisation of diagnostic traits

After completion of the data collection and the image processing, the next phase of the project involved experimenting with various landmark placement arrangements on the images and processing the information to provide increasingly improved results (results being measured by visually improved definition between species groups, usually best seen on a Principal Components graph – see 3.6.1.2 below).

Landmarks are finite points placed on and around an object, so that for each object being compared, there is a corresponding, matching site for each landmark on each specimen in the group.

There are a number of different names for the types of landmarks used in shape analyses. For this study, landmarks were based on the definitions provided by Dryden and Mardia (1998, pages 3-4):

> *"An **anatomical landmark** is a point assigned by an expert that corresponds between organisms in some biologically meaningful way, e.g. the corner of an eye or the meeting of two sutures on a skull."*
>
> *"**Mathematical landmarks** are points located on an object according to some mathematical or geometrical property of the figure, e.g. at a point of high curvature or at an extreme point."*
>
> *"**Pseudo-landmarks"** are constructed points on an organism, located either around the outline or in between anatomical or mathematical landmarks."*

There are further types of landmark to which reference is generally made in the literature. Again, from Dryden and Mardia (1998, pages 4-5):

> *"**Type I landmarks** occur at the joins of tissues/bones; **type II landmarks** are defined by local properties such as maximal curvatures and **type III landmarks** occur at extremal points or **constructed** landmarks, such as maximal diameters and centroids."*

For the purposes of this study, the only truly homologous **anatomical** (Type I) landmarks for crown enamel surfaces demonstrating varying degrees of wear would be the five junction points where each cusp joins the next cusp along the perimeter edge of the tooth. All other landmarks used are the equivalent of **pseudo** (Type III) or "constructed" landmarks, such as the geometrically calculated centre of each molar, the maximal diameters (mesiodistal and buccolingual), the perimeter markers and the geometric centres of cusp arcs, etc..

Landmarks were placed on the teeth using ImageJ software, using a large, high definition computer screen purchased for this study to maximise accuracy. The siting of the landmarks is described in detail below. The landmarks for each image were scaled to convert their coordinates from pixel measurements to millimetre measurements, using the scale bar photographed with each image. Landmarks were thus expressed as x and y coordinates according to their location on each image itself. In order to standardise all the images, these x and y coordinates were then "centred", using Excel software, so that for all images, the landmark at the MD:BL intersection reference point at the centre of the tooth was at x=0, y=0 and all the landmarks around the tooth were

expressed as actual measurements in millimetres from the origin were then calculated as Euclidian coordinates around the origin.

Although analytical methods such as Procrustes superimposition can translate, scale and rotate the data without any requirement on the analyst to do so beforehand, other methods (such as log se_m) work with comparative linear measurements. Expressed as vectors from the origin in millimetres, the data are also compatible with measurements (e.g. mesiodistal and buccolingual diameters) in other databases worldwide, so the centring of the data is useful for all types of analysis used in the study.

Referring back to 2.3 and Figures 2.11 and 2.12 above, the diagnostic traits of the fossil teeth requiring to be landmarked are as follows:

a) Overall size (usually measured by the mesiodistal and buccolingual diameters)
b) Relative width in relation to overall size (usually measured by the ratio between the mesiodistal diameter and the buccolingual diameter)
c) Basic shape of the tooth (measured in a shape analysis by applying evenly-spaced, mathematically calculated landmarks "pseudo-landmarks" or Type III around the perimeter of the tooth.)
d) Cusp arrangement (relative width of cusp arcs at the perimeter and length from the centre of the tooth to the centre of each cusp; general direction of the midline of the cusp from the centre to the perimeter of the tooth).

In all of the models for landmark placements that were examined to maximise digitisation of the diagnostic traits of the crown surface, the following criteria were required to be met:

- *minimal reliance on anatomical landmarks on the crown surface that are subject to erasure as a result of wear or damage*. Since teeth were all in differing stages of wear, and some were effectively "blank canvasses" except for traits visible around the peripheral margins, this would preclude the placement of landmarks on the peaks of cusps and even fovea, the latter of which, while being well embedded into the enamel of teeth, are at different surface levels and undergo differential wear. In heavily worn teeth, it is difficult to distinguish between pits in the tooth due to damage and the fovea themselves, if still present. Furthermore, some of the molars in the fossil record, while very worn and damaged (with fovea and cusp-peaks obliterated), are either of vital importance (due to being holotypes or proxies for holotypes) or they may be among very few specimens from a specific taxonomic group, so their inclusion into the model would be ideal, despite being damaged, in order to establish whether it is correctly identifying (via quantitative methods) what morphologists are establishing (using qualitative observations) in terms of taxonomic classifications. If internal landmarks can be calculated mathematically by means of identifiable anatomical features still visible around the perimeter of a damaged tooth, then even that damaged tooth can often be included into the model.
- *High emphasis to be placed on overall size and shape (width and length, perimeter shape)*. Morphologists traditionally place great emphasis on overall size and shape for classification purposes. Mesiodistal and buccolingual diameters are

used widely in comparative research studies (e.g. Moggi-Cecchi et al. 2010; Benazzi et al. 2011; Leakey et al. 2012), as they are indicative of both overall size of the tooth and their relative width, while perimeter shape comparisons give a broad idea of cusp arrangement. Quantification of these three parameters (length, breadth, basic outer shape) is paramount.

- *Calculation of the centre of the tooth should ideally be simplified for repeatability and not be reliant on a computerised calculation of a mathematical "centroid"*. Apart from practical considerations (repeatability; access to identical software; maximising of simplicity in locating MD:BL intersections), some teeth are diagnostically characterised by larger or smaller, unbalanced or protruding individual cusps. A mathematical calculation of a centroid may effectively ignore the importance of these characteristically protruding cusps, particularly if they have narrow cusp arcs, as a centroid is effectively calculated to find the average distance between landmarks. In the case of a tooth with protruding mesial cusps, particularly the diagnostic metaconid (such as in the case of *Australopithecus afarensis*), it is useful if the centre point were not "averaged" to minimise this diagnostic difference in cusp length from the centre. If the centre point were based simply on the mid-point of the mesiodistal axis (and the buccolingual axis), distances from this centre to the perimeter edge of a very protruding cusp will then be uniformly emphasised. This should provide a means to differentiate between species when conducting geometric morphometric analyses. This is also exactly in keeping with the regularly used "uncorrected mesiodistal diameter" and the "maximum buccolingual" diameter of size calculation ((Wood and Abbott, 1983) – refer to 3.4.4.), and this suits a study based on occlusal photographs very well – these diameters can be

delineated by a rectangle superimposed upon the photograph as described above, which itself then forms a "bounding box" around the tooth, the centre of which can be quickly calculated in a standardised, easily repeatable way.

- *Cusp arrangement to be a major feature of the choice of landmark placement*. In addition to the overall breadth and perimeter shape of the tooth, the relative surface areas of each cusp vis-à-vis the other four (or five) cusps is highly diagnostic (Aiello & Dean 1990; Hillson 1996; Wood et al. 1983). Fortunately, cusp arcs at the perimeter of molars usually remain identifiable despite wear on the crown. If the geometric centre of the tooth and the cusp arcs can be identified (or inferred in the case of damaged teeth, by using the antimere and adjoining molars as a guide if available), additional landmarks marking the midline of the cusps and the distance of the middle of the cusp at the perimeter from the geometric centre of the tooth can be calculated mathematically to provide additional information that should equate to relative cusp length, width and orientation vis-à-vis the MD:BL intersection reference point at the centre of the tooth.
- *Landmarks to be placed with maximal ease and speed, to be easily repeatable for other researchers to use, yet to achieve maximum impact for the model.* In choosing landmark placements, it would be less than ideal if the method of calculation for these placements were to be so complicated as to make the model unwieldy to use. It should also be a quick process, to enable any new tooth to be analysed efficiently, for instance, at the site of an excavation, to confirm any initial observer-based qualitative analysis with quantifiable modelling. It was decided to use evenly-placed landmarks around the perimeter of the tooth rather than semi-sliding landmarks, for instance. Ease and speed should not, however,

outweigh the importance of the careful placement of the landmarks for maximal diagnostic capability.

Taking all of the above criteria into consideration, several landmark models using increasingly improved and balanced landmark placement arrangements were considered, to optimise the capacity to distinguish between groups. Ultimately, an arrangement of 49 landmarks (5 "anatomical" / Type I and 44 "pseudo" / "constructed" / Type III landmarks), 29 of which measured overall size and perimeter shape, and a further 20 of which measured the cusp arrangement at the perimeter and at the mathematical centres of the cusps, provided a satisfactory level of differentiation between species groups, both for extant species and for the fossil specimens.

Four landmark models were considered to optimise landmark placements:

a) Landmark model #1: Perimeter shape alone. A 72-point fan was overlain over the image of each tooth (centred on the intersection of the mesiodistal and buccolingual axes – see below in 3.4.4. for a definition of the mesiodistal and buccolingual diameters). Landmarks (or more correctly stated, "pseudo-landmarks"/ Type III landmarks) were placed around the outer perimeter of each tooth at every 5˚ around the tooth. Pairwise regression analyses were conducted on the resultant 72 radial data points (distances from the centre of the tooth to each perimeter landmark) to test for shape correlation. This landmark model was rejected because the perimeter shape, particularly of fossil and extant *Homo sapiens* teeth, is not clearly indicative of the cusp arrangement of the teeth. There are often only very minor indentations along the perimeter of

the tooth to indicate where cusps meet the edge of the tooth, and in the case of very smooth cusp edges, the indentation at the perimeter edge of the tooth does not always give an accurate indication of the actual breadth of the cusp.

b) Landmark model #2: Inner cusp arrangement alone. The mathematical centres of each cusp were calculated by bisecting the radius from the centre of the tooth to the perimeter of the tooth through the midline of each cusp (as measured by an arc drawn across the width of each cusp at the perimeter). The five resultant landmarks were then joined by three pseudo-landmarks between each (20 landmarks in total), describing a differentially irregular pentagon for each tooth. 72 radial measurements were then taken from the centre of the tooth to this pentagon shape and the data for each tooth was compared in pairwise regression analyses. This landmark model was rejected as it did not adequately describe overall size and shape parameters for the tooth as a whole, and it did not easily cater for teeth with a sixth (diagnostic) cusp. Since size, shape and cusp arrangement are vital for the morphometric analysis of each tooth, it was decided to combine both perimeter shape and inner cusp arrangement.

c) Landmark model #3: Outer perimeter and inner cusp pentagon. The twenty landmarks calculated for Experiment 2 above were added to 24 perimeter landmarks (one landmark every 15˚on a rotary basis around the perimeter of the tooth rather than every 5˚, so that the perimeter landmarks would not outweigh the interior landmarks) plus a landmark at the centre of the tooth, to make a total of 45 landmarks. With this model there was still a certain lack of weighting on cusp arrangement, especially in respect of the direction of the cusps from the

central point to the perimeter mid-points of the cusp arcs, and again the landmarking of a sixth (diagnostic) cusp remained problematic. A more balanced landmark arrangement could be achieved by removing some of the less important mathematically-generated internal pseudo-landmarks and replacing these with additional mathematical landmarks depicting a second "layer" of cusp patterning to include a "cusp direction" component.

d) Landmark model #4: Final selection - shape, size, inner and outer cusp arrangements. This 49-landmark arrangement is henceforth known as "the landmark model". The landmarks are shown in Figure 3.10.

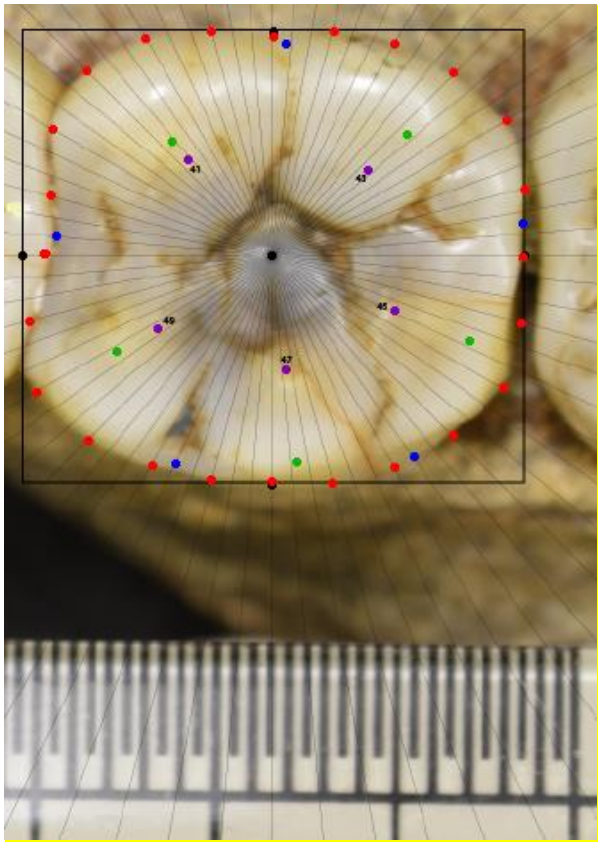

Figure 3.10 Landmark model: 5 anatomical (Type I) landmarks (blue) plus 44 Type III/pseudo/constructed landmarks

This 49-landmark model was chosen so that optimised distributions of landmarks could be placed on the main diagnostic features utilised by morphometricians, as follows:

- **Diameters (relative size and width); centre intersection**

  Emphasis placed on the length and breadth of the tooth (4 pseudo / ”constructed” / Type III landmarks (landmarks 2-5) on the “bounding box” surrounding the tooth on the 2D image, delineating the maximum length and width of the tooth at the mesial, distal, buccal and lingual extremities of the bounding box); Landmark #1 is geometrically placed at the centre of the bounding box (in Adobe Illustrator, the centre is automatically located by the software, but this point is easily reproducible by drawing lines from the corners of the bounding box and finding the centre).

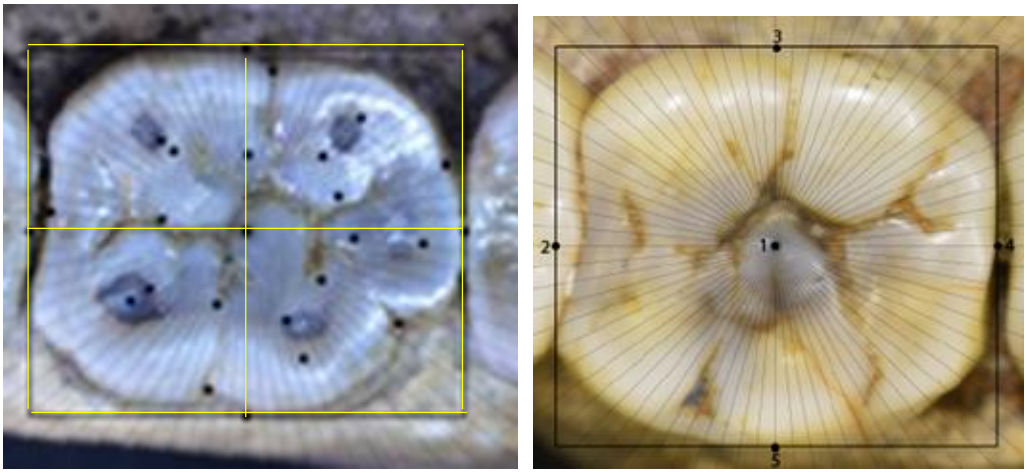

Figure 3.11 Landmarks 1-5: centre, overall size and relative width

- **Overall shape – perimeter, approximately half of the landmarks:**

  Adequate weighting given to perimeter shape (approximately half of the landmarks – 24 out of 49 (landmarks 6 to 29), evenly spaced around the perimeter to facilitate reproducibility); see Figure 3.12.

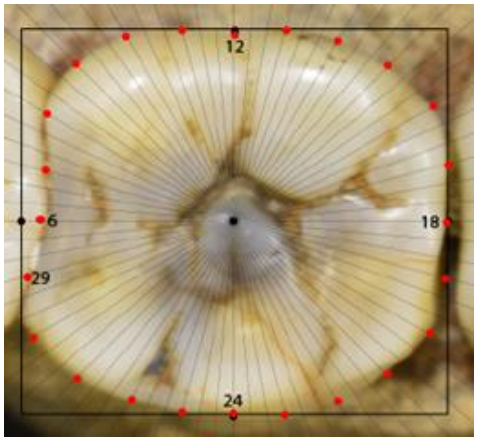

Figure 3.12 Landmarks 6-29: perimeter shape

- **Cusp arrangement: perimeter arc junctions, midline, geometric centres, cusp orientation:** Inner and outer cusp arrangement arranged with 20 landmarks (landmarks 30 to 49): 5 landmarks (anatomical, homologous landmarks, equivalent to Type I landmarks, circled in the image below) at the junctions of the cusp arcs at the perimeter; 5 landmarks at the midpoint of the cords subtended between the arc junctions at the perimeter, thus marking the reference point to calculate the midline of the cusps; 5 mathematical landmarks at the geometric centres of each of the five main cusps (calculated as the midpoint from the MD:BL centre reference point of the tooth to the midpoint of the cusp arc using the midline arc cord marker as a guide), and landmarks at the midpoint between each of these 5 main cusp-centre landmarks (20 landmarks in total, landmarks 30 to 49), forming an inner pentagon with projections from the five vertices of the pentagon towards the centre of the cusp arcs, to show the orientation of the cusps. In the case of a tooth with an extra cusp, known as a "tuberculum sextum" or C_6 (Aiello & Dean, 1990; Hillson, 1996; Wood et al, 1983), which is diagnostic for certain fossil species, the midpoint pseudo-landmark on the hypoconulid is projected

outwards to mark the C_6, and to modify the inner pentagon to become a hexagon, as shown in Figure 3.13:

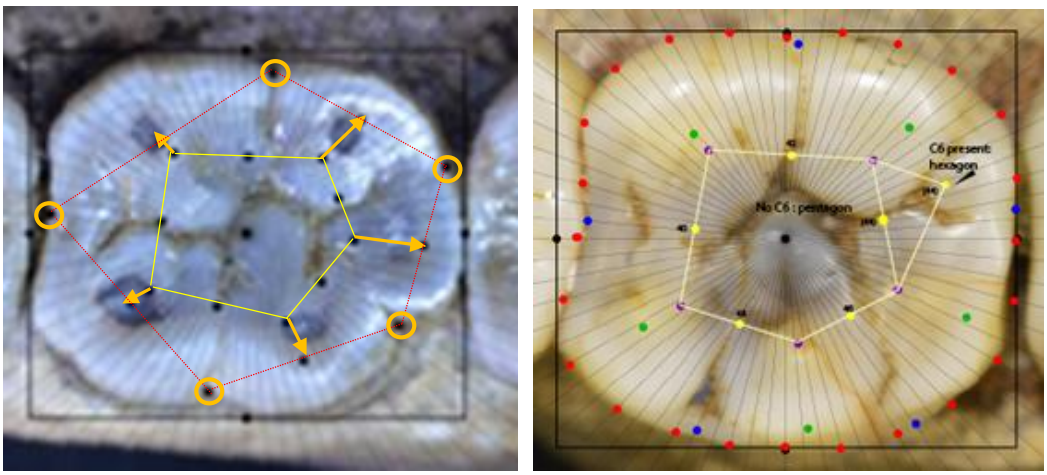

Figure 3.13 Landmarks 30-49: inner and outer cusp arrangement,cusp orientation

This landmark model provided a good balance between overall size and relative width; overall shape (perimeter), and outer and inner cusp arrangements. Landmarking the cusps in this manner provided an advantage over methods that focus on relative cusp areas, because a "wide, shallow" cusp can have the same surface area as a "narrow, elongated" cusp. Length, width and orientation of the cusps is measured not only by the distances of the landmarks from the central landmark but by distances between themselves, and having two landmarks located along the midline of the cusps (one at the midpoint of the cusp arc cord and one at the mathematical centre of the cusp) has the advantage of determining cusp orientation as well as further adding to a differentiation between "wide, shallow" cusps and "narrow, elongated" cusps, as the distances between these two midline markers will be different in either case, as shown in Figure 3.14:

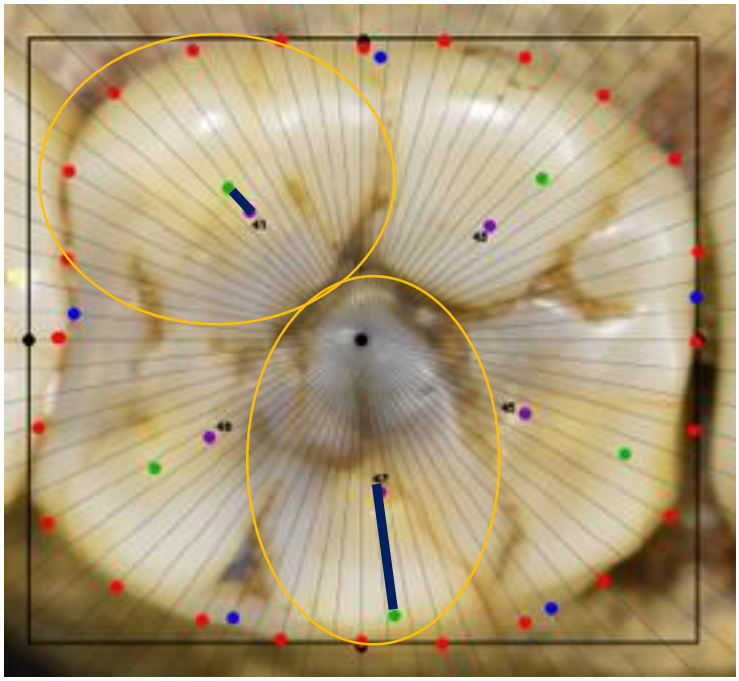

Figure 3.14 Image to show cusp midline differences for differently oriented cusps. (The cusp-midline landmarks add a third differentiator between cusps of similar area but different orientation, in that the length between the two cusp-midline landmarks will be different for extended, narrow cusps as compared to flatter, wide cusps. The other two differentiators will be the direction of the cusps (also indicated by these two landmarks on each cusp (blue and purple landmarks on the image above)), and the overall size and shape of the cusps, marked by the blue, green and purple landmarks in the image above)

These 49 landmarks formed the "inputs" of data to the majority of the analyses used for this study (see 3.6 for a description of these analyses):

- Landmarks 1-5 were utilised for most of the linear dimension analyses
- Landmarks 1-49 were the inputs for the Procrustes-based analyses (including the principal components analyses and the discriminant function analyses)
- Vectors calculated from landmark #1, radially to each of the remaining landmarks (2-49), provided the straight-line measurements used as inputs to the log se_m analyses.

There is some discussion as to how many landmarks to use in morphometric analyses. For this particular study, it was felt that more inputs rather than less would maximise the possibility of achieving diagnostic resolution between species groups in the

principal components and discriminant function analyses. This reasoning has been used successfully by researchers in dentition studies (Skinner et al. 2009). This premise is also true for the log se_m analyses, where a minimum number of 10 inputs is required, but where improved accuracy of results is achieved as the number of inputs increased. For this reason, the five anatomical (Type I) landmarks have been supplemented by 44 mathematically-placed landmarks.

A descriptive summary of the exact positioning of the landmarks used for this model and the rationale therefor is given in Table 3.5 below.

Table 3.5 Descriptive summary of landmark placements

Landmark N°	Placement	Comments
1 Type III (constructed)	MD:BL diameter intersection reference point at the geometric centre of the tooth, calculated at the centre of the "bounding box" delineating the maximal mesial, distal, buccal and lingual points on each tooth.	This landmark is dependent on the correct horizontal alignment of the MD diameter. See 3.4.3 for a description of the observer error tests for this landmark placement.
2 – 5 Type III	Placed at the mid-points of the four sides of a rectangle defining the mesiodistal and buccolingual diameters of the tooth. (Using a clock analogy, these were placed at 9 o'clock (mesial edge), 12 o'clock (lingual), 3 o'clock (distal) and 6 o'clock (buccal), which are designated in the study as 0°, 90°, 180° and 270° respectively)	These markers delineate the maximal length and breadth of the molars, as visible from an occlusal view photograph. They then form a proxy for the MD and BL diameters ("uncorrected" and "maximum" respectively, as defined by B. Wood (Wood & Abbott 1983)
6 – 29 Type III	Placed every 15° degrees clockwise around the perimeter of the molar best describing the actual crown shape, as visible from the occlusal view. Point 6 starts at 0° along the side-wall of the tooth (at "9 o'clock" from the centre, along the mesial edge of the tooth)	So as not to create morphometric artefacts due to differential wear between teeth, the side wall of the tooth, particularly where it meets the cemento-enamel junction (where visible) can be treated as a guide for the overall crown shape.
30, 32, 34, 36, 38 Anatomical Landmarks (Type I)	Placed at the perimeter extremities of the intersections of the five main cusps (at the points best describing the intersection of adjoining cusps where their average margins generally tend towards the side wall of the tooth – this may not be exactly the same point as the indent made into the perimeter wall between the cusps, if this indent is skewed by following the rounding effect of either of the cusps in question). Landmark 30 starts at the junction between the protoconid and the	

	metaconid (the two mesial cusps) and landmark placement proceeds clockwise.	
31, 33, 35, 37, 39 Type III	Placed at the mid-point of the five cords drawn between the cusp intersections, starting from the midpoint of the cord describing the arc of the metaconid (mesiolingual cusp) and proceeding clockwise.	These points describe the mathematical midpoints of the cusp "widths" at the perimeter of the tooth.
41, 43, 45, 47, 49 Type III	Placed at the mid-point of the five radii drawn from the centre (landmark 1) to the perimeter of the tooth, drawn through the midpoints of the cusp centres (landmarks 31, 33, 35, 37, 39), starting from the central point of the metaconid (mesiolingual cusp) and proceeding clockwise.	These points describe the mathematical "centre" of each cusp, since they are midway along the length of the cusp and midway across the width thereof.
40, 42, 44, 46, 48 Type III	Placed at the midpoint between landmarks 41, 43, 45, 47 and 49 above, to describe an inner pentagon with apices at the mathematical midpoints of each cusp, starting midway between the centre of the protoconid (mesiobuccal cusp) (landmark 49) and the metaconid (mesiolingual cusp) (landmark 41) and proceeding clockwise.	
44 – special exception	Where there is a visible sixth cusp (C_6 or "tuberculum sextum"), this landmark is placed midway between landmarks 43 (the mid-point of the entoconid, or distolingual cusp) and landmark 34 (the intersection along the perimeter wall of the tooth of the entoconid and the hypoconulid (distal cusp) of the tooth.	Where there is a C_6 present, the inner "pentagon" describing the centre points of each cusp therefore becomes a hexagon.

Footnotes to landmark placement:

1) Where crown enamel is damaged at the perimeter, if the original perimeter of the tooth can be inferred with sufficient accuracy from the antimere of the tooth in question, landmark placements should be made using this inferred perimeter. If this results in a consistently divergent pattern of grouping of the teeth in the geometric morphometric analyses (for example, in the PC analyses, if the left and right antimeres consistently do not group together), corrections to the inferred landmarks can be tried, before discarding the damaged tooth completely from the study.
2) Where a P_4 has created a marked, artificial concavity to the mesial edge of the M_1 in question, landmarks may be situated slightly outside of the resultant visible perimeter of the tooth, so as to reduce the level of concavity. Since "uncorrected" mesiodistal measurements are being used (Wood & Abbott 1983), there is no need to extrapolate these corrected landmark placements so as to infer a fully convex edge to the mesial perimeter of the tooth. With all teeth being treated in an identical manner (straighter, rather than overly concave or convex mesial margins), the definition between groups in the analyses should not be prejudiced).

3.6 Methods - analyses

Analyses were first conducted on the "**inputs**" to the study (the **landmarks**) to test for the importance of retaining size as a factor in distinguishing between different species, firstly on the extant species, and thereafter on the African Plio-Pleistocene lower first molars.

Thereafter, testing was conducted on the "**outputs**" of the shape/shape-and-size analyses (the **results** of the initial analyses) using several different analytical methods, to see if the same results would be obtained no matter which type of analysis was utilised ("results" meaning the identification of species groups and of any potentially anomalous specimens that failed to group as expected within their species groups on the initial analyses).

Phase I - testing of "**inputs**" – the **Landmark Model**

- Testing of the adequacy of the landmark model's ability to differentiate between extant species using a Principal Components Analysis based firstly on "Procrustes Shape Space" (shape only analysis – data rotated, translated and scaled, based on a full Procrustes superimposition) and secondly on "Procrustes Form Space" (Mitteroecker et al. 2004), which is a "shape-and-size" analysis (Dryden & Mardia 1998) – data rotated and translated but size accounted for by including the log of the centroid size within the analysis. The purpose of conducting both of these analyses is to ascertain the role of size in species

differentiation in the context of lower first molars (see below, 3.6.1.2 and 4.2. for a fuller explanation of these analyses).

- Decision to include or exclude size from future shape analyses, based on the outcomes of the "Procrustes Shape Space" and "Procrustes Form Space" analyses carried out on extant species data.
- Principal Components Analysis on fossil M_1 data, to test whether the same landmark model and the same type of analysis, using the same criteria for the choice of the second axis in the plot, would also apply to the African Plio-Pleistocene fossil hominin lower first molars (i.e. whether the same parameters as applied to the extant species would result in a reasonable level of species differentiation for the fossil species groups.)

Phase II - Testing of "**outputs**" (additional types of analyses to test the robustness of the initial **results** – species groups and anomalous specimens).

Once a satisfactory level of diagnostic capability of the landmark model was established (based on 49 landmarks (see 3.5)) and tested visually, using principal components analyses (as described below), a number of additional studies were conducted on the extant species and on the fossil sample, using various analytical methods. The rationale for using multiple methods to analyse the same data was as follows:

- To obtain additional information not necessarily evident from the principal components analyses (trends over time, for example);
- To compare analytical methods for coherence between themselves;

- Most importantly, to confirm the results of the principal components analyses, particularly in the case of anomalies identified visually on the PC plots. This is an exploratory study: an emphasis was placed on testing data using various analyses, rather than on conducting in-depth analyses based on one methodology alone.

3.6.1 Analytical methods used for the study

3.6.1.1 Generalised Procrustes Analysis (GPA)

This analysis is designed to quantify differences in shape between specimens compared to a calculated average shape. For this analysis, landmark coordinates are translated, rotated and scaled (standardised in size), and a pure shape analysis is conducted (Rohlf & Slice 1990). This method also offers the flexibility of being able to conduct a partial Procrustes superimposition (no scaling of the data, but translation and rotation still performed). Figure 3.15 below illustrates this. Such transformations are useful when size is a significant differentiating factor between specimens, in which instance it is useful to retain the size element when conducting principal components analyses.

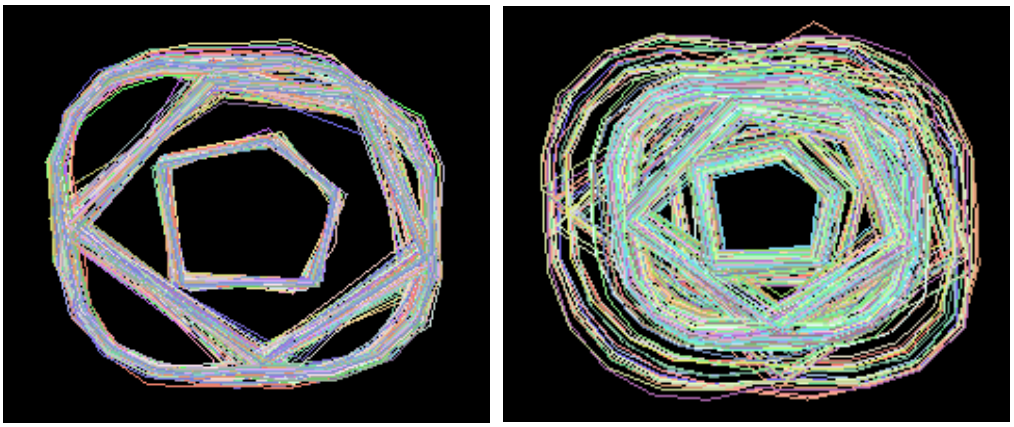

a **b**

Figure 3.15 Example of Procrustes wireframe overlays (of 49 landmarks from the images of 80 lower M1 specimens from 4 extant species (showing inner cusp-pattern pentagon, outer cusp-breadth pentagon and outer perimeter) (This study)). The specimens in image "a" have been translated (moved to the same base coordinate for each image), rotated (oriented in the same direction) and scaled (standardised to a single size along the main axis of the image) to allow for an average shape to be calculated; the specimens in picture "b" have been translated and rotated but not scaled. It can be seen that

with scaling (a), the specimens show more similarity, whereas with size factored in (b), there is more information upon which to differentiate between specimens. From the images above, the importance of the role of size in differentiating between specimens can be inferred, and this analysis provides the basis for the decision to conduct principal components analyses based on both shape space and form space.

Ultimately, a "Procrustes Distance Matrix" can be produced to summarise in a series of "distance vectors" for each fossil tooth, how similar or different it is in shape from all the other fossil teeth individually, as well as from the average. Once specimens have been rotated, translated and scaled, they are superimposed and analysed for differences, purely in shape. A "Procrustes distance" is calculated for each specimen from all the other specimens, and a matrix is produced of these distances. The lower the distance, the more closely grouped the specimens are in terms of their shape alone.

This analysis was carried out using the software programmes ImageJ, Excel and Morphologika.

3.6.1.2 Principal Components Analysis (PCA or PC)

(Bookstein 1991; Zelditch et al. 2004)

This is an analysis (in the case of this current study, based on two-dimensional landmarks) which identifies the individual components of the shape (and size, if factored into the analysis) of each specimen that contribute most towards variability between them. These components are then ranked according to the amount of covariance they contribute towards the total variance (variability) between the specimens. The main components (the "principal components") can then be used as axes in a 2-dimensional or 3-dimensional scatter plot of the specimens in the analysis, and this should ultimately group the specimens visually in terms of their main shape differences and in terms of their main shape-and-size differences in the case of a PC

based on Procrustes form space (shapes rotated and translated but size factored in by adding the log of the centroid value for each shape (Mitteroecker et al. 2004)).

The main aim of this analysis in the context of this present study was to provide a basic way of visualising the main shape and/or size contributors to differences between groups of known species (extant species) and to use the results from the known species to compare patterns of variability within groups of fossils based on the same parameters. In addition, by using both "shape space" and "form space" (shape-and-size) analyses with a PCA, it can be immediately apparent whether it is only shape that differentiates between groups or whether size is a major differentiator, along with shape. Morphologika software offers this flexibility to choose either option.

Each principal component can be examined in turn to identify which particular aspect(s) of variability are being identified for that component. With a view to providing 2-dimensional plots of the groupings of specimens for each analysis conducted, the most important components were examined.

PC analysis was used during Phase I ("testing of inputs") and during Phase II (testing of the results). During the landmark model testing phase (see 4.2 below), PC analyses were carried out on the samples from the four extant species included in the study, firstly on the basis of shape alone and secondly with size retained (size added as a variable) to test the importance of the role of size in distinguishing between species of known biological (extant) species. Once a decision could be made as to whether to include or to exclude a size component with the data in the analyses on the extant species, PC analyses were then applied in the chosen format to the fossil specimens.

In the case of the fossil specimens the same criteria retained for the extant species were applied to the fossil specimens to see if:

- During Phase I - they would group together visually, generally according to their expected species groups (confirming the methodology (using Procrustes shape space or Procrustes form space) and the adequacy of the landmark inputs to identify species groups, at least broadly, and to discern patterns of sexual dimorphism in the extant species groups repeated in the fossil groups) and
- During Phase II – it could be ascertained whether there was overlap between species groups in the fossil sample, whether patterns of species variability could be inferred, and whether any anomalous specimens could be identified that failed to group with their expected species groups (as determined mainly by the holotypes for each species). The first PCA was plotted for the 36 fossil specimens alone. Thereafter, the analysis was repeated with different extant species as "outgroups", to check that the results were consistent. The purpose of adding an "outgroup species" to a PCA graph is to check for the graph's ability to provide visual resolution between species. Whilst a small amount of overlap between species (particularly those presumed to be closely related) is to be expected, if specimens from a known "non-fossil" species (that should group separately from the other (fossil) specimens in the chart) find themselves dotted within the groups of fossils in the chart, the PCA could be inaccurately grouping the fossils. If, however, the additional "outgroup" extant species does group more or less separately from the fossils, additional comfort can be drawn from the knowledge that the PC chart is identifying and separating the species groups successfully.

This analysis was carried out by means of software programmes including ImageJ, Excel and Morphologika;

3.6.1.3 General tooth dimension analysis

(Buccolingual (BL) (width of tooth) and mesiodistal (MD) (length of tooth) diameter analyses, including a MD:BL ratio analysis of fossil teeth over time. (See 2.7.3 below for a fuller definition of these diameters)).

As discussed in 2.3, a major indicator of taxonomic grouping for molar teeth is the overall size and the general width of the tooth (is the molar "narrow" or "wide"?), and these parameters are always the first to be considered by morphologists and morphometricians.

It is not only the general size of the tooth but the ratio between length and breadth (the MD:BL ratio) that can provide useful information about tooth morphology and the implications for taxonomic classifications that go with it. The following analyses were conducted using this particular set of general molar characteristics:

- A comparison of MD and BL measurements for 76 modern human lower first molars from various population groupings in Southern Africa. The MD and BL diameters of 19 female left M_1s were compared with their respective antimeres, as well as with the left and the right M_1s from 19 males from the same population groups. The aim of this analysis was to establish whether there was a variation in the size of antimeres and whether variability in molar size could be attributed to sexual dimorphism.
- A plot of MD and BL diameters for the four extant primate species in the study (modern humans, chimpanzees, bonobos and gorillas). The aim of this analysis was to establish whether clear boundaries existed between the four species,

simply by visualising their general molar dimensions (without taking cusp patterns into consideration). From a simple chart of mesiodistal vs. buccolingual diameters, it might also be possible to see whether variability within a group is attributable to size differences, shape differences or both. In the case of highly sexually dimorphic primates (such as gorillas), this information will be useful in predicting whether variability in teeth in the fossil record could be due to sexual dimorphism.

- A plot of MD and BL diameters of the 36 fossil specimens used in the study, with indicators to show "square teeth", "relatively broad teeth" and "relatively narrow teeth". This kind of plot should highlight cases where specimens do not group together as predicted, in terms of their relative size, width and length. Questions could then be asked about potential misclassifications or variability due to sexual dimorphism, based on the results of the analyses of the modern human and the extant great ape species molar dimensions described above.
- A plot of the MD:BL ratios over time. If a trend can be determined over time, and there are some anomalous specimens that fail to fit the trend, this could indicate misclassification or sexual dimorphism.

All of these analyses were conducted using Microsoft Excel.

3.6.1.4 Discriminant Function Analysis (DFA or DF)

(Fisher 1936; Poulsen & French 2013; Stockburger 2013)

This is a type of distance matrix analysis that compares numerical data that typify or characterise each specimen and seeks to discriminate between categories of specimens, effectively confirming or rejecting the specimen's probability of belonging to predetermined groups of specimens (in this case, species groups). The DF analysis for

this study is carried out at a preliminary level and makes use of the results already obtained from the PC analysis. The aim of this analysis is to check whether specimens that regularly failed, in the preceding analyses, to group according to their presumed taxa will likewise be highlighted as anomalies in terms of their groupings in the DFA.

The DFA was conducted first on the extant species to test its ability to group specimens correctly. If there is a failure for the analysis to group known biological species accurately, then the results of such an analysis on the fossil specimens would be meaningless. The inputs to the DFA were taken from a subset of the PC scores from the principal components (form space) analyses. The number of PC scores to include was the result of a test conducted for accuracy and sensitivity (Skinner et al. 2008). If too many PC scores are used as inputs, the values eventually contribute too much "noise" and the results are inconclusive as the analysis will not be sensitive enough and will fail to identify potential misclassifications. If too few PC scores are used as inputs, a slight but taxonomically insignificant outlier value in one of the landmarks on a specimen from any given species might cause it to be misclassified by the DFA. In order to test the sensitivity of the analysis, the DFA was run for the extant species using the first 3, 4, 5, 6, 7, 8, 9, and 10 PC scores and the results were recorded. These are set out in table 3.6 below.

Table 3.6 Sensitivity test to establish the number of PC score inputs to include in a discriminant function analysis. **80 specimens from 4 extant species were subjected to DFA analyses using from 3 to 10 PC scores for each analysis. The percentage of correctly-identified species classifications for each species were recorded**

Species	No of PC scores	3	4	5	6	7	8	9	10
		% correctly classified							
Gor. Gorilla		100	100	100	100	100	100	100	100
P. paniscus		95	95	100	100	100	100	100	100
H. sapiens		70	75	90	85	85	100	100	100
P. trog.schw		95	95	95	100	100	100	100	100
Average		90	91.3	96.3	96.3	96.3	100	100	100

It can be seen from Table 3.6 that inputs from the first 8 PCs are just sensitive enough to classify the specimens 100% correctly. The data were then checked for normality of distribution, using a Shapiro-Wilk test (df = 20 per species), since one of the assumptions upon which this analysis is based is that the data should be normally distributed within groups (Manly 2005). The first 8 PC scores were tested for each of the four extant species and the results confirmed normality of distribution. Once the parameters for this test had been established for the extant species, the same test was then also applied to the DFA that included the fossil sample.

This analysis was carried out using Excel and SPSS software

3.6.1.5 A "log se_m" regression analysis combined with a correlation analysis

(Thackeray et al. 1997**;** Thackeray 2007a**;** Braun et al. 2004**;** Thackeray & Odes 2013)

The log se_m analysis is based on comparisons of the log-transformed standard error of the slope (m) of the regression lines calculated for pairwise comparisons of measurements of any two specimens. In this study, 48 measurements per tooth have been compared together, based on the distances, in mm, of landmarks 2-49 from the central MD-BL intersection marker, landmark #1.

In any regression analysis, a limited sample of data points is used to assess the relationship, if any, between two sets of variables. Regression analyses test how highly correlated two sets of variables are. Such tests can also be used to calculate the slope "m" of the regression line (the coefficient of x in the equation for the regression line, y = mx +c, the line that should predict the value of y for any possible value of x, based on the values that have been included in the correlation calculation). Also part of the equation is the constant c, which is the y intercept of the line. For a log se_m analysis, an additional error value is the focus of the analysis, this being the log transformed "standard error of the slope m", which effectively describes the amount of "scatter" there is between the datapoints plotted and the line. Below are three examples of pairwise regressions based on 48 measurements each taken from a) two very similar teeth (KNM-ER 992, left and right antimeres); b) two moderately similar teeth (OH 16 (R) and OH 7 (L)); and c) two dissimilar teeth (Peninj 1 (L) and AL 288-1 (R)). The degree of scatter increases in direct proportion to the degree of dissimilarity between the measurements being compared. Figures 3.16 a), b) and c) illustrate these differences in degree of scatter.

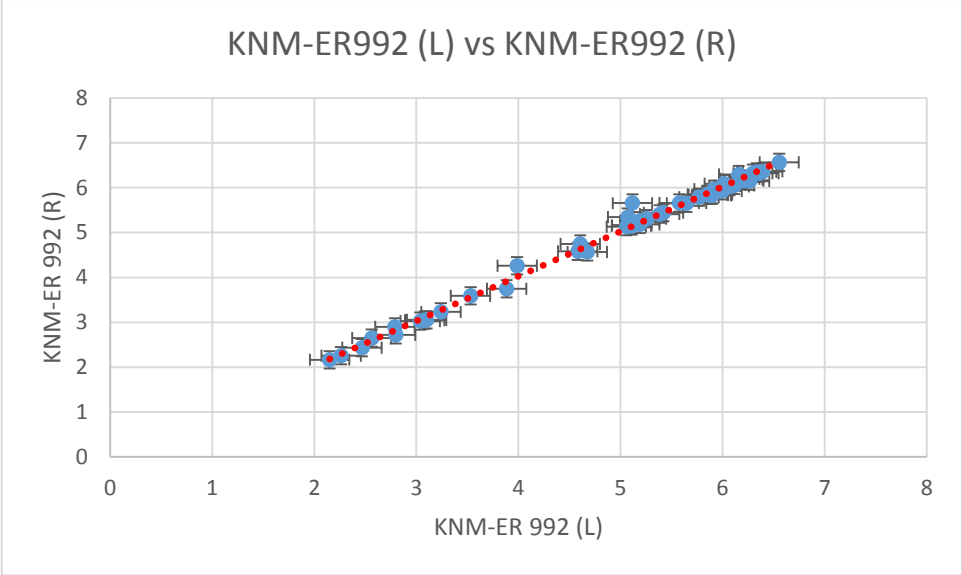

Figure 3.16 a) – Illustrative plot of a regression of 48 pairwise measurements between two antimeres from the same specimen (low degree of scatter around the regression line; slope ≈1.0 (because both teeth are of almost identical size)). The $\log_{10}$ of the standard error of the slope ("log se_m") will be well below the average calculated for all conspecific pairwise comparisons.

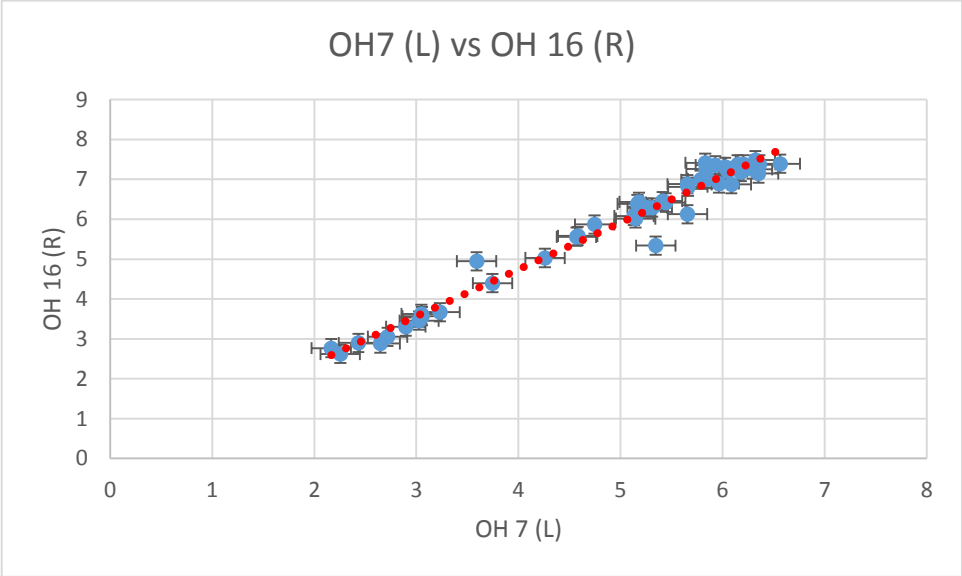

Figure 3.16 b)– Illustrative plot of a regression of 48 pairwise measurements between two molars of different specimens from the same species (average degree of scatter around the regression line; slope > 1.0 (because OH 16 (R) is larger than OH 7 (L))). The $\log_{10}$ of the standard error of the slope ("log se_m") will be around the average value calculated for all conspecific pairwise comparisons.

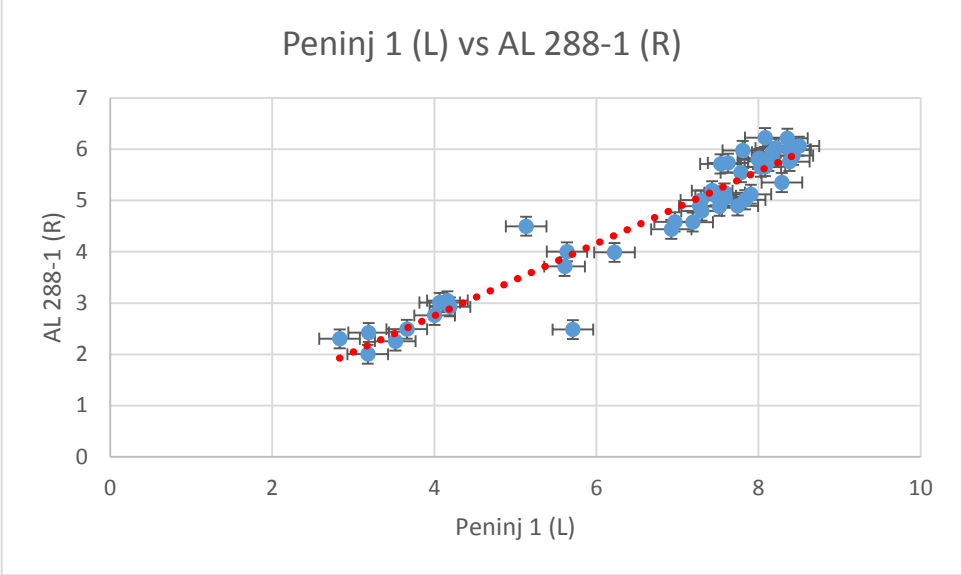

Figure 3.16 c)– Illustrative plot of a regression of 48 pairwise measurements between two morphologically distinct molars of different species (high degree of scatter around the regression line; slope < 1.0 (because AL 288-1 (R) is much smaller than Peninj 1 (L)). The $\log_{10}$ of the standard error of the slope ("log se_m") will be well above the average value calculated for all conspecific pairwise comparisons.

Thackeray (1997) found that on average, the log to base 10 of the standard error values for the slope m for all pairwise comparisons of *intra-specific (conspecific) specimens* are distributed normally around a central tendency (mean) of -1.61 (with a standard deviation of +/- 0.23, based on a study including over 70 different taxa), as depicted in Figure 3.17:

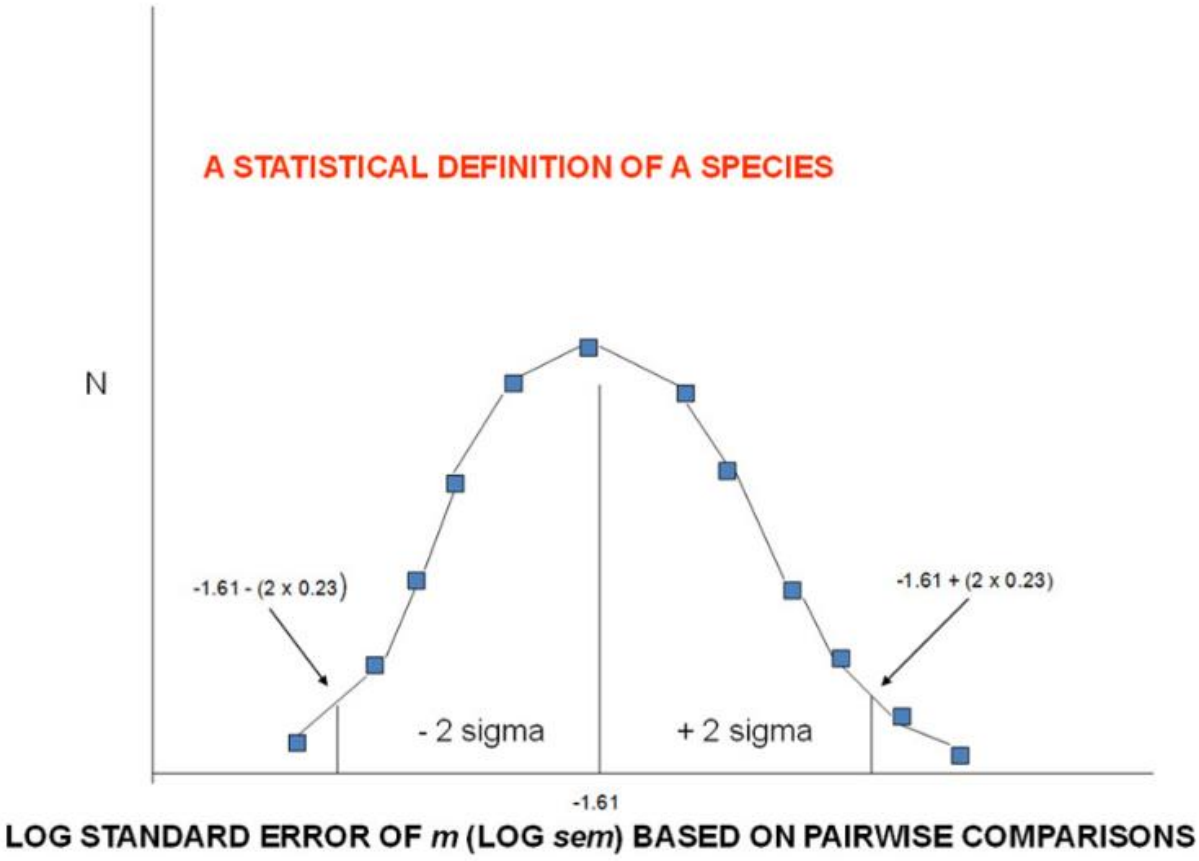

Figure 3.17 A statistical definition of a species (based on cranial data). Source: Thackeray and Odes (2013). This normal curve describes the expected range of log se_m values to fall within an approximate 95% probability range for two specimens of "the same species". Here, the mean is -1.61 and the standard deviation (sigma) is 0.23, based on analyses of pairs of conspecific specimens (> 70 taxa).

It should be noted that the log se_m method was initially conceived as a probability analysis to make comparisons between two similarly-sized specimens that are suspected to be from the same species ("Probabilities of conspecificity" – Thackeray, 1997). Once an average log se_m value can be calculated to stand as a proxy for a "species constant" for dental data (which might not be identical to the species constant for cranial data or other skeletal element data), a *probability* function can be calculated to determine whether specimen A and specimen B are likely to be of the same species. Once a mean and a standard deviation can be calculated for all the log se_m outputs within each species an assessment can be made as to probabilities of conspecificity between individual pairs of specimens. If a log se_m value for a comparison of two

similarly-sized specimens is a higher value than the mean value plus 1.96 standard deviations from the mean (approximated in the graph above to the "cut-off" value of "+2 sigma"), there will be less than a 2.5% probability that the specimens being compared are from the same species.

By way of illustration, in Figure 3.18 below, 5400 pairwise comparisons have been made for cranial measurement data (source: Gordon & Wood, 2013, S.O.M.), first between conspecific pairs of *Homo sapiens* (n= 2775 pairwise comparisons) and then between inter-species pairs of *Homo sapiens* on the one hand and *Pan troglodytes* on the other (n=2625 pairwise comparisons). If any of the inter-specific (*Homo sapiens* vs. *Pan troglodytes*) log se_m values were to fall within the 95% confidence interval for *conspecific* pairwise comparisons (between *Homo sapiens* and *Homo sapiens*), this would indicate that there is a high probability that the crania are from the same species. In this particular instance, the upper 95% confidence value for conspecific pairwise comparisons is -1.478: thus any log se_m values lower than -1.478 would indicate that the specimens being compared have a high probability of conspecificity. As can be seen, the inter-species pairwise comparisons (*Homo sapiens* vs. *Pan troglodytes*) all fall well above a value of -1.478 and there is no instance for which a specimen from the *Homo sapiens* sample would be considered to have any probability of conspecificity with any specimen from the *Pan troglodytes* sample used in this analysis of cranial comparisons.

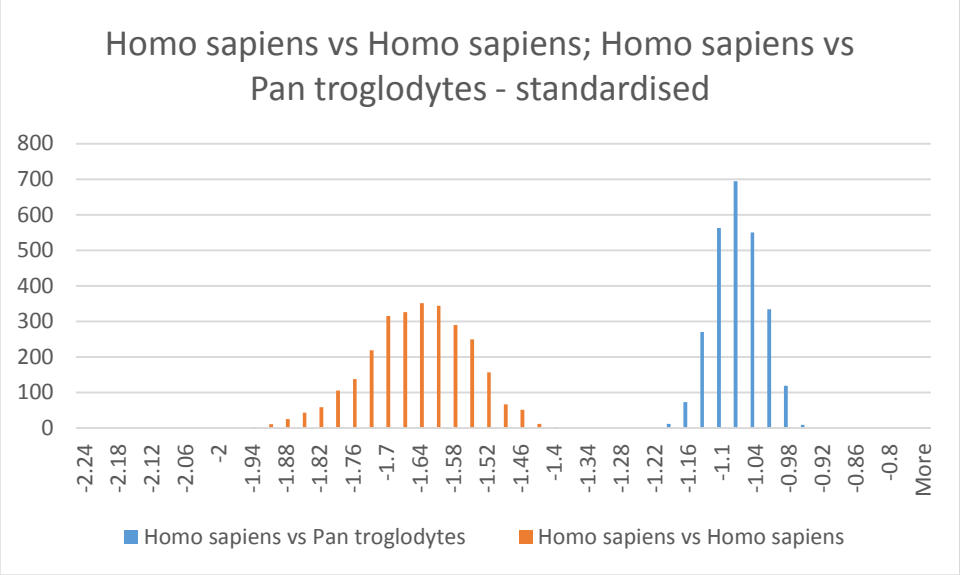

Figure 3.18 Illustrative frequency diagram for log se_m values for 2775 intra-species comparisons of cranial measurements of *Homo sapiens* (red), compared to 2625 inter- species comparisons (*Homo sapiens* vs. *Pan troglodytes* (blue)). As can be seen, the intra- and inter-species values for *Homo sapiens* and *Pan troglodytes* do not overlap.

It needs to be recalled that for each pairwise comparison between any two specimens, two different log se_m values will be produced: the first value being calculated when specimen A is placed on the x axis with specimen B on the y axis, and a second value when specimen A is placed on the y axis with specimen B on the x axis. These values are both placed in a log se_m matrix with paired values being located equidistantly from each other, reflected orthogonally to each other via the (empty) diagonal in the matrix. A partial matrix is reproduced in Table 3.7 below to illustrate this point:

Table 3.7 Illustrative log se_m matrix showing paired x-on-y and y-on-x values for pairwise comparisons (intra-specific (yellow) and inter-specific (orange)).

	OH7L	OH7R	OH16R	SK6L	SK6R	SK23L	SK23R
OH7L		-1.870	-1.581	-1.325	-1.393	-1.333	-1.300
OH7R	-1.863		-1.645	-1.366	-1.425	-1.367	-1.333
OH16R	-1.631	-1.701		-1.352	-1.364	-1.355	-1.367
SK6L	-1.432	-1.479	-1.409		-1.709	-1.802	-1.676
SK6R	-1.494	-1.533	-1.415	-1.704		-1.639	-1.523
SK23L	-1.393	-1.433	-1.365	-1.755	-1.598		-1.710
SK23R	-1.339	-1.379	-1.356	-1.608	-1.461	-1.690	

When two specimens are similarly sized and have similar morphologies, it is expected that not only will there be very little scatter around the slopes m of the two regression lines (which will be similar in their coefficient m due to the similar size of the specimens), but that the two log se_m values produced will also be close in value, both being low values (in the above example, the two intra-specific comparisons shown in yellow produce paired values of -1.645 and -1.701 (differential of 0.057) and of -1.802 and -1.755 (differential of 0.047)). This is due mainly to two phenomena: firstly, specimens that are nearly identical will produce very little scatter of datapoints around the two regression lines because of their similarity in morphology. Secondly, if the specimens are nearly identical in size as well as shape, their regression lines will both approach a gradient of 1 (45˚), so the vertical (y) and horizontal (x) measurements of each datapoint to each line will be similar. In such instances, the values of the two standard errors of the slopes and thus the two log se_m values for the x-on-y and the y-on-x pairwise regressions will be very close to each other in value. If, however, specimen A is of a different size and morphology to specimen B, not only will the amount of scatter around the regression line be larger but also the coefficients of the slopes are expected to be dissimilar due to the difference in size, and the calculated value of the larger degree of scatter around both slopes is thus expected to be further exaggerated for the two lines individually since one line will be more vertical and the other more horizontal. In these cases, the log se_m values are expected to be higher in value with more divergence between them (in the above example, the paired values (in orange) are -1.432 and -1.325, with a differential between the two of 0.107) because the y measurements will be larger than the x measurements in the one instance, and the x measurements will be larger than the y measurements in the other, so both slopes (m)

and both log se_m values need to be examined to test for such divergences in value between them. Two examples illustrate this point in Figure 3.19 below. Antimeres are similar in both size and morphology, so their lines will be almost at a gradient of 1, and the degree of scatter between them is reduced due to similarities in shape. A small, narrow tooth (KNM-ER 992 L in this example) and a large, relatively wider tooth with a different arrangement of landmarks (Peninj 1 L) will present very different paired log se_m values:

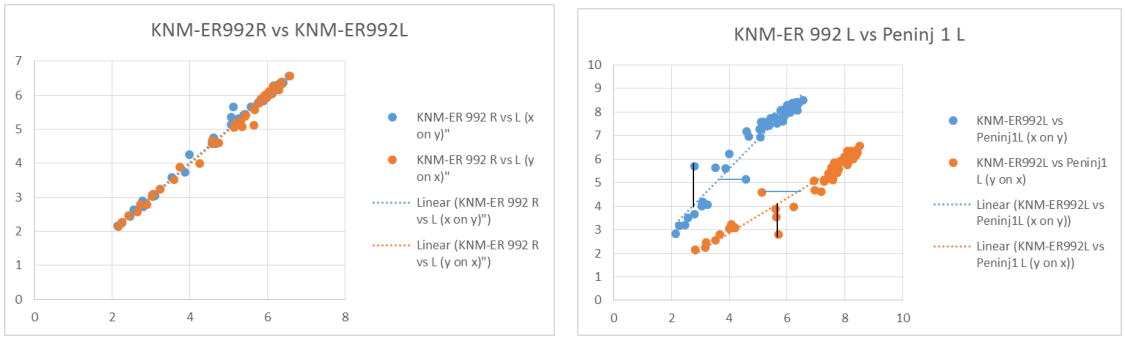

a) b)

Figure 3.19 Illustrative examples of x-on-y and y-on x pairwise comparisons for a) conspecific, almost identically-sized specimens and b) differently-shaped and differently-sized specimens from different species. **In the case of non-specific, differently sized comparisons (b), the horizontal distances (x-values) from each point to both lines differ, as do the vertical (y-value) distances. In the case of the conspecific pair (a), both lines are almost on an equal gradient of 1, so the vertical and horizontal distances from either line are almost equidistant. The degree of scatter for the conspecific pair is also very small. The paired log se_m value in the first instance are -1.911 and -1.910 (differential of 0.001 between them) and in the second instance, they are -1.304 and -1.531 (differential of 0.227 between them).**

Tables 3.8 and 3.9 below summarise the expectations in terms of log se_m values for these two scenarios:

Table 3.8 Expectations for pairwise comparisons between two specimens of similar size and morphology (likely to be "conspecific"):

Log se_m values	Log se_m values	"false positives"
Both values tending to be low values if conspecific	Smaller differential between the two values (smaller degree of scatter around the lines and closer slope coefficients minimising the difference in values).	Less probable

Table 3.9 Expectations for pairwise comparisons between two specimens of different size and morphology (unlikely to be "conspecific"):

Log se_m values	Log se_m values	"false positives"
At least one value tending to be high; usually both	Higher differential between the two values (High degree of scatter and different slope coefficients maximising the differential between the two values)	More probable, based on the lower of the two values.

For these reasons, when comparing specimens of variable size and morphology, an analysis of only one of the two log se_m values is not adequate: it is useful to analyse the log se_m matrix carefully to identify cases where the "differential" between the two values is highly divergent, as this will provide confirmation that although one of the two values might imply a probability of conspecificity, the other one may imply the opposite probability, thus these are not likely to be members of the same species. This "differential" is named the "delta value" between the two log se_m values (Dykes and Thackeray, unpublished manuscript). Two specimens with a high delta value between the two log se_m values can be said to show a high variability of size, morphology or, more usually, both.

A further helpful analysis is to take the average value between both log se_m values for each pairwise comparison. By comparing the average of the two pairwise log se_m values, an idea can be obtained more of the morphometric (rather than size-based)

differences between the two specimens, since the average log se_m value would be indicative of the value obtained if both regression lines (i.e. both slopes) were averaged themselves. By comparing the average log se_m values alongside the delta values for each pairwise comparison against the group averages for both types of value, a better-informed assessment can be made regarding probabilities of conspecificity between each pair of specimens.

Another note of caution should be employed for species where there is a high degree of sexual dimorphism. There might be a wider range of log se_m values for intra-species comparisons in the case of gorillas, for example, with some high delta values occurring between large males and juvenile males or females of the same species. The opposite would be expected to be true of a species where relatively little sexual dimorphism is evident for the skeletal element being compared – for example, in the case of crania of modern *Homo sapiens.* The scenario described in the second of the two tables above can thus apply to scenarios of dissimilarity between species as well as to scenarios of dissimilarity within the same species where a high degree of sexual dimorphism is evident, particularly if morphological differences accompany size differences between the genders (such as is the case for male and female gorilla crania).

3.6.2 Summary – analyses carried out

Several analyses with distinct methodological bases were chosen for this exploratory study, principally aimed at confirming trends in size and shape features between teeth, as well as the identification of potential misclassifications of any of the specimens chosen for the study (Table 3.10). With an emphasis on independent approaches to

confirm initial findings, rather than carrying out one single type of analysis in great depth, the level of detail used for each analysis was necessarily fairly limited, but despite this, the methods were adequate to test initial visual results from the PC plots.

Table 3.10 Summary table of analyses

Analysis	Aim
Linear Dimension analyses	a) To test for basic differences between species, genders and antimeres b) To test for trends of relative dimensions between fossil specimens (species diagnostics; trends over time)
Generalised Procrustes Analysis	a) Shape analysis used as the basis for further analyses (PCA, etc.) b) Flexibility of this GM method ("Full" or "Partial" superimposition) allows for the role of size to be examined in differentiating between specimens (relevant in the case of teeth) c) Procrustes Distance Matrix compares shapes, quantifying shape "distances" of one specimen to another.
Principal Components Analysis	Main uses for this study: a) Provides a basic spatial visualisation of the main factors of shape (or size-and-shape) variability (covariance) between specimens. b) Flexibility of carrying out two analyses – based on "Procrustes Shape Space" and "Procrustes Form Space", allowing for an immediate visual comparison of grouping of specimens with size factored in or out of the analysis.
Discriminant Function Analysis	A classification analysis that can potentially identify misclassifications of specimens in terms of their allocated groups.
Log se_m	A probability function that aims to assess the likelihood of two specimens being conspecific or not

CHAPTER FOUR – RESULTS

4.1 Introduction

As discussed in 3.6 above, the study was divided into two phases. Phase I was carried out, a) to test the "inputs" to the analyses to see if the qualitative diagnostics of teeth from different species were being adequately translated into quantitative data so that species groups plotted out on a PC analysis in the expected way (did morphometrics reflect morphology?); and b) to ascertain the significance of retaining size in the principal components analyses on the teeth, which was conducted firstly on the extant species specimens and secondly on the fossils. Based on the results from Phase I, Phase II was aimed at analysing the teeth using a suite of differing types of analysis, to test the robustness of initial results.

Results are set out as follows:

<u>Phase I PCA</u>	Visualisation of species groupings to confirm adequacy of inputs (landmark model; role of size in species diagnostics) A) Extant species, shape analysis B) Extant species, "shape-and-size" analysis C) Fossil species, "shape-and-size" analysis, visual check for expected basic grouping of species to confirm inputs
<u>Linear dimension analyses</u>	Modern *Homo sapiens:* - MD:BL plot - Tooth area and dimension statistical comparisons Extant Primate Species: - MD:BL plot - Tooth area and dimension statistical comparisons Fossil molars: - MD:BL plot - MD:BL plot over time - Identification of potential anomalies

Phase II PCA	Visual analysis of grouping patterns, identification of potential anomalies - Extant species: shape and size analysis with examination of grouping patterns (sexual dimorphism, etc.) - Fossils: shape and size analysis with examination of grouping patterns and potential anomalies - Fossils with extant species as outgroups : Fossils plus *Pan paniscus* Fossils plus *Pan troglodytes* Fossils plus *Gorilla gorilla* Fossils plus modern *Homo sapiens* Fossils plus four extant species together
Procrustes distance matrix	Shape analysis on fossil specimens by species group
Discriminant Function Analysis	- Extant species - Fossil specimens – identification of anomalies
Log se_m analysis	- Extant species • Intra-specific comparisons • Inter-specific comparisons - Fossil specimens • Intra-specific comparisons • Matrix analysis by species; inter-specific comparisons for larger groups • Identification of potential anomalies

4.2 Phase I – Testing of "inputs" – landmark model tests to ascertain the importance of scaling in the analyses

Since the results of this phase of landmark testing are used to dictate the format of the principal components analyses for the remainder of the study ("shape only" analysis, or "shape-and-size" analysis?), this section will include a full discussion of the results obtained from the principal components analyses on the extant species and the fossil species. In the "Discussion" chapter, only the results of Phase II (the actual analysis of the data itself) will be included.

4.2.1 Extant species – Test for species differentiation with and without size included as a parameter using a principal components analysis

The landmark model (49 landmarks) was tested for its ability to differentiate diagnostically between species, using the 80 molars selected to represent the four extant species used in the study, before being applied to the 36 fossil molar specimens (see Materials, 3.2.2. above). Using this landmark placement model, a principal components analysis was carried out in Morphologika (O'Higgins & Jones, 2006), having first transformed the data using a full Procrustes superimposition (see also 3.6 for a discussion on the methods used for the study).

4.2.2 Prior expectations from shape-only analyses vs. size-and-shape analyses

In the absence of size considerations to distinguish between species, it was expected, based on visual inspections of the images captured for this study and on measurements taken (see Figure 4.1 and paragraph 4.3.1.2 below), that the three great ape species might overlap somewhat on a shape-only analysis, particularly in the case of bonobos (*Pan paniscus*) and common chimpanzees (*Pan troglodytes).* Both of these species might also overlap slightly with the gorilla specimens in the absence of size considerations, particularly if the chimpanzee or bonobo specimens were slightly narrower than usual, or if the gorilla specimens were wider than the average. As for the modern *Homo sapiens* sample, molar shape was much more unpredictable than for the other species.

Modern *Homo sapiens*: rounded and regular; usually relatively wider than the great ape species, although width is variable	Gorillas: very large, but proportionally, consistently very narrow with uneven, pronounced cusps
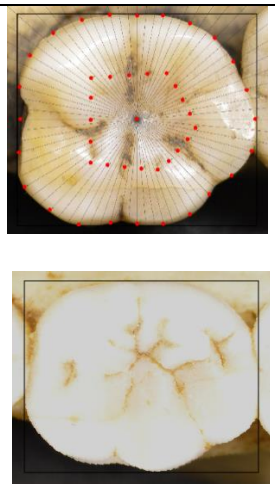	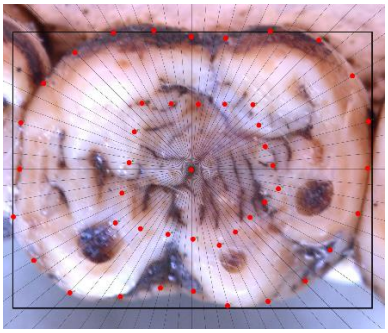
Chimpanzees: consistently narrow; uneven cusps	Bonobos : consistently narrow; uneven cusps
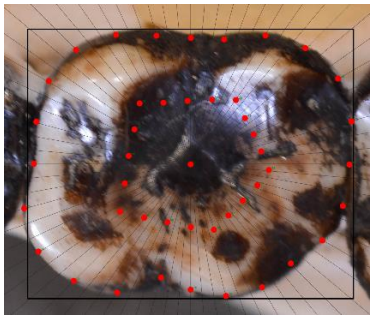	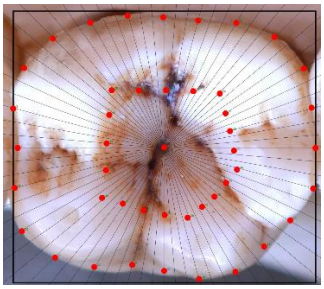

Figure 4.1 Typical shapes of modern human, gorilla, chimpanzee and bonobo mandibular first molars.

To confirm the importance of size when comparing teeth, the principal components analysis was first performed as normal, based on Procrustes "shape space" (with the PCA being based on a full Procrustes superimposition, whereby objects are translated, rotated and scaled to factor size differences out between them) and secondly in Procrustes "form space" (the log of the centroid is factored in as a variable to the analysis to enable size to be analysed as well as shape (Mitteroecker et al. 2004)).

4.2.3 Results of the shape-only and size-and-shape analyses

The following figures (Figures 4.2 and 4.3) illustrate the differences between a shape analysis and a size-and-shape analysis, in the context of teeth:

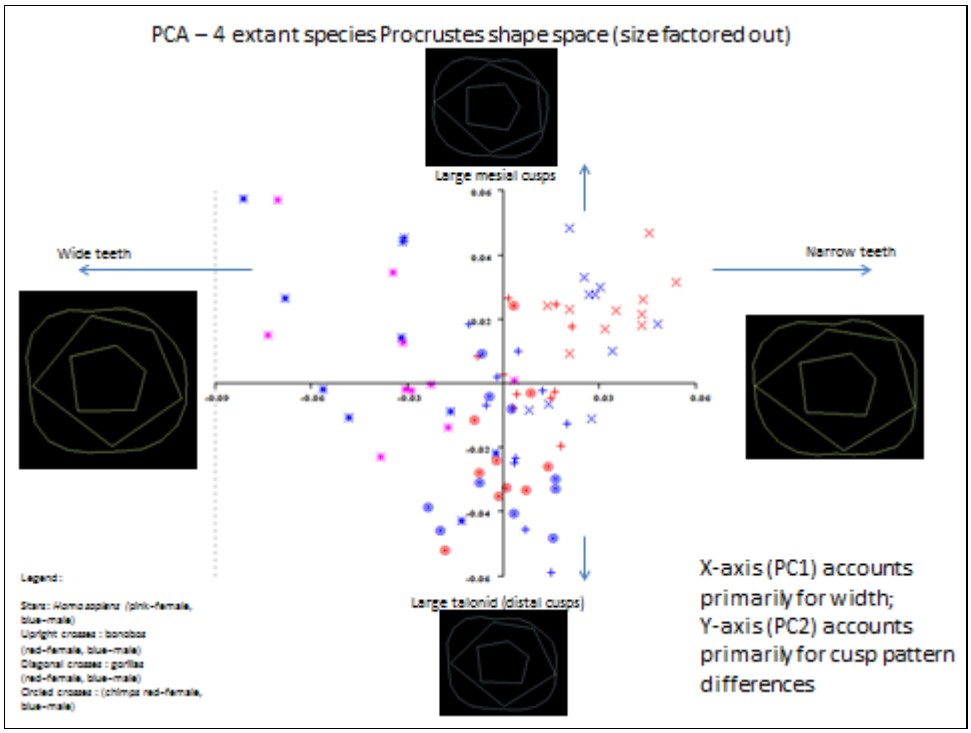

Figure 4.2 – Procrustes shape space analysis of lower first molars of four extant species (n=20 per species; 49 landmarks each specimen); in this analysis, data are rotated, translated and scaled. **With size differences between specimens not factored into the analysis, and shape alone determining the covariance results, relative width of tooth becomes a major distinguishing factor as shown by PC1 along the x-axis (reflected by the relative warps wireframe images; PC1: 28% of the covariance). There is significant overlap between species, particularly chimps and bonobos, once size is no longer a factor to differentiate between molars.**

Since size has been factored out of this (shape only) analysis, the primary differentiator between species is relative width of tooth, and this is the main factor depicted along the x-axis (PC1= 28.0% of the variance). PCs 2 and 3 accounted mainly for some elements of cusp arrangement changes (PC2= 25.4% of the variance). With no size differentiation, there is overlap between bonobos and gorillas, bonobos and chimpanzees and chimpanzees and gorillas where their relative width is similar, as well as some overlap between modern *Homo sapiens,* chimpanzees and bonobos.

A second Principal components analysis was then conducted with the addition of a size factor (log of the centroid size added), to produce a "size-and-shape" analysis (Procrustes "form space"). The results are shown in Figure 4.3 below.

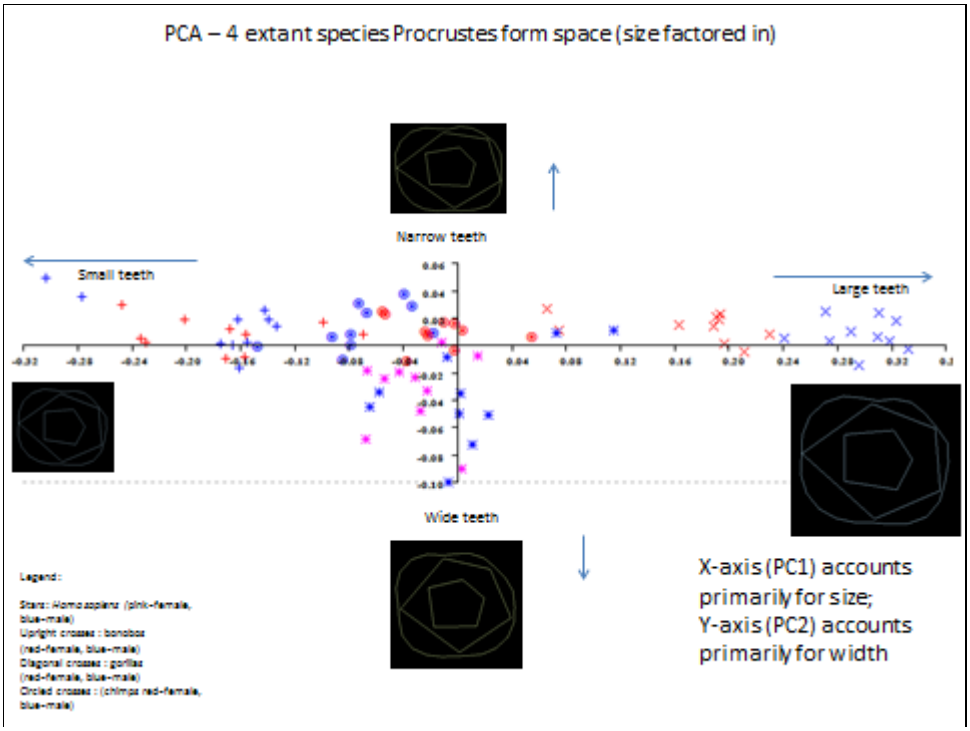

Figure 4.3 – Procrustes form space analysis of lower first molars of four extant species (n=20 per species; 49 landmarks per specimen); in this analysis, data are rotated and translated and *size is added* to the analysis by means of the log of the centroid size. **With size now differentiating between specimens, size itself becomes the major determining differentiator between molars (x-axis, PC1: 90.6% of covariance), with relative width (formerly the main contributor to covariance) now accounting for most of the covariance along the y-axis, PC2. There is less overlap between species, particularly between chimps and bonobos and no longer any overlap at all between gorillas and bonobos; size-related sexual dimorphism between male and female gorillas also now becomes apparent.**

In this size-and-shape analysis, size is now the dominating factor along the x-axis (PC1 = 90.6% of the variance), with relative width of the tooth (formerly PC1) now accounting for the second principal component (y-axis: PC2 = 2.8% of the variance). Along both axes there is an element of cusp pattern change and perimeter shape change in addition to the size and relative width components, although size is now highly correlated to PC1 due to the log of the centroid size being a variable in the analysis. The correlations between centroid size and the first principal components axes from both analyses are shown below in figure 4.4.

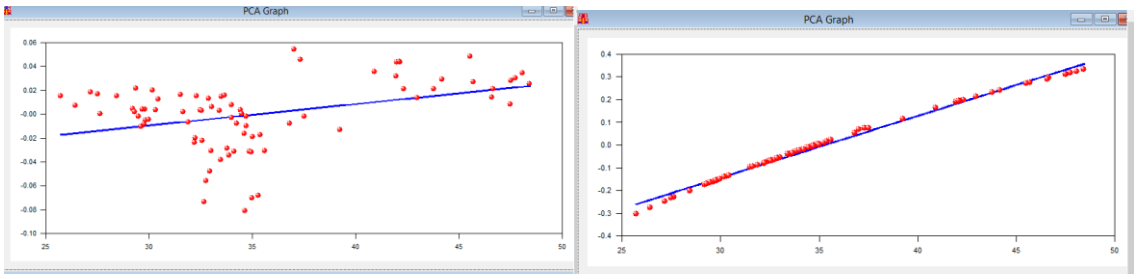

a) b)

Figure 4.4 PCA results for 4 extant species: PC1 correlated to centroid size, a) using Procrustes shape space which includes scaling; R^2= 0.132; b) with size factored in to the variables by means of the log of centroid size (Procrustes form space; R^2= 0.997). The high correlation in b) is to be expected, since the log of centroid size is a variable in the shape analysis. There are components of peripheral shape and cusp arrangement also represented within the first principal component.

In the "form space" analysis, there is still some slight overlap between species towards the middle of the chart, but with size factored into the analysis, gorilla specimens no longer overlap with bonobo specimens or chimpanzee specimens. Modern *Homo sapiens* molars, which overlap in size with a few large bonobo teeth, some similarly-sized chimpanzee teeth and one very small female gorilla tooth are seen to overlap in size range (around the middle of the x-axis, where "medium-sized teeth" are grouped), but the majority of the Modern *Homo sapiens* sample tends to be wider than the molars of the great ape species, thus they tend to group towards the negative side of the y-axis, where wider teeth are located. In addition to the above, gorilla male molars no longer overlap with gorilla female molars for the sample used. Overall, the results from this principal components plot are in keeping with the observations made in 4.2.2 above, in that the species groups are reasonably differentiated, with some overlap at the extremes, just as is observed in nature.

In sum, the results of these analyses show that size appears to be a major diagnostic feature for differentiating between species, followed by relative width, and then by changes in cusp pattern arrangement. Overlaps on the PC plot concur with potential areas of overlap discussed in 4.2.2 above (small chimpanzees-large bonobos; very

narrow modern *Homo sapiens* teeth with medium-sized great ape teeth (i.e. mainly chimpanzee teeth, and the smallest female gorilla tooth).

In light of the above, for the remainder of the study, it was decided to proceed with principal components analyses based on Procrustes **form space**, in the knowledge that the first principal component in any graph based on form space would have a high correlation with the **size** of the specimens (because the log of centroid size is included as a variable for each shape in the analysis), together with additional contributions that would be made factors of variability in peripheral shape and of cusp arrangement. The choice of y-axis (the selection of the remaining principal component for depiction in the graphs – PC2 or PC3, for instance) would in each case be based primarily on which principal component was most reflective of **relative tooth width**, because in the analyses conducted on the extant species based purely on shape (with size factored out), the first principal component then accounted primarily for relative width differences, together with some factor of shape/cusp arrangement variability. (Furthermore, relative tooth width is, as noted in Figure 4.2 above, a primary diagnostic feature used by morphologists to make taxonomic assessments of lower first molars, so it is useful to ensure that the y-axis reflects relative width as well as some feature of cusp variation in each case).

In Morphologika, it is possible to inspect the shape changes being depicted along each axis using the wireframe tool. Relative warps (showing a visual depiction of shape change) can be examined visually using the slider tool in the software. It is therefore possible to examine PC2, PC3 and additional principal components by selecting them as the y-axis component and viewing the change in the shape of the wireframe relative

warps as the slider progresses from the minimum value to the maximum value. In this manner, it is possible to determine which of the principal components accounts mainly for changes in width (together with some measure of cusp arrangement variability) and which of the principal components accounts mainly for cusp arrangement variation alone, with little contribution made by tooth width variation.

4.2.4 Fossil hominin species – application of parameters identified in extant species analysis to test for fossil species differentiation using PCA

The 49-landmark model was then similarly applied to images of the fossil hominin molars, and the data were analysed in Morphologika, using a Procrustes form-space principal components analysis as described above. A regression analysis between PC1 and centroid size determined that PC1 was highly correlated to size (which is logical, since each shape in "Procrustes form space" is anyway multiplied by the log of the centroid size). Importantly, there is a component of cusp arrangement also reflected along the same axis (in particular, the absence or presence of a sixth cusp), as seen by the relative warp changes along the axis. Using relative warp factors similarly as a guide for the choice of which principal component to reflect along the y-axis, it was determined that it was PC3 that reflected principally the relative width of the teeth (together with a factor contributed by variability in cusp arrangement, notably the size of the metaconid). Once PC3 had been selected to reflect principally relative width of tooth, it could be seen that relatively wide teeth would plot towards the negative side of the y-axis and relatively narrow teeth would plot towards the positive side. Before any attempt was made to colour code the specimens according to their currently accepted species classifications, predictions were made as to where on the plot each species would be expected to be located, based on the morphological diagnostic features

examined prior to embarking on the landmark model assessments (2.3.6 above). Figure 2.11 is repeated below by way of explanation for the basis of the predictions for the locations of the specimens on the PC plot. Although the PC analysis is not identifying solely overall size along the x-axis and solely overall width along the y-axis (there are cusp pattern features also being identified in the analysis for both axes), the majority of the covariance along each axis is explained by the "gross size" (x-axis) and "relative width" (y-axis) features.

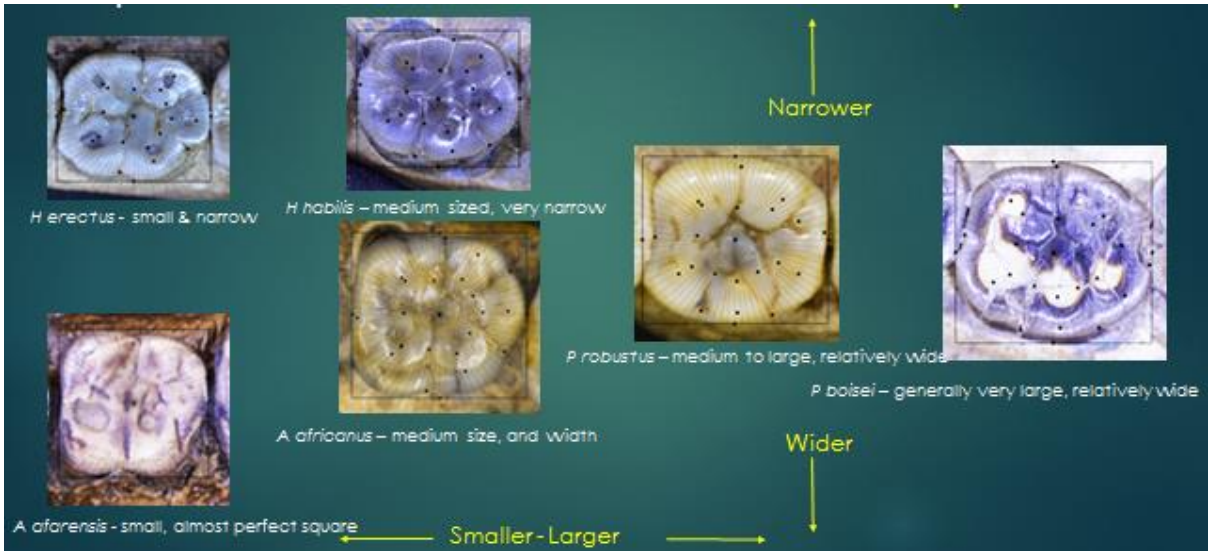

(Figure 2.11 repeated). Molars are arranged on this chart according to relative size (left to right) and relative width (narrow to wide, top to bottom). This is the type of arrangement to be expected for the arrangement of species groups on a PC plot where PC1 (x-axis) reflects mainly size differences and where PC2 or 3, as the case may be, (y-axis) reflects mainly width variability.

A. afarensis, for example, should plot to the left of the y-axis (where x would be negative, where relatively smaller teeth should be grouped), because typical *A. afarensis* molars are smaller on average than *A. africanus* molars and certainly significantly smaller than *P. robustus* and *P. boisei* molars, but being generally very wide teeth with large metaconids, they would be found towards the negative extreme of the y-axis; *Paranthropus robustus* should be found along the positive side of the x-axis, being extremely large, with a C_6 present. Less square in shape than *A. afarensis,* but not as

narrow as *H. habilis,* these molars would be scattered on either side of the x-axis. *Homo erectus* should be in the negative x but positive y quadrant, being the smallest in overall size of the fossil molars, but also very narrow compared to the others in the sample. Molars falling into the "Early *Homo*" group – *Homo habilis, Homo rudolfensis*, for example, would be expected to be close to the y axis (neither as large as *Paranthropus* nor as small as *Homo erectus*) but above the x-axis (on the narrower side); *Australopithecus africanus*, by contrast, while also "medium-sized" compared to *Paranthropus* and *Homo erectus,* should fall below the x-axis, being wider than the "Early *Homo*" group. Figure 4.5 illustrates these expected positions on the PC plot, while Figure 4.6 shows that specimens largely grouped as predicted once colour codes for species were added.

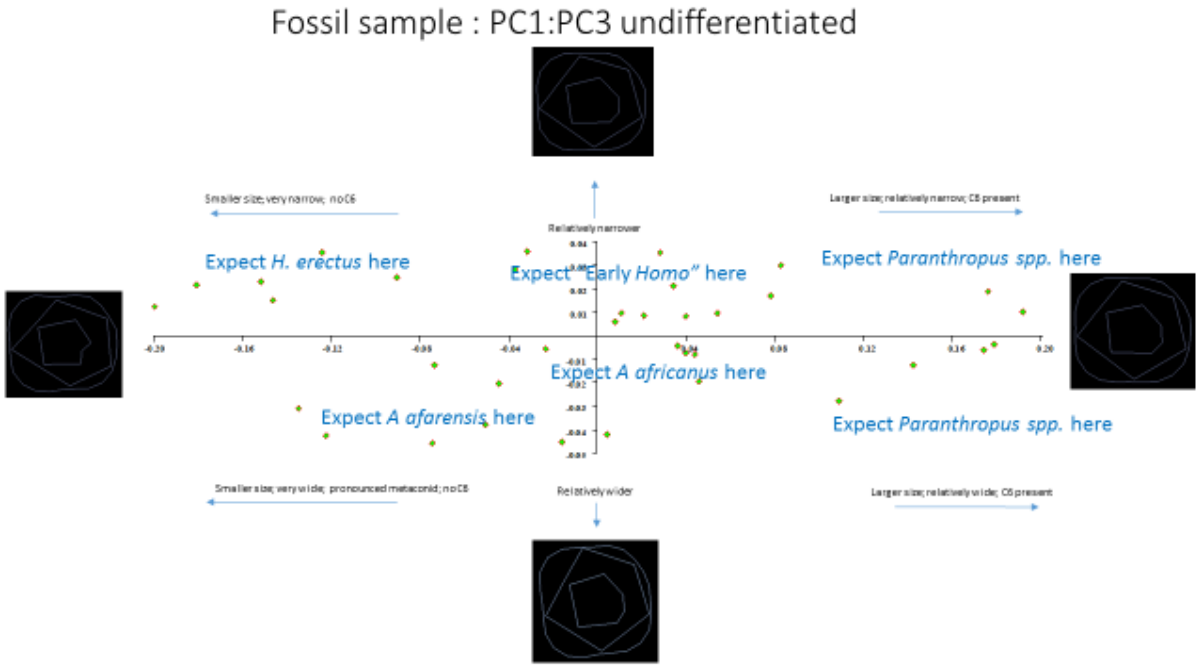

Figure 4.5 "Undifferentiated" Procrustes form space principal components analysis of lower first molars of African Plio-Pleistocene lower first molars attributed to seven species (n=36) **to test the landmark model's ability to differentiate correctly between currently accepted species; in this analysis, data are rotated and translated *and size is factored in to the analysis*. PC1 accounts primarily for size plus the absence or presence of a sixth cusp, PC3 (y-axis) accounts mainly for relative width of tooth plus elements of cusp differences (particularly in the relative size of the metaconid).**

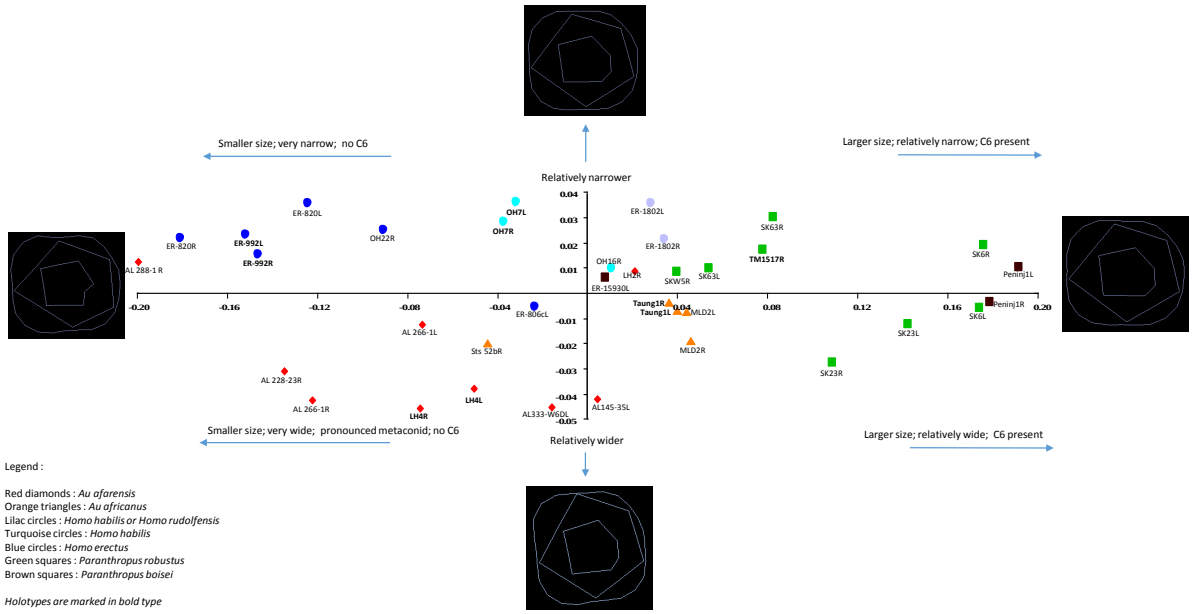

Figure 4.6 "Colour-coded" Procrustes form space principal components analysis of lower first molars of African Plio-Pleistocene lower first molars from seven presumed species (n=36) **to confirm the landmark model's ability to differentiate between currently accepted species; the currently allocated species groups largely plot according to the quadrants/zones in which they were predicted to be found according to the expectations shown in Figure 2.11 above.**

Since most specimens from each species group were located in the areas where they would be expected to be found on the PC plot, the landmark model (based on 49 landmarks) was considered to have adequately "translated", in a quantitative manner, the diagnostic features of various fossil molar species, as described above in 2.3.6 in qualitative terms. There were a few specimens that failed to group perfectly in the areas where they would most be expected to be located on the plot. These are analysed separately in Phase II of the study (testing of "outputs").

4.2.5 Implications of (Phase I) "inputs" tests for the remainder of the study (testing of "outputs", Phase II)

For the remainder of the study, the landmark model of 49 landmarks, based on Procrustes Form Space (size factored in as a variable) was adopted for all principal components analyses and discriminant function analyses. The model proved to be adequately balanced for these analyses to be able to identify size and relative width traits as well as more subtle characteristics of cusp arrangements of the lower first molars for both extant and fossil species.

Log se_m results were discussed, with qualifications, in the light of the absence or presence of size as a distinguishing factor between species, both extant and fossil.

Once the "inputs" had been adequately tested, the remainder of the study focused on testing the "outputs" – the initial findings as described by the PC

4.3 Phase II – testing of "outputs" – additional analyses carried out on the specimens

4.3.1 Linear Dimension analyses

4.3.1.1 Modern humans (*Homo sapiens)*:

Mesiodistal (uncorrected) and buccolingual (maximum) diameter measurements were taken using callipers from 38 male-female paired individuals of modern *Homo sapiens* housed at the Raymond Dart Collection at the University of the Witwatersrand (see Tables 4.1 and 4.2). Area measurements ("computed crown area" / CCA = MD*BL

diameters) as well as the mesiodistal:buccolingual ratios (MD/BL diameters) were compared for left and right antimeres from both genders and then comparisons were made between genders to ascertain how much variability in size and width of tooth there might be within the human sample. The measurements and ratios are presented in Table 4.1 below. Mesiodistal and buccolingual diameters for molars of both genders were then plotted on a graph, presented in Figure 4.7. Lastly, statistical analyses were conducted to ascertain the differences in area (computed crown area, MD*BL) and in MD:BL ratio between antimeres for each gender and between genders. Results are set out in Tables 4.2 and 4.3.

Table 4.1 Measurements from lower first molars of modern *Homo sapiens*

M1													
Accession no	Pop group	m/f	age	tooth	MD	BL	MD/BL	MD antimere	BLantimere	MD FL-MR.ar	BL FL-MR.ant	MD gender	BL gender
2179	EURO	F	19	MAND M1 L	10.21	10.07	1.01	1.00	0.99	0.98	1.01	0.95	0.98
863	XOSA	F	20	MAND M1 L	11.41	10.08	1.13	1.02	1.00	1.02	0.90	1.07	0.93
935	ROLO	F	20	MAND M1 L	10.55	10.16	1.04	1.00	1.04	0.95	0.92	0.96	0.90
381	ZULU	F	29	MAND M1 L	11.54	11.16	1.03	1.02	1.08	0.96	1.06	0.94	1.03
1319	ZULU	F	20	MAND M1 L	10.42	10.32	1.01	0.98	1.00	0.96	0.98	0.92	0.95
4035	S.A.N.	F	22	MAND M1 L	10.72	9.66	1.11	1.01	1.04	0.88	0.79	0.84	0.77
1263	SOTHO	F	18	MAND M1 L	11.36	10.05	1.13	0.96	1.00	1.06	0.96	1.05	0.97
900	SWAZ	F	26	MAND M1 L	10.44	9.26	1.13	0.97	0.97	0.84	0.79	0.86	0.80
263	SHAN	F	30	MAND M1 L	10.84	10.78	1.01	0.96	0.98	0.94	1.00	0.92	1.02
1903	VEND	F	24	MAND M1 L	10.91	10.06	1.08	1.00	0.95	0.89	0.89	0.93	0.89
1954	NDEB	F	30	MAND M1 L	10.14	9.40	1.08	0.99	0.99	0.91	0.90	0.91	0.93
1483	TSWA	F	19	MAND M1 L	11.76	10.49	1.12	1.00	0.97	0.93	0.91	0.93	0.90
3319	MIXED	F	33	MAND M1 L	10.62	9.66	1.10	1.01	0.96	1.01	0.96	1.04	1.05
3607	MIXED	F	40	MAND M1 L	11.84	11.21	1.06	1.04	0.99	1.15	1.09	1.15	1.06
84	FING	F	38	MAND M1 L	11.01	10.13	1.09	1.00	0.99	0.94	0.94	0.94	0.98
3894	N/S	F	35	MAND M1 L	11.41	10.31	1.11	0.98	0.95	0.95	0.95	0.96	0.96
3469	MIXED	F	25	MAND M1 L	11.22	10.40	1.08	0.99	0.96	0.93	0.90	0.93	0.91
27	BUSH	F	N/A	MAND M1 L	11.29	10.27	1.10	1.00	0.97	0.99	0.97	1.02	0.95
320	BUSH	F	N/A	MAND M1 L	10.41	9.98	1.04	1.02	1.07	0.85	0.93	0.79	0.90
					10.95	10.18	1.08	1.00	0.99	0.95	0.94	0.95	0.94
Accession no	Pop group	m/f	age	tooth	MD	BL	MD/BL	MD antimere	BLantimere	MD FL-MR.ar	BL FL-MR.ant	MD gender	BL gender
2179	EURO	F	19	MAND M1 R	10.25	10.20	1.00					0.98	1.02
863	XOSA	F	20	MAND M1 R	11.20	10.10	1.11					1.00	0.90
935	ROLO	F	20	MAND M1 R	10.60	9.75	1.09					0.96	0.88
381	ZULU	F	29	MAND M1 R	11.33	10.38	1.09					0.95	0.98
1319	ZULU	F	20	MAND M1 R	10.60	10.33	1.03					0.97	0.98
4035	S.A.N.	F	22	MAND M1 R	10.58	9.32	1.14					0.87	0.76
1263	SOTHO	F	18	MAND M1 R	11.79	10.06	1.17					1.10	0.97
900	SWAZ	F	26	MAND M1 R	10.75	9.53	1.13					0.87	0.82
263	SHAN	F	30	MAND M1 R	11.35	10.97	1.03					0.98	1.02
1903	VEND	F	24	MAND M1 R	10.93	10.58	1.03					0.89	0.93
1954	NDEB	F	30	MAND M1 R	10.21	9.54	1.07					0.91	0.91
1483	TSWA	F	19	MAND M1 R	11.74	10.78	1.09					0.93	0.93
3319	MIXED	F	33	MAND M1 R	10.50	10.02	1.05					1.00	0.99
3607	MIXED	F	40	MAND M1 R	11.42	11.38	1.00					1.11	1.11
84	FING	F	38	MAND M1 R	11.01	10.25	1.07					0.94	0.95
3894	N/S	F	35	MAND M1 R	11.68	10.85	1.08					0.97	1.00
3469	MIXED	F	25	MAND M1 R	11.37	10.84	1.05					0.95	0.94
27	BUSH	F	N/A	MAND M1 R	11.34	10.59	1.07					0.99	1.00
320	BUSH	F	N/A	MAND M1 R	10.25	9.36	1.10					0.84	0.87
					10.99	10.25	1.07					0.96	0.95
Accession no	Pop group	m/f	age	tooth	MD	BL	MD/BL	MD antimere	BLantimere	MD FL-MR.ar	BL FL-MR.ant	MD gender	BL gender
3109	EURO	M	15	MAND M1 L	10.78	10.24	1.05	1.03	1.03				
973	XOSA	M	18	MAND M1 L	10.70	10.80	0.99	0.96	0.97				
1860	ROLO	M	22	MAND M1 L	11.03	11.34	0.97	1.00	1.03				
3360	ZULU	M	47	MAND M1 L	12.33	10.88	1.13	1.03	1.03				
3770	ZULU	M	23	MAND M1 L	11.27	10.88	1.04	1.03	1.03				
4037	S.A.N.	M	24	MAND M1 L	12.83	12.49	1.03	1.06	1.02				
691	SOTHO	M	18	MAND M1 L	10.79	10.40	1.04	1.01	1.00				
1570	SWAZ	M	32	MAND M1 L	12.20	11.56	1.06	0.99	0.99				
924	SHAN	M	30	MAND M1 L	11.76	10.57	1.11	1.02	0.99				
821	VEND	M	25	MAND M1 L	11.77	11.33	1.04	0.96	1.00				
927	NDEB	M	37	MAND M1 L	11.09	10.07	1.10	0.99	0.97				
1264	TSWA	M	23	MAND M1 L	12.58	11.68	1.08	0.99	1.01				
2093	MIXED	M	23	MAND M1 L	10.18	9.22	1.10	0.97	0.91				
3421	MIXED	M	60	MAND M1 L	10.34	10.54	0.98	1.00	1.03				
861	FING	M	34	MAND M1 L	11.77	10.37	1.14	1.00	0.96				
3906	N/S	M	40	MAND M1 L	11.85	10.77	1.10	0.99	0.99				
3386	MIXED	M	34	MAND M1 L	12.03	11.41	1.05	1.00	0.99				
173	BUSH	M	N/A	MAND M1 L	11.10	10.85	1.02	0.97	1.03				
28	BUSH	M	N/A	MAND M1 L	13.12	11.08	1.18	1.08	1.04				
					11.55	10.87	1.06	1.00	1.00				
Accession no	Pop group	m/f	age	tooth	MD	BL	MD/BL	MD antimere	BLantimere	MD FL-MR.ar	BL FL-MR.ant	MD gender	BL gender
3109	EURO	M	15	MAND M1 R	10.47	9.97	1.05						
973	XOSA	M	18	MAND M1 R	11.17	11.19	1.00						
1860	ROLO	M	22	MAND M1 R	11.06	11.02	1.00						
3360	ZULU	M	47	MAND M1 R	11.96	10.56	1.13						
3770	ZULU	M	23	MAND M1 R	10.89	10.56	1.03						
4037	S.A.N.	M	24	MAND M1 R	12.12	12.23	0.99						
691	SOTHO	M	18	MAND M1 R	10.73	10.42	1.03						
1570	SWAZ	M	32	MAND M1 R	12.36	11.67	1.06						
924	SHAN	M	30	MAND M1 R	11.57	10.73	1.08						
821	VEND	M	25	MAND M1 R	12.27	11.33	1.08						
927	NDEB	M	37	MAND M1 R	11.18	10.43	1.07						
1264	TSWA	M	23	MAND M1 R	12.67	11.56	1.10						
2093	MIXED	M	23	MAND M1 R	10.54	10.09	1.04						
3421	MIXED	M	60	MAND M1 R	10.29	10.26	1.00						
861	FING	M	34	MAND M1 R	11.72	10.78	1.09						
3906	N/S	M	40	MAND M1 R	12.02	10.85	1.11						
3386	MIXED	M	34	MAND M1 R	12.01	11.55	1.04						
173	BUSH	M	N/A	MAND M1 R	11.44	10.58	1.08						
28	BUSH	M	N/A	MAND M1 R	12.20	10.70	1.14						
					11.51	10.87	1.06						

Column headings: MD = Mesiodistal diameter; BL= Buccolingual diameter; MD or BL antimere = the ratio of the mesiodistal or buccolingual diameter for one tooth compared to its antimere; MD or BL "FL-MR" is the ratio of the female left tooth to the corresponding male right tooth in the same population group in the mesiodistal or the buccolingual diameter. MD or BL "gender" is the ratio of the mesiodistal or buccolingual diameter to the same side tooth of the opposite gender within the same population group. Females = pink; Males = blue; Averages = white.

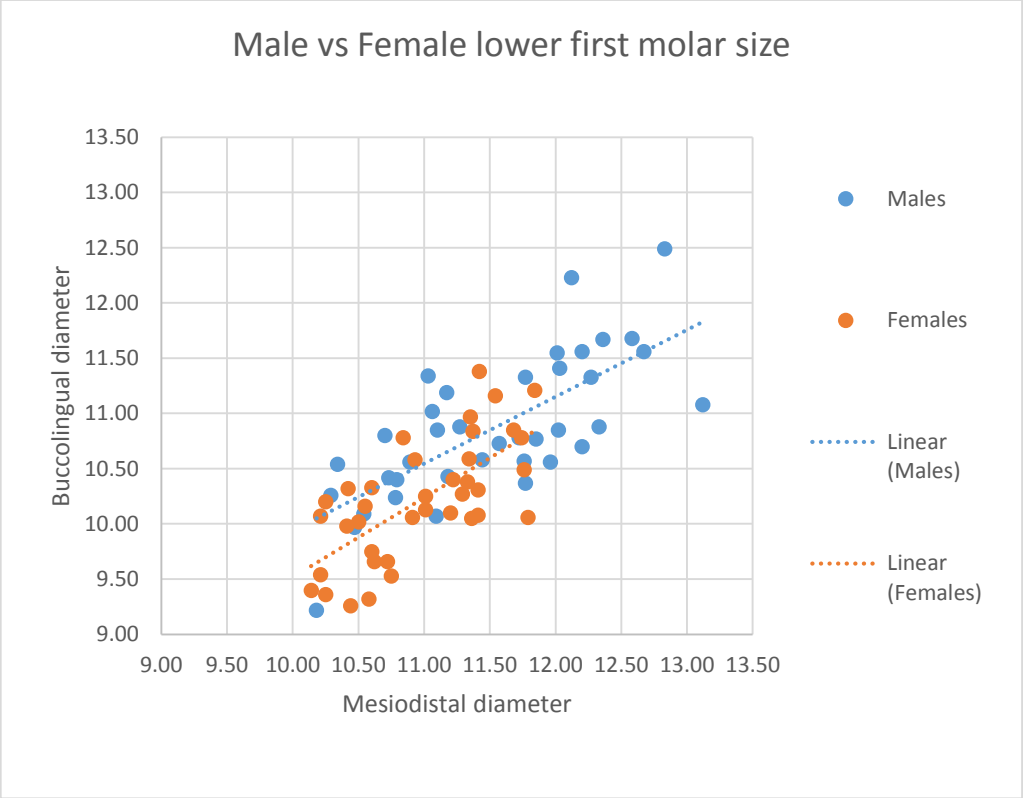

Figure 4.7 Graph of mesiodistal and buccolingual diameters for mandibular first molars of modern human males and females. Mesiodistal diameters are plotted along the x-axis and buccolingual diameters along the y-axis. Males are plotted in blue and females in red, with trend lines inserted for each.

As can be seen from the scatter diagram above (Figure 4.7) and the tables below (Tables 4.2-4.3), female molars are generally smaller and narrower than male molars. There is generally a slight difference between left molars and right molars with a strong bias towards wider teeth on the right and narrower teeth on the left, particularly in males. On average, there is about an eight percent difference in the relative width of a female left M_1 and a male right M_1, as measured by the mediodistal:buccolingual ratio.

Table 4.2 Mesiodistal and buccolingual diameter comparisons for modern human female and male left and right lower first molars. ("Area" = CCA = MD*BL)

	Average	Std Deviation	N=
Female Lower M1 Area (mm²)	**112.31**	**10.31**	**38**
Female Lower Left M1 Area (mm²)	**111.69**	**10.05**	**19**
Female Lower Right M1 Area (mm²)	**112.94**	**10.80**	**19**
Male Lower M1 Area (mm²)	**125.66**	**14.64**	**38**
Male Lower Left M1 Area (mm²)	**125.96**	**15.98**	**19**
Male Lower Right M1 Area (mm²)	**125.37**	**13.62**	**19**
Female Lower M1 MD:BL	**1.08**	**0.04**	**38**
Female Lower Left M1 MD:BL	**1.08**	**0.04**	**19**
Female Lower Right M1 MD:BL	**1.07**	**0.04**	**19**
Male Lower M1 MD:BL	**1.06**	**0.05**	**38**
Male Lower Left M1 MD:BL	**1.06**	**0.06**	**19**
Male Lower Right M1 MD:BL	**1.00**	**0.06**	**19**
Area : Male lower right M1 vs. Female lower left M1		**13% larger**	**38**
Width : Female lower left M1 vs. Male lower right M1		**8% narrower**	**38**

Table 4.3 – Descriptive statistics: Modern *Homo sapiens* sample

Area Male Right / Female Left		*MD:BL Male Right - Female Left*	
Mean	1.13127817	Mean	1.07665515
Standard Error	0.03702575	Standard Error	0.02078438
Median	1.10863835	Median	1.10479697
Mode	#N/A	Mode	#N/A
Standard Deviation	0.16139151	Standard Deviation	0.09059702
Sample Variance	0.02604722	Sample Variance	0.00820782
Kurtosis	0.98562429	Kurtosis	-0.81247
Skewness	0.45825425	Skewness	0.05609699
Range	0.69659466	Range	0.30898498
Minimum	0.79543633	Minimum	0.93667774
Maximum	1.49203098	Maximum	1.24566272
Sum	21.4942852	Sum	20.4564478
Count	19	Count	19
Confidence Level(95.0%)	0.07778822	Confidence Level(95.0%)	0.04366637

4.3.1.2 Extant primate species:

Representative specimens of lower M_1s from the four extant species (gorillas, humans, chimpanzees and bonobos) were compared for overall shape, using mesiodistal and buccolingual dimensions. Figure 4.8 illustrates these dimensions graphically:

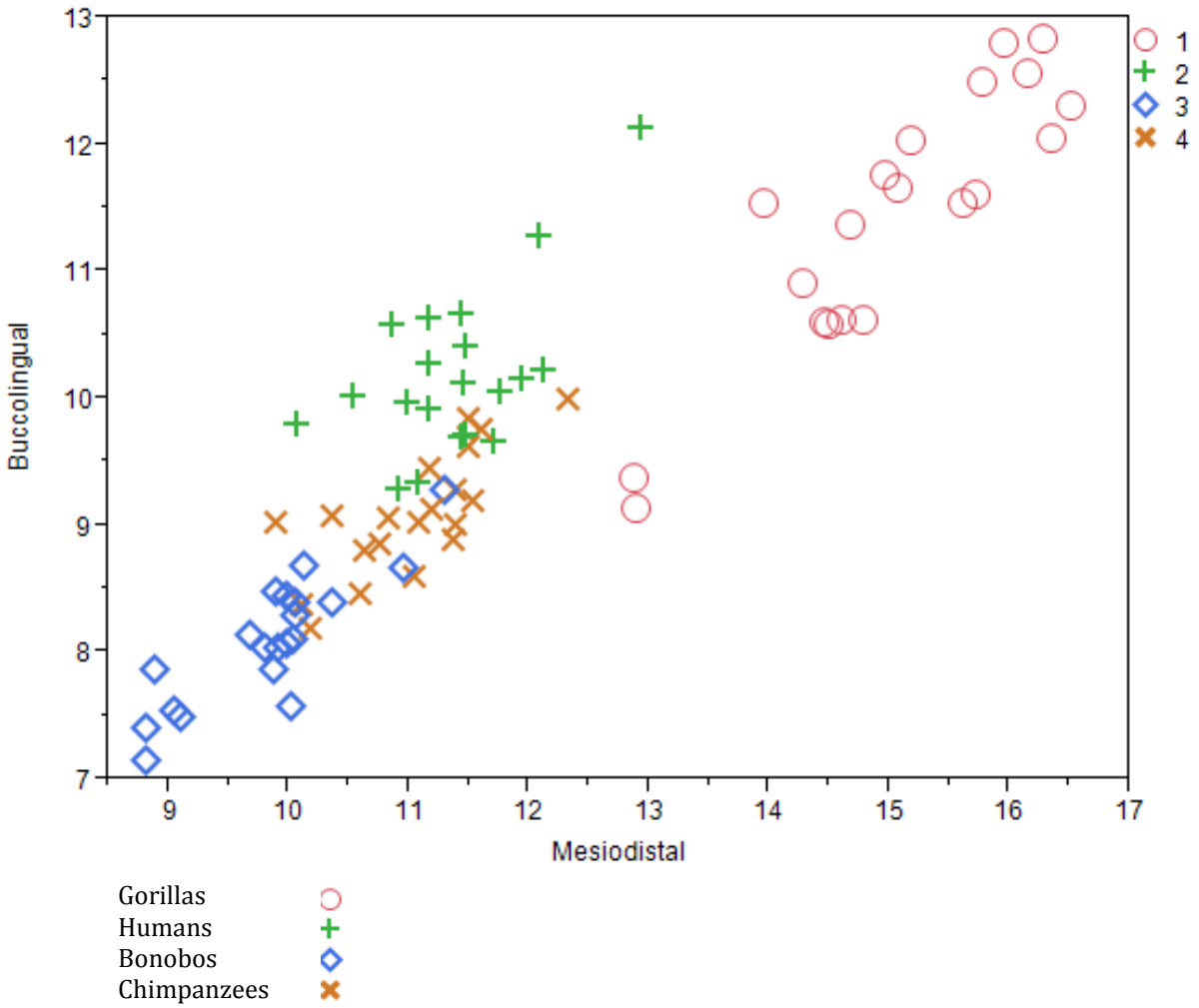

Figure 4.8 Graph showing the mesiodistal:buccolingual measurements of mandibular first molars of four extant primates.

(Measurements are taken from occlusal views of photographs. Gorillas: n= 20; modern humans: n=20; bonobos: n=20; chimpanzees: n=20)

Mesiodistal and buccolingual diameter measurements for a sample of mandibular first molars from individuals representing the four species studied show a wide disparity in size (from extremely small bonobo teeth (average: 80mm^2) to very large gorilla teeth (average: 172mm^2)). For all three great ape species, the data points fall roughly along the same axis on the graph, indicative of similar mesiodistal:buccolingual (MD:BL) ratios for these species, with gorillas being narrower on average than the other ape species (Gorillas – average MD:BL: 1.32; chimpanzees – average MD:BL: 1.21; bonobos –

average MD:BL: 1.21), and all three great ape species being significantly narrower on average by comparison to modern *Homo sapiens* – average MD:BL: 1.07. In terms of the ranges of relative width for each species, the MD:BL for gorillas ranged from 1.41 (extremely narrow) to 1.21 (more in the range of the chimpanzees and the bonobos), for chimpanzees the ratio ranged from 1.10 to 1.28 and for bonobos it ranged from 1.13 to 1.32 (the latter being similar to the average relative width of the gorilla sample: were it not for the size factor, some of the bonobo teeth would be difficult to tell apart from the gorilla sample). Only a very few of the most narrow modern *Homo sapiens* lower first molars overlapped with the widest bonobo and chimpanzee molars. The *Homo sapiens* sample ranged from a narrow MD:BL of 1.18 to an extremely wide 0.97.

Between genders, all of the primate species appear to show a tendency for female molars to be slightly narrower than male molars on average.

Between antimeres, in the great ape species there was a slight difference in mesiodistal:buccolingual ratios of up to about 2% between left and right teeth, particularly in the case of female gorillas and both genders of bonobos, but there was no more consistent pattern, as is the case with modern *Homo sapiens,* of right teeth being generally wider than left teeth (left lower first molars were wider than right lower first molars in only 37% of the cases in the modern *Homo sapiens* sample).

Gorillas in particular show a wide variation in size (the largest male in the sample had an area of 208.81 mm^2 and the smallest female had an area of 117.76 mm^2). Notably,

not one of the female gorilla teeth overlapped with the male sample in size (determined by crown area). Female gorilla teeth ranged in area between 117.76 mm^2 and 175.64 mm^2; male gorilla teeth ranged between 175.96 mm^2 and 208.81 mm^2. None of the other apes demonstrated such extreme sexual dimorphism: indeed, the bonobo specimens were almost identical in area between males (average = 79.27 mm^2) and females (average = 80.51 mm^2), whilst the chimp female teeth were on average larger than the male teeth in the sample chosen for study (105.89 mm^2 and 94.73 mm^2 on average, respectively).

Unlike the three great ape species, the modern human (MH) specimens show a higher degree of variability in both size and relative width. Male teeth ranged from 93.86 mm^2 and 125.66 mm^2 in area, and females between 95.32 mm^2 and 132.73 mm^2 placing these teeth within the size range of the largest bonobos, all of the chimps and some of the smaller (female) gorillas. In the case of the MH specimens, however, most of the teeth are significantly wider than those of the ape species. There is some overlap, however, because of the wide range of MD:BL ratios, from 1.18 at the narrowest and 0.97 at the most wide, with an average of 1.07.

These statistics are summarised in Table 4.4 a), b) and c).

Table 4.4 Summary table of area and width data for extant species ("Area" = CCA = MD*BL)

a) Gorilla

Gorilla	Average	Std Deviation	N=
Female Lower M1 Area (mm²)	151.61	18.45	10
Female Lower Left M1 Area (mm²)	150.75	19.18	5
Female Lower Right M1 Area (mm²)	152.47	19.89	5
Male Lower M1 Area (mm²)	193.38	11.93	10
Male Lower Left M1 Area (mm²)	193.30	11.33	5
Male Lower Right M1 Area (mm²)	193.47	13.85	5
Female Lower M1 MD:BL	1.34	0.06	10
Female Lower Left M1 MD:BL	1.33	0.08	5
Female Lower Right M1 MD:BL	1.35	0.04	5
Male Lower M1 MD:BL	1.30	0.04	10
Male Lower Left M1 MD:BL	1.30	0.05	5
Male Lower Right M1 MD:BL	1.30	0.04	5
Area : Male lower right M1 vs. Female lower left M1		28% larger	20
Width : Female lower left M1 vs. Male lower right M1		2% narrower	20

b) Bonobo

Bonobo	Average	Std Deviation	N=
Female Lower M1 Area (mm²)	80.51	11.78	10
Female Lower Left M1 Area (mm²)	78.13	11.36	5
Female Lower Right M1 Area (mm²)	82.88	13.01	5
Male Lower M1 Area (mm²)	79.27	8.62	10
Male Lower Left M1 Area (mm²)	80.05	8.88	5
Male Lower Right M1 Area (mm²)	78.49	9.33	5
Female Lower M1 MD:BL	1.22	0.05	10
Female Lower Left M1 MD:BL	1.24	0.05	5
Female Lower Right M1 MD:BL	1.21	0.05	5
Male Lower M1 MD:BL	1.20	0.03	10
Male Lower Left M1 MD:BL	1.18	0.01	5
Male Lower Right M1 MD:BL	1.23	0.03	5
Area : Male lower right M1 vs. Female lower left M1		0.5% larger	20
Width : Female lower left M1 vs. Male lower right M1		1% narrower	20

c) Chimpanzee

Chimpanzee	Average	Std Deviation	N=
Female Lower M1 Area (mm²)	105.89	8.35	10
Female Lower Left M1 Area (mm²)	108.12	8.69	5
Female Lower Right M1 Area (mm²)	103.65	8.30	5
Male Lower M1 Area (mm²)	94.73	8.95	10
Male Lower Left M1 Area (mm²)	95.59	11.58	5
Male Lower Right M1 Area (mm²)	93.87	6.67	5
Female Lower M1 MD:BL	1.22	0.03	10
Female Lower Left M1 MD:BL	1.22	0.03	5
Female Lower Right M1 MD:BL	1.21	0.03	5
Male Lower M1 MD:BL	1.21	0.06	10
Male Lower Left M1 MD:BL	1.20	0.07	5
Male Lower Right M1 MD:BL	1.22	0.05	5
Area : Male lower right M1 vs. Female lower left M1		13% smaller	20
Width : Female lower left M1 vs. Male lower right M1		0.5% narrower	20

In summary, great ape lower first molars in the sample are generally relatively narrow to very narrow (particularly gorilla lower first molars), the major differentiator between species being size; modern *Homo sapiens* lower first molar teeth are variable in size and particularly in relative width compared to the great ape species, but on the whole, although they may overlap with certain of the great ape lower first molars, the modern *Homo sapiens* molars are generally significantly wider than those of the great ape species.

4.3.1.3 Fossil molars:

Mesiodistal and buccolingual diameter measurements from occlusal photographs were plotted against each other for the 36 mandibular first molar specimens taken from the fossil record (Figure 4.9). Trend lines were added to the graph to indicate MD:BL ratios of 1:1, 1:1.06 and 1:1.16 respectively. Teeth falling close to the 1:1 line on the plot are square in occlusal aspect. Very narrow teeth fall below the 1:1.16 trend line.

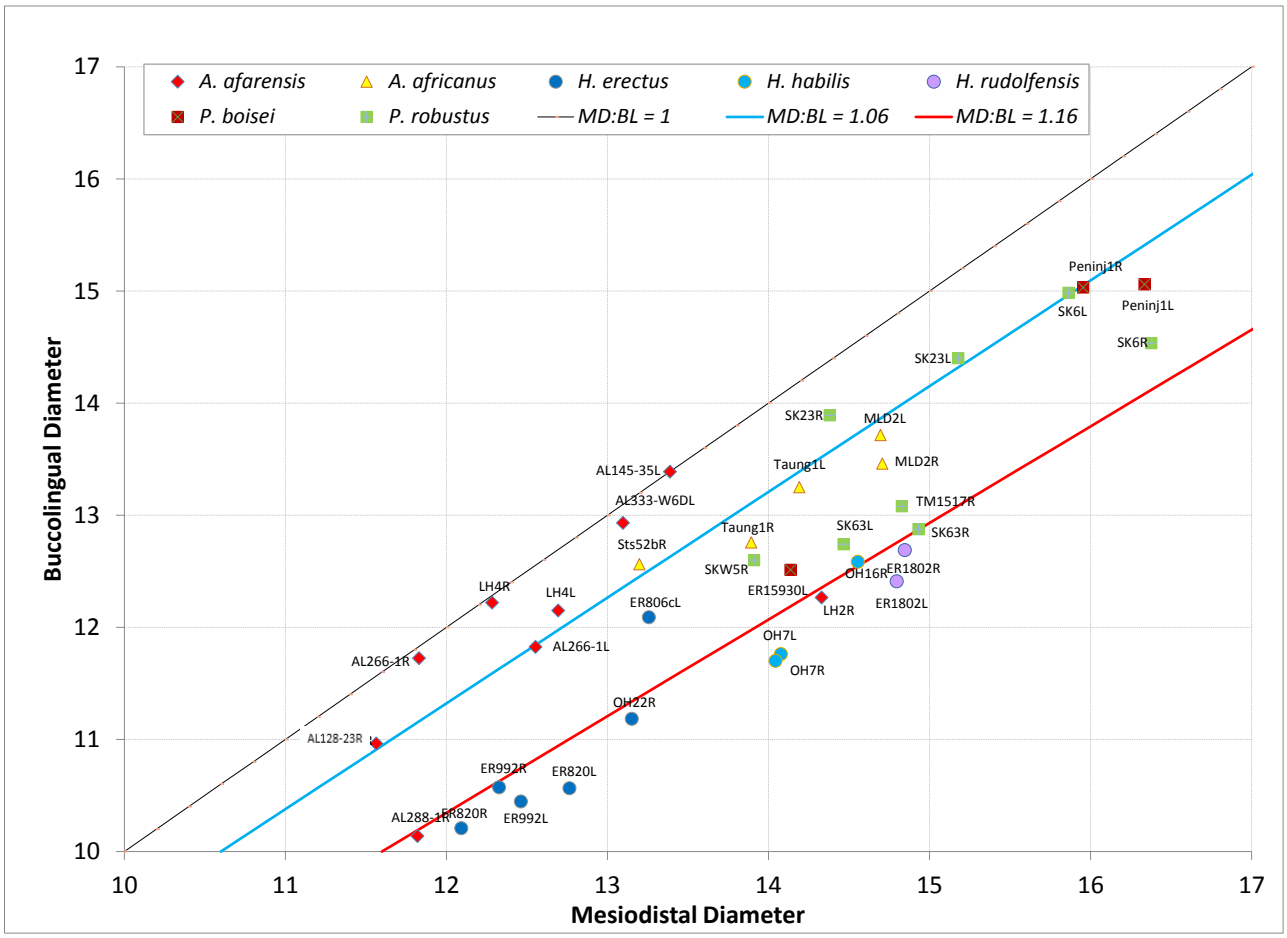

Figure 4.9 Mesiodistal (x-axis) and buccolingual (y-axis) measurements for M_1s of 36 fossil specimens, taken from occlusal photograph views.

It can be seen from Figure 4.9 that the squarest teeth are among the *Australopithecus afarensis* species group, which are also among the teeth with the smallest mesiodistal diameter in the sample. Most of these specimens have a similar MD:BL ratio to the holotype, LH 4. The narrowest teeth are mainly within the *Homo* group. AL 288-1 and LH 2 (both specimens of *Australopithecus afarensis*) also fall into this "very narrow tooth" category, indicating that within this single species, some of the most square and some of the narrowest teeth are represented. *Australopithecus africanus* and *Paranthropus* lower first molars range between these two extremes of overall width. Representatives from both *Paranthropus boisei* and *Paranthropus robustus* are among the largest teeth overall in the sample. The remaining specimens from both

Paranthropus species group closely with specimens from *Australopithecus africanus.* KNM-ER 806c (currently classified as *Homo erectus*) appears to be wider than the remaining specimens from any of the *Homo* groups, with a MD:BL ratio close to that of the *Paranthropus* and *Australopithecus africanus* specimens. It is similar in length to Sts 52b but not quite as wide. OH 16 *(Homo habilis)* is larger and wider than the holotype for the species and appears to group somewhere between *Homo rudolfensis* and *Paranthropus.*

The MD:BL ratios from the occlusal views of the 36 specimens were then plotted against the geological ages of each specimen (see "Materials and Methods", Table 3.3), to detect very general trends through time from more robust/wide molars in more primitive species to more gracile/narrow molars in more modern species. The results are depicted in Table 4.10 below. There appears to be a general trend from very square teeth to narrower teeth over time. Exceptions to this trend are AL 288-1 and LH 2, which are very narrow teeth, with much the same MD:BL ratios as the holotype of *Homo ergaster* (African *Homo erectus*), which appeared in the record around two million years later in time.

In both of the linear plots there is some differentiation visible between certain antimeres, where these are present, with some antimeres appearing narrower than their counterparts. Photographs were examined in each instance, to verify that measurements based on the occlusal views of the photographs were taken as correctly as could be expected, and it was confirmed that in instances where most differentiation was noted from the plots, there were distinct shape variations between the two

antimeres in the occlusal view. As discussed in 3.2.2.1 above, it was decided to retain antimeres in the study.

As in the case with the modern *Homo sapiens* sample, many of the left antimeres appear from their occlusal photographs to be more narrow than their right counterparts (with the notable exception of Taung 1 and MLD 2, the two *Australopithecus africanus* specimens studied that had both antimeres in good condition), in which instances, the right antimeres are more narrow than the left antimeres in the occlusal view. This finding should, however, be treated as tentative due to the small sample size, and it is recommended that antimeric laterality bias in the hominin record (as well as in modern humans and other extant primates) be examined in more detail using an expanded sample.

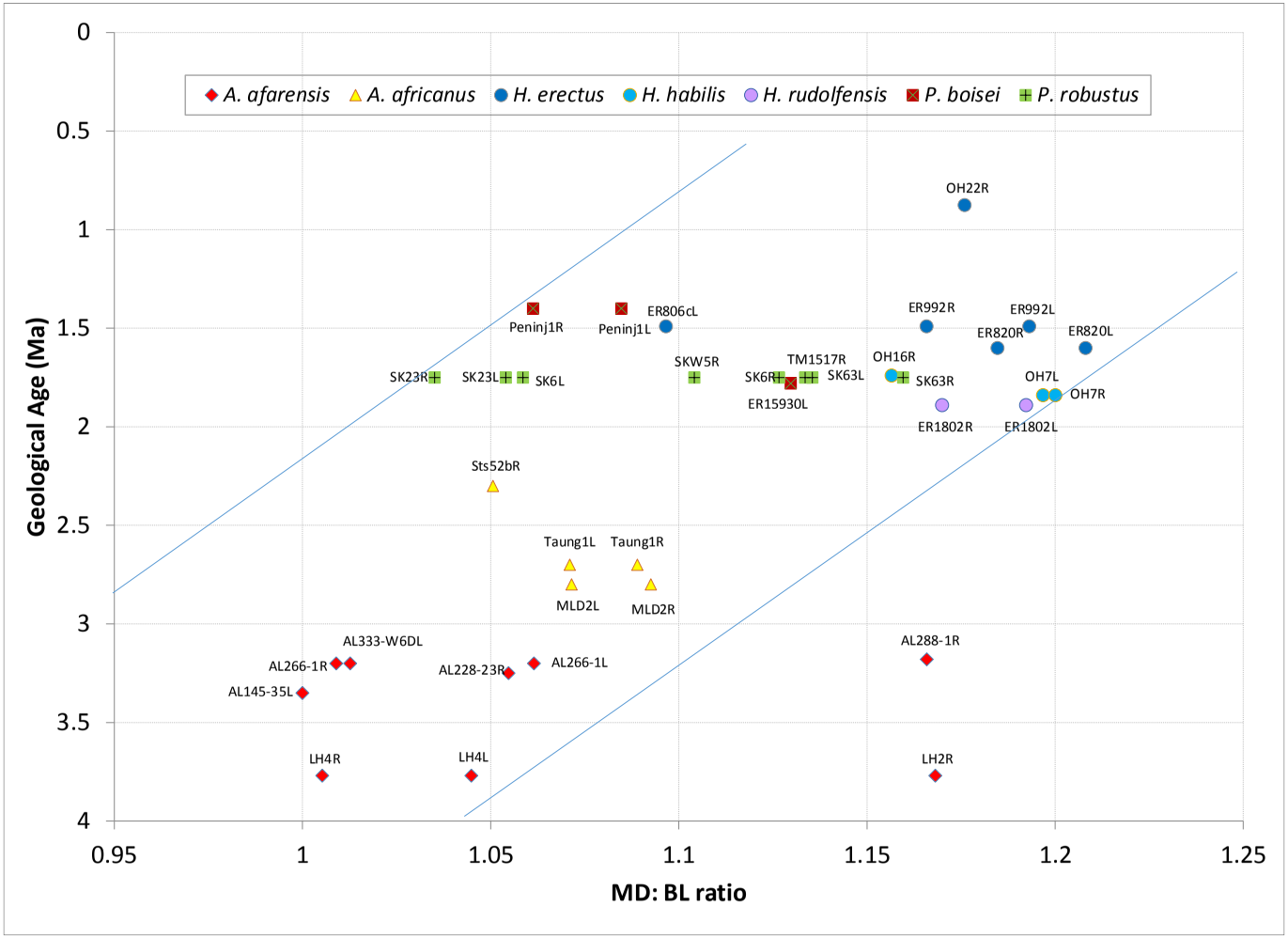

Figure 4.10 M_1 MD:BL ratios (x-axis) plotted against time (y-axis) for 36 fossil samples.
(Mesiodistal and buccolingual measurements taken from occlusal view photographs.)

In sum, therefore, based on occlusal image data, the linear dimensions of certain specimens appear to be relatively anomalous in terms of their currently accepted species groupings, by comparison to the holotypes for each of their groups. These would be:

- AL 288-1 and LH 2, which appear significantly narrow by comparison to the *Australopithecus afarensis* holotype and other similarly square-shaped teeth from the same species group;
- KNM-ER 806c, which is more *Australopithecus africanus*-like in dimensions and significantly larger and wider than the holotype of *Homo ergaster/erectus*;
- Sts 52b, which appears to be more narrow than the other specimens studied from the *Australopithecus africanus* species, including the holotype, Taung 1, which groups well in linear dimensions with MLD 2;
- OH 16, which is larger and wider than either the holotype for *Homo habilis* or the larger *Homo rudolfensis*, seems to group better with small specimens from the *Paranthropus robustus* group.
- KNM-ER 15930, which appears to be a very small and narrow *Paranthropus boisei,* as measured against Peninj 1, which is a mandibular proxy for the holotype, OH 5; this specimen groups more readily with small specimens from *Paranthropus robustus,* including the holotype, TM 1517.

4.3.2 Principal components analyses based on Procrustes form space

4.3.2.1 Extant species

The Principal Components Analysis chart (based on a Procrustes superimposition with size added as a variable in the form of the log of the centroid (Procrustes Form Space) (Mitteroecker et al. 2004)) is repeated below in Figure 4.11 for purposes of presenting the results thereof:

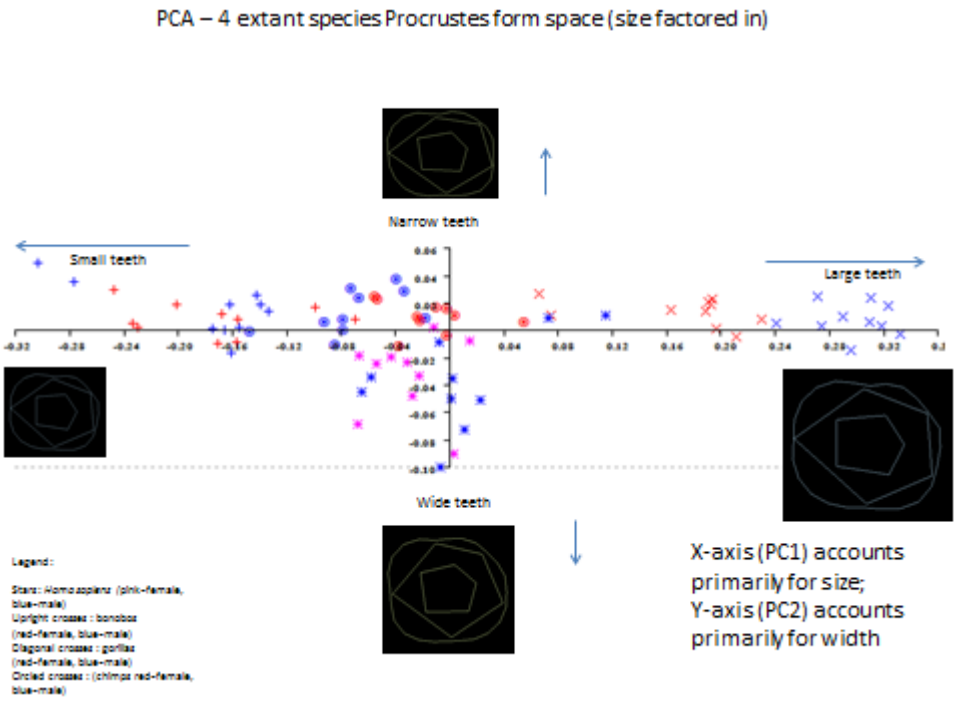

Figure 4.11 Principal Components graph for sample of lower first molars of four extant primate species (20 specimens per species), based on 5 anatomical landmarks and 44 mathematically-placed landmarks per specimen. PC1 (x-axis) accounts primarily for size, with some shape change. PC2 (y-axis) represents mainly changes in width, together with some shape change.

Bonobo, chimpanzee and gorilla specimens group in a narrow band, almost completely above the x axis, denoting small variations in the relative narrowness of these three great ape species' lower first molars compared with the majority of the modern *Homo sapiens* sample, which in general tend to be wider teeth. The species are grouped along the x axis in order of size, with bonobos being the smallest teeth in the sample, with a

slight overlap with the smallest chimpanzee teeth before the larger gorilla molars appear to the right of the y axis, females first and then males, towards the positive extreme of the axis. The modern *Homo sapiens* sample groups along the x axis in the same range as that for chimpanzees (teeth of similar size), but the majority of the variability within the modern *Homo sapiens* sample is not accounted for by size (as in the great ape species) but by relative width differences. Two outliers of the *Homo sapiens* group are grouped with the smallest of the female gorilla teeth: these were the largest teeth from the whole modern *Homo sapiens* sample (antimeres of the male Tswana specimen), chosen to reflect maximum variability for the ensuing analyses of the four extant species (see Table 4.1).

Sexual dimorphism is not clearly identified for bonobos, chimpanzees or modern *Homo sapiens.* However, for the gorilla sample, sexual dimorphism is significant. There is no overlap between female and male specimens in the gorilla sample, confirming linear dimension data. The differences are largely due to size factors rather than relative width factors (the specimens are spread horizontally rather than vertically in the plot).

4.3.2.2 Fossil species

The PCA "form space" (size and shape) plot for the fossil sample conducted under Phase I is repeated below, in this instance for purposes of identification of anomalies and species group patterns. Thereafter, the same specimens were analysed with each of the four extant species in turn as "species outgroups". Lastly, the same analysis was conducted on the fossils plus all four extant species.

A detailed list of the first three PC scores and the rationale for selecting PC2 or PC3 for each principal components plot (to represent width plus some aspect of cusp arrangement, as discussed in 4.2.3) for all the principal components analyses conducted on the fossil sample and the extant species outgroups is provided in Appendix 3.

In the first principal components analysis (36 fossil specimens alone), PC1 accounted mainly for size and cusp arrangement (x-axis; 72,5% of the covariance; PC1 98,2% correlated to centroid size, with the absence or presence of a C_6 shown along this axis). PC3 was chosen for the y-axis as this accounted primarily for the highly diagnostic relative width of the teeth (PC3 accounted for 4% of the covariance), with an element of cusp arrangement as well.

As discussed in 4.3.1.3 above, once the specimens were colour-coded according to their currently accepted species groups and compared with expectations of where they should be located on the PC plot, most of the predictions as to which fossil species should group into which quadrants or areas of the graph were confirmed. Anomalies included the following specimens:

- AL 288-1 *(Australopithecus afarensis)*: groups with *Homo erectus;*
- LH 2 (*Australopithecus afarensis)*: groups with medium-sized teeth such as OH 16 (a large, wider specimen of *Homo habilis*), KNM-ER 15930 (classified as *Paranthropus boisei*) and specimens from the *Australopithecus africanus* group;
- Sts 52b *(Australopithecus africanus)*: groups with the smaller teeth to the negative side of the x-axis;
- KNM-ER 15930 (*Paranthropus boisei*): groups with smaller teeth, outside of the range of the smallest *Paranthropus robustus* in the fossil sample;

- OH 16 *(Homo habilis):* groups closer to *Australopithecus africanus* than to the holotype of *Homo habilis* (OH 7)
- KNM-ER 806c *(Homo erectus)*: groups with the wider and larger teeth to the negative side of the y-axis, closer to *Australopithecus africanus*.

Species groupings, outside of the above anomalies were patterned as follows:

- *Australopithecus afarensis* – most specimens grouped around the holotype, LH 4, being square and small with a pronounced metaconid (cusp patterns including the size of the metaconid was a feature of PC3, selected with "relative width" to represent the y-axis). The grouping was not tight, reflecting diversity of occlusal crown shapes, but other than the two specimens already mentioned, the group was positioned on the plot in the general area where it should be predicted to be located. Size as well as width variability was noted.
- *Australopithecus africanus* – unfortunately this is a small sample. However, other than Sts 52b, which is smaller than the other specimens in its occlusal view, there was a close association between Taung 1 molars and those of MLD 2, in the centre of the plot, as expected.
- *Early Homo – Homo habilis* (with the exception of OH 16 as mentioned above) plotted in an area designated for medium-sized, narrow teeth, and *Homo rudolfensis* plotted in an area designated for larger teeth (slightly narrower than those of *Australopithecus africanus* and *Paranthropus robustus*).
- *Homo erectus* – This group, with the exception of KNM-ER 806c, as mentioned above, was very cohesive, plotting in a narrow band of "small, narrow" molars on the PC plot. This group shows more variation in size rather than in width of crown.

- *Paranthropus boisei* and *Paranthropus robustus* – *Paranthropus boisei*, with the exception of KNM-ER 15930 mentioned above, are located on the chart in the area where they would most be expected to be located, representing the largest teeth in the whole fossil sample analysed. However, very close by KNM-ER 15930 are SK 6 and SK 23, which are representatives of *Paranthropus robustus.* The remaining *Paranthropus robustus* molars are in a second group of smaller teeth, grouping closely towards the more "medium-sized" teeth (*Homo rudolfensis* and *Australopithecus africanus).*

Further PC analyses were performed using the four extant species as "outgroups" against the fossil sample to test for recurrent outliers and anomalies. Each species was individually added to the fossil data, with axes chosen in each case to represent the main diagnostic features of the lower first molars in each case (mainly size and cusp arrangement on the x-axis and tooth breadth plus at least one more shape feature change on the y-axis, as before).

Finally, a PC analysis was performed on the fossil sample against all four extant species at once, to test the range of variability found within the fossil sample against extant species.

These charts are presented in the following order:

- Fossils alone (Figure 4.12)
- Fossils with bonobos as the outgroup (Figure 4.13)
- Fossils with chimpanzees as the outgroup (Figure 4.14)

- Fossils with gorillas as the outgroup (Figure 4.15)
- Fossils with modern humans as the outgroup (Figure 4.16)
- Fossils with all four extant species (Figure 4.17).

Output data from the Principal Components analyses are given in Appendix 3, with an explanation of the rationale for choosing either PC2 or PC3 for the y-axis in each graph (choice based on the PC that most represented variability in width of tooth plus some factor of cusp arrangement variability, as discussed in 4.2.3 above).

Unsurprisingly, the bonobo and chimpanzee graphs are very similar. The fossil data points are easier to read on the chimpanzee PC plot.

Generally, good resolution between species was visible from the PC plots. Certain specimens tended to show up consistently as anomalies on each chart, and these were by and large confirmed by the other analyses.

The same six fossil specimens identified on the fossil-only PC plot as being potentially "anomalous" (namely, AL 288-1; LH 2; Sts 52b; KNM-ER 15930; KNM-ER 806c and OH 16) continue to appear as specimens that do not group well with their allocated species groups as represented by the holotype or the proxy for the holotype (in the case of *Paranthropus boisei*). One of these specimens, AL 288-1 not only fails to group well against the holotype for the species group to which it is allocated (*Australopithecus afarensis)* but in the plots with chimpanzee and modern *Homo sapiens* molars as outgroups, this specimen groups better with the extant species than with the fossil specimens. This particular tooth is closer in overall dimensions and relative width to

chimp teeth and to modern *Homo sapiens* than it is to its species holotype and the majority of the teeth in the sample allocated to the species from the Afar region.

A pattern of sexual dimorphism, seen from the PC plot including the gorilla teeth as the species outgroup might be mirrored in the *Paranthropus spp.* group. Again, there is not much differentiation between Peninj 1 (*P. boisei*) and SK 6 (*P, robustus*), but rather a spread of molars from Peninj 1 in a group of "larger" molars of both species to SKW 5 (and arguably KNM-ER 15930) in a group of "smaller" molars (if KNM-ER 15930 is not misclassified, then again, of both species). The spread is greater along the x-axis rather than the y-axis, as with gorillas, indicating that if the *Paranthropus* group is divided into smaller and larger teeth due to sexual dimorphism, this is manifested mainly by size/length difference, rather than large variations in width of tooth. The same pattern is evident for *Homo erectus* specimens, but *Australopithecus afarensis* specimens appear to vary both in size and in overall width, which is more reminiscent of the pattern seen in modern *Homo sapiens,* where the spread is more noticeable along the y-axis than along the x-axis.

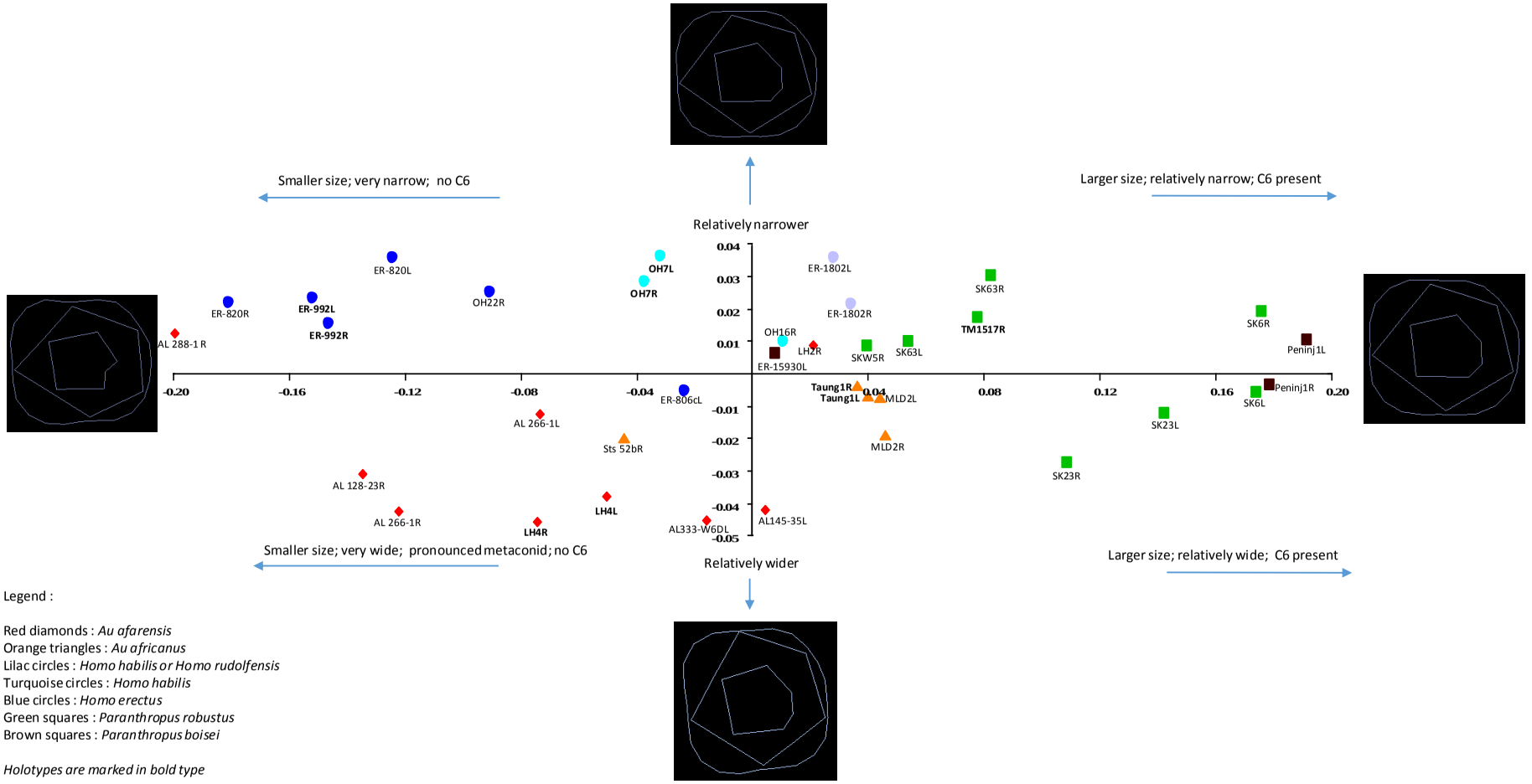

Figure 4.12 Principal Components graph (colour-coded data points) for fossil M_1 sample of lower first molars (36 specimens from 7 species, based on 49 mathematically-placed landmarks per specimen). PC1 (x-axis) accounts primarily for size, with C_6 and some shape change as depicted. PC3 (y-axis) represents mainly changes in width.

Fossils with Bonobos as a species outgroup - PC1 : PC3

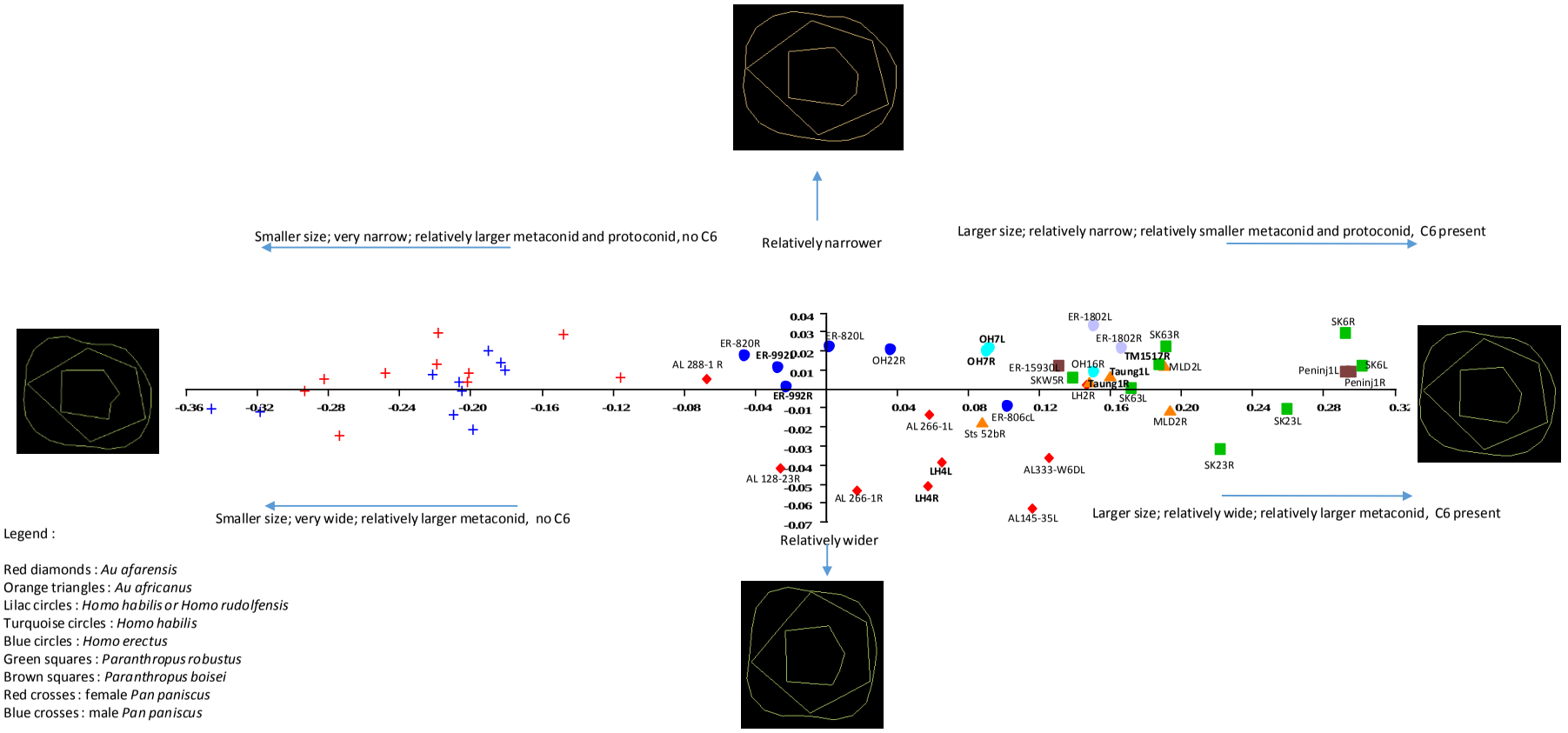

Figure 4.13 Principal Components graph (fossil M_1 sample) with bonobo sample (n=20) as a species outgroup PC1 (x-axis) accounts primarily for size, with C_6 and some shape change as depicted. PC3 (y-axis) represents mainly changes in width, plus an element of shape change as depicted.

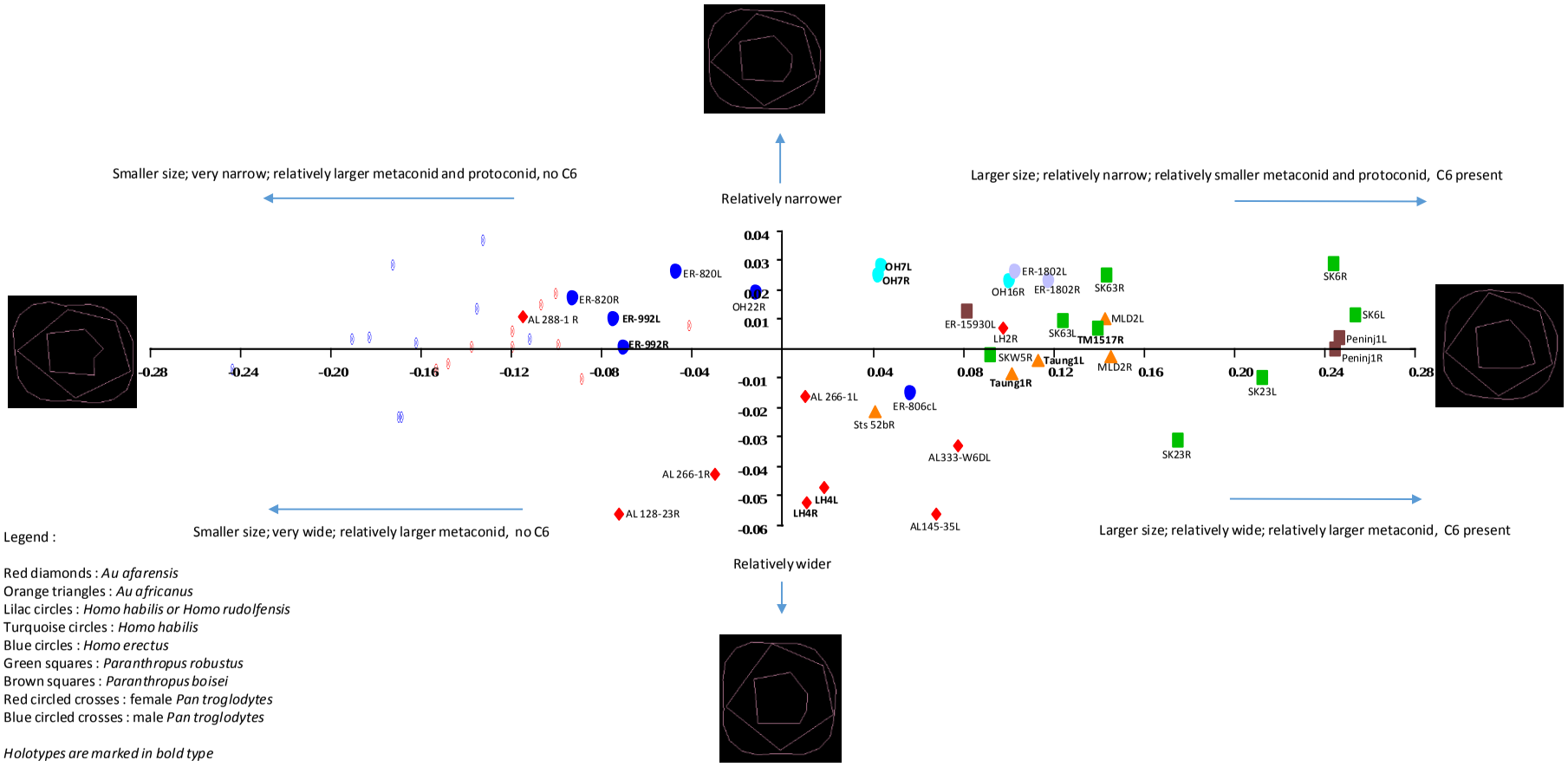

Figure 4.14 Principal Components graph (fossil M_1 sample) with chimpanzee sample (n=20) as a species outgroup PC1 (x-axis) accounts primarily for size, with C_6 and some shape change as depicted. PC3 (y-axis) represents mainly changes in width, plus an element of shape change as depicted.

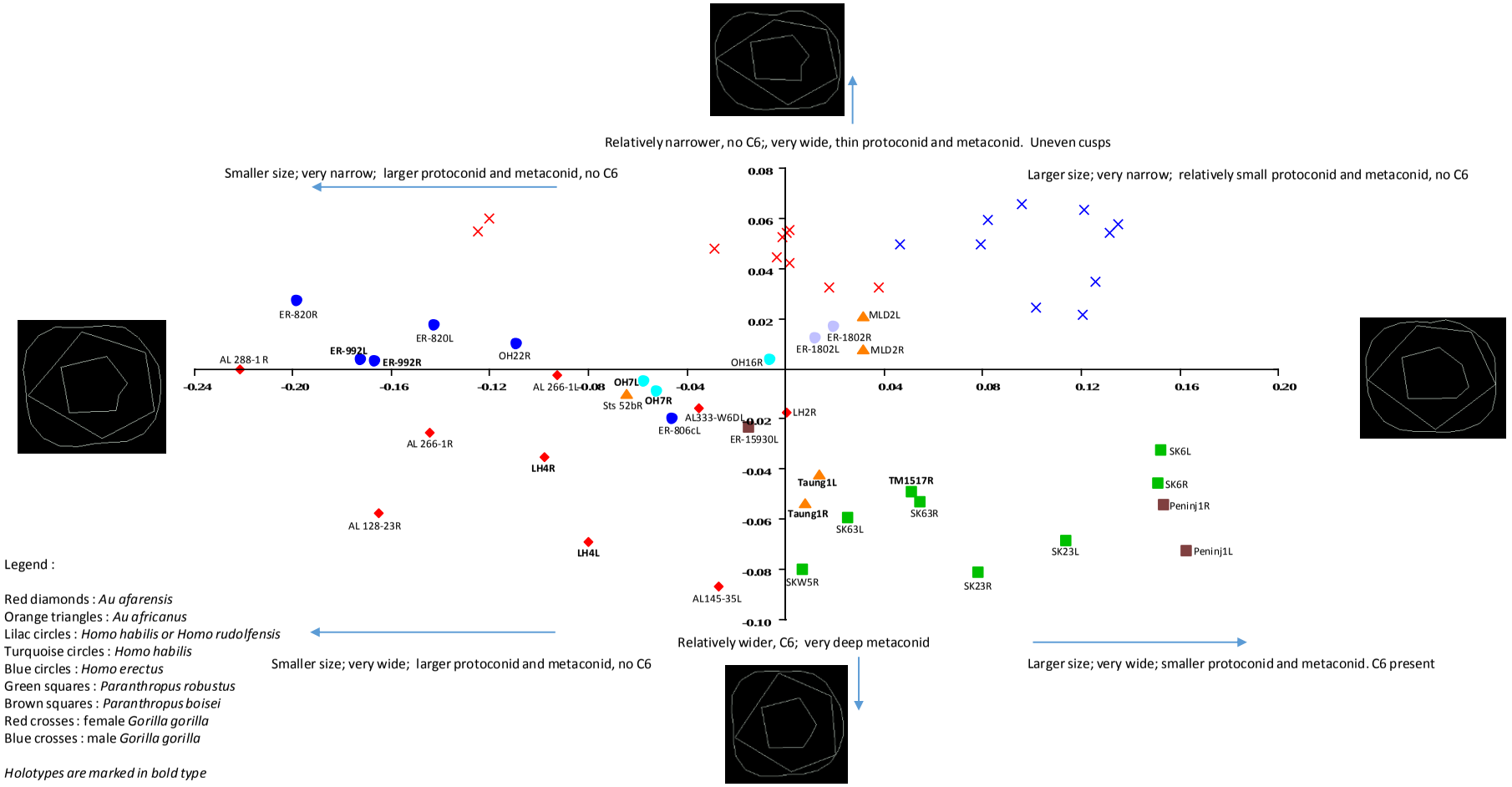

Figure 4.15 Principal Components graph (fossil M_1 sample) with gorilla sample (n=20) as a species outgroup PC1 (x-axis) accounts primarily for size, with C_6 and some shape change as depicted. PC3 (y-axis) represents mainly changes in width, plus an element of shape change as depicted.

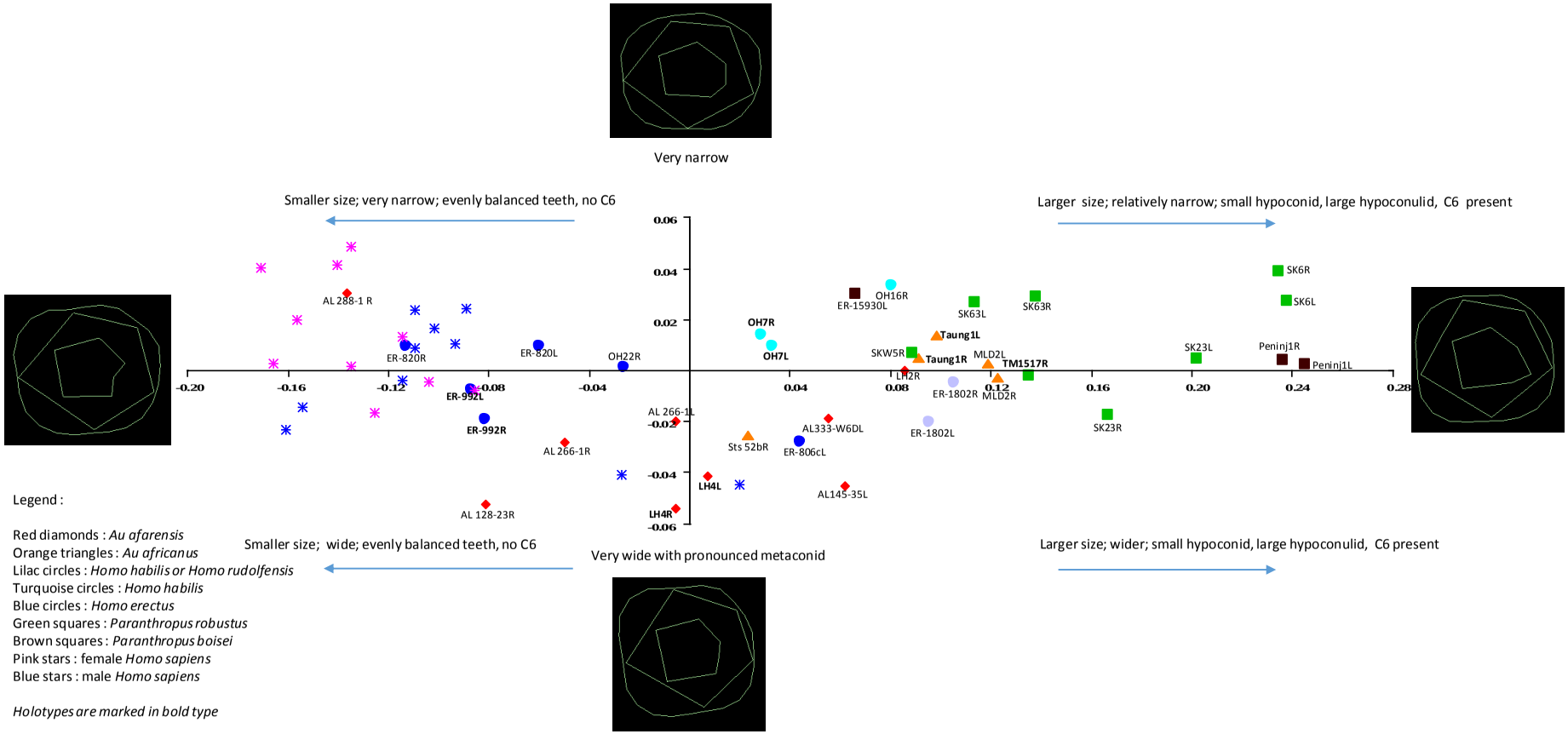

Figure 4.16 Principal Components graph (fossil M_1 sample) with modern human sample (n=20) as a species outgroup PC1 (x-axis) accounts primarily for size, with C_6 and some shape change as depicted. PC3 (y-axis) represents mainly changes in width, plus an element of shape change as depicted.

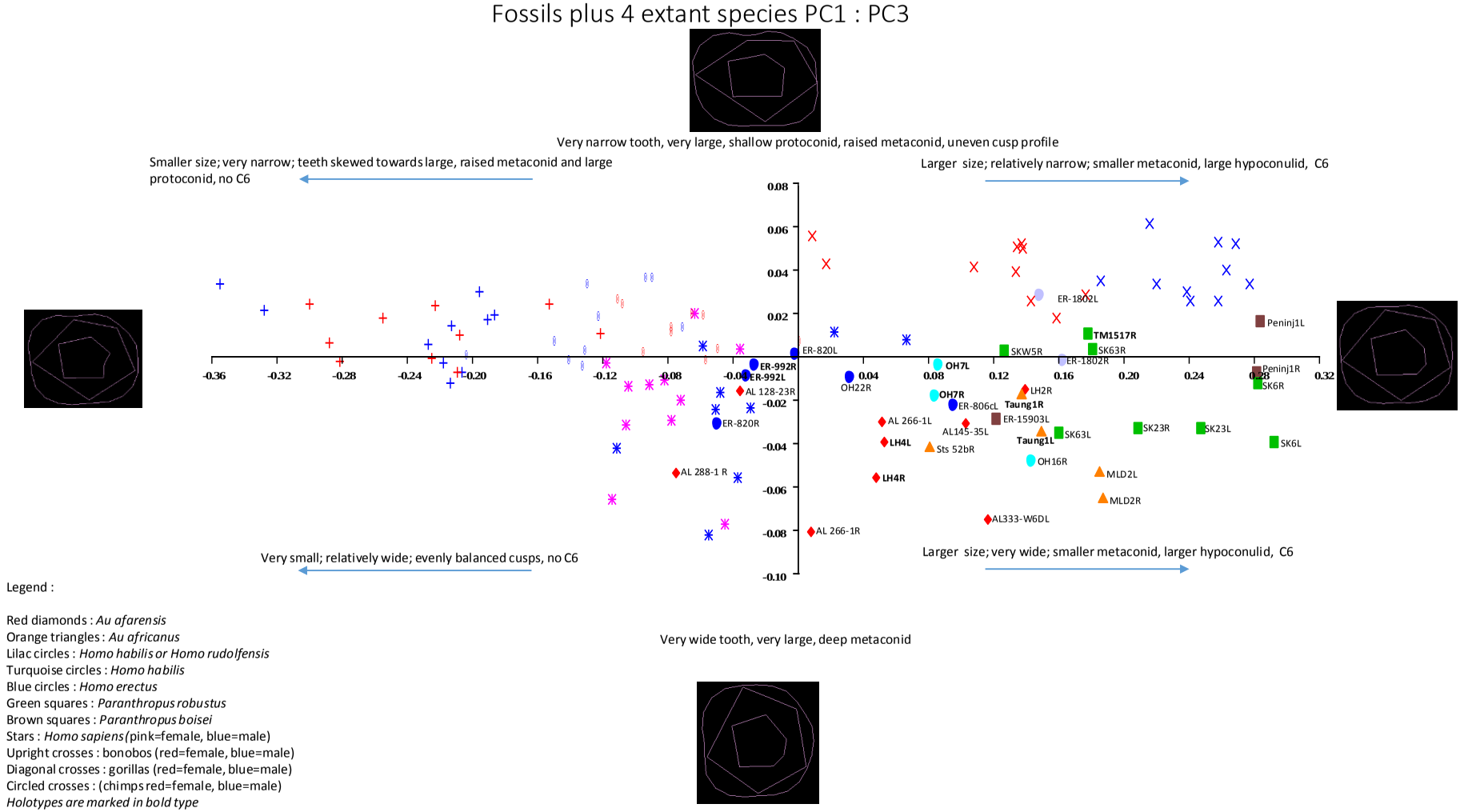

Figure 4.17 Principal Components graph (fossil M_1 sample) with four extant species samples (n=20 per species) PC1 (x-axis) accounts primarily for size, with C_6 and some shape change as depicted. PC3 (y-axis) represents mainly changes in width, plus an element of shape change as depicted.

4.3.3 Basic Procrustes distance matrix analysis between fossil species

The preliminary results of the Procrustes distance analysis are presented according to species group, as currently classified.

Table 4.5 Procrustes distance matrix: *Australopithecus afarensis*

	AL145-35L	AL128-23R	AL266-1L	AL266-1R	AL288-1R	AL333-W60L	LH2R	LH4L	LH4R
AL145-35L		0.09970	0.13502	0.14016	0.16290	0.14062	0.10104	0.10164	0.11570
AL128-23R	0.09970		0.08792	0.13310	0.14429	0.11806	0.07490	0.08345	0.08551
AL266-1L	0.13502	0.08792		0.07574	0.08185	0.06662	0.06393	0.10726	0.06430
AL266-1R	0.14016	0.13310	0.07574		0.08063	0.06013	0.09517	0.13028	0.07245
AL288-1R	0.16290	0.14429	0.08185	0.08063		0.07583	0.09011	0.13801	0.10412
AL333-W60L	0.14062	0.11806	0.06662	0.06013	0.07583		0.09266	0.10712	0.06384
LH2R	0.10104	0.07490	0.06393	0.09517	0.09011	0.09266		0.08866	0.07571
LH4L	0.10164	0.08345	0.10726	0.13028	0.13801	0.10712	0.08866		0.08426
LH4R	0.11570	0.08551	0.06430	0.07245	0.10412	0.06384	0.07571	0.08426	
0.09841	0.12460	0.10337	0.08533	0.09846	0.10972	0.09061	0.08527	0.10509	0.08323

Procrustes distances for *Australopithecus afarensis* as a group average at just under 0.1, which is the highest average distance for any of the species groups, and individual Procrustes distances are very varied. Comparing teeth to the holotype (LH 4), the main anomaly appears to be AL288-1 (R). This specimen also has the highest single Procrustes distance of 0.16 (from AL145-35L), this latter specimen being closer in shape to the Laetoli specimens and to AL 128-23R. One surprise in this matrix is that certain of the specimens group more closely with LH 4 (R) than they do with the left antimere of this same specimen. Both of these antimeres were damaged and needed part of their perimeter inferred for the analyses, but were included due to their importance as holotypes. It is suspected that this distance matrix has identified differences between the antimeres around the perimeter of the tooth, due to the larger number of landmarks attributed to the perimeter and external shape, as opposed to the cusp pattern (28 landmarks and 20 landmarks respectively – this total excludes landmark #1). The wide diversity in overall shape of specimens within this group are confirmed by the PC analysis.

Table 4.6 Procrustes distance matrix: *Australopithecus africanus*:

	MLD2L	MLD2R	Sts52bR	Taung1L	Taung1R
MLD2L		0.04845	0.06866	0.10593	0.12537
MLD2R	0.04845		0.06121	0.10949	0.12850
Sts52bR	0.06866	0.06121		0.08295	0.09716
Taung1L	0.10593	0.10949	0.08295		0.04641
Taung1R	0.12537	0.12850	0.09716	0.04641	
0.08741	0.08710	0.08691	0.07749	0.08619	0.09936

In this grouping, Taung1L and R seem to be quite distant from MLD2L and R, despite their closeness on the PCA graph. The reason for this is that Taung1 L and R had cusp landmark sited for the presence of a sixth cusp, C_6. Sts52b is consistently "distant" from all the other teeth in the group. This result is still consistent with the PC analysis, in that Taung 1 L and R group quite close to *Paranthropus* specimens with a sixth cusp.

Table 4.7 Procrustes distance matrix: *Homo erectus:*

	OH22R	KNM-ER806cL	KNM-ER820L	KNM-ER820R	KNM-ER992L	KNM-ER992R
OH22R		0.09205	0.05501	0.06567	0.05292	0.05505
KNM-ER806cL	0.09205		0.08418	0.09750	0.07551	0.06796
KNM-ER820L	0.05501	0.08418		0.06191	0.04301	0.03699
KNM-ER820R	0.06567	0.09750	0.06191		0.06020	0.06878
KNM-ER992L	0.05292	0.07551	0.04301	0.06020		0.02956
KNM-ER992R	0.05505	0.06796	0.03699	0.06878	0.02956	
0.06309	0.06414	0.08344	0.05622	0.07081	0.05224	0.05167

These teeth have generally small distances from each other, showing a consistent grouping. The exception is KNM-ER 806cL, which does not group well with *Homo erectus.* This finding is confirmed on the PC plots.

Table 4.8 Procrustes distance matrix: *Homo habilis* (turquoise) and *Homo rudolfensis* (lilac):

	OH7L	OH7R	OH16R	KNM-ER1802L	KNM-ER1802R
OH7L		0.03333	0.08227	0.06446	0.05356
OH7R	0.03333		0.06539	0.07287	0.04867
OH16R	0.08227	0.06539		0.11728	0.07619
KNM-ER1802L	0.06446	0.07287	0.11728		0.05592
KNM-ER1802R	0.05356	0.04867	0.07619	0.05592	
0.06699	0.05840	0.05507	0.08528	0.07763	0.05858

In this group, OH 16 appears to be more of an outlier from the *habilis* group than does KNM-ER 1802, which is currently classified as *Homo rudolfensis.*

Table 4.9 Procrustes distance matrix: *Paranthropus boisei:*

	KNM-ER15930L	Peninj1L	Peninj1R
KNM-ER15930L		0.12251	0.08542
Peninj1L	0.12251		0.05895
Peninj1R	0.08542	0.05895	
0.08896	0.10397	0.09073	0.07219

There are not enough photographed undamaged specimens from this taxon to make reasonable judgements regarding the results of this analysis. However, grouping *Paranthropus boisei* with *Paranthropus robustus* (see below), it can be seen that KNM-ER 15930, while classified with *Paranthropus boisei*, does not fit very well with this group. It groups best (within the *Paranthropus* clade, at least) with SK 6 *(Paranthropus robustus)*.

Table 4.10 Procrustes distance matrix: *Paranthropus robustus:*

	SK6L	SK6R	SK23L	SK23R	SK63L	SK63R	SKW5R	TM1517R
SK6L		0.05336	0.06150	0.08323	0.06761	0.08001	0.10358	0.08482
SK6R	0.05336		0.05478	0.07363	0.05717	0.04669	0.07288	0.06099
SK23L	0.06150	0.05478		0.04453	0.05671	0.05808	0.07939	0.06672
SK23R	0.08323	0.07363	0.04453		0.07102	0.07067	0.08005	0.06868
SK63L	0.06761	0.05717	0.05671	0.07102		0.05512	0.09221	0.07868
SK63R	0.08001	0.04669	0.05808	0.07067	0.05512		0.06178	0.05692
SKW5R	0.10358	0.07288	0.07939	0.08005	0.09221	0.06178		0.06612
TM1517R	0.08482	0.06099	0.06672	0.06868	0.07868	0.05692	0.06612	
0.06811	0.07630	0.05993	0.06025	0.07026	0.06836	0.06132	0.07943	0.06899

This is another very homogenous group. All of the members of this group were landmarked for a sixth cusp (C_6).

Table 4.11 Procrustes distance matrix: *Paranthropus boisei* and *robustus* together:

	KNM-ER1590L	Peninj1L	Peninj1R	SK6L	SK6R	SK23L	SK23R	SK63L	SK63R	SKW5R	TM1517R
KNM-ER1590L		0.12251	0.08542	0.06715	0.07954	0.09418	0.10584	0.09241	0.09517	0.10975	0.09624
Peninj1L	0.12251		0.05895	0.11449	0.08282	0.08393	0.07820	0.10486	0.07400	0.06835	0.05507
Peninj1R	0.08542	0.05895		0.07268	0.05917	0.05818	0.06185	0.08920	0.07104	0.06997	0.04872
SK6L	0.06715	0.11449	0.07268		0.05336	0.06150	0.08323	0.06761	0.08001	0.10358	0.08482
SK6R	0.07954	0.08282	0.05917	0.05336		0.05478	0.07363	0.05717	0.04669	0.07288	0.06099
SK23L	0.09418	0.08393	0.05818	0.06150	0.05478		0.04453	0.05671	0.05808	0.07939	0.06672
SK23R	0.10584	0.07820	0.06185	0.08323	0.07363	0.04453		0.07102	0.07067	0.08005	0.06868
SK63L	0.09241	0.10486	0.08920	0.06761	0.05717	0.05671	0.07102		0.05512	0.09221	0.07868
SK63R	0.09517	0.07400	0.07104	0.08001	0.04669	0.05808	0.07067	0.05512		0.06178	0.05692
SKW5R	0.10975	0.06835	0.06997	0.10358	0.07288	0.07939	0.08005	0.09221	0.06178		0.06612
TM1517R	0.09624	0.05507	0.04872	0.08482	0.06099	0.06672	0.06868	0.07868	0.05692	0.06612	

These two species group so well together that if judgements could be based on lower first molars alone (and within the limitations of this small sample), an argument could be made that they are possibly one species, their only difference being a matter of geography (*P. boisei* being found in East Africa and *P. robustus* being found in South Africa). There is less shape difference between Peninj 1(R) and TM 1517, for instance, than there is between the antimeres of Peninj 1. Peninj 1 (R) also groups very closely with SK 6 (R) and SK 23 (L). KNM-ER 15930 appears to be poorly grouped, not only with its holotype proxy but also with most of the specimens of *P. robustus* as well, considering that its Procrustes distances are above the average for this latter group except in one instance.

The full Procrustes distance matrix (36 specimens x 36 specimens) can be found in Appendix 4. This analysis has been limited to a basic overview, for the purposes of this exploratory study.

4.3.4 Results obtained from the preliminary discriminant function analysis and probability predictions for groupings of fossils.

A preliminary discriminant function analysis (DFA) was carried out, using the first 8 PC scores of the Procrustes form-space PCA analysis of the extant species specimens (n=80) and the fossil specimens (n=36). The choice of 8 PCs was as a result of a sensitivity test of the ability of the DFA to discriminate between species, as carried out on the four known (extant) species, as described in 3.6.1.4. above.

The results of the DFA are presented in Tables 4.12 a) and b) below. Potential misclassifications were as follows:

4.3.4.1 Extant species

- One female gorilla left molar grouped better with *Homo rudolfensis.* Looking at the PC plot of the 116 specimens together (Figure 4.17) there is one gorilla tooth that falls midway between the left and the right antimeres of KNM-ER 1802.
- Bonobo specimens and chimpanzee specimens were all correctly grouped
- With respect to the modern *Homo sapiens* sample, the right and left antimeres of the large Tswana male specimen (the largest teeth in the whole sample of Modern *Homo* sapiens) group better with the *Homo erectus* group. This particular specimen does, in fact, group closer to OH 22 and KNM-ER 820 (L) than it does to the rest of the modern *Homo sapiens* sample on Figure 4.17.

4.3.4.2 Fossil specimens

- The sole outlier in the *Australopithecus afarensis* group on the DFA was AL 288-1, which as seen in all the analyses thus far, groups closer to modern *Homo sapiens* specimens (see Figure 4.17) due to its small size and extreme narrowness as compared to the rest of its group.
- In the *Australopithecus africanus* group, Taung 1, the holotype, groups better with the *Paranthropus robustus* group. This is the only specimen from *Australopithecus africanus* that was landmarked for a sixth cusp, normally a diagnostic feature of *Paranthropus robustus.* The two Taung antimeres fall directly between SKW 5 and SK 6 (L) on the PC plot of the 116 specimens together in Figure 4.17. On the contrary, Sts 52b, which is classified as *Australopithecus africanus,* is predicted instead to belong to the *Australopithecus afarensis* group. This result is in keeping with the findings from PC plots and linear dimension analyses.
- In the *Homo erectus* group, KNM-ER 806c is predicted to group better with the *Australopithecus africanus* group.
- All other specimens grouped according to their currently assigned species groups.

Tables 4.12 a) and b) present the results of the DFA for the four extant species and the fossil species respectively.

Table 4.12 a) Discriminant function analysis results - extant species

Specimen	Actual Group	Actual Group	Predicted Group	Highest Group				
				Predicted Group	P(D>d | G=g)		P(G=g | D=d)	Squared Mahalanobis Distance to Centroid
					p	df		
Gorgorg7318M3_F_L	*Gorilla gorilla*	2	*Homo rudolfensis*	10**	.453	8	.680	7.800
Gorgorg7318M3_F_R	*Gorilla gorilla*	2	*Gorilla gorilla*	2	.852	8	.990	4.055
Gorgorg7556M2_F_L	*Gorilla gorilla*	2	*Gorilla gorilla*	2	.894	8	1.000	3.567
Gorgorg7556M2_F_R	*Gorilla gorilla*	2	*Gorilla gorilla*	2	.796	8	1.000	4.634
Gorgorg7732M1_M_L	*Gorilla gorilla*	2	*Gorilla gorilla*	2	1.000	8	1.000	.386
Gorgorg7732M1_M_R	*Gorilla gorilla*	2	*Gorilla gorilla*	2	.941	8	1.000	2.889
Gorgorg7732M2_M_L	*Gorilla gorilla*	2	*Gorilla gorilla*	2	.849	8	1.000	4.086
Gorgorg7732M2_M_R	*Gorilla gorilla*	2	*Gorilla gorilla*	2	.871	8	1.000	3.840
Gorgorg7732M3_F_L	*Gorilla gorilla*	2	*Gorilla gorilla*	2	.907	8	.999	3.400
Gorgorg7732M3_F_R	*Gorilla gorilla*	2	*Gorilla gorilla*	2	.915	8	1.000	3.291
Gorgorg7732M5_M_L	*Gorilla gorilla*	2	*Gorilla gorilla*	2	.250	8	1.000	10.215
Gorgorg7732M5_M_R	*Gorilla gorilla*	2	*Gorilla gorilla*	2	.307	8	1.000	9.429
Gorgorg7732M6_M_L	*Gorilla gorilla*	2	*Gorilla gorilla*	2	.528	8	1.000	7.085
Gorgorg7732M6_M_R	*Gorilla gorilla*	2	*Gorilla gorilla*	2	.774	8	.996	4.849
Gorgorg7732M7_M_L	*Gorilla gorilla*	2	*Gorilla gorilla*	2	.515	8	1.000	7.199
Gorgorg7732M7_M_R	*Gorilla gorilla*	2	*Gorilla gorilla*	2	.513	8	1.000	7.224
Gorgorg7732M8_F_L	*Gorilla gorilla*	2	*Gorilla gorilla*	2	.855	8	1.000	4.027
Gorgorg7732M8_F_R	*Gorilla gorilla*	2	*Gorilla gorilla*	2	.780	8	1.000	4.791
Gorgor732M15_F_L	*Gorilla gorilla*	2	*Gorilla gorilla*	2	.096	8	1.000	13.507
Gorgor732M15_F_R	*Gorilla gorilla*	2	*Gorilla gorilla*	2	.091	8	1.000	13.677
Ppan11354_M_L	*Pan paniscus*	3	*Pan paniscus*	3	.617	8	1.000	6.274
Ppan11354_M_R	*Pan paniscus*	3	*Pan paniscus*	3	.067	8	1.000	14.619
Ppan13201_F_L	*Pan paniscus*	3	*Pan paniscus*	3	.949	8	1.000	2.759
Ppan13201_F_R	*Pan paniscus*	3	*Pan paniscus*	3	.518	8	.998	7.177
Ppan29026_F_L	*Pan paniscus*	3	*Pan paniscus*	3	.166	8	1.000	11.691
Ppan29026_F_R	*Pan paniscus*	3	*Pan paniscus*	3	.995	8	.999	1.363
Ppan29027_F_L	*Pan paniscus*	3	*Pan paniscus*	3	.782	8	.973	4.766
Ppan29027_F_R	*Pan paniscus*	3	*Pan paniscus*	3	.895	8	.972	3.551
Ppan29028_M_L	*Pan paniscus*	3	*Pan paniscus*	3	.986	8	.920	1.836
Ppan29028_M_R	*Pan paniscus*	3	*Pan paniscus*	3	.621	8	.551	6.234
Ppan29050_M_L	*Pan paniscus*	3	*Pan paniscus*	3	.861	8	.995	3.962
Ppan29050_M_R	*Pan paniscus*	3	*Pan paniscus*	3	.513	8	.995	7.222
Ppan29053_M_L	*Pan paniscus*	3	*Pan paniscus*	3	.546	8	.935	6.913
Ppan29053_M_R	*Pan paniscus*	3	*Pan paniscus*	3	.845	8	.940	4.130
Ppan29055_F_L	*Pan paniscus*	3	*Pan paniscus*	3	.858	8	.996	3.987
Ppan29055_F_R	*Pan paniscus*	3	*Pan paniscus*	3	.948	8	.998	2.762
Ppan84036M03_M_L	*Pan paniscus*	3	*Pan paniscus*	3	.848	8	.969	4.105
Ppan84036M03_M_R	*Pan paniscus*	3	*Pan paniscus*	3	.928	8	.988	3.106
Ppan84036M11_F_L	*Pan paniscus*	3	*Pan paniscus*	3	.653	8	.990	5.951
Ppan84036M11_F_R	*Pan paniscus*	3	*Pan paniscus*	3	.780	8	.915	4.785
Hs_A27Bush_F_L	*Homo sapiens*	4	*Homo sapiens*	4	.077	8	.942	14.188
Hs_A27Bush_F_R	*Homo sapiens*	4	*Homo sapiens*	4	.112	8	1.000	12.984
Hs_A84FING_F_L	*Homo sapiens*	4	*Homo sapiens*	4	.264	8	1.000	10.020
Hs_A84FING_F_R	*Homo sapiens*	4	*Homo sapiens*	4	.783	8	1.000	4.758
Hs_A173BUSH_M_L	*Homo sapiens*	4	*Homo sapiens*	4	.159	8	.998	11.822
Hs_A173BUSH_M_R	*Homo sapiens*	4	*Homo sapiens*	4	.154	8	.999	11.938
Hs_A281SOTHO_M_L	*Homo sapiens*	4	*Homo sapiens*	4	.763	8	1.000	4.947
Hs_A281SOTHO_M_R	*Homo sapiens*	4	*Homo sapiens*	4	.712	8	1.000	5.419
Hs_A861FING_M_L	*Homo sapiens*	4	*Homo sapiens*	4	.852	8	1.000	4.052
Hs_A861FING_M_R	*Homo sapiens*	4	*Homo sapiens*	4	.569	8	.995	6.703
Hs_A1263SOTHO_F_L	*Homo sapiens*	4	*Homo sapiens*	4	.093	8	1.000	13.596
Hs_A1263SOTHO_F_R	*Homo sapiens*	4	*Homo sapiens*	4	.120	8	.972	12.780
Hs_A1264TSWA_M_L	*Homo sapiens*	4	*Homo erectus*	8**	.011	8	.474	19.801
Hs_A1264TSWA_M_R	*Homo sapiens*	4	*Homo erectus*	8**	.173	8	.820	11.549
Hs_A1483TSWA_F_L	*Homo sapiens*	4	*Homo sapiens*	4	.343	8	1.000	8.986
Hs_A1483TSWA_F_R	*Homo sapiens*	4	*Homo sapiens*	4	.968	8	1.000	2.363
Hs_A3421_MIXED_M_L	*Homo sapiens*	4	*Homo sapiens*	4	.246	8	.995	10.279
Hs_A3421_MIXED_M_R	*Homo sapiens*	4	*Homo sapiens*	4	.412	8	.971	8.224
Hs_A3607MIXED_F_L	*Homo sapiens*	4	*Homo sapiens*	4	.084	8	.999	13.905
Hs_A3607MIXED_F_R	*Homo sapiens*	4	*Homo sapiens*	4	.710	8	1.000	5.439
Pan_t_sch83006M15_M_L	*Pan troglodytes schweinfurthii*	5	*Pan troglodytes schweinfurthii*	5	.852	8	.995	4.060
Pan_t_sch83006M15_M_R	*Pan troglodytes schweinfurthii*	5	*Pan troglodytes schweinfurthii*	5	.815	8	.973	4.442
Pan_t_sch83006M17_M_L	*Pan troglodytes schweinfurthii*	5	*Pan troglodytes schweinfurthii*	5	.481	8	1.000	7.524
Pan_t_sch83006M17_M_R	*Pan troglodytes schweinfurthii*	5	*Pan troglodytes schweinfurthii*	5	.512	8	.996	7.234
Pan_t_sch83006M21_M_L	*Pan troglodytes schweinfurthii*	5	*Pan troglodytes schweinfurthii*	5	.798	8	.812	4.616
Pan_t_sch83006M21_M_R	*Pan troglodytes schweinfurthii*	5	*Pan troglodytes schweinfurthii*	5	.952	8	.976	2.690
Pan_t_sch83006M22_M_L	*Pan troglodytes schweinfurthii*	5	*Pan troglodytes schweinfurthii*	5	.656	8	.996	5.919
Pan_t_sch83006M22_M_R	*Pan troglodytes schweinfurthii*	5	*Pan troglodytes schweinfurthii*	5	.617	8	.998	6.270
Pan_t_sch83006M32_F_L	*Pan troglodytes schweinfurthii*	5	*Pan troglodytes schweinfurthii*	5	.798	8	.909	4.616
Pan_t_sch83006M32_F_R	*Pan troglodytes schweinfurthii*	5	*Pan troglodytes schweinfurthii*	5	.843	8	.988	4.152
Pan_t_sch83006M37_F_L	*Pan troglodytes schweinfurthii*	5	*Pan troglodytes schweinfurthii*	5	.519	8	.569	7.164
Pan_t_sch83006M37_F_R	*Pan troglodytes schweinfurthii*	5	*Pan troglodytes schweinfurthii*	5	.588	8	.698	6.529
Pan_t_sch91060M406_F_L	*Pan troglodytes schweinfurthii*	5	*Pan troglodytes schweinfurthii*	5	.821	8	.982	4.386
Pan_t_sch91060M406_F_R	*Pan troglodytes schweinfurthii*	5	*Pan troglodytes schweinfurthii*	5	.924	8	.992	3.157
Pan_t_sch91060M410_F_L	*Pan troglodytes schweinfurthii*	5	*Pan troglodytes schweinfurthii*	5	.853	8	1.000	4.043
Pan_t_sch91060M410_F_R	*Pan troglodytes schweinfurthii*	5	*Pan troglodytes schweinfurthii*	5	.989	8	.999	1.684
Pan_t_sch91060M414_M_L	*Pan troglodytes schweinfurthii*	5	*Pan troglodytes schweinfurthii*	5	.909	8	.801	3.375
Pan_t_sch91060M414_M_R	*Pan troglodytes schweinfurthii*	5	*Pan troglodytes schweinfurthii*	5	.979	8	.981	2.077
Pan_t_sch91060M422_F_L	*Pan troglodytes schweinfurthii*	5	*Pan troglodytes schweinfurthii*	5	1.000	8	.998	.530
Pan_t_sch91060M422_F_R	*Pan troglodytes schweinfurthii*	5	*Pan troglodytes schweinfurthii*	5	.666	8	.983	5.831

Table 4.12 b) Discriminant function analysis results - fossil specimens

Specimen	Actual Group	Actual Group	Predicted Group	Highest Group				
				Predicted Group	P(D>d | G=g) p	P(D>d | G=g) df	P(G=g | D=d)	Squared Mahalanobis Distance to Centroid
AL145-35L	*Australopithecus afarensis*	6	*Australopithecus afarensis*	6	.020	8	1.000	18.235
AL228-23R	*Australopithecus afarensis*	6	*Australopithecus afarensis*	6	.081	8	.984	14.045
AL266-1L	*Australopithecus afarensis*	6	*Australopithecus afarensis*	6	.156	8	.939	11.886
AL266-1R	*Australopithecus afarensis*	6	*Australopithecus afarensis*	6	.171	8	.997	11.573
AL288-1R	*Australopithecus afarensis*	6	*Homo sapiens*	4**	.153	8	.547	11.957
AL333-W6DL	*Australopithecus afarensis*	6	*Australopithecus afarensis*	6	.588	8	.989	6.529
LH2R	*Australopithecus afarensis*	6	*Australopithecus afarensis*	6	.379	8	.545	8.580
LH4L	*Australopithecus afarensis*	6	*Australopithecus afarensis*	6	.005	8	.958	21.809
LH4R	*Australopithecus afarensis*	6	*Australopithecus afarensis*	6	.851	8	.998	4.063
MLD2L	*Australopithecus africanus*	7	*Australopithecus africanus*	7	.373	8	.992	8.650
MLD2R	*Australopithecus africanus*	7	*Australopithecus africanus*	7	.155	8	.402	11.916
Sts52bR	*Australopithecus africanus*	7	*Australopithecus afarensis*	6**	.584	8	.498	6.568
Taung1L	*Australopithecus africanus*	7	*Paranthropus robustus*	12**	.287	8	.817	9.692
Taung1R	*Australopithecus africanus*	7	*Paranthropus robustus*	12**	.484	8	.958	7.498
OH22R	*Homo erectus*	8	*Homo erectus*	8	.363	8	.694	8.763
KNM-ER806cL	*Homo erectus*	8	*Australopithecus africanus*	7**	.020	8	.843	18.196
KNM-ER820L	*Homo erectus*	8	*Homo erectus*	8	.722	8	.960	5.324
KNM-ER820R	*Homo erectus*	8	*Homo erectus*	8	.804	8	.995	4.556
KNM-ER992L	*Homo erectus*	8	*Homo erectus*	8	.978	8	.986	2.097
KNM-ER992R	*Homo erectus*	8	*Homo erectus*	8	.784	8	.956	4.750
OH7L	*Homo habilis*	9	*Homo habilis*	9	.897	8	.970	3.534
OH7R	*Homo habilis*	9	*Homo habilis*	9	.992	8	.962	1.566
OH16R	*Homo habilis*	9	*Homo habilis*	9	.396	8	.992	8.395
KNM-ER1802L	*Homo rudolfensis*	10	*Homo rudolfensis*	10	.991	8	.995	1.601
KNM-ER1802R	*Homo rudolfensis*	10	*Homo rudolfensis*	10	.991	8	.964	1.601
KNM-ER15930L	*Paranthropus boisei*	11	*Paranthropus boisei*	11	.075	8	.729	14.276
Peninj1L	*Paranthropus boisei*	11	*Paranthropus boisei*	11	.558	8	.972	6.799
Peninj1R	*Paranthropus boisei*	11	*Paranthropus boisei*	11	.893	8	.991	3.584
SK6L	*Paranthropus robustus*	12	*Paranthropus robustus*	12	.428	8	.961	8.061
SK6R	*Paranthropus robustus*	12	*Paranthropus robustus*	12	.711	8	1.000	5.432
SK23L	*Paranthropus robustus*	12	*Paranthropus robustus*	12	.938	8	.994	2.935
SK23R	*Paranthropus robustus*	12	*Paranthropus robustus*	12	.490	8	.881	7.439
SK63L	*Paranthropus robustus*	12	*Paranthropus robustus*	12	.626	8	1.000	6.193
SK63R	*Paranthropus robustus*	12	*Paranthropus robustus*	12	.909	8	1.000	3.367
SKW5R	*Paranthropus robustus*	12	*Paranthropus robustus*	12	.118	8	1.000	12.829
TM1517R	*Paranthropus robustus*	12	*Paranthropus robustus*	12	.688	8	.983	5.639

A cursory examination of the squared Mahalanobis distances (vector distances of specimens from the mean centroid value for each group) also confirms observations already made at the species level concerning variability. Gorillas and modern humans show more intra-species variability than do chimpanzees and bonobos. Of the fossil species, the widest within-group variability was shown by *A. afarensis.*

4.3.5 Results of Log se_m on radial measurements of landmarks

4.3.5.1 Four extant species

6320 pairwise x-on-y and y-on-x regression analyses were carried out on the 80 specimens representing four extant species used for the study, based on 48 radial measurements calculated for each specimen from the centre of each tooth to each of the anatomically or mathematically-placed landmarks (landmarks 2-49) used for the geometric morphometric analyses. The $\log_{10}$ of the standard error of each slope m (log se_m) was calculated and the results were then placed into an 80 x 80 matrix. The average of the two log se_m values of these were placed in a separate matrix. Lastly, delta values (differentials) were calculated between the minimum and the maximum log se_m values of each of the pairwise comparisons, with the figures placed in a third matrix. Due to the size of these matrices, it is not possible to reproduce them in their entirety within this dissertation but these are available in Excel format. Instead, the 20 x 20 intra-species matrices for each of the four extant species are provided in Appendix 5, and summary data for the full matrices of inter- and intra-species log se_m and delta values are given below.

Table 4.13 Summary of average log se_m values for conspecific pairwise comparisons of gorilla, chimpanzee, bonobo and modern *Homo sapiens*

Gorilla vs Gorilla		*Pan troglodytes vs Pan troglodytes*		*Homo sapiens vs Homo sapiens*		*Pan paniscus vs Pan paniscus*		*All conspecific comparisons*	
AVERAGE LOG SEm		**AVERAGE LOG SEm**		**AVERAGE LOG SEm**		**AVERAGE LOG SEm**		**AVERAGE LOG SEm**	
Mean	**-1.6428**	Mean	**-1.6577**	Mean	**-1.5389**	Mean	**-1.6439**	Mean	**-1.6208**
Standard Error	0.0094	Standard Error	0.0067	Standard Error	0.0092	Standard Error	0.0071	Standard Error	0.0044
Median	-1.6542	Median	-1.6509	Median	-1.5375	Median	-1.6453	Median	-1.6275
Mode	#N/A	Mode	#N/A	Mode	#N/A	Mode	#N/A	Mode	#N/A
Standard Deviation	**0.1300**	Standard Deviation	**0.0917**	Standard Deviation	**0.1262**	Standard Deviation	**0.0973**	Standard Deviation	**0.1221**
Sample Variance	0.0169	Sample Variance	0.0084	Sample Variance	0.0159	Sample Variance	0.0095	Sample Variance	0.0149
Kurtosis	1.1683	Kurtosis	0.3368	Kurtosis	0.1628	Kurtosis	0.1856	Kurtosis	0.4020
Skewness	0.1421	Skewness	-0.1699	Skewness	-0.4338	Skewness	-0.0659	Skewness	0.1303
Range	0.8778	Range	0.5084	Range	0.6181	Range	0.5283	Range	0.8778
Minimum	-2.1135	Minimum	-1.9291	Minimum	-1.9035	Minimum	-1.9142	Minimum	-2.1135
Maximum	-1.2357	Maximum	-1.4207	Maximum	-1.2854	Maximum	-1.3859	Maximum	-1.2357
Sum	-312.1230	Sum	-314.9622	Sum	-292.3934	Sum	-312.3319	Sum	-1231.8106
Count	190.0000	Count	190.0000	Count	190.0000	Count	190.0000	Count	760.0000
Confidence Level(95.0%)	0.0186	Confidence Level(95.0%)	0.0131	Confidence Level(95.0%)	0.0181	Confidence Level(95.0%)	0.0139	Confidence Level(95.0%)	0.0087

Pairwise intra-specific (conspecific) comparisons of the four species examined showed average log se_m values for these species grouping around a central tendency of -1.6208, with a standard deviation of 0.1221 (n= 760, based on 1520 pairwise comparisons). Histograms showing frequency distributions of the log se_m values for the four intra-species pairwise comparisons are shown in Figure 4.18 below:

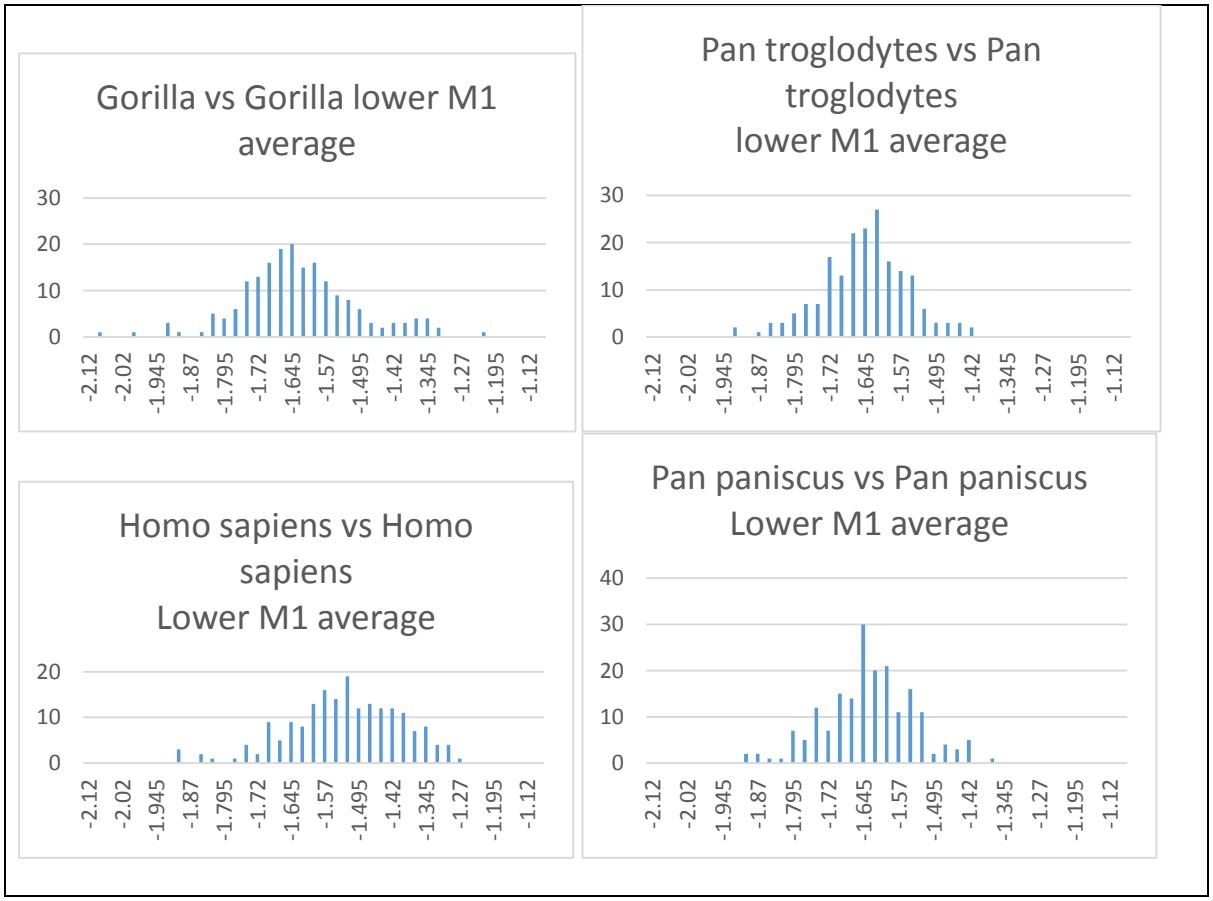

Figure 4.18 Frequency distributions of average log se_m values for intra-specific pairwise comparisons lower first molars of gorilla, chimpanzee, bonobo and modern *Homo sapiens*

As can be seen from the summary statistics and the histograms above, the log se_m analysis confirms that the modern *Homo sapiens* sample shows a greater level of intra-specific shape variability of first molar shape than do the three great ape species samples. The average log se_m values for the three great ape species is lower than that for the modern *Homo sapiens* sample, and the values for the latter sample are fairly evenly spread across a range of higher values (than the overall mean for all four species) in the histograms.

Further informing the intra-specific comparisons are the differentials between the maximum and the minimum log se_m values for each individual pairwise comparison (delta values, see 3.6.1.5):

Table 4.14 Summary of differentials (delta values) between pairs of log se_m values for comparisons of conspecific pairs of gorilla, chimpanzee, bonobo and modern *Homo sapiens*

Gorilla vs Gorilla		*Pan troglodytes vs Pan troglodytes*		*Homo sapiens vs Homo sapiens*		*Pan paniscus vs Pan paniscus*		*4 intra-species comparisons*	
Delta Values		**Delta Values**		**Delta Values**		**Delta Values**		**Delta Values**	
Mean	**0.0706518**	Mean	**0.0483288**	Mean	**0.0468516**	Mean	**0.056339579**	Mean	**0.055543**
Standard Error	0.0038327	Standard Error	0.0025392	Standard Error	0.0029304	Standard Error	0.003162861	Standard Error	0.00161
Median	0.0680662	Median	0.0444319	Median	0.0351178	Median	0.051406764	Median	0.046033
Mode	#N/A	Mode	#N/A	Mode	#N/A	Mode	#N/A	Mode	#N/A
Standard Deviation	**0.0528298**	Standard Deviation	**0.0350004**	Standard Deviation	**0.0403925**	Standard Deviation	**0.043597024**	Standard Deviation	**0.044372**
Sample Variance	0.002791	Sample Variance	0.001225	Sample Variance	0.0016316	Sample Variance	0.0019007	Sample Variance	0.001969
Kurtosis	0.057379	Kurtosis	0.6307892	Kurtosis	1.2135324	Kurtosis	-0.088121143	Kurtosis	0.737093
Skewness	0.7427472	Skewness	0.8821239	Skewness	1.2786478	Skewness	0.70459574	Skewness	1.004157
Range	0.2040443	Range	0.1799394	Range	0.1845722	Range	0.19205656	Range	0.20421
Minimum	0.0004049	Minimum	0.0002706	Minimum	0.0002891	Minimum	0.000239628	Minimum	0.00024
Maximum	0.2044492	Maximum	0.18021	Maximum	0.1848612	Maximum	0.192296188	Maximum	0.204449
Sum	13.423843	Sum	9.1824633	Sum	8.9017982	Sum	10.70451996	Sum	42.21262
Count	190	Count	190	Count	190	Count	190	Count	760
Confidence Level(95.0%)	0.0075603	Confidence Level(95.0%)	0.0050088	Confidence Level(95.0%)	0.0057805	Confidence Level(95.0%)	0.006239043	Confidence Level(95.0%)	0.00316

Since log se_m values reflect levels of scatter around two different slopes with two different y-intercepts, the delta values are able to provide additional information about size variation in addition to the shape variability, between the two specimens being compared. The average delta value for all four species was 0.056. The species showing most size variation in this instance is the gorilla species, which is consistent with its being the species with the most sexual dimorphism evident in size differences between

males and females. The species with the least variation was the modern *Homo sapiens* group, again consistent with previous results: the modern *Homo sapiens* lower first molar sample showed the most variability in terms of shape, but less variability in terms of size, between the four species.

Comparison between species were then carried out. The results are presented in Table 4.15.

Table 4.15 Summary of average log se_m values for inter-specific pairs of gorilla, chimpanzee, bonobo and modern *Homo sapiens*

Gorilla vs Pan troglodytes		*Gorilla vs Pan paniscus*		*Pan troglodytes vs Pan paniscus*	
Mean	-1.5344	Mean	-1.5103	Mean	-1.6163
Standard Error	0.0056	Standard Error	0.0046	Standard Error	0.0042
Median	-1.5416	Median	-1.5065	Median	-1.6123
Mode	#N/A	Mode	#N/A	Mode	#N/A
Standard Deviation	0.1116	Standard Deviation	0.0926	Standard Deviation	0.0837
Sample Variance	0.0125	Sample Variance	0.0086	Sample Variance	0.0070
Kurtosis	0.7624	Kurtosis	1.0104	Kurtosis	-0.0607
Skewness	0.3222	Skewness	0.4006	Skewness	-0.0518
Range	0.7109	Range	0.5578	Range	0.4701
Minimum	-1.8597	Minimum	-1.7619	Minimum	-1.8574
Maximum	-1.1487	Maximum	-1.2042	Maximum	-1.3873
Sum	-613.7698	Sum	-604.1271	Sum	-646.5304
Count	400.0000	Count	400.0000	Count	400.0000
Confidence Level(95.0%)	0.0110	Confidence Level(95.0%)	0.0091	Confidence Level(95.0%)	0.0082
Gorilla vs Homo sapiens		*Pan troglodytes vs Homo sapiens*		*Pan paniscus vs Homo sapiens*	
Mean	-1.3709	Mean	-1.4819	Mean	-1.4754
Standard Error	0.0046	Standard Error	0.0043	Standard Error	0.0040
Median	-1.3746	Median	-1.4886	Median	-1.4773
Mode	#N/A	Mode	#N/A	Mode	#N/A
Standard Deviation	0.0927	Standard Deviation	0.0869	Standard Deviation	0.0798
Sample Variance	0.0086	Sample Variance	0.0075	Sample Variance	0.0064
Kurtosis	-0.6325	Kurtosis	-0.2688	Kurtosis	-0.6032
Skewness	0.1630	Skewness	0.3156	Skewness	0.0283
Range	0.4480	Range	0.4549	Range	0.3967
Minimum	-1.5733	Minimum	-1.6873	Minimum	-1.6691
Maximum	-1.1253	Maximum	-1.2324	Maximum	-1.2723
Sum	-548.3417	Sum	-592.7737	Sum	-590.1733
Count	400.0000	Count	400.0000	Count	400.0000
Confidence Level(95.0%)	0.0091	Confidence Level(95.0%)	0.0085	Confidence Level(95.0%)	0.0078

The above inter-specific comparisons are based on averaged Log se_m values and confirm previous results, such as the PCA plots performed in Procrustes shape space: with most of the effects of size removed from the comparisons, there is little to differentiate a bonobo lower first molar from a chimpanzee lower first molar (Singleton *et al.*, 2011). The log se_m values for comparisons between these two species, at an average of -1.616, is almost the same as the average log se_m value reported in table 4.13 above for conspecific comparisons (-1.621) of lower first molars for the four species examined in this study, and is very close to the value of -1.61 calculated by Thackeray (1997) to be

the average log se_m value for conspecific pairwise comparisons, based on pairwise comparisons of cranial data within more than 70 taxa. Comparisons between gorillas and the two species of *Pan* give reasonably similar mean values to each other, at -1.534 and -1.510. Comparisons between modern *Homo sapiens* and the three great ape species show higher log se_m values, as a result of a greater variability in shape, of -1.476 and -1.482 respectively between modern *Homo sapiens* and bonobos and chimpanzees, and a significantly high value of -1.371 between modern *Homo sapiens* and gorillas, the latter of whose lower first molars are, on average, the most narrow of all the four species, those of modern *Homo sapiens* being, on average, the most wide. Average log se_m value comparisons between the four different species can be visualised by means of the following histograms (Figure 4.19), which are arranged in order of similarity in shape between species:

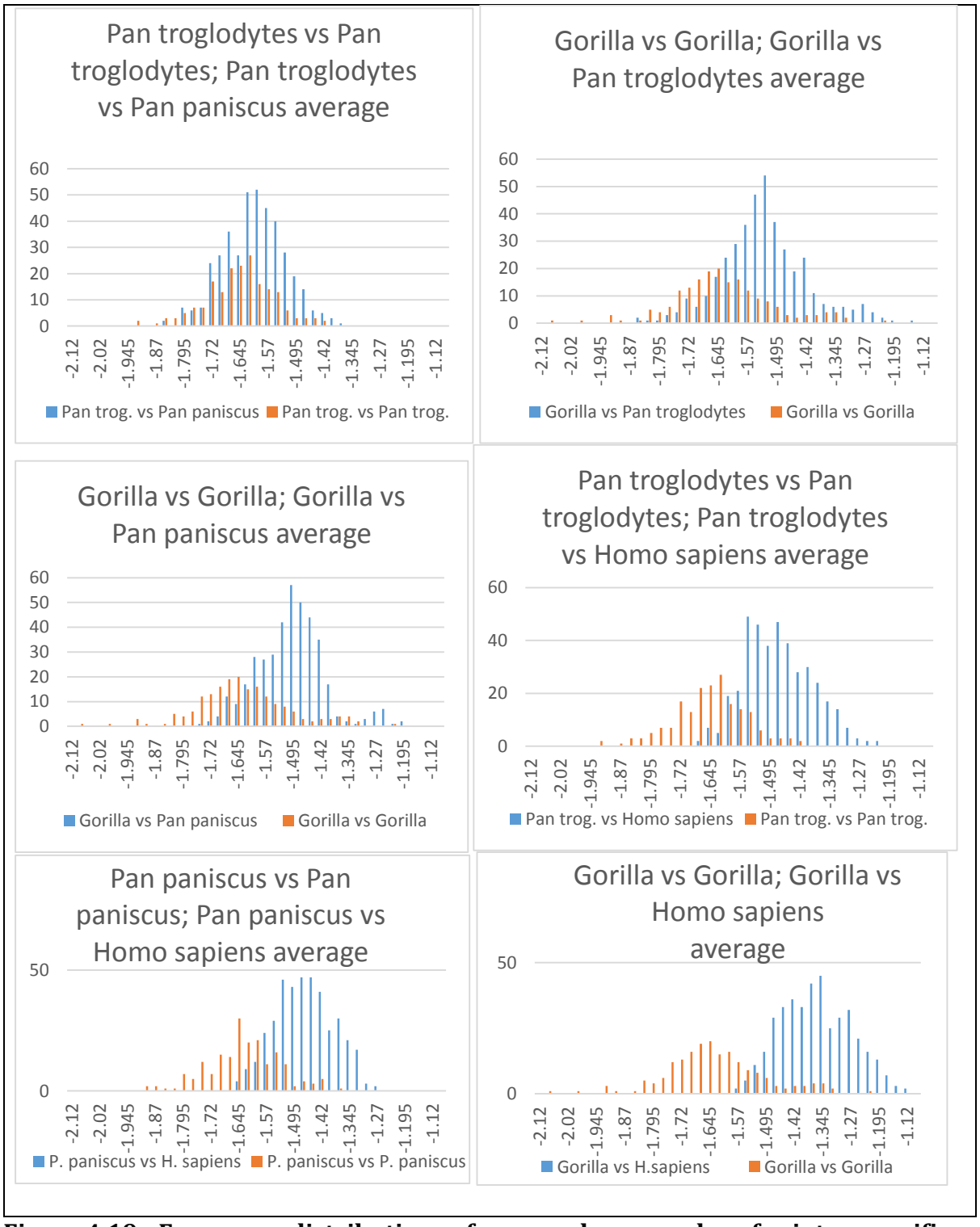

Figure 4.19 Frequency distributions of average log se_m values for inter-specific pairwise comparisons of lower first molars of gorilla, chimpanzee, bonobo and modern *Homo sapiens*, shown in order of shape similarity. Size variation is not reflected in these comparisons as the two log se_m values for each pairwise comparison were first averaged.

Note: in areas of overlap between species, it might appear that there are many specimens in the area of the overlap. It needs to be remembered that if one specimen (e.g. of *Homo sapiens*) genuinely overlaps with another species (e.g. *Gorilla gorilla*), there will be up to 38 log se_m values (or 19, in the case of averaged log se_m values) to represent that single overlap (each specimen from species A will have 19 pairwise comparisons to other members of species B in the x-on-y pairwise comparisons and a further 19 on the y-on-x pairwise comparisons).

Turning to the differentials between the two log se_m values for individual pairwise comparisons (delta values) between specimens from different species, the average inter-specific delta value was calculated to be 0.194 +/- 0.128 (n=2400 delta values measured from 4800 pairwise comparisons). This figure is almost four times higher than the intra-specific mean delta value of 0.056. Here again, the importance of size as well as morphology in dental comparisons is being recognised in the calculations. The mean delta values for inter-specific comparisons between each species are presented below in Table 4.16:

Table 4.16 Summary of log se_m delta values for inter-specific pairs of gorilla, chimpanzee, bonobo and modern *Homo sapiens*

Gorilla vs Pan troglodytes		*Gorilla vs P paniscus*		*Pan troglodytes vs Pan paniscus*	
Delta Values		**Delta Values**		**Delta Values**	
Mean	0.2578499	Mean	0.3725567	Mean	0.1161679
Standard Error	0.0036714	Standard Error	0.0039086	Standard Error	0.0030684
Median	0.2659901	Median	0.3767551	Median	0.1123224
Mode	#N/A	Mode	#N/A	Mode	#N/A
Standard Deviation	0.0734271	Standard Deviation	0.078172	Standard Deviation	0.0613689
Sample Variance	0.0053915	Sample Variance	0.0061109	Sample Variance	0.0037661
Kurtosis	-0.16918	Kurtosis	-0.164806	Kurtosis	-0.347431
Skewness	-0.333208	Skewness	-0.214155	Skewness	0.3215579
Range	0.3846592	Range	0.3967454	Range	0.3006679
Minimum	0.0400313	Minimum	0.1487754	Minimum	0.0003723
Maximum	0.4246905	Maximum	0.5455207	Maximum	0.3010402
Sum	103.13998	Sum	149.02268	Sum	46.467161
Count	400	Count	400	Count	400
Confidence Level(95.0%)	0.0072176	Confidence Level(95.0%)	0.007684	Confidence Level(95.0%)	0.0060323
Gorilla vs Homo sapiens		*Pan troglodytes vs Homo sapiens*		*Pan paniscus vs Homo sapiens*	
Delta Values		**Delta Values**		**Delta Values**	
Mean	0.249365	Mean	0.0463726	Mean	0.1238364
Standard Error	0.0037089	Standard Error	0.0018891	Standard Error	0.0031928
Median	0.2544056	Median	0.0363637	Median	0.114876
Mode	#N/A	Mode	#N/A	Mode	#N/A
Standard Deviation	0.0741772	Standard Deviation	0.0377821	Standard Deviation	0.0638566
Sample Variance	0.0055023	Sample Variance	0.0014275	Sample Variance	0.0040777
Kurtosis	-0.013742	Kurtosis	2.0548094	Kurtosis	0.1460617
Skewness	-0.547132	Skewness	1.3341432	Skewness	0.5649211
Range	0.383352	Range	0.2237051	Range	0.3429993
Minimum	0.0023739	Minimum	0.0001208	Minimum	0.0016568
Maximum	0.3857259	Maximum	0.2238259	Maximum	0.3446561
Sum	99.745981	Sum	18.54905	Sum	49.534558
Count	400	Count	400	Count	400
Confidence Level(95.0%)	0.0072913	Confidence Level(95.0%)	0.0037138	Confidence Level(95.0%)	0.0062769

The highest average delta value (0.373) was between gorillas and bonobos, which represented the largest and smallest of the molar teeth in the study respectively. The lowest average delta value (0.046) was between chimpanzees and modern *Homo sapiens,* indicative of species with similarly-sized teeth.

The results of these log se_m comparisons can be summarised as follows (Table 4.17):

Table 4.17 Summary of results from log se_m analyses: extant species

Comparison	Average log se_m	Delta value	Comment
Average intra-species values	-1.621	0.056	
Average inter-species values	-1.498	0.194	
Gorilla vs. Gorilla	-1.643	0.071	Higher than average shape similarity Higher than average size variability
Chimpanzee vs. Chimpanzee	-1.6577	0.048	Highest average shape similarity Low average size variability
Homo sapiens vs. Homo sapiens	-1.539	0.047	Lowest average shape similarity Lowest average size variability
Bonobo vs. Bonobo	-1.644	0.056	Higher than average shape similarity Average size variability close to mean
Gorilla vs. Chimpanzee	-1.534	0.258	Similarity in shape but large difference in size. Very low probability of overlap between specimens
Gorilla vs. Bonobo	-1.510	0.373	Similarity in shape but extreme difference in size. No probability of overlap between specimens despite shape similarity
Chimpanzee vs. Bonobo	-1.616	0.116	Extreme similarity in shape and twice the intraspecific average difference in size. Some probability of overlap between specimens.
Gorilla vs. Homo sapiens	-1.371	0.249	Generally very dissimilar in shape, large average difference in size. Low probability of overlap between specimens
Chimpanzee vs. Homo sapiens	-1.482	0.046	Slight shape similarity, very close in size. High probability of overlap between specimens
Bonobo vs. Homo sapiens	-1.475	0.124	Slight shape similarity, more than twice the intraspecific average difference in size. Low probability of overlap between specimens

4.3.5.2 African Plio-Pleistocene fossil hominin species

1260 pairwise x-on-y and y-on-x regression analyses were carried out on the 36 lower first molars representing African Plio-Pleistocene fossil hominin species used for the study, based on 48 radial measurements calculated for each specimen from the centre

of each tooth to each of the mathematically-placed landmarks (landmarks 2-49) used for the geometric morphometric analyses. The $\log_{10}$ of the standard error of each slope m ($\log se_m$) was calculated and the results were then placed into a 36 x 36 matrix. The average of the two $\log se_m$ values of these were placed in a separate matrix. Lastly, delta values (differentials) were calculated between the minimum and the maximum $\log se_m$ values of each of the pairwise comparisons, with the figures placed in a third matrix. The main 36 x 36 matrix is provided in Appendix 6, and summary data for the full matrices of inter- and intra-species $\log se_m$ and delta values are given below.

Certain of the currently classified species have unusually high shape diversity between them (reflected in higher $\log se_m$ values), while the *Homo* groups show similar diversity to that of modern humans and other primates, as shown in Table 4.18:

Table 4.18 Average intra-species $\log se_m$ values for fossil M_1 specimens as currently classified:

Current taxon	A. afarensis	A. africanus	Homo erectus	Homo habilis/rudolfensis	Paranthropus boisei/robustus
Average log se_m	-1.437	-1.521	-1.625	-1.701	-1.566
Standard deviation	0,125	0,134	0,160	0,096	0,110
Count (n)	72	20	30	20	110

In view of the average $\log se_m$ values for the extant primate species of -1.6208 (+/- 0.1221; n=1520) it can be said that any pairwise $\log se_m$ results that are higher than -1.6208 + (1.96 x 0.1221), that is, any pairwise $\log se_m$ output above -1.3815 within any species group might well require further scrutiny in terms of taxonomy. The average Log se_m value for all fossil species together (including potentially misclassified or anomalous specimens) is -1,57.

The paired x-on-y and y-on-x log se_m values ("delta values", see 3.6.1.5) further inform the intra-species comparisons. Intra-species values are shown in Table 4.19.

Table 4.19 Average intra-species delta values for fossil M_1 specimens as currently classified:

Current taxon	A. afarensis	A. africanus	Homo erectus	Homo habilis/rudolfensis	Paranthropus boisei/robustus
Average log se_m	0.071	0.050	0.040	0.036	0.058
Standard deviation	0.046	0.033	0.024	0.027	0.038
Count (n)	36	10	15	10	55

The delta values incorporate size differences into the analysis. It is not surprising that *A. afarensis,* which includes a tiny, narrow specimen such as AL 288-1 and several larger and squarer specimens, would have the largest average delta, with the highest standard deviation. The smallest delta value was for the "Early *Homo*" group. The *Homo erectus* group has the next smallest delta value: this value would have been 0.031, were it not for the inclusion of the unusually large specimen, KNM-ER 806c. The group consisting of the two *Paranthropus* species has a high delta value with a moderate standard deviation, which would be in keeping with what was seen from the PC plots: the specimens are not as diversely scattered as those of *A. afarensis;* they form two main groups, with specimens, particularly in the smaller group, being very close in size to each other, but (as a group) not close in size to the larger specimens in the *Paranthropus* clade.

Intra-species log se_m matrices are set out in Tables 4.20 to 4.25 below:

Table 4.20 Log se_m matrix - *Australopithecus afarensis:*

		AL145-35L	AL128-23R	AL266-1L	AL266-1R	AL288-1R	AL333-W60L	LH2R	LH4L	LH4R
		1	2	3	4	5	6	7	8	9
AL145-35L	1		-1.526	-1.428	-1.407	-1.369	-1.421	-1.400	-1.247	-1.423
AL128-23R		-1.402		-1.510	-1.401	-1.333	-1.479	-1.463	-1.291	-1.540
AL266-1L	3	-1.397	-1.602		-1.592	-1.514	-1.570	-1.582	-1.267	-1.490
AL266-1R	4	-1.342	-1.459	-1.558		-1.492	-1.609	-1.390	-1.223	-1.451
AL288-1R	5	-1.240	-1.328	-1.417	-1.429		-1.325	-1.439	-1.135	-1.278
AL333-W60L	6	-1.436	-1.617	-1.616	-1.689	-1.468		-1.450	-1.350	-1.669
LH2R	7	-1.447	-1.634	-1.660	-1.503	-1.615	-1.483		-1.308	-1.486
LH4L	8	-1.237	-1.404	-1.288	-1.279	-1.253	-1.325	-1.251		-1.472
LH4R	9	-1.383	-1.623	-1.481	-1.477	-1.366	-1.614	-1.399	-1.442	

The mean log se_m is -1.437, and the standard deviation is 0.125 (n=72). This group presents the most variability in shape between all of the current fossil taxonomic groups. The mean log se_m between specimens allocated to this species and those allocated to other species is -1.404. This implies that on shape alone, there is almost as much diversity within this single species group as there is between the specimens in this group and specimens from other species groups. The mean inter-specific delta value between *A. afarensis* and other species groups is 0.086, which is not greatly different to the mean value for comparisons within the group, of 0.071, confirming this unusual intra-species diversity, with size also being factored in to the analysis – so both size and shape are extremely varied within this species.

To highlight some results for individual specimens, AL 288-1, identified as an outlier or anomaly by other analyses, remains a significant anomaly in this analysis as well. As was noticed from the linear dimensions analyses, this specimen is extremely narrow by comparison with other specimens of the group, with the exception of LH 2, the other comparatively narrow specimen in the group. AL 288-1 and LH 2 produce very low values for pairwise comparisons with other specimens in the group. The delta value between these two specimens of divergent size is a very high 0.176, well over double

the average for this disparate group, of 0.071, reflecting the large size difference between the two specimens. LH 2 itself might seem to group better overall with AL 266-1 (L), the larger, but relatively more narrow, of the two AL 266-1 antimeres. The delta value in this instance is 0.078, which is not far away from the mean value for the group. Comparing it to AL 128-23R, however, although one of the log se_m values is as high as -1.634, the second value is -1.479, which represents a delta value of 0.171. The "size-and-shape" analysis therefore indicates a large difference between the two specimens. LH 2 groups very poorly, however, with the holotype for *A. afarensis,* LH 4, with values averaging -1.361 for comparisons between these two specimens. This value is higher than the value of -1.3815, which, based on the 95% confidence limit for comparisons of conspecific pairs of (extant) species, would indicate that there is a high probability that these two specimens are not conspecific, although due to the high average value for this group, no firm assessments can be made.

In respect of the holotype for *A. afarensis,* some caution should be applied in the case of the log se_m analysis, particularly, due to the fact that for this species, both of the antimeres of the holotype were damaged to some degree, specifically around the perimeter edge (as previously noted, this specimen was considered too important to exclude from the study). With 28 landmarks of the 48 utilised in this analysis being allocated to perimeter shape (and maximal diameters judged from the perimeter), and with no statistically differential weighting being conferred by this methodology on any of the landmarks that most contribute to covariance in the shape analysis, any observer error made in the inferred perimeter shape will be emphasised by the log se_m analysis. Such errors may not be emphasised, for instance, in a principal components analysis or a discriminant function analysis based on PC scores. For log se_m pairwise comparisons

between the two antimeres directly, there is an average log se_m value of -1.457, which is not as low a value as might be expected for antimeres. The delta value is, however, 0.03, which is well below average for the group, and is even well below the average delta value for any of the extant species' intra-species averages, so although the antimeres are different in shape, the degree of antimeric variability is not as excessive as might first appear. In the case of the two other very different antimeres, those of AL 266-1, on the other hand, the average log se_m value is a lower -1.575 (well below the average for the group). The delta value is 0.034, which reflects a low to moderate size difference between these antimeres, as confirmed by the linear dimensions analyses.

Table 4.21 Log se_m matrix - *Australopithecus africanus:*

		MLD2L	MLD2R	Sts52bR	Taung1L	Taung1R
		10	11	12	13	14
MLD2L	10		-1.744	-1.675	-1.459	-1.432
MLD2R	11	-1.733		-1.688	-1.426	-1.422
Sts52bR	12	-1.587	-1.611		-1.463	-1.459
Taung1L	13	-1.391	-1.368	-1.483		-1.667
Taung1R	14	-1.349	-1.351	-1.464	-1.653	

The mean log se_m is -1.521, and the standard deviation is 0.134 (n=20). This is compared to an average log se_m value for comparisons between specimens within the group and specimens of other species of -1.450 (+/- 0.049). The average delta value for intra-species and inter-species comparisons are 0.050 and 0.068 respectively. The apparent discrepancy in this group is presented by Taung1, which is actually the holotype of the species. Taung1 has an identifiable sixth cusp, and the landmarks placed on these would accentuate this difference in terms of shape alone.

Table 4.22 Log se_m matrix - *Homo erectus:*

		OH22R	KNM-ER806c	KNM-ER820L	KNM-ER820R	KNM-ER992L	KNM-ER992R
		15	16	17	18	19	20
OH22R	15		-1.402	-1.653	-1.761	-1.695	-1.692
KNM-ER806cL	16	-1.425		-1.401	-1.498	-1.462	-1.468
KNM-ER820L	17	-1.632	-1.357		-1.755	-1.673	-1.751
KNM-ER820R	18	-1.693	-1.407	-1.709		-1.751	-1.729
KNM-ER992L	19	-1.653	-1.396	-1.653	-1.776		-1.910
KNM-ER992R	20	-1.651	-1.403	-1.731	-1.755	-1.911	

The mean log se_m for within-group pairwise comparisons is -1.625, and the standard deviation is 0.160 (n=30). Inter-group comparisons between these specimens and other species give an average value of -1.459. This group is much more cohesive and the log se_m values approach those of the extant species groups. The specimen that seems to fit less well with this group is KNM-ER 806c. It is both different in size (as witnessed by the wider divergence between the two values for each pairwise comparison – showing that the slopes of the two regression lines calculated for an x-on-y and a y-on-x regression are different) and in shape (higher log se_m outputs across the board, most of them higher than the inter-species pairwise average for this group). The mean log se_m for *Homo erectus,* with KNM-ER 806c excluded from the group falls to -1.727. Intra-species average delta values are 0.040 (including KNM-ER 806c) and 0.031 (excluding this specimen from the group). The mean delta value between this species group and other species groups is 0.108.

Table 4.23 Log se_m matrix - *Homo habilis* and *Homo rudolfensis*
(There is only one specimen in the *Homo rudolfensis* group, so intra-species comparisons for *rudolfensis* were not possible.)

		OH7L	OH7R	OH16R	KNM-ER1802L	KNM-ER1802R
		21	22	23	24	25
OH7L	21		-1.870	-1.581	-1.696	-1.716
OH7R	22	-1.863		-1.645	-1.635	-1.764
OH16R	23	-1.631	-1.701		-1.521	-1.673
KNM-ER1802L	24	-1.753	-1.699	-1.529		-1.742
KNM-ER1802R	25	-1.770	-1.824	-1.677	-1.738	

The mean log se_m is -1.701, and the standard deviation is 0.096 (n=20). The average between this species and specimens from other species groups is -1.472 (+/-0.130). This group is the most cohesive in terms of shape comparisons of all the other groups, despite the inclusion of *Homo rudolfensis* with *Homo habilis.* In fact, the two antimeres of KNM-ER 1802 group more closely with the two antimeres of OH 7 than does OH 16 (OH 16 is classified with OH 7 as *Homo habilis,* while KNM-ER 1802 is currently classified as *Homo rudolfensis.* OH 16 is larger and wider than OH 7*).* The average delta values for intra-species and inter-species comparisons respectively are 0.036 and 0.070 respectively.

Table 4.24 Log se_m matrix - *Paranthropus boisei* and *Paranthropus robustus*
(*Paranthropus boisei* was represented only by two antimeres from Peninj 1 and the left tooth of KNM-ER 15930. Since KNM-ER 15930 groups poorly with the *Paranthropus* genus in general, these two specimens were not representative enough as a group to produce meaningful statistics as a *boisei* group by themselves. The results for *Paranthropus boisei* are presented together with *Paranthropus robustus*).

		KNM-ER15930L	Peninj1L	Peninj1R	SK6L	SK6R	SK23L	SK23R	SK63L	SK63R	SKW5R	TM1517R
		26	27	28	29	30	31	32	33	34	35	36
KNM-ER15930L	26		-1.367	-1.438	-1.377	-1.363	-1.363	-1.353	-1.375	-1.328	-1.397	-1.423
Peninj1L	27	-1.492		-1.730	-1.626	-1.624	-1.665	-1.600	-1.695	-1.638	-1.651	-1.791
Peninj1R	28	-1.547	-1.714		-1.728	-1.596	-1.728	-1.606	-1.565	-1.510	-1.628	-1.682
SK6L	29	-1.482	-1.607	-1.724		-1.709	-1.802	-1.676	-1.640	-1.537	-1.572	-1.625
SK6R	30	-1.462	-1.599	-1.586	-1.704		-1.639	-1.523	-1.727	-1.629	-1.543	-1.678
SK23L	31	-1.421	-1.598	-1.677	-1.755	-1.598		-1.710	-1.597	-1.571	-1.599	-1.575
SK23R	32	-1.391	-1.513	-1.535	-1.608	-1.461	-1.690		-1.559	-1.469	-1.522	-1.512
SK63L	33	-1.380	-1.576	-1.462	-1.540	-1.632	-1.544	-1.526		-1.656	-1.521	-1.687
SK63R	34	-1.375	-1.560	-1.448	-1.479	-1.576	-1.560	-1.478	-1.697		-1.568	-1.633
SKW5R	35	-1.379	-1.509	-1.501	-1.449	-1.426	-1.523	-1.466	-1.498	-1.503		-1.635
TM1517R	36	-1.456	-1.700	-1.607	-1.553	-1.611	-1.551	-1.508	-1.715	-1.619	-1.686	

The mean log se_m for the *Paranthropus* clade as a whole is -1.566, and the standard deviation is 0.110 (n=110). The least cohesive member of this grouping, in terms of shape, is KNM-ER 15930, which seems to fit poorly with both *P. boisei* and *P. robustus* in the analysis, having numerous values above -1.3815 (the upper 95% confidence limit for conspecific pairs) . If that particular specimen were removed from the group as a whole, the mean log se_m would then be -1.601 for *Paranthropus spp.*, and the standard deviation 0.086 (n=90). Thus, with the exception of KNM-ER 15930, *Paranthropus boisei* (represented by Peninj 1, which is a mandibular proxy for OH 5, the holotype of *Paranthropus boisei*) and the *Paranthropus robustus* specimens group extremely well together.

The mean inter-species log se_m value (for pairwise comparisons between specimens of *Paranthropus spp.* and specimens of other species in the sample) is -1.409 (including KNM-ER 15930 with the *Paranthropus* group), or -1.356 (excluding this specimen). Average delta values are 0.058 for intra-species comparisons including KNM-ER 15930, 0.057 excluding this specimen from the group, and 0.093 for inter-species comparisons.

Taking the *Paranthropus* grouping as a whole, with the exception of KNM-ER 15930 due to its frequent status as an anomalous specimen within this group (in this and other analyses), the large size of the group as a whole allows for reasonably robust comparisons between average log se_m values for each specimen on an individual basis, both intra-species (*within* the group) and inter-species (*outside of* the group). The results are shown in Table 4.25.

Table 4.25 Average log se_m values for M_1s of *Paranthropus* specimens compared to specimens from other species groups and to specimens within the *Paranthropus* group.

Log sem values	Peninj1L	Peninj1R	SK6L	SK6R	SK23L	SK23R	SK63L	SK63R	SKW5R	TM1517R
avg value between groups	-1.32335	-1.36339	-1.35203	-1.33761	-1.34058	-1.33917	-1.38221	-1.33622	-1.38502	-1.41114
avg value within group (excl. KNM-ER 15930)	-1.59725	-1.58549	-1.60461	-1.58151	-1.63356	-1.56588	-1.63256	-1.57023	-1.58785	-1.64652

As discussed above, the mean within-group log se_m value for all the extant species in this study is -1.621, with a standard deviation of 0.1221. For the *Paranthropus* group (excluding KNM-ER 15930), the average within-group log se_m value for these specimens is -1.601. None of the within-group average log se_m values for this group fall above -1.566, which is less than one standard deviation away from the mean for all extant species groups of -1.621. Based on these values, there is a high probability of conspecificity for the specimens attributed to *Paranthropus* (TM 1517, Peninj 1, SK 6, SK 23, SK 63 and SKW 5). On the other hand, when each specimen is compared pair-wise with specimens from other fossil species, the average log se_m value for these specimens is calculated to be -1.357, which is well outside the 95% confidence interval of -1.382 ((-1.621 + (0.122 x 2). Based on these values, there would be a low probability of conspecificity between these specimens and specimens from other species groups. The log se_m values not only confirm the integrity of the approach taken by Thackeray (*ibid.*) but confirm the results of the other analyses, in particular the Procrustes distance matrix.

4.3.5.3 Potential anomalies – log se_m analysis

Comparisons were made between the log se_m values of anomalous specimens (those with higher than expected within-group log se_m values), with those of specimens from

other taxonomic groups. By examining the 36 x 36 matrix in Appendix 6, it can be seen that for this analysis:

- AL 288-1 *(Australopithecus afarensis)* groups better with *Homo erectus, Homo habilis* and *Homo rudolfensis* than it does with any of the specimens in the *Australopithecus afarensis* group. The same is true, to a lesser extent, of LH 2.
- LH 4 (L) which is a surprise anomaly in this group, still groups better with *Australopithecus afarensis* than it does with any other species group. The average log se_m value for this specimen in pairwise comparisons with specimens from other species is -1.241, with a range of -1.293 and -1.135. This confirms the supposition that perceived shape differences along the inferred perimeter of the two antimeres of this holotype specimen may be being highlighted by the log se_m analysis, but not enough for this specimen (and/or its antimere) to be considered to be a misclassification, belonging rather to a different species. (This is borne out by the discriminant function analysis.)
- Taung 1 *(Australopithecus africanus)* groups slightly better with *Paranthropus robustus* than it does with *Australopithecus africanus.* As pointed out before, however, this is due to the presence of the C_6 on the molars of Taung 1, which is diagnostic of *Paranthropus.* On a shape analysis alone, this grouping is not unexpected, and such was also confirmed by the DFA. In terms of size, Taung 1 is small relative to *Paranthropus* specimens.
- KNM-ER 806c (currently grouped with *Homo erectus)* appears to be an anomaly. It groups marginally better in terms of shape with *Paranthropus*, but is small for this group.
- OH 22 appears to group just as well, if not better, with *Homo rudolfensis* than with *Homo erectus.* In terms of size, however, it is considerably smaller.

- KNM-ER 15930 seems to group better with OH16 and the *Australopithecus africanus* group (without C_6) than it does with *Paranthropus boisei* or *Paranthropus robustus.*

Comparison of log se_m results with other analyses:

By and large, the results from the log se_m analysis compare well with the Procrustes distance matrix. Both these analyses primarily compare shape differences. When size is included in the comparison, such as in the case of the principal components analyses based on Procrustes form space, a tooth such as OH 22 (R) groups more closely with *Homo erectus* than it does with *Homo rudolfensis,* for example. The linear dimension analyses (Figures 4.9 and 4.10) also confirm that the relative proportions (MD:BL ratios) are very similar in the case of comparisons between KNM-ER 15930 and OH 16, between OH 22 and *Homo rudolfensis,* between KNM-ER 806c and specimens of *Paranthropus*, and between AL 288-1 and *Homo erectus* specimens but the size differences, visible on Figure 4.9, preclude OH 22 being grouped with *Homo rudolfensis* in a shape-and-size analysis. Providing that the dates given for each specimen are correct, cross-checking the log se_m "anomalies" with figure 4.10 (MD:BL ratios plotted against time), it would appear that KNM-ER 15930, AL 288-1 and KNM-ER 806c persist as the most significant anomalous specimens.

4.4 Summary tables of results of analyses

Two summary tables (Tables 4.26 and 4.27) summarise the results of each type of analysis conducted as follows:

4.26- Species grouping patterns (for main "groups", excluding potential anomalies)
4.27- Potential anomalies highlighted by each analysis

Table 4.26 Species grouping patterns detected by each type of analysis

Analyses confirming patterns observed Patterns observed	Linear/ statistics	PCA	Procrustes Matrix	DFA	Log se_m
Modern *Homo sapiens* – M_1 molars extremely **variable** in width, less variable in length; generally-speaking, wider than great ape species but some overlap	**X**	**X**	**N/A**	**X**	**X**
***Gorilla gorilla* -** M_1 molars much **less variable** in width. Extremely large, narrow teeth. Extreme sexual dimorphism witnessed by size differences rather than relative width differences	**X**	**X**	**N/A**	**X**	**X**
***Pan troglodytes* -** M_1 molars of medium size and relatively narrow. **Less variability** than for modern *Homo sapiens.* Sexual dimorphism not evident as in *Gorilla gorilla.* Similarly shaped molars to bonobo molars and to wider gorilla molars, but generally much larger.	**X**	**X**	**N/A**	**X**	**X**
***Pan paniscus* -** M_1 molars relatively narrow and extremely small. **Less variability** than for modern *Homo sapiens.* Sexual dimorphism not evident as in *Gorilla gorilla.* Similarly shaped molars to chimpanzee molars and to wider gorilla molars, but generally much smaller, no overlap in size with gorilla molars.	**X**	**X**	**N/A**	**X**	**X**
***Australopithecus afarensis* -** M_1 molars (those similar to holotype) smaller than *A. africanus* but much squarer. Distinctive shape with almost perpendicular buccolingual groove. If anomalies are included, this is the **most diverse group** with the most extreme variability of both size and overall shape of all the species examined.	**X**	**X**	**X**	**X**	**X**
***Australopithecus africanus* -** M_1 molars are "medium-sized" and of "medium" relative width compared to other fossil species. Mesial cusps reasonably large compared to talonid, with slight diagonal buccolingual groove. The sample is very small, so that if Taung 1 is separated away due to the presence of a C_6 and if	**X**	**X**	**?**	**?**	**?**

Sts 52b is isolated due to other differences, the group becomes fractured into its 3 specimen components, leaving little left for meaningful comparisons. Therefore there are question marks placed for some of the analyses.					
Homo habilis and ***Homo rudolfensis -*** M_1 molars are "medium-sized" and very narrow (*H. habilis)* or relatively narrow (*H. rudolfensis)*. Metaconid very wide, protoconid small, buccolingual groove at very steep angle	**X**	**X**	**X**	**X**	**X**
Homo erectus - M_1 molars are the smallest and among the narrowest of all species groups included in the study. Little variability in this group, and the small variability seen is mainly in terms of size rather than relative width. Similar general occlusal morphology to earlier Pleistocene *Homo* species.	**X**	**X**	**X**	**X**	**X**
Paranthropus boisei and ***Paranthropus robustus -*** M_1 molars from both species group closely together in a "large" group as well as a "smaller" group. Large talonid relative to mesial cusps. Metaconid slightly larger than protoconid, so buccolingual groove similar to that of *A. africanus.*	**X**	**X**	**X**	**X**	**X**

Table 4.27 Specimens identified as potential anomalies by each type of analysis

Analyses confirming potential anomalies Potential anomaly	Linear/ statistics	PCA	Procrustes Matrix	DFA	Log se_m
AL 288-1 – *A. afarensis* - *visibly different from the remainder of its group. Small, extremely narrow, almost chimp-like.*	**X**	**X**	**X**	**X**	**X**
LH 2 – *A. afarensis* - *Much larger specimen than remainder of the sample for this species (MD diameter: 14.0mm, compared with 11.8mm and 11.9mm for the holotype* (White 1977)*).*	**X**	**X**	**No**	**No**	**X**
LH 4 (L) – *A. afarensis* - *damaged left tooth of holotype*	**No**	**No**	**X**	**No**	**No**
Sts 52b –***A. africanus* -** *smaller than the holotype and MLD 2 in the occlusal view.*	**X**	**X**	**No**	**X**	**No**
Taung 1 – *holotype for* ***A. africanus*** *but with sixth cusp that is usually more diagnostic of* ***P. robustus.***	**No**	**No**	**X**	**X**	**X**
OH 16 – *H. habilis* – *larger in dimension than holotype.*	**X**	**X**	**X**	**No**	**No**
KNM-ER 806c – *H. erectus* – *larger in dimensions than the remainder of the group*	**X**	**X**	**X**	**X**	**X**
KNM-ER 15930 – *Paranthropus boisei* – *very much smaller than the holotype proxy*	**X**	**X**	**X**	**No**	**X**

CHAPTER FIVE – DISCUSSION

5.1 Extant primate species

As can be seen from Table 4.26 (summary table of results – species level), all of the analyses performed on the selected samples representing the four extant species seemed to confirm trends that might be expected from visual examinations of the morphology and basic odontometrics of the molar teeth of the four species. Despite the preliminary nature of most of the analyses, initial results tended to be largely in agreement concerning species variability patterns and potential anomalies detected.

The mesiodistal:buccolingual (MD:BL) plots and comparative statistics for modern humans (see 4.3.1.1) and for the four extant species (including modern humans) (see 4.3.1.2) give a very general picture of how well these analyses can be used to group species or to detect certain trends regarding species overlaps and sexual dimorphism.

In modern humans, there is a wide range in the diversity of both the overall size and the width of teeth. Generally speaking, however, there is a trend for female M_1s to be smaller and narrower on average than male M_1s. (Tables 4.1-4.3, Figure 4.7). This finding is consistent with research conducted by Thackeray et al. (2005), who found that modern *Homo sapiens* males showed average M_1 MD:BL ratios of 1.06 +/-0.02 (n=23), while the corresponding value for female modern *Homo sapiens* is 1.11 +/-0.05 (n=25).

The diversity of both tooth size and width is more evident when modern human teeth are compared to other extant primate teeth from the great ape species (Figure 4.8).

While some species have extremely divergent size ranges (gorillas, for instance), their overall shape remains largely similar, while the human sample shows a high degree of diversity in terms of shape, in comparison to the other species studied. The homogeneity in tooth shape for the three ape species is evident from the fact that the overall ratios between the mesiodistal and the buccolingual diameters remain within a very narrow band, and this is interestingly true of gorillas, as this species shows a very clear pattern of sexual dimorphism: the females in the sample do not overlap with the males in terms of their size, but there is no substantial difference in overall relative width (after size is factored out). There is some overlap between males and females in the remaining three species groups. These features in the ape species, particularly gorillas (high diversity in size but very low diversity in overall shape between males and females) are taken into consideration when examining similar charts for the fossil samples, and in particular, those for which large variability in size and/or shape is thought to be due to sexual dimorphism.

Also of note is the fact that even though modern human teeth are diverse in both shape, and to a lesser degree, size, the overlaps generally between species on the linear charts and on the PC plots are low enough for the species to be reasonably distinguishable from the other three species examined. Some overlaps are visible, particularly between species that are presumed to have diverged only recently (bonobos and chimpanzees, (Prüfer et al. 2012)) and between modern *Homo sapiens* and some of the unusually large, small or relatively wide (as the case may be) specimens of the great ape species. The modern *Homo sapiens* sample used for the PCA, DFA and log se_m analyses was specifically chosen from the larger sample initially studied from the Raymond Dart collection to ensure that the whole range of variability was represented (very small

`teeth, very large teeth, very narrow teeth and very square teeth). What can be seen, even from these small representative samples, is that overlaps do occur in nature. In the case of bonobos and chimpanzees, these overlaps might anyway be expected due to the presumed recent divergence time between the species and due to potential interbreeding (Vervaecke et al. 2004) during periods when the Congo River has dried up or during periods of change in natural refugia due to climate changes (Nichol 1999). Lastly, overlaps between bonobos, chimpanzees and modern *Homo sapiens* may be expected due to overlaps in the genomes of the three species in different combinations (apart from a large portion of overlap of the genomes between all three species, there are additional overlaps shared only between two of the three species at a time : modern humans with bonobos; modern humans with chimpanzees, chimpanzees with bonobos; these paired overlaps (to the exclusion of the third species in the group) are presumed to be due to potential incomplete lineage sorting (Prüfer et al. 2012)). Genomic factors may be at the root of similarities between gorillas and modern *Homo sapiens* and between gorillas and chimpanzees. 30% of the gorilla genome is either closer to *Homo sapiens* than it is to *Pan troglodytes* or closer to *Pan troglodytes* than it is to *Homo sapiens*. Again, this has been attributed to incomplete lineage sorting (Scally et al. 2012).

These overlaps in nature are confirmed by the analyses used in this preliminary study and are taken into consideration when analysing patterns of grouping of species groups among the fossil specimens, as well as in respect of the rejection or acceptance of the hypotheses being tested.

5.2 Fossil species

5.2.1 *Australopithecus afarensis*

In the *A. afarensis* group, one of the species in the fossil record that has been hypothesised to show great sexual dimorphism, all but two of the specimens in the sample fall within a reasonably narrow range in terms of their MD:BL ratios. These molars are characterised by being almost as broad as they are long, but small compared to the other Australopiths. Most of them fall between the 1:1 and 1:1.06 ratio lines. The only exceptions in this sample are AL 288-1 ("Lucy") and LH2 (a gracile juvenile from Laetoli which had originally been classified by White (1977) as being allocated to the "*Homo* sp."). Both of these specimens group more readily with specimens allocated to *Homo.* In the case of LH 2, a medium-sized, narrow molar, it groups well with specimens classified as *Homo habilis* and *Homo rudolfensis,* while AL 288-1 is as narrow as, but smaller than, all of the *Homo erectus* specimens in the study. It is interesting to note that Don Johanson, who discovered AL 288-1, wrote that the small size and narrowness of the molars was puzzling, as such features had hitherto been considered to be "modern" rather than "primitive" (Johanson & Edey 1981:260-263; 281).

When the fossil MD:BL ratios are compared over time (Figure 4.10), there is a clear trend from very wide, square teeth (*A. afarensis* of the type closest to the holotype in shape*)* via medium sized, medium-width molars *(A.* africanus) to, on the one hand very small, narrow teeth (*Homo erectus),* and on the other hand, of large, very slightly proportionally narrower teeth on the side of the most robust species *(P. robustus* and *P. boisei*).

Again, in the time-trend analysis, two very notable exceptions occur in the *A. afarensis* group, these being AL 288-1 and LH 2. These teeth are exceptionally narrow (LH 2 being much larger in size, however, than AL 288-1) and neither of these specimens seem to fit with their species group for that reason in the time-related linear dimension analysis.

The same two suspected anomalies (AL 288-1 and LH 2) are also identified by the Principal Components analyses, taking cusp arrangements into the analysis over and above the simple linear dimensions. ***Australopithecus afarensis*** specimens generally grouped well together in the lower left quadrant of the PC chart as predicted (in this quadrant, one would predict that the generally smallish but relatively very wide teeth should group together).

AL 288-1 plots at the negative end of the x axis (the "smallest tooth"), and which is also above the x axis ("narrower teeth") whereas the rest of the *afarensis* group are below it (on the "wider" side of the axis): it thus groups with the "narrow teeth" (*Homo erectus)* in the PC analysis for the fossil sample alone. When chimpanzees or humans are added to the PC analysis as "species outgroups" to check for the correct grouping of the fossils in the PC analyses, AL 288-1 consistently groups away from the fossil specimens and towards these two species (Figures 4.14 and 4.16). Indeed, Don Johanson, who discovered AL 288-1, completed his PhD on primate mandibles and in his first book about "Lucy" he states on more than one occasion that this specimen is much more chimpanzee-like than the others, with "an odd lower jaw", which he initially assigned to a different species than that assigned to the Laetoli and the larger Hadar specimens (Johanson and Edey, 1981; Johanson & Taieb 1976). These latter specimens all had a

square, robust mandible with considerably larger dentition than did AL 288-1, prompting Johanson to state, when noticing the similarities between the Hadar and the Laetoli specimens, "But not Lucy. She's different". It was later, in discussions with Tim White that Johanson started to consider allometry and sexual dimorphism.

The holotype for *A. afarensis* is LH 4 from Laetoli. It has close affinities with larger specimens from Hadar. The teeth are typically very square-looking, not just because they are often as wide as they are long, but because the two buccal cusps (the protoconid and the hypoconid) are almost directly opposite the two lingual cusps (the metaconid and the entoconid), with the fifth cusp, the hypoconulid, being very much flattened and centralised along the distal margin of the tooth (see 2.4.2.1).

Figure 5.1 below shows AL 288-1 between two typical *Australopithecus afarensis* specimens, between a chimpanzee and a bonobo and between a *Homo erectus* specimen and a modern human specimen. It can be confirmed from these photographs that AL 288-1 appears to group more readily with a chimpanzee specimen or a specimen of *Homo erectus* or *Homo sapiens* than it might with the more typical teeth of the *Australopithecus afarensis* hypodigm, which are typically very much wider teeth with accentuated metaconids. Not only is this specimen very similarly shaped to the chimpanzee specimen pictured, but the wear patterns on the teeth appear similar as well. It also groups on the PC analyses with modern humans. The mandible shape is considerably different (more chimpanzee-like) but the tooth is very small and similarly proportioned to that of much more modern specimens. Indeed, AL 288-1 groups well to the left of KNM-ER 992, the holotype of *Homo ergaster* ("African *Homo erectus"*) and KNM-ER 820, the smallest of the *erectus* group (implying that it is still smaller than it)

on all of the PC plots, including those with modern primates included as "outgroup species". AL 288-1 fails to group with the remainder of the *A. afarensis* sample in the study, no matter which outgroup species is added to the PC analysis.

Australopithecus afarensis AL 266-1 R (mirrored)	*Australopithecus afarensis* AL 288-1 (Lucy)	*Australopithecus afarensis* LH4 L (holotype)
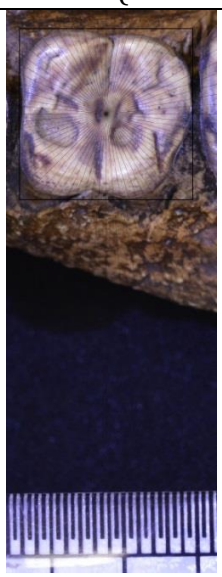		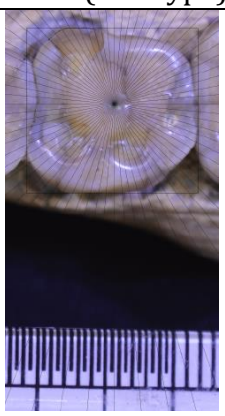
Bonobo	AL 288-1 (Lucy)	Chimpanzee
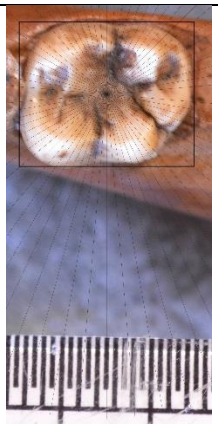		
Homo erectus (KNM-ER 820)	AL 288-1 (Lucy)	Modern human
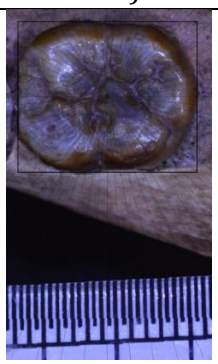		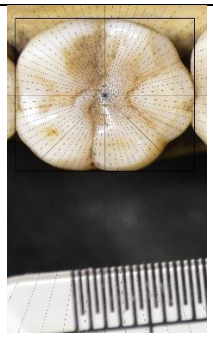

Figure 5.1 M_1 of AL 288-1 ("Lucy") compared with other specimens from *A. afarensis* (AL 266-1 and LH 4), bonobos, chimpanzees, *Homo erectus* and a modern human.

The second potential anomaly, LH 2, is a juvenile. Its mesiodistal diameter is unusually large for the species (14mm for LH 2 (R) as opposed to 11.8mm for the holotype, LH 4 (R) – "corrected" MD diameters, (White 1977)); because the uncorrected MD diameter is used for this study, the odontometric differences are increased, since LH 2 is larger and a juvenile tooth, still in good condition; while LH 4 has undergone interstitial wear, in addition to it being shorter along the mesiodistal axis). LH 2 was also photographed from a cast, and inferences needed to be made about the boundaries of the tooth enamel which appears damaged at the cervical margin as well as on the mesial side of the crown. If allowance was made for a discoloured area to be added on the buccal side (taken to be below the cervical margin) LH 2 would group closer to Taung1, the holotype of *Australopithecus africanus.* There is no sign of the larger, bulbous metaconid typical of the more robust *A. afarensis* specimens. This molar was described by T. White as having a protostylid (White 1977), which is more diagnostically typical of *Australopithecus africanus* mandibular first molars. The buccolingual measurements measured by White (*ibid.*) are again above average for *Australopithecus afarensis* (Alemseged et al. 2005), and marginally larger than Taung 1 (Wood 1991). Overall, this molar does appear to be less square than the holotype, and more similarly proportioned to *Australopithecus africanus.* It lacks the prominent metaconid of the more typical specimens from *A. afarensis* and has a buccolingual groove similar in angle to *A. africanus.* The similarity between LH 2 and *Australopithecus africanus* can be confirmed by visual inspection of images presented in Figure 5.2 below.

Australopithecus afarensis AL 266-1 R (m)	*Australopithecus afarensis* LH 2 R (m)	*Australopithecus afarensis* LH4 L (holotype)	*Australopithecus africanus* Taung1 R (m)
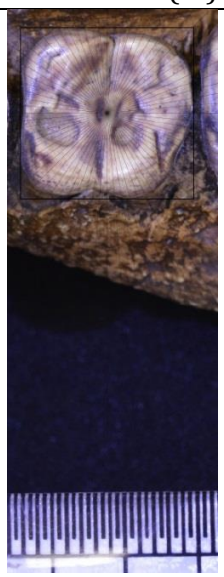	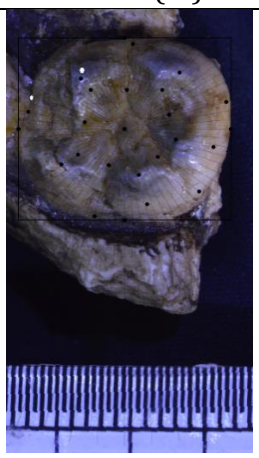		

Figure 5.2 Comparison between the M_1 of LH2 (*Australopithecus afarensis)* with other *A. afarensis* specimens and with the holotype of *Australopithecus africanus*

With such wide ranging diversity between specimens in the *Australopithecus afarensis* group (from the tiny AL 288-1 to the large LH 2, and from the extremely narrow AL 288-1 to the extremely square holotype and specimens such as AL 266-1 (R)) it is of little surprise that the Procrustes distance matrix and the Log se_m analyses both reflect this lack of cohesion among members of the species, with high values across the board being reflected in the respective matrices for both analyses.

Interestingly, the DFA, which is based on eight PC scores confirms the extreme anomalous status of AL 288-1, classifying it with the extant species (*Homo sapiens)* due to its extreme small size and narrowness, rather than with any of the fossil species groups, yet it does not find that LH 2 is misclassified.

In sum, *Australopithecus afarensis* is a highly species diverse group, characterised on the one hand by robust U-shaped mandibles with very square lower first molars and on the other by comparatively narrow (LH 2) or significantly narrow (AL 288-1) molars (and in the case of AL 288-1, certainly, with a gracile, V-shaped mandible). D. Johanson and T. White, along with other researchers, attribute these very marked differences to sexual dimorphism (Johanson & Edey 1990; Leonard & Hegmon 1987; Leonard 1991; Lockwood et al. 2000; Reno et al. 2003, 2010) but other researchers have challenged this assumption (Schmid 1989; Richmond & Jungers 1995; S.-H. Lee 2005; Ferguson 1989; Gordon et al. 2008). Reno et al., (2003 and 2010) cite the large range of variability in modern *Homo sapiens* to conclude that *A. afarensis* was within this range. However, in this study, on examination of the MD:BL plots for the lower first molars of modern humans and other primates, there is sometimes a marked difference in size, but not so much in the width of the tooth at the same time. This is particularly true of gorillas, but even with the human group, while female molars are possibly 8% more narrow than male molars on average (as calculated from the limited sample in this study), the difference between AL 288-1 and AL 145-35 is nearer 17%. Ferguson (1989) advances the idea that "great dental variation is usually the result of widespread geographic distribution". He goes on to echo Brace, (C L Brace 1979; Brace et al. 1987) that dental size varies with the amount of self-domestication (the degree of technology used in food production, processing and consumption). Australian aborigines traditionally had unspecialised technology, an omnivorous diet and the largest teeth of modern *Homo sapiens* (Campbell 1925), whilst populations that have used agriculture and food processing technology to greater degrees typically have the smallest teeth (see, for instance, Dahlberg, 1960; Brace & Mahler, 1971; Brace et al. 1987: Figure 2 page 709; Larsen, 1995; Dempsey & Townsend, 2001; Pinhasi et al. 2008; Emes et al.

2011). That diet affects dental crown size is a well-recognised assumption (see, for example, Wolpoff, 1996, page 444). Several studies have been conducted into the probable diet of *Australopithecus afarensis* (among them Ryan & Johanson, 1989; Teaford & Ungar, 2000; Ungar, 2004; Grine et al., 2006; Estebaranz et al. 2009). By and large, these studies conclude that the diet of *Australopithecus afarensis* may have been closest to that of modern gorilla species. This is in keeping with other studies such as Rak et al., (2007), which went as far as to suggest that so gorilla-like were certain specimens of *Australopithecus afarensis* in their mandibular ramus morphology, the species may not have been an ancestor of modern humans but of robust Australopiths.

Based on the findings of Reno et al. (2003 and 2010), the range of variability within *Australopithecus afarensis* does not exceed the range of variability found within modern *Homo sapiens.* However, the preliminary findings from this present study, exploratory though it might be, might possibly more in keeping with those of Ferguson (1989), who challenges the idea that the two distinct morphologies in this group can be attributed to sexual dimorphism and who points out that the geographical range of the species is far less than that of *Homo habilis* (specimens attributed to this species have been found both in southern and eastern Africa), and considerably smaller than the range of geographical spread of modern *Homo sapiens*. Certainly, the range of *Australopithecus afarensis* was fairly limited: the distance between Hadar and Laetoli and other sites where this species has been discovered is around 900km. Modern *Homo sapiens* has populated virtually the entire globe, encountering numerous different ecological niches and having introduced farming technology and advanced food processing in certain areas, which might account for the size variability coupled with marked shape variability (the latter being less marked in the extremely sexually dimorphic gorilla,

which exhibits extreme size variability in the lower first molars but relatively less shape variability). This pattern (size differences, but not a great deal of shape variability) is visible in the *Paranthropus* clade, and for *Paranthropus,* gorilla-like variability due to sexual dimorphism is the most likely explanation. By comparison to modern *Homo sapiens*, in *Australopithecus afarensis*, extreme variability in both size and shape is a puzzle and based on preliminary findings here does not seem to fit with a pattern of sexual dimorphism. Nor does the wide range of variability in the lower first molars of modern *Homo sapiens* fit an explanation attributed solely to sexual dimorphism: in the context of this study, it would appear that in the case of modern *Homo sapiens,* it is regional or population variation that seems to explain the wide variation in tooth shape and size. Male and female European teeth (in this study) and Middle Eastern teeth (papers cited above) are both extremely small for both genders alike, Tswana teeth (this study) and Australian aboriginal teeth (Campbell 1925) are again large by comparison, for both genders. To say that all small, gracile teeth in a varied sample like modern *Homo sapiens* are female and all large, robust teeth are male, as has been suggested in the case of *Australopithecus afarensis* molars, would be equivalent to saying that all European or Middle Eastern molars in *Homo sapiens* belong to females and all megadont teeth belong to males, which is clearly not the case. In a study of third mandibular premolars conducted by Leonard and Hegmon (1987) AL 288-1 (a presumed female of *A. afarensis*) is characterised as a V-shape mandible with a mesially-angled P_3 similar to ramapithecines and AL 333w-60 (a presumed male of *A. afarensis*) represents a U-shaped mandible with a buccally-oriented P_3, similar to later australopithecines such as MLD 2 (*A. africanus*) (Leonard and Hegmon 1987, page 53). Further to this, the presumed female premolars had a different morphology (unmolarised, compared to a more derived state of molarisation in the presumed males). These researchers conclude

that males and females evolved differentially, with different selective pressures acting on the males and females of *A. afarensis,* causing the females to exploit a restricted, arboreal habitat, while the males exploited a "more terrestrial habitat with a high proportion of low-quality foods in the diet" (*ibid.,* page 61). Lee (2005) has applied resampling methods to test whether various skeletal elements of *A. afarensis* jointly reflect a similar type of sexual dimorphism as that reflected in modern *Homo sapiens,* gorillas or chimpanzees, in the same way. The result was that variability was within the same range as gorillas in the femur, that sexual dimorphism in the humerus was similar to that in modern *Homo sapiens* and that canine dental variability was similar to that in chimpanzees, but that taken together, skeletal elements as a whole did not match the type of sexual dimorphism seen in any living human or ape. Schmid (1989) argues that "Lucy" and the presumed males of *A. afarensis* cannot be considered to be the same species.

Despite what seem to be reasonable grounds for sympathising with this viewpoint, however, a note of caution should be considered. The somewhat extraordinary range of variability between specimens posited to belong to *Australopithecus afarensis* has a parallel in the extreme variability found between specimens from Dmanisi, Georgia. The disparate collection of Dmanisi mandibular remains seems to find a counterpart in both the gracile, V-shaped mandible of Lucy and the robust, U-shaped mandibles of the presumed "male" members of *A. afarensis* (Skinner et al. 2006). Unlike the fossil collections of the Hadar region, where certain specimens were surface finds or near-surface finds in the ever-changing landscape of dried and constantly-eroding river courses, making dating and provenance less than ideally secure, in the case of Dmanisi, there is much more compelling evidence to consider these specimens to be of one single

penecontemporary palaeodeme: they were all found within the same member of rock in the same location. It is difficult to imagine a scenario wherein this well-grouped assemblage could have comprised more than one hominin species. Such is the extraordinary craniodental and postcranial variability presented by this collection, however, that some have argued in favour of a multiple species scenario at this site (e. g., Schwartz, 2000). Others, nevertheless, while recognising the highly variable, somewhat mosaic, nature of the craniodental and postcranial remains, consider the context of the assemblage, and argue for a single fossil species at the site (S. H. Lee 2005; Lordkipanidze et al. 2007; Rightmire et al. 2008; Martinón-Torres et al. 2008; Van Arsdale & Lordkipanidze 2012; Lordkipanidze et al. 2013).

Variability within a fossil hominin species cannot incontrovertibly be based upon morphometric observations made on lower first molar specimens representing four extant species. As far as the scope of this study is concerned, however, conclusions are bound to be drawn on the basis of limited samples of modern *Homo sapiens,* gorilla, chimpanzee and bonobo, and the concept of rapid morphological variability occurring in modern *Homo sapiens* as a result of farming and food technology seems interesting. Further work is therefore recommended in the context of *A. afarensis* as a whole and for AL 288-1 in particular (to encompass the remaining dentition and other skeletal elements) in order to confirm whether AL 288-1 represents a second morphotype within *A. afarensis* or even a distinct species altogether, or whether sexual dimorphism could explain the significant differences between this specimen and the more robust specimens more typical of the species.

5.2.2 *Australopithecus africanus*

In the linear dimension analyses, the *A. africanus* specimens all cluster along an axis associated with a MD:BL ratio of approximately 1:1.05 – 1:1.08, differing only in size. As an apparent outlier, Sts 52b is slightly wider and smaller in the occlusal view than the remaining specimens in the sample.

The PC analyses confirm the potentially anomalous status of Sts 52b. This particular specimen groups better, according to the PC analyses, with some of the *Australopithecus afarensis* samples and with KNM-ER 806c, which itself does not group perfectly with *Homo erectus* (into which it is currently classified). This grouping might be an artefact from the landmark placements, however, as Sts 52b is a much worn tooth. Nevertheless, the main damage is only in the hypoconid area and judging by the mesiodistal diameter (uncorrected), it does appear to be smaller and thus proportionally squarer (according to the hypoconid-metaconid diameter) than the other *A. africanus* specimens (see Figure 5.3 for a visual comparison). This specimen has previously been identified by other researchers as being anomalous and perhaps belonging to a different species (Kimbel & White 1988; Clarke 2008; Fornai et al. 2013).

Australopithecus africanus Taung1 R (m)	*Australopithecus africanus* Sts 52b	*Australopithecus africanus* MLD2 L
	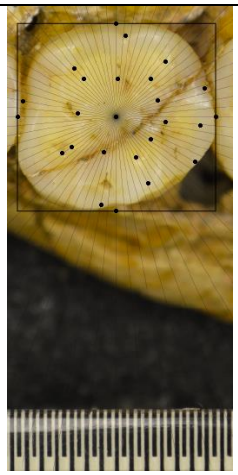	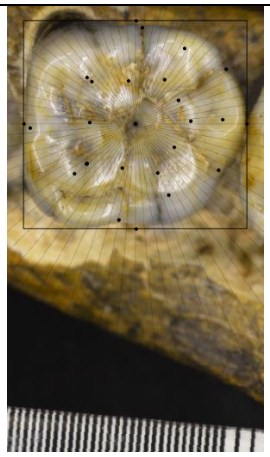
Australopithecus afarensis AL 266-1 (L)	*Australopithecus africanus* Sts 52b	*Homo erectus* KNM-ER 806c
	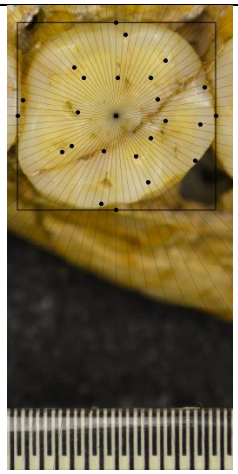	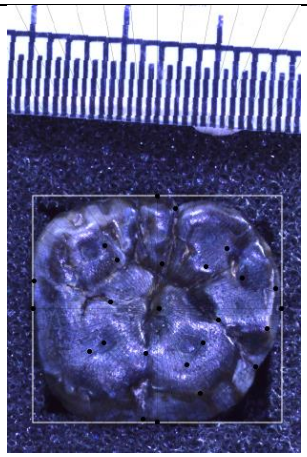

Figure 5.3 M_1 of Sts52b pictured with a) Taung1 and MLD2 (both *Australopithecus africanus)* and with AL266-1 (L) and KNM-ER 806c, the two closest specimens to it on the PC chart, Figure 4.12. **This specimen has the general (square) dimensions of *A. afarensis* , although it does not share exact features with typical specimens from this group.**

A further point of discussion with respect to the PC analysis results for the *Australopithecus africanus* group is that the holotype, Taung 1, groups very well together with MLD 2 on the Fossil PCA (Figure 4.12) as well as the majority of the PC analyses including an extant species as a "species outgroup" (for example, with

chimpanzees as an outgroup (Figure 4.14), with bonobos as an outgroup (Figure 4.13), and with modern humans as an outgroup (Figure 4.16)), despite Taung 1 having a sixth cusp (C_6), which was landmarked as such (giving it an inner "hexagon" instead of a "pentagon" in the landmark placements). Taung 1 also groups very well on the PC analysis plots with SKW 5 and SK 63 (L), which are two very small specimens from the *Paranthropus robustus* group. It might be questioned whether the presence of the C_6 has influenced this grouping, but MLD 2 (L) also groups closely with SKW 5 and SK 63 (L) (Figure 4.12). One of the major differences between the smaller *Paranthropus robustus* specimens is the fact that the hypoconid tends to be more centrally placed along the buccal margin of the crown, rather than being oriented more distally, as is the case of the *Australopithecus africanus* specimens, as witnessed in Figure 5.4.

Australopithecus africanus Taung1 R (m)	*Paranthropus robustus* SKW5	*Paranthropus robustus* SK63 L
	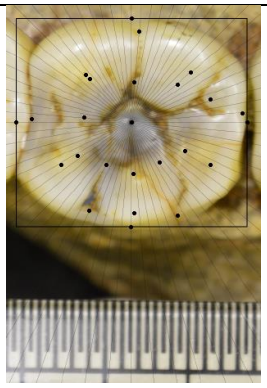	

Figure 5.4 M_1 of Taung 1, with a visible sixth cusp, compared with similarly-sized *Paranthropus* specimens

The analyses that do highlight Taung 1 as a potential anomaly are the Procrustes distance matrix, the DFA and the Log se_m analyses, all of which seem to have identified the presence of the C_6 and the resultant slight buccal shift of the hypoconulid in the holotype. Taung 1 grouped well in the log se_m analyses with the other specimens with a

C_6, notably KNM-ER 806c and specimens from the *Paranthropus* hypodigm, particularly SK 6, despite the latter being significantly larger in size.

The sample size for this species is already very small. MLD 2 is represented by both antimeres, which are morphologically very typical of *Australopithecus africanus* (Aiello & Dean 1990; Hillson 1996). Sts 52b is represented by a single tooth due to excessive damage in the antimere and Taung 1, the holotype, has the C_6 present in the LM_1. The DFA thus splits the sample into its three specimen components: it confirms the anomalous status of Sts 52b, grouping it with *Australopithecus afarensis*, in keeping with its position on the PC plot in the lower left quadrant of the chart. It groups Taung 1 with *Paranthropus* due to the presence of the C_6, leaving only MLD 2 to represent *Australopithecus africanus* legitimately. The sample size in this instance is therefore problematic and a recommendation should be to enlarge it in future to include as many other specimens as possible. (Within the scope of this preliminary study, the sample size was limited due to access problems and due to damage to the crown enamel in the case of many of the specimens to which access was granted. Once further studies are undertaken to include maxillary dentition, there are a good number of specimens already accessed that can be included, and it is hoped that more specimens can be added).

5.2.3 *Homo erectus*

The whole ***Homo erectus*** group is well aligned together on the linear dimension analyses and on the Principal Components plots, the specimens generally group closely together in the upper left quadrant of the Fossil PC plot (Figure 4.12), which is the

location in which teeth that are the smallest and most narrow of the 36 specimens in the fossil sample would be predicted to be grouped. The only exception to this grouping is KNM-ER 806c, which falls more readily into a grouping consisting of *Australopithecus africanus* and "Early *Homo" (Homo habilis; Homo rudolfensis*) and KNM-ER 15930 which is currently classified as *Paranthropus boisei,* but which does not group well with Peninj 1, a proxy for the holotype of the species). These results confirm initial observations made on the basis of the linear dimensions analyses, which also identifies KNM-ER 806c as a potential anomalous outlier.

KNM-ER 806c was described by B. Wood as "a left M_1 crown with five cusps and a C_7, arranged in a Y pattern" (Wood, 1991, page 206). However, as Figure 5.5 shows, there is a very noticeable sixth cusp on the tooth as well as the C_7. (Wood did note a C_6 on the M_2 and M_3).

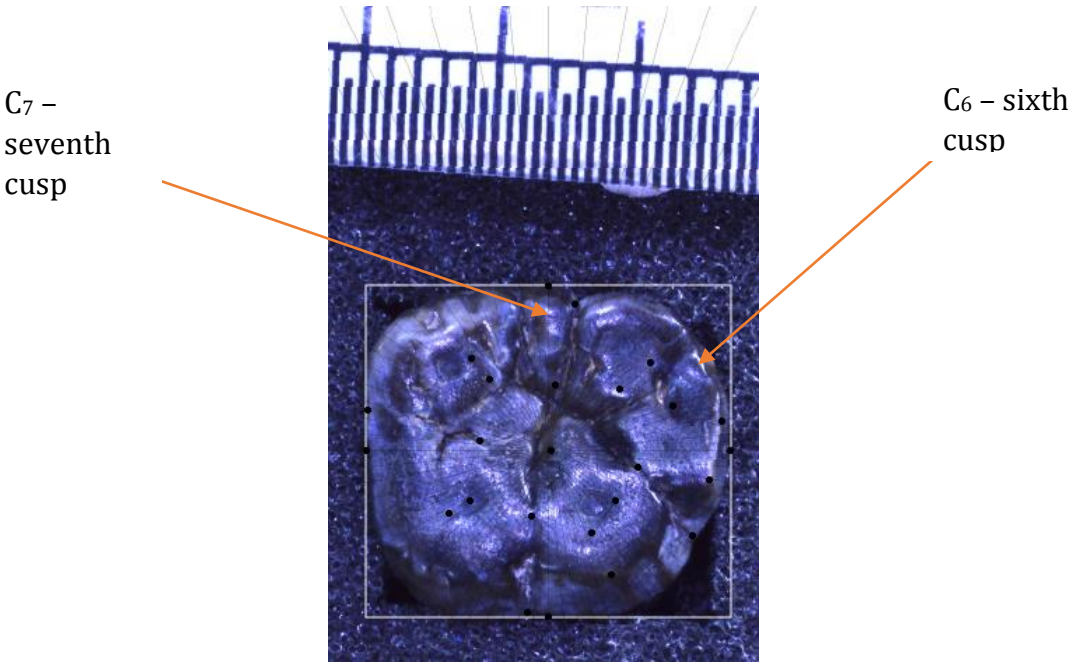

Figure 5.5 M_1 of KNM-ER 806c (L), showing the sixth and seventh cusps

Were it purely the presence of the C_6 that could be responsible for KNM-ER 806c grouping away from the later *Homo* specimens and grouping rather with *Australopithecus africanus* and with earlier *Homo* species and *Paranthropus* specimens, it could be proposed that unlike Taung1, which still groups with other specimens of its species (MLD 2) on the PC analyses, despite its having a C_6, (absent in MLD 2), this tooth's C_6 may have skewed the results of the PC analysis because of the presence of this C_6. However, KNM-ER 806c is anomalous in every single one of the analyses carried out, from the linear dimension analyses (MD and BL; MD:BL plots) to the geometric morphometric analyses, to the log se_m analysis to be discussed below. When compared visually to some of the specimens near to which it groups on the PC analysis, similarities can be seen, while clear differences can be observed between this tooth and *Homo erectus* (Figure 5.6).

Homo erectus KNM-ER 992 L	*Homo erectus* KNM-ER 806c	*Homo erectus* KNM-ER 820 R(m)
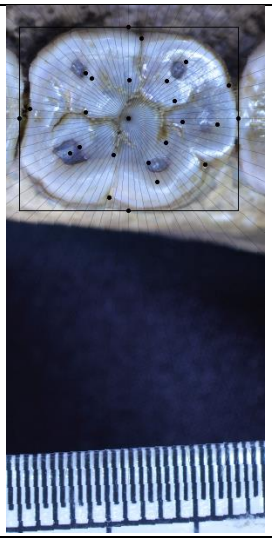	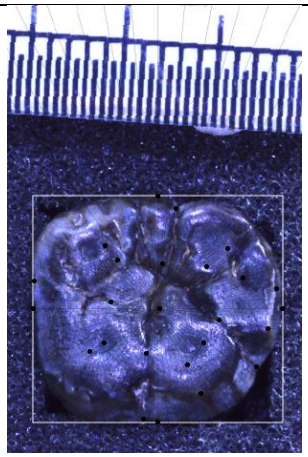	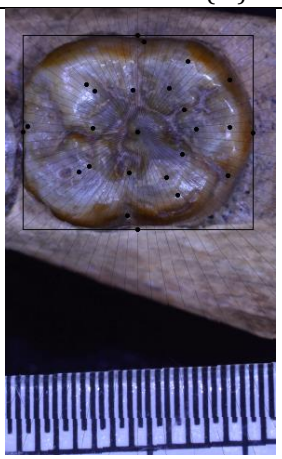
Australopithecus africanus Taung1 R (m)	*Homo erectus* KNM-ER 806c	*Australopithecus africanus* MLD2 L
	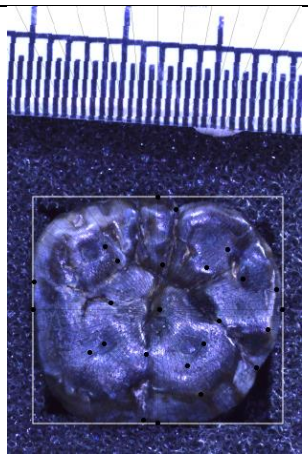	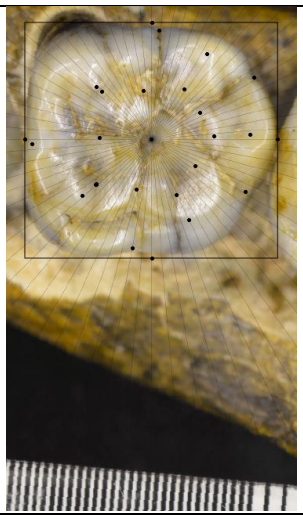
Paranthropus boisei KNM-ER 15930 L	*Homo erectus* KNM-ER 806c	*Homo habilis* OH 16 R(m)
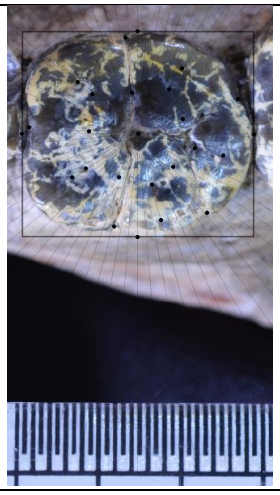	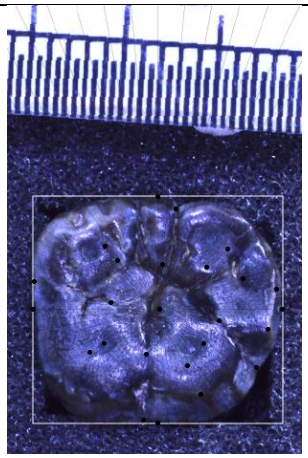	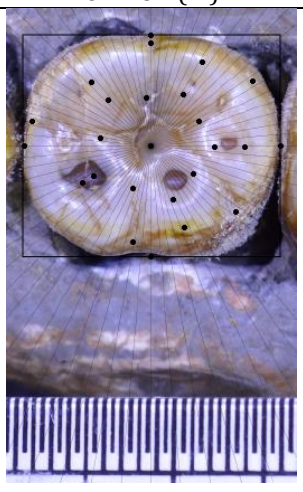

Figure 5.6 M_1 of KNM-ER 806c (middle column), compared to a) other *Homo erectus* specimens, b) *Australopithecus africanus* specimens and c) KNM-ER 15930 *(Paranthropus boisei)* and OH 16 (*Homo habilis).*

In keeping with the PCA results, it can be seen from the visual comparisons that KNM-ER 806c is altogether a larger and wider tooth than others classified as *Homo erectus* (of which KNM-ER 992 is the holotype of the African equivalent, *Homo ergaster*). There are significant shape similarities between KNM-ER 806c and MLD 2, including the presence of a C_7 and the existence of a protostylid of sorts (see 4.2.2.2); on MLD 2 this protostylid seems to extend all the way along the buccal side of the crown wall. KNM-ER 806c is also similar to Taung 1 and shares a similar overall cusp arrangement with OH16 *(Homo habilis),* which, although not quite as replete with surface features, has a raised area reminiscent of a C_6 coupled with a similarly-sited fovea on the hypoconulid. The hypoconid of OH 16, which is very slightly damaged (for which allowance has been made) is in a similar position to that of KNM-ER 806c, as are the protoconid and the metaconid. These observations would largely confirm the results of the PC plot, which places KNM-ER 806c closer to late Australopiths and early *Homo* than to *Homo erectus,* and the DFA, which places this specimen within *Australopithecus africanus,* thus confirming the similarities between this specimen and MLD 2, that can be seen from a visual comparison.

The Procrustes distance matrix and the log se_m analysis both confirmed that *Homo erectus* seemed to be the most cohesive of all the fossil species groups, with the sole exception again of KNM-ER 806c. Log se_m values for this specimen range between -1.357 and -1.498 for within-species comparisons. The log se_m analysis would group this specimen marginally better with specimens from the *Paranthropus* clade, possibly due to the landmarking of the C_6. Other specimens in the *Homo erectus* group range in value from -1.632 to -1.761 (values between different specimens) and if antimeres are

considered, the values are as low as -1.911. These very low values imply a high probability of conspecificity (Thackeray 2005; Thackeray 1997; Thackeray et al. 1997) for the remaining specimens within this group.

5.2.4 *Homo habilis; Homo rudolfensis*

These specimens group well together on the linear dimension analyses with the exception, perhaps, of OH 16, which is a specimen from *Homo habilis* (of which the holotype, OH 7, is extremely narrow) but which has a greater relative width than the typically wider *Homo rudolfensis* specimens, grouping closer to specimens of *Paranthropus robustus.*

These two species group quite predictably on the PC plot around the centre of the x-axis (being "medium-sized") and on the positive side of the y-axis (being very narrow teeth). Nevertheless, there is also a significant grouping of these "early *Homo"* molars, particularly *Homo rudolfensis,* with *Australopithecus africanus* and the smallest *Paranthropus robustus* teeth (SKW 5, SK 63 and TM 1517, which are all "medium-sized" and a little narrow, compared to the larger *P. robustus* and *P. boisei* specimens). The exception to this is OH 7, the holotype of *Homo habilis,* which is extremely narrow and does not group very closely with the "medium-sized" teeth.

It is interesting that the "medium-sized" teeth group most closely together, near to the origin of the PC plot in the area where both x and y are positive (see Figure 4.12). Four in particular group extremely closely: OH 16, KNM-ER 15930, KNM-ER 1802 and SKW 5, all of which are currently classified as being from different species. OH 16 and KNM-ER

15930 are extremely closely grouped on the PC plot, and their overall morphology bears this out, with relative cusp proportions being extremely similar, as well as their MD:BL ratio. There are also distinct similarities between KNM-ER 15930 and KNM-ER 1802 (R). SKW 5 does, however, have a more buccocentrally-sited hypoconid, while the other three specimens have a more distally-sited hypoconid (see Figure 5.7).

Homo habilis OH 16 R (m)	*Paranthropus boisei* KNM-ER 15930 L	*Homo rudolfensis* KNM-ER 1802 R (m)	*Paranthropus robustus* SKW5
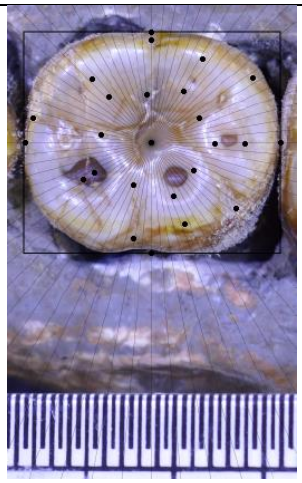	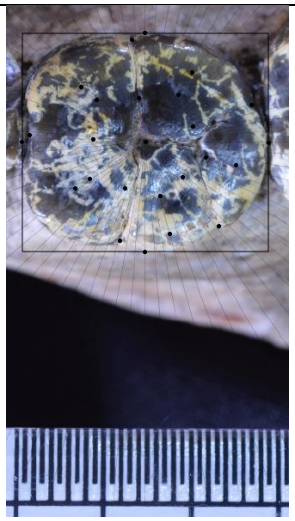	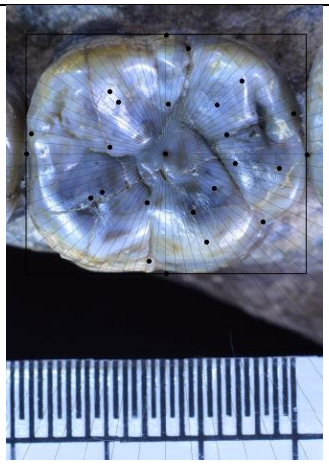	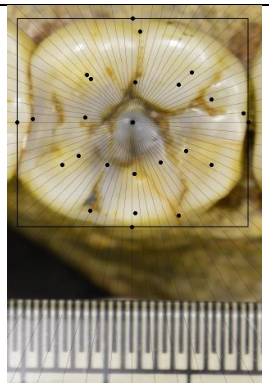

Figure 5.7 Close PCA grouping of four M_1 molars each from different species

The similarities between the overall morphology of these molars (particularly OH 16 and KNM-ER 15930) are perhaps more marked than the similarities between OH 16 and OH 7, which are both classified as *Homo habilis.* OH 7 groups to the left of the y axis (where x is negative, implying a smaller size overall) and since it plots quite high along the positive side of the y axis, it is very much on the narrower side compared with OH 16. It has a wide metaconid, similar to that of KNM-ER 1802, with similar MD:BL proportions, but it is significantly smaller than this tooth. Its overall proportions are similar to KNM-ER 820 (*Homo erectus)* but in this instance OH 7 is larger (Figure 5.8).

Homo habilis OH 16 R (m)	*Homo habilis* OH 7 L	*Homo erectus* KNM-ER 820 R(m)	*Homo rudolfensis* KNM-ER 1802 L
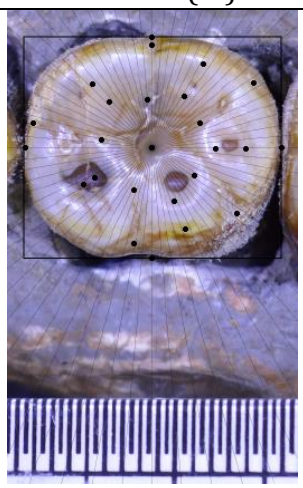	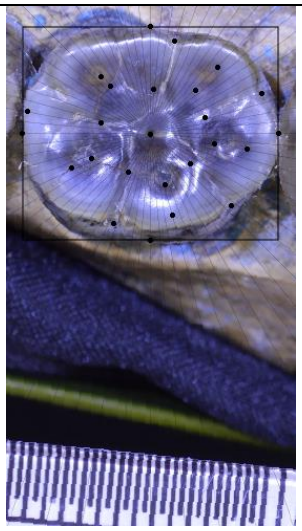	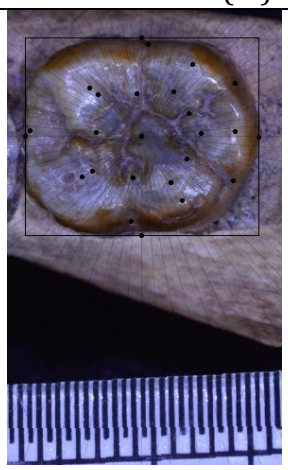	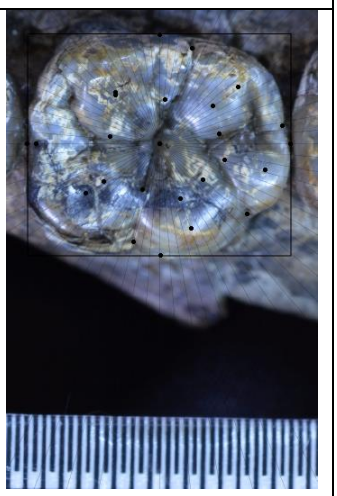

Figure 5.8 M_1 of OH 7 (*Homo habilis* holotype*)* compared to other specimens

The Procrustes distance matrix found the early Pleistocene *Homo* specimens to be reasonably homogenously grouped together, although OH 16 (classified as *Homo habilis)* generally exceeded the average distance between specimens. This finding was not, however, confirmed by the DFA, which found OH 16 to be correctly classified, and by the Log se_m analysis, which found this whole group to be likewise cohesive with values ranging from -1.521 to -1.824 (not including antimeres; if antimeres are included, the lowest value is -1.870).

5.2.5 *Paranthropus boisei; Paranthropus robustus*

These specimens group well together on the linear dimension analyses. Peninj 1 (a typically large specimen of *P. boisei*) groups closely with SK 6 (a very large *P. robustus*), while KNM-ER 15930 (a relatively diminutive specimen of *P. boisei*) is more closely associated with the smallest specimen of *P. robustus* in the study, SKW 5. Thus, both

species are grouped well together in two groups, one consisting of large teeth and the other consisting of small teeth.

P. boisei and *P. robustus* are generally considered to be sister taxa (Wood, 2011). Though they are separated geographically (*P. boisei* being located only in East Africa; *P. robustus* being located only in South Africa), according to the dimensional analyses and the PCA plots, there seems little to differentiate the two species in respect of the shape of their mandibular first molars. Although the sample for *Paranthropus boisei* is extremely small, the inclusion of Peninj 1 (which matches OH 5 well in terms of size and overall proportions), can be considered to be a type specimen, representative of the species as a whole, and if so, the data thus would seem to support the contention by Robinson (1960) that morphological similarities between the two taxa would suggest that they be grouped together under the single genus *Paranthropus* (at the time, *Paranthropus boisei* had been named *Zinjanthropus boisei* (Leakey, 1959)). KNM-ER 15930, as noted, fits better with very small examples of *P. robustus* although it is far closer to OH 16 (*Homo habilis*) than it is to Peninj 1, in both shape and size. Thackeray and Prat (2009) noted that OH 5, the holotype of *Paranthropus boisei* and TM 1517, the holotype of *Paranthropus robustus,* had a high probability of conspecificity, based on cranial shape parameters, but cautioned that further analyses should be undertaken, as the boundaries between these species are difficult to determine.

There are visible morphological similarities between the two species of *Paranthropus.* The cusp patterns are very similar: the boundary between the metaconid and the entoconid falls almost directly perpendicular to the centre of the tooth in all three cases. The hypoconids are located more centrally along the buccal edge rather than tilted distally, with the distal margin dominated by a large hypoconulid (see 2.4.2.5). The

significant similarities between *Paranthropus boisei* and *Paranthropus robustus* is of interest in light of the tendency for some authors to ignore comparative specimens from South Africa when describing new data from East Africa (Leakey et al., 2012, for instance). When one considers that a number of the species of early Pleistocene fauna and flora that were present in Southern Africa at the time were also present in East Africa (Grine et al. 2012), it should not be impossible to conceive of a hominin species that might also have inhabited both areas, and perhaps these are not two separate species at all. With the discovery of some extremely large molars at Gondolin cave in South Africa, which have been attributed to *Paranthropus robustus* (*ibid.*), it would appear that the whole size range represented by *Paranthropus robustus* is also represented by *Paranthropus boisei.* Previous analyses have, however, distinguished the two groups based on relative cusp sizes (Wood et al. 1983), and there are craniodental features that are typically cited to distinguish the two species. The landmark model used for this study was designed to maximise the relative cusp proportion data that was subsequently utilised for the PC analyses and the statistical analyses. The results show close affinities between Peninj 1 and SK 6. Figure 5.9 shows visual comparisons between these closely-grouped specimens.

Paranthropus boisei Peninj1 L	*Paranthropus boisei* Peninj1 R (m)	*Paranthropus robustus* SK 6 L	*Paranthropus robustus* SK 23 L

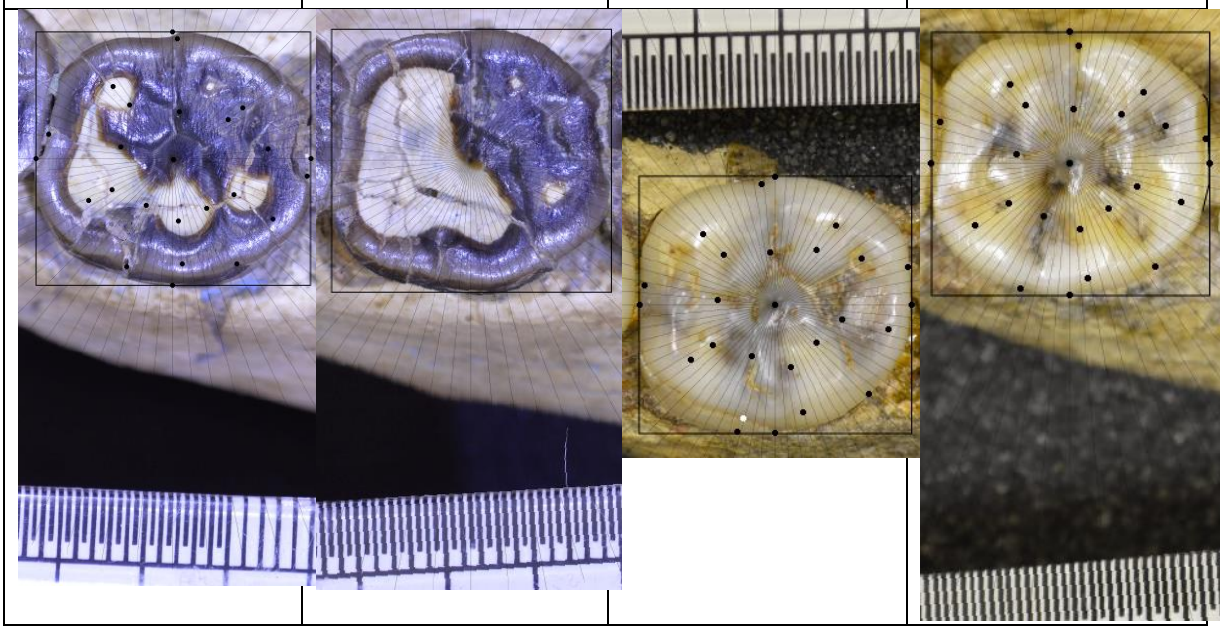

Figure 5.9 PCA grouping of "robust" *Paranthropus* M_1 specimens

The second, smaller-sized group of *Paranthropus* specimens, allocated to both *P. robustus* and *P. boisei,* falls within the general area of a central grouping of "medium-sized" and "slightly narrower" molars (including *Homo habilis* and *Homo rudolfensis*). The four specimens in this smaller group are TM 1517 (the holotype of *Paranthropus robustus)*, SK 63, SKW 5 and KNM-ER 15930, the latter of which is currently classified as falling into the *Paranthropus boisei* clade. SKW 5 and SK 63 group very closely together, both on the PCA plot and visually (Figure 5.10).

Paranthropus boisei KNM-ER 15930 L	*Paranthropus robustus* SKW 5	*Paranthropus robustus* SK 63 L	*Paranthropus robustus* TM 1517
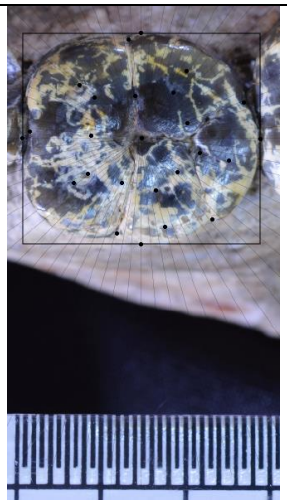	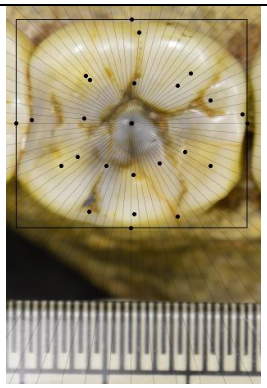		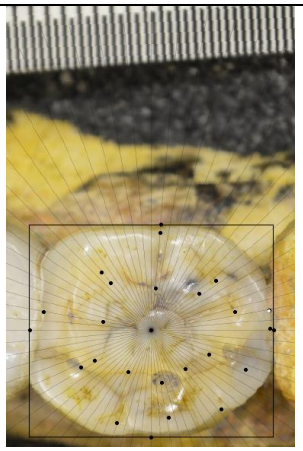

Figure 5.10 Principal components grouping of smaller *Paranthropus* M_1 specimens

If KNM-ER 15930 is correctly classified as a small *Paranthropus boisei*, then the fact that there are two distinct groupings of *Paranthropus* (large and robust on the one hand; medium-sized and slightly narrower on the other) might imply a very wide degree of sexual dimorphism within the *Paranthropus* clade in both South Africa and in East Africa, similar to the degree of sexual dimorphism in gorillas today. Looking at the linear dimension analyses and the PC plots, more specifically the chart which includes gorillas as a species outgroup (Figure 4.15), the amount of variation between the two groups of *Paranthropus* (large specimens and small specimens of both species) does seem to mimic that of the gorilla group. In the gorilla sample, males group to the right of the females on the PC chart (they are larger in size) but they both plot within a similar vertical bandwidth denoting overall similarities in relative width for both genders. The two groupings within the *Paranthropus* group mimics this pattern of "significant size variation but little width variation". The anomalous specimen continues to be KNM-ER 15930, however, which groups in the bottom left quadrant of the plot, towards the "early *Homo"* group, whereas the others group to the right of the y

axis (the bottom right quadrant on this particular plot). Interestingly, Taung 1 groups with the smaller, narrower *Paranthropus robustus* group on this graph, probably because the presence of a C_6 would have been a primary factor influencing the first principal component in this instance.

All of the *Paranthropus* specimens have been landmarked for the presence of a C_6, with the exception of KNM-ER 15930, which is relatively undamaged and does not show a C_6 to be obviously present. TM 1517 is very worn and the C_6 was inferred partly because it is the holotype of *Paranthropus robustus,* and all of the other specimens of *P. robustus* that were included in this study did have a C_6 present, but more importantly, a C_6 is visible on the enamel-dentine junction image supplied by Professor José Braga of Toulouse University . As mentioned, Taung 1 (*Australopithecus africanus)* and KNM-ER 806c were also landmarked for a (very visible) C_6. At a later stage, it would be useful to re-work all the analyses in this study without taking the C_6 into account, to see if this would markedly alter the species groupings on the principal components plots.

The *Paranthropus boisei/robustus* group is also reasonably cohesive on the Procrustes distance matrix, and in the log se_m analysis, with the exception again of KNM-ER 15930, the values for which range from -1.328 to -1.547 when compared to specimens attributed to the same genus. This specimen groups better in this analysis with specimens attributed to *Homo habilis* (especially OH 16)*, Homo rudolfensis* (KNM-ER 1802), OH 22 (*Homo erectus*) and MLD 2 (*A. africanus*). This finding therefore confirms the findings from the principal components analyses. The log se_m values for pairwise comparisons between KNM-ER 15930 and OH 16 are -1.615 and 1.567. Peninj 1 groups extremely well with SK 6 (-1.728/-1.724) and with SK 23 (-1.728/-1.677), again

confirming the results from the PC analyses. The close log se_m values for both the x-on-y and the y-on-x regressions between Peninj 1 and SK 6 confirm the very low degree of scatter around the regression line. SK 63 and TM 1517 also group well together (-1.715/-1.687), again confirming the grouping presented by the PC analyses. Also of note are an extremely low se_m values for the pairwise comparisons between TM 1517 (the holotype of *Paranthropus robustus*) and Peninj 1 (the mandibular proxy for the holotype of *Paranthropus boisei*), the values being -1.791/-1.700. This implies a high probability of conspecificity between these two specimens and confirms similar interpretations by Thackeray (1997) and Thackeray & Prat (2009) based on pairwise cranial comparisons between TM 1517 and OH 5 (the holotype of *Paranthropus boisei*).

Notably, however, the DFA differentiates the three *P. boisei* molars and the larger group of *P. robustus* molars from each other, with no misclassifications identified for specimens of either species, confirming the need for further analysis (Thackeray & Prat, 2009). Under this scenario, the seemingly anomalous specimen, KNM-ER 15930, tiny as it may be, would simply reflect extreme sexual dimorphism within *P. boisei,* just as SKW 5 would represent a small female specimen of *P. robustus.* Indeed, A. Walker and F. E. Grine (Grine 2007) considered this specimen to be of great importance, since "for whatever taphonomic reasons, mandibles at the small end of the size range […] are not common in the collections" (page 248).

Due to the very limited sample of lower first molars from *Paranthropus boisei* to which access was available for this study, it will be necessary to continue analysing specimens from this species (for instance, the holotype, OH 5, which includes maxillary, rather than mandibular, dentition) so that more robust conclusions can be reached as to similarities

between these two species. Dietary differences between the species (Lee-Thorp 2011; Cerling et al. 2011) should be considered alongside morphological distinctions before reaching any conclusions.

5.3 Discussion of potential anomalous specimens

- AL 288-1 *(A. afarensis):* highly anomalous, as confirmed by every type of analysis conducted. This study, though preliminary in nature, would suggest that this specimen does not group well within the *Australopithecus afarensis* paradigm. More research should be conducted to ascertain from other skeletal elements as well as the remaining dentition, whether *A. afarensis* consists of several morphotypes, or whether extreme sexual dimorphism or a highly unusual level of within-species variability might explain the vast differences between this specimen and the bulk of the more robust specimens from the species, or whether this specimen is misclassified.
- LH 2 *(A. afarensis)*: anomaly identified by the PCA and confirmed by linear dimension analyses and by the Log se_m analysis. A larger sample size is recommended for study, to assess the range of variability between specimens attributed to this species.
- Sts 52b *(A. africanus):* anomaly identified by the PCA and confirmed by linear dimension analyses and by the discriminant function analysis. A much larger sample size of *A. africanus* is required to establish whether, as suspected by Ronald Clarke, there are at least two morphotypes within the species (Clarke 2008).

- OH 16 *(H. habilis):* anomaly identified by the PCA and confirmed by the linear dimension analyses and by the Procrustes Distance Matrix. The dimensions of this specimen were initially likened to those of Australopithecines by Phillip Tobias (Leakey et al. 1964). This study would seem to confirm that OH 16 is more "robust" in morphology than OH 7, the holotype, based on uncorrected diameters from the occlusal view of the crown.
- KNM-ER 806c (*H. erectus):* highly anomalous, all analyses identified this specimen as being misclassified. It includes features that are diagnostic of both gracile and robust Australopiths, and it is of little surprise that the DFA classifies this specimen with *Australopithecus africanus.*
- KNM-ER 15930 *(Paranthropus boisei):* this specimen was identified as being anomalous in all but the discriminant function analysis. Whilst it is certainly possible that this specimen might represent a tiny female of *Paranthropus boisei*, most of the analyses did pick up additional shape components that confirmed a lack of close grouping of this molar within the *Paranthropus* hypodigm.

Other specimens that were identified by analyses other than the principal components analysis were:

- LH 4 (L) *(Australopithecus afarensis):* (anomalous only on the Procrustes distance matrix with some high values on the log se_m analysis). This specimen was included, despite it being very damaged, because of its importance as the holotype for *A. afarensis.* Neither the PCA nor, importantly, the DFA (based on 8 principal components axes) identified this specimen as anomalous. This implies that though the contour may be shaped differently (possibly due to incorrect inferences concerning the outline of the broken metaconid), the cusp pattern for

both antimeres was well-matched, and the main axes of covariance that distinguish well between any two species are recognised by the analyses that are designed to differentiate between specimens in this way, whilst those analyses (Procrustes distance matrices and Log se_m analyses) that analyse distances between all landmarks in an equally-weighted way identify regions in one area (in this instance, probably the metaconid) where shape is different. However, whilst log se_m values for within-species pairwise comparisons were on the high side for this molar, the between-species comparisons for this specimen precluded it being classified as anything other than *Australopithecus afarensis.*

- Taung 1: The Procrustes distance and log se_m matrices identified this specimen as anomalous, grouping better with *Paranthropus robustus.* This was confirmed by the DFA. The reason for this is the presence of a C_6, which is usually considered to be diagnostic of *Paranthropus* species (Wood et al. 1983; Aiello & Dean 1990; Hillson 1996). Phillip Tobias (1973; 1978) suggested that this juvenile skull may be a robust Australopithecine or a "derived" *Australopithecus africanus* (*c.f.* F. E. Grine, 2007, pp. 302-304).

5.4 Re-working of the PCA analysis with the exclusion of the six main anomalies

The six anomalies identified by the PC analysis of the fossil specimens are highlighted in Figure 5.11 below:

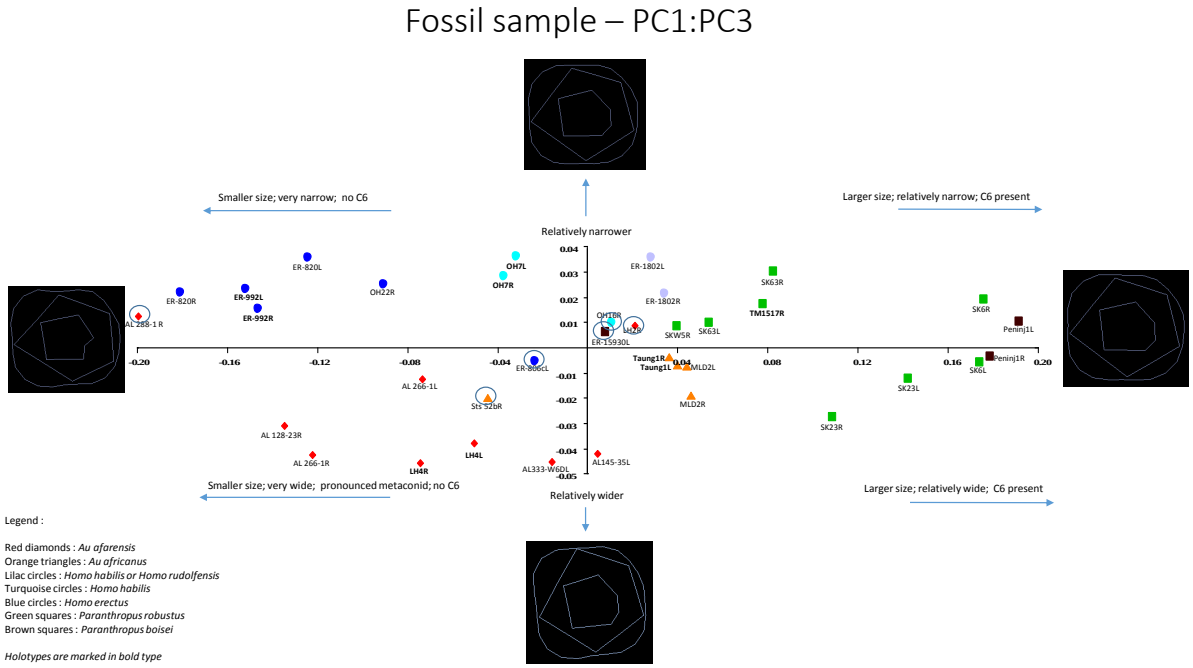

Figure 5.11 Principal Components Analysis of 36 fossil M_1 specimens showing six anomalous specimens

If all six of the anomalous specimens are removed from the fossil PC chart, the species groupings become remarkably distinct from each other and all species groups are reasonably well defined, as shown in Figure 5.12 below:

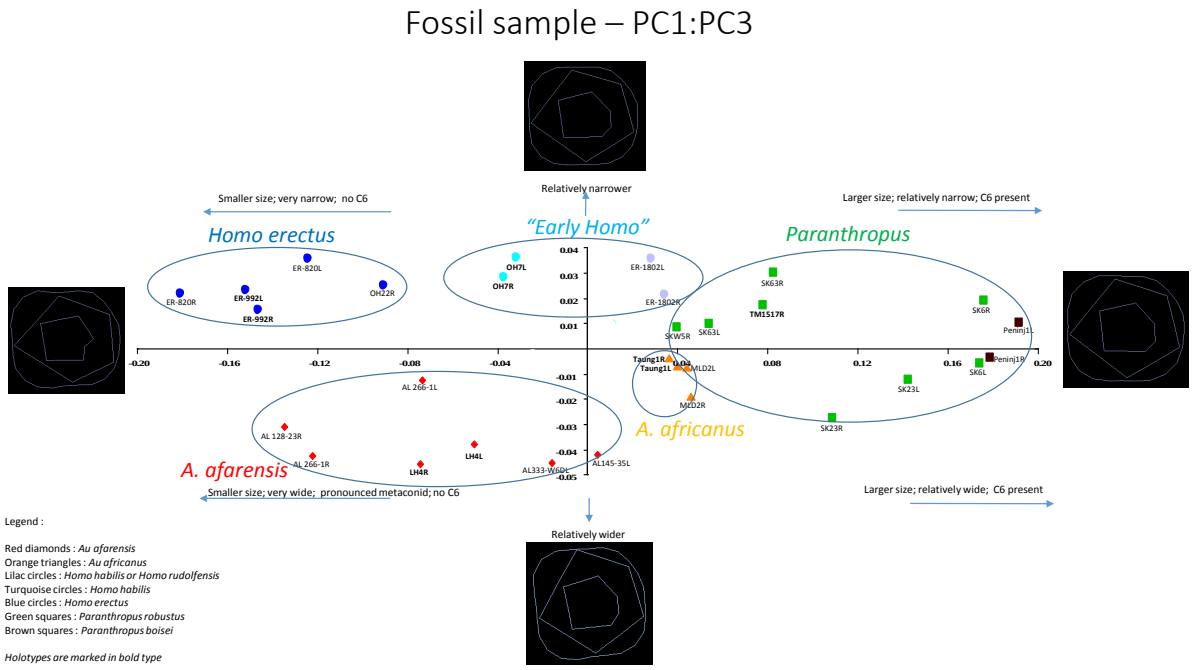

Figure 5.12 Principal Components Analysis of fossil M_1 specimens showing well-defined species groupings after exclusion of 6 anomalous specimens

This is not to say, however, that there are perfectly delineated boundaries between species, rendering them as completely discrete species. What this PC plot shows is that it is possible to use a landmark placement model that is capable of combining overall shape and size together with cusp pattern arrangement in such a way as to produce a visual overview showing the various species included in the study, grouped together as they are currently defined, in a predictable pattern. The area on the plot around which species group most closely together (*A. africanus, P. robustus,* Early Pleistocene *Homo*) (indeed, the area where the majority of the potential anomalies are located) is equivalent to a period straddling the Plio-Pleistocene boundary during which there is

debate over the certainty of allocations of some specimens to each of the species represented at this time (see 1.3). Indeed, if the time element is also added, the placement of the species groups on the plot (Figure 5.13) also shows a logical progression of change in the morphology of lower first molars that seems to fit with the expected chronological order of appearance of the species included in this study:

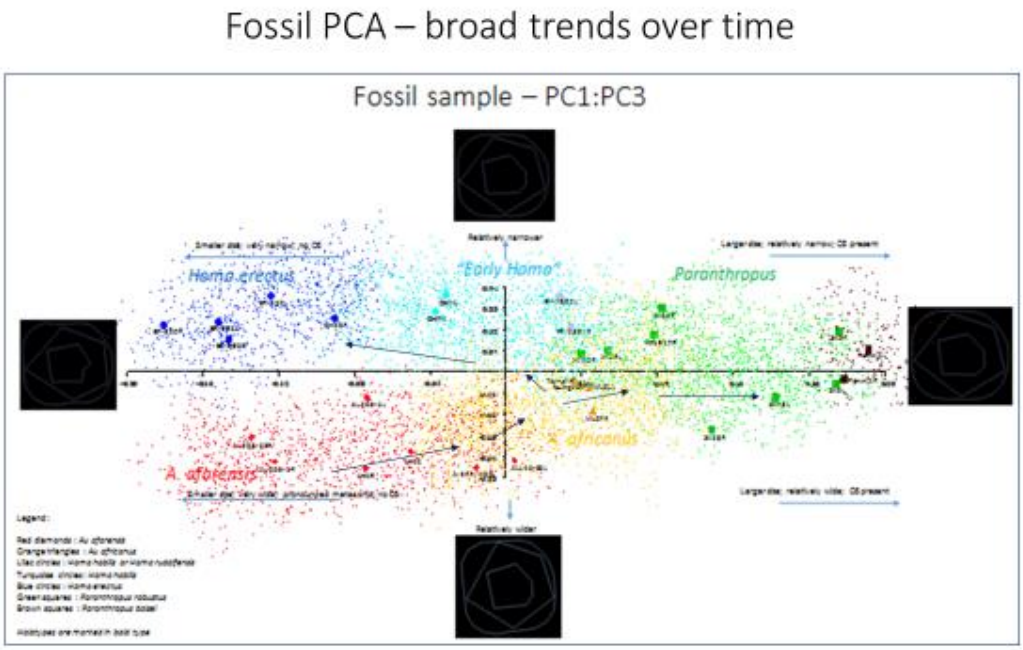

Figure 5.13 Schematic colour-coded graph relating to time. **Principal components analysis of fossil M_1 specimens showing trends over time from square teeth to narrowish/large teeth and narrow/small teeth. Starting at bottom left, very square teeth *(A. afarensis,* in red) trend towards medium-sized and "medium-width" teeth *(A. africanus,* in orange). Thereafter there is a split towards, on the one hand, slightly narrower but very much larger *P. robustus* and *P. boisei* (in green and dark brown, respectively), and on the other hand, the *Homo* clade, which has increasingly smaller and narrower molars as time progresses (turquoise for early Pleistocene *Homo* species and dark blue for *Homo erectus*).**

It is not within the scope of this study to enter the debate over lineages - the sample size is small and consists of only a single dental element (lower first molars). However, the trends over time raise some compelling questions. It would be interesting in future to add further dental and skeletal elements to the study, to see if these same orderly trends continue to be detected.

5.5 Re-working of the log se_m analysis with the exclusion of the six main anomalies

As far as the log se_m analysis is concerned, the average value for pairwise conspecific comparisons of the four extant species is -1.6208 +/- 0.1221 (n = 1520). The average intra-species log se_m value is for the fossil sample (with potential anomalies included) is -1.57. If the six potential anomalies identified by the PC analyses are removed from the sample (these being AL 288-1; LH 2; Sts 52b; OH 16; KNM ER 806c; KNM-ER 15930) the re-worked log se_m averages for the species groupings of *Australopithecus afarensis, Australopithecus africanus, Homo erectus, Homo habilis/rudolfensis* and *Paranthropus boisei/robustus* are calculated to be -1.584, -1.500, -1.727, -1.756 and -1.602 respectively, resulting in a new mean log se_m value for African Plio-Pleistocene hominin mandibular first molars of -1.607, with a standard deviation of 0.102 (n=176 pairwise comparisons). These averages (both for extant and fossil specimens) are therefore remarkably close to the mean log se_m value of -1.610 +/-0.230 calculated by Thackeray (2007a) based on comparisons of cranial data of conspecific vertebrates (n=1252 specimens). Thackeray has proposed -1.61 as an approximation of a biological species constant (T) (Thackeray 2007a), demonstrating this value to be a central tendency around which values for intra-species comparisons cluster together, producing a probability function that approximates a normal distribution. The values calculated for extant and fossil specimens in this study are also very close to the values calculated for cranial data of conspecific chimpanzees calculated by Adam Gordon and Bernard Wood, using the log se_m method in a recent study (Gordon & Wood 2013, Table 4); see below in Table 5.1 for a summary of values from this study (dental comparisons), together with comparisons of cranial data from Gordon & Wood's research:

Table 5.1 Log se_m mean and standard deviation values – comparisons obtained from different studies

Author	Data type	Species	Average log se_m	Standard deviation
(This study)	Dental	Extant primate species	-1.62	0.122
(This study)	Dental	Fossil specimens (excl. anomalies)	-1.61	0.102
Thackeray (2007a)	Cranial	Vertebrate species (> 70 taxa)	-1.61	0.230
Gordon & Wood (2013)	Cranial	*Pan paniscus* (female-female)	-1.61	0.087
Gordon & Wood (2013)	Cranial	*Pan paniscus* (male-male)	-1.62	0.095
Gordon & Wood (2013)	Cranial	*Pan paniscus* (female-male)	-1.61	0.094
Gordon & Wood (2013)	Cranial	*Pan troglodytes* (female-female)	-1.62	0.100
Gordon & Wood (2013)	Cranial	*Pan troglodytes* (male-male)	-1.60	0.109
Gordon & Wood (2013)	Cranial	*Pan troglodytes* (female-male)	-1.60	0.116

Generally speaking, the log se_m values obtained for within-species pairwise comparisons and for between-species pairwise comparisons (see Appendix 6 for the full 36 x 36 pairwise matrix of log se_m values) thus confirm the approach championed by Thackeray in the context of log se_m values and probabilities of conspecificity (Thackeray 2005; Thackeray 1997; Thackeray et al. 1997; Thackeray 2007a).

Despite having conducted an analysis that calculated log se_m average intra-species values to be consistently close to the proposed species constant of T= -1.61, the approach in general has been challenged by Adam Gordon and Bernard Wood (Gordon & Wood 2013), primarily because the method would occasionally appear to identify probabilities of conspecificity between specimens of different species. As explained in 3.6.1.5, "false positives" might occur in one of the two pairwise comparisons (x-on-y or y-on-x) for the two specimens being compared, for various reasons; it is usually possible to identify such potential errors by including an additional analysis of the delta values (differentials between the two log se_m values).

In summary, the analyses by and large confirmed each other (see Table 4.26). Six main anomalies were identified by the PCA. By excluding these anomalies from the analysis,

there is a high definition between species groupings in the expected areas of the PCA plot (notwithstanding the possibility that boundaries between species might be indistinct), borne out by a trend through time that reflects the correct order of appearance on the PCA plot of the species studied. The exclusion of the same six anomalies from the log se_m analysis also render an average value of -1.607 for the intra-species comparisons of the fossil species groups, which is very close to the expected average value of -1.61 for conspecific pairwise comparisons.

5.6 Antimeres

Most of the hominin antimeres included in this study followed the pattern observed for modern *Homo sapiens,* of right antimeres being wider and/or more robust than their left counterparts (the exception being *A. africanus* in this sample studied). Further research, to include additional dentition types and enlarged sample sizes should be undertaken to see if this trend is repeated in other molars, both in modern *Homo sapiens* and in fossil hominins.

5.7 Link between dental morphology and diet and/or sexual dimorphism

This study has identified some patterns of variability in the lower first molar morphology of fossil species groups that might be a reflection of what has been observed in the case of extant species groups. In the case of the *Paranthropus* species, it is possible to see a similar pattern of variability as that evident in the molars of *Gorilla gorilla* (dictated by sexual dimorphism: size differences but no significant shape difference, between genders). It is therefore expected that the difference between large

P. robustus and small *P. robustus* molars is explained by sexual dimorphism rather than by dietary differences between the two "size groups" within the same species. The same might well be true of *P. boisei* specimens (to be confirmed with larger samples).

The pattern of variability within *Australopithecus afarensis* is, however, puzzling. Very significant variability exists between certain specimens within this species (notably between AL 288-1, "Lucy" and the remainder of the group in the sample studied here). Typically, great differences in the shape of molars of modern *Homo sapiens* are cited as an example to use as a benchmark for "variability within a species". In modern *Homo sapiens*, certain population groups have been exposed to farming, soft grains such as wheat and rice, and food technology (high degrees of food processing resulting in a soft diet), whilst within other groups, an ancient type of hunter-gatherer existence is still observed, with roots, fruits and harder, often uncooked foodstuffs forming the majority of the diet of these communities. Diet-related tooth size differences are not restricted to males or females in these groups, and it is geography/technology that is posited to determine the variability, not gender. This has bearing on the validity of using modern *Homo sapiens* as a comparative sample against which to measure fossil hominin dentition, because none of the species in the African Plio-Pleistocene period had access to widescale farming of grains and food processing technology.

It is not within the scope of this study to include additional dietary-related research or comparative analyses of sexual dimorphism in regional dentition of modern *Homo sapiens*, *Pan troglodytes* or any of the other extant species usually studied for variability comparisons. However, the results from this current study suggest numerous other

avenues of enquiry that would be pertinent to the question of the amount of variability that can be expected within any single species. If there are "special circumstances" that could explain extraordinarily large ranges of variation in the molars of extant species (in this instance, the globally-ranging but differentially "modernised" *Homo sapiens*), then these circumstances should not be overlooked by researchers, if a fair comparison is to be made.

In particular, a study should be undertaken to examine the possible effects on dentition of a dietary change in a community evolving from a hunter-gatherer (pre-pastoral) lifestyle to a pastoral lifestyle. If dental photographs of pre-pastoral and 20th century specimens of San populations spanning several millennia can be obtained, it is hoped that some trends in morphological change of molar dentition over time, as dietary change takes place, might be observable. In particular, it should be investigated whether differential change, should it be identified, affects males and females within this group over the period in question at different rates.

Additionally, specimens from *Gorilla gorilla gorilla* and *Gorilla beringei graueri* could be studied together with a detailed description of any differences in the diets of these two lowland gorilla species, with a view to quantifying the expected degree of variability of two closely-related species. Mountain gorilla dentition images might also be collected for further comparison. The results of such a study might inform a discussion regarding the amount of variability to be expected, for instance, between *Paranthropus boisei* and *Paranthropus robustus.*

CHAPTER SIX – CONCLUSIONS

6.1 Review of the aims of the project

This project was focused on original analyses conducted on mandibular first molars from seven African Plio-Pleistocene hominin taxa (*Australopithecus afarensis, Australopithecus africanus, Homo rudolfensis, Homo habilis, Paranthropus robustus, Paranthropus boisei and Homo erectus*) and from four extant species (*Homo sapiens, Gorilla gorilla gorilla, Pan troglodytes schweinfurthii and Pan paniscus*). These analyses sought to assess the probability that certain African Plio-Pleistocene specimens currently attributed to species of *Australopithecus, Paranthropus* and *Homo* may belong to other species or other genera than those currently accepted for the specimens.

The principal questions that needed to be addressed were as follows:

- Can a species be defined numerically: how much variability is to be expected within a species and do clear boundaries exist between species?
- What are the traditionally accepted diagnostic features of molar teeth that distinguish the various species groups in the fossil record? How can these diagnostic features best be represented by landmark placements on the images, so that each feature is correctly emphasised for purposes of analysis?
- Can the application of various morphometric techniques and other numerically-based methodologies confirm or falsify the results obtained?
- Is it possible to assess trends over time and/or geographical distance in hominin tooth morphology?

- Is it possible to discern the influences on molar tooth size and/or shape of sexual dimorphism in extant species, and can this be applied to analyses of tooth morphology variation in the fossil record?
- Based on morphometric studies molars of extant species, are the currently accepted ranges of variability within taxonomic groupings of hominin fossils reasonable, or are there particular species groups that might warrant further study due to there being an unexpected amount of variability between specimens in the group, or very little variation between two or more groups?

Looking at each of these questions in turn, and in the knowledge that this study is exploratory in nature, is based on one dental element (lower first molars) and uses small sample sizes, some tentative conclusions can be made as follows:

6.1.1 Quantification of species variability and the existence of clear boundaries between species

Variability within any single "known" (biological, extant) species can be quantified and visualised with varying degrees of success, using any number of techniques. The real question being asked, however, is whether a universally-applicable measure of within-species variability can be applied to all species, present and past. Clearly, different species have differing ranges of variability between them and further to this, small ranges of variability in one skeletal element (such as the cranium) might be coupled with large ranges of variability in another (such as dental data) – such is the case of modern *Homo sapiens* (high variability in dental morphology, relatively low variability in cranial data) and gorillas (high variability in cranial morphology, relatively low variability in the overall *shape* of molars, although *size* differences between genders are

observed). This study has used several methodologies that can identify patterns of variability for certain extant species and inferences can be made, based on these, about the expected patterns to be found in the fossil record for certain species. However, the scope of the study is narrow (lower first molars; small samples) and whatever conclusions are made here are considered to be preliminary in nature, to be added to existing research on other dental and skeletal elements and to be amplified via further research on the remaining post-canine dentition of these and other specimens. Certainly, one firm conclusion can be made about the boundaries between species: these are not clear; overlaps between species exist in biological species today, so it is to be expected that overlaps likewise must have existed between fossil species.

6.1.2 Diagnostic features of lower first molars; development of a landmark model

The landmark model (3.5) developed for this study has translated fairly adequately the morphological features (size, overall shape, cusp arrangements), diagnostic of the various species of African Plio-Pleistocene hominin lower first molars included in the study, as detailed in 2.3, so as to be able to visualise these species on a PC plot with species clustering in predictable locations. Whilst the scope of the study is too limited to discuss questions of lineage and whether species as they are currently defined for African Plio-Pleistocene hominins are correctly defined as such, the research presented here may have the potential to be put to use to highlight suspected anomalies or to match any lower first molar discovered to others in the database, to confirm its allocation into a particular species group. It is hoped that as the sample size is increased and a larger database of specimens is created, the preliminary findings here

will be increasingly reinforced, to provide a comparative morphometric collection for use, possibly in the field.

6.1.3 Confirmation of results using additional analytical methods

A selection of additional methodologies has been applied to test the initial results from the PCA, by and large confirming species groups – homogeneity and variability – as well as the anomalous status of certain of the specimens chosen for the study. It is hoped that future research will include further methods, further statistical tests on the methods already used, and consist of larger sample sizes, in order to continue to confirm the potentially anomalous status of specimens identified as outliers in this present study, and to identify further potential anomalies.

6.1.4 Trends over time and geographical distance

Whilst it has not been possible to assess geographical trends with any degree of certainty (indeed, lower first molars from South Africa and East Africa share similar morphology in both species within the *Paranthropus* clade, for instance, although the two species are considered separate, based on other skeletal/cranial/dietary diagnostics), broad trends over time have become evident. Figure 5.13 demonstrates this most effectively. From the small, square molars typical of the *Australopithecus afarensis* holotype, a general narrowing over time becomes evident: molars in *Australopithecus africanus* are longer mesiodistally (and are therefore relatively narrower). From there, species fall into two categories – *Paranthropus* species, with molars that are relatively slightly narrower but larger or even significantly larger than

those of *Australopithecus africanus*, and *Homo* species, with increasingly significantly smaller, narrow teeth. Both of these areas of interest (time trends; geographical trends) will be useful to target for further research.

6.1.5 Evidence of sexual dimorphism – patterns identified: extant and fossil species

Gorilla teeth were found to display the greatest degree of sexual dimorphism in lower first molars, among the four extant species included in the study. On the PC plots figuring this species (confirming the linear dimensions analyses), this sexual dimorphism is evidenced in size differences between the two genders, rather than in significant shape or width variation between the two. A similar pattern was observed for the *Paranthropus* clade, which showed evidence of two main groupings defined by size variability rather than by large variability in tooth width or shape. The other species that has historically been theorised to demonstrate extremely significant levels of sexual dimorphism is *Australopithecus afarensis.* In this study, the pattern of variability demonstrated by the specimens chosen for the sample for this species encompassed a group that clustered around the holotype (smallish, square-shaped teeth, which have been considered to be male specimens), a larger, narrower tooth, and a tiny, very narrow tooth, considered to be female (AL 288-1: "Lucy"). The only similar pattern of variability seen among the extant species, wherein a single species reflects both size *and* more particularly, shape variability, was that of the modern *Homo sapiens* group. Nevertheless, the variability for this group appears to be narrower in range than for *A. afarensis,* and size differences were not so much a factor of sexual dimorphism as of ethnic variability: both male and female specimens of European descent had very

small, squarish teeth, as did the San ("Bushman") teeth in the study; other groups, male and female both, had very large teeth, such as the Tswana group, which tended to be large and narrow in both genders. Further research with expanded samples of specimens from Modern *Homo sapiens* (and from *Pan troglodytes*) is recommended.

6.1.6 Range of variability observed within species in the fossil record; identification of cases of unexpectedly little variation or higher than expected variability

Results are presented in tabular form (Table 6.1) for species highlighted by this question:

Table 6.1 Summary table of assessment of range of variability of fossil species

Inter/intra-species variability	Species	Comments
Intra-species	*A. afarensis*	* Extremely wide range of size and shape variability observed * Patterns of occlusal mandibular first molar variability do not appear to mimic patterns seen in extant species included in this study * Sexual dimorphism does not seem to be an adequate answer, but further research should be conducted to address this possibility * Possibly two or more morphotypes might be represented within this species; alternatively one or more specimens within the sample analysed are misclassified. * Further research required particularly into AL 288-1 (Lucy), due to its recurrent highly anomalous status.
Intra-species	*P. robustus*	* Large size variability, moderate width/shape variability, mimics the pattern of sexual dimorphism seen in *Gorilla gorilla*
Intra-species	*P. boisei*	* Large size variability, moderate width/shape variability, mimics the pattern of sexual dimorphism seen in *Gorilla gorilla*
Inter-species	*P. robustus/P. boisei*	* Lower first molar morphology almost indistinguishable between these species (excluding potential anomaly, KNM-ER 15930). * An enlarged sample, including additional dentition and further specimens (e.g. OH 5, the holotype, which has maxillary dentition) is required before making firm conclusions about the degree of variability evident in the molars of these two sister species. * Cranial variability morphometric comparisons between these two species, as well as those of intra-species cranial variability of another species with high degrees of variability (e.g. *A. afarensis*) would be useful. * Further research into the geographic spread of other hominins (e.g. *A. africanus* and *H. habilis*, with specimens identified in South Africa and East Africa for both species) should further inform the debate as to whether *Paranthropus* individuals could have inhabited both areas without necessarily being delineated into two separate species.
Inter-species	*H. habilis/ H. rudolfensis*	* Molars from both species group fairly closely, especially OH 16 (*H. habilis*) and KNM-ER 1802 *(H.*

		rudolfensis). Attempts should be made to include further specimens in the sample.
Inter-species	*H. rudolfensis/ H. habilis/ H. erectus*	* While a progression from larger molars to smaller molars is evident over time, analyses based on pure shape differences show some similar metrics between these species.
Inter-species	*A. africanus/ P. robustus*	Taung 1 (the holotype for *A. africanus*) has a sixth cusp and groups better with small specimens from *P. robustus.*
Inter-species	*A. africanus/ Early Pleistocene Homo*	* There are morphological affinities and close groupings on principal components analyses between some specimens allocated to *A. africanus* and to early Pleistocene *Homo,* as well as between *A. africanus* and KNM-ER 806c, currently attributed to *Homo erectus/ergaster.* Further comparisons with larger sample sizes and additional dental-skeletal elements are needed to ascertain whether there are overlaps between specimens attributed to these species.
Intra-species	*A. africanus*	* One specimen in this limited sample (Sts. 52b) appears to be smaller and squarer than the remaining specimens, grouping towards *A. afarensis.* Comparisons between this specimen and others considered to be from a second *A. africanus* morphotype (Clarke 2008), as well as between this specimen and new hominin material discovered recently at the nearby Rising Star cave complex (when accessible) should be considered for the future.
Intra-species	*P. robustus*	KNM-ER 15930 should be examined more thoroughly to assess how well it groups within *Paranthropus boisei* (larger sample required) and within the *Paranthropus clade* in general
Intra-species	*H. erectus*	KNM-ER 806c appears to be misclassified and has different morphology and size from the holotype, KNM-ER 992. Additional dentition from this specimen should be compared with additional *H. erectus* dentition and *A. africanus* dentition in particular.

6.2 Potential anomalies detected

Six anomalies were identified by the principal components analyses on the fossil sample, which were confirmed by most, if not all, of the other analyses used to test the initial PCA findings. These were:

AL 288-1 (currently classified as *A. afarensis* but which repeatedly failed to group within this species group);

LH 2 (currently classified as *A. afarensis* but which is significantly larger and narrower in dimension than most of the specimens in the sample);

Sts 52b (currently classified as *A. africanus*);

OH 16 (currently classified as *Homo habilis.* Groups between *H. rudolfensis* and *A. africanus* as it is significantly larger and wider than OH 7, the holotype);

KNM-ER 15930 (currently classified as *P. boisei* but is significantly smaller than the holotype and seems to differ in morphology to the other *Paranthropus* specimens);

KNM-ER 806c (currently classified as *H. erectus* but has more affinities in size and morphology with *A. africanus*).

There can be at least four possible conclusions to draw from these anomalous results:

a) The specimen may be **misclassified** into its current taxon. This kind of conclusion would be made in the case of specimens that differ excessively from other specimens in their currently-accepted species groups both in size and in shape. On examination of the images of the anomalous specimens in conjunction with the shape analyses and overall dimension metrics, KNM-ER 806c and AL 288-1 stand out as potential candidates for this outcome, as well as KNM-ER 15930, perhaps. The Procrustes distance between KNM-ER 806c and the

remaining specimens of the *Homo erectus* group is 0.083. If this specimen were excluded from the group, the average Procrustes distance between the other specimens falls to 0.053. The log se_m value for pairwise comparisons between KNM-ER 806c and the remaining specimens from *Homo erectus* averages -1.422. If this specimen were excluded from the group, the mean log se_m value for pairwise comparisons between the remaining specimens would fall to -1.727. The resultant low value is indicative of very close taxonomic grouping between specimens, as is the low Procrustes distance, once this anomalous specimen is removed. The Procrustes distance between KNM-ER 15930 and Peninj 1 (the mandibular proxy for the holotype of *Paranthropus boisei*) is 0.123, which is very high relative to the *Paranthropus* group as a whole (the average Procrustes distance for this group would fall to 0.070 if this specimen were excluded), and the log se_m value for pairwise comparisons between KNM-ER 15930 and Peninj 1 is a high -1.461, compared to -1.602, which is the value for the *Paranthropus* group as a whole after exclusion of this apparently anomalous specimen.

b) An extreme form of **sexual dimorphism** or some other factor influencing morphological variability within a species might be the reason for an apparent anomalous grouping. This could be the case for OH 16. Its mean log se_m value in pairwise comparisons with other specimens from the group is -1.620, which shows a good deal of cohesion with other members of its current species grouping. However, the average Procrustes distance between this specimen and others in the group (0.085 on average) is fairly high, but the range of values between specimens representing this small sample of Early Pleistocene *Homo* is very variable. This outcome might also be the case for KNM-ER 15930, and more detailed shape analyses are recommended to investigate this anomaly.

c) Some species themselves have an unusually wide range of shape variability, comprising more than one **morphotype**. This certainly seems true of *Australopithecus afarensis,* wherein there are currently two (or more) distinct morphotypes for lower first molars (very square teeth on the one extreme and very tiny, narrow, chimpanzee-like teeth on the other extreme). AL 288-1 and LH 2 may be appearing as repeated anomalies for the reason that their morphotype is considerably different, both in size and in shape, to the holotype and the majority of other specimens attributed to *Australopithecus afarensis*. In the case of *A. afarensis,* however, more research is required to try to establish whether the higher-than-expected range of variability among lower first molars is indicative of the existence of two distinct species, rather than two morphotypes within a single species. The other species which may contain a second morphotype is *Australopithecus africanus,* and a second species has been proposed instead for certain specimens currently attributed to this group (*Australopithecus prometheus,* (Clarke 2008)).

d) Anomalies could be due to observer **error**, **damage** to teeth or other **technical reasons**. In the case of LH 4, antimere differences observed most particularly in the log se_m analysis could be due to incorrect observer inferences regarding perimeter shape, as a result of damaged areas on both antimeres. A methodology such as log se_m, which places no special weighting on any particular landmark, will distinguish morphological differences according to the number of landmarks allocated to each different type of shape feature. In this study, 28 of the 48 measurements used for the log se_m analysis were weighted towards perimeter and outer shape of the teeth, with only 20 being allocated to cusp arrangement. On the PCA, however, size, outer shape and cusp arrangement

differences were all factored in to both axes, because the sample included specimens with very different cusp arrangements (including the presence of a C_6 or unusually pronounced metaconids) and the most distinctive differentiators between species were already identified in the first few principal components. The DFA utilised eight sets of PC scores. Thus on the studies that discriminated for the features that most differentiated diagnostic features between groups, neither of the antimeres of LH 4 were identified as being anomalous: they were clearly representative of *A. afarensis*. The decision could have been made to eliminate these damaged teeth from the study but the results proved interesting enough to keep them present: other than highlighting the different emphases of the methodologies used, both antimeres still grouped together. Even in the log se_m analysis, for which high values were reported for LH 4 (L), there was no other species group into which it would be classified more readily, and the only group for which it had log se_m values within 95% confidence levels was its allocated group, *A. afarensis.* One of the outcomes requiring to be tested was whether, in the case of specimens with unusually different antimeres, either one (and one only) of the antimeres might be highlighted as being misclassified. Even in such instances as LH 4 and AL 266-1, where antimeres were significantly "different" (around the perimeter) from each other, the analyses did not identify either antimere as "misclassified", because their cusp arrangements were both in keeping with their allocated species group. When a specimen with antimeres was highlighted as "misclassified", such as Taung 1, both antimeres were grouped in the same way for the same reasons.

6.3 Limitations of this study and opportunities for further research.

This study has been limited to mandibular first molars of 36 African Plio-Pleistocene hominin fossils and of small samples of four extant species (n=20 each for *Homo sapiens, Gorilla gorilla gorilla, Pan paniscus* and *Pan troglodytes*). For these results to be verified, the sample sizes should ideally be greatly increased and the remaining post-canine dentition taken into account (both mandibular and maxillary dentition). The analyses used to confirm anomalies have also been carried out in a preliminary manner, and with larger sample sizes, additional statistical tests could be conducted on each analysis.

Whilst the landmark placement model appears to have been very successful in providing well-weighted data reflecting the main morphological characters of lower first molars, this model will need to be tested further in the context of the remaining post-canine dentition (with modifications for the maxillary dentition), as well as against diagnostic metrics from 3D images of the enamel-dentine junction.

Further research can also be considered to resolve questions pertaining to currently accepted species groupings in the Plio-Pleistocene period:

- The inclusion of larger samples and additional molar types of extant primate species should be analysed to provide more conclusive data to assess the extent of size variation and/or the range of shape variation influencing sexual dimorphism within a species;

- Further research comprising larger samples and additional molar types (using additional gorilla subspecies to inform comparative analyses based on geographical range and/or moderate dietary variations) to shed more light on the question as to whether *Paranthropus robustus* and *Paranthropus boisei* should be considered as separate species, or whether they should be subsumed into one species;
- Additional specimens of *Australopithecus africanus* should be analysed to test for the existence of two distinct morphotypes (Clarke 2008; Fornai et al. 2013);
- A much larger sample size for extant species, coupled with a study into diet-related morphological change (in pre-pastoral and recent modern humans, for example) may inform further research into the question of whether the distinct morphotypes currently observed within the *Australopithecus afarensis* group can be attributed to sexual dimorphism, or whether there are two (or more) distinct species in this group.
- Additional landmark models and further morphological methodologies should be investigated. Further refinements are currently being made to the log se_m approach (Thackeray & Dykes, unpublished manuscript) and these can be implemented in additional studies.
- Additional statistical tests should be added to each of the analytical methodologies carried out to confirm results.

6.4 Final conclusions

Based on the results of this study, the hypotheses formed at the beginning of the study are reviewed in the context of lower first molars of African Plio-Pleistocene fossil hominins:

- HSQ: *"Status Quo Hypothesis"*: *all African Plio-Pleistocene first molar specimens discovered to date, including holotypes, are correctly classified into their current taxa*. Certain specimens assessed during the course of this study are extremely anomalous. The conclusion reached is that some specimens, even in the small sample analysed here, are misclassified.
(HSQ rejected)

- H0: *The observed degree of variability in lower first molar shape and size within extant species is so narrow in range that when the same parameters are applied to samples of African Plio-Pleistocene fossil hominin dental specimens discovered to date, they should be recognisable as discrete species*. The observed range of variability in lower first molar shape and size within extant species is varied. The range of variability within extant species is not so narrow as to be able to recognise fully discrete species, using the analyses in this study. There are small areas of overlap between the species analysed. Furthermore, the "within-group" range of variability in size between gorilla molars, for instance, is very wide, due to sexual dimorphism. When such a pattern is similarly applied to the fossil record, the *Paranthropus* clade as a whole displays similar patterns that are probably better explained by sexual dimorphism and on the basis of this study,

Paranthropus boisei is not readily distinguishable from *Paranthropus robustus* (based on LM_1 shape and size alone). The range of variability observed for lower first molar size and, more particularly, for shape in the lower first molars of modern *Homo sapiens* is extremely large, with different population groups displaying size and shape variations for both genders. Some very large, narrow teeth overlap with small female gorilla teeth, and small, narrow teeth overlap with chimpanzee teeth. The fossil species that displays the most variability in both size *and* shape is *Australopithecus afarensis,* but the vast differences between "Lucy" (tiny and narrow, in a V-shaped, gracile mandible) and the holotype or other specimens with "square" molars within U-shaped, robust mandibles have been attributed to sexual dimorphism, which is puzzling in the light of patterns of sexual dimorphism evident within the modern *Homo sapiens* sample, wherein teeth from one population group (e.g. Tswana) are large and narrow (both male and female specimens) and others (e.g. European) are small and squarish (both male and female specimens). With regard to lower first molars, it appears that specimens of the *Australopithecus afarensis* group fail to be recognised as one discrete species.
(HO hypothesis cannot be rejected – boundaries between species are not fully discrete).

- H2: *The observed degree of variability in first molar shape and size within extant species is so wide in range that when the same parameters are applied to specimens attributed to currently-accepted species groups in the African Plio-Pleistocene period, this would result in all species of that period being subsumed into one species group*. The four extant species assessed in this study demonstrated varying ranges of variability, mainly in size and to a lesser extent, in shape. However, as expected, the four species did not group together as a homogenous single group: although there were minor overlaps, generally distinct species groups were observed. Likewise, in the case of African Plio-Pleistocene

hominin fossils, even before removing the six anomalous specimens identified during the course of this study, many distinct species groups were also observed, with some small overlaps. The exclusion of these six anomalies from the analyses resulted in the removal of some of these overlaps. Even though some species did appear to be reasonably homogenously grouped together (early Pleistocene *Homo – Homo habilis* and *Homo rudolfensis;* and the *Paranthropus* clade – *Paranthropus robustus* and *Paranthropus boisei*), it cannot be postulated that all of the species during the African Plio-Pleistocene period can be subsumed into one single species group.
(H2 hypothesis rejected).

- H3: *There are no clear boundaries between species*. On the basis of the lower first molars included in the extant species and Hominin fossil samples, clear boundaries were not always evident between species, although there was enough separation between the bulk of the specimens in each species to perceive groupings in general. However, the findings from this study would not support the contention that there are no clear boundaries at all between species.
(H3 hypothesis cannot be fully rejected, due to some overlaps).

Significant, recurrent anomalous results from this study, do, however, make an acceptance of H1 possible:
- H1: *At least some of the African Plio-Pleistocene specimens currently attributed to species of Homo, Paranthropus or Australopithecus may be misclassified*.

Based on dentition alone (and bearing in mind that many of the specimens examined comprised only dentition with no other skeletal element for comparative purposes),

some of the specimens examined in this study may indeed be misclassified at the species level (e.g. perhaps Sts 52b and OH 16) or at the genus level (e.g. KNM-ER 806c and possibly Taung 1, OH 16 and KNM-ER 15930). AL 288-1 is highly anomalous but it is not possible to tell at this juncture at what level it might be misclassified; more research is required to confirm the possibility that the range of variability within *Australopithecus afarensis* is too wide to encompass one single species.

H1: can be accepted.

This project has served, in an exploratory fashion, to address several issues which would be useful to examine using enlarged samples and additional analytical methodologies in ongoing future research.

BIBLIOGRAPHY

Aiello, L. C., Collard, M., Thackeray, J. F., & Wood, B. A. (2000). Assessing exact randomization-based methods for determining the taxonomic significance of variability in the human fossil record. *South African Journal of Science*, *96*, 179–183.

Aiello, L., & Dean, C. (1990). *An introduction to human evolutionary anatomy* (pp. 133–159). Academic Press.

Albrecht, G. H. (1980). Multivariate analysis and the study of form with special reference to canonical variate analysis. *American Zoologist*, *20*, 679–693.

Alemseged, Z., Wynn, J. G., Kimbel, W. H., Reed, D., Geraads, D., & Bobe, R. (2005). A new hominin from the Basal Member of the Hadar Formation, Dikika, Ethiopia. *Journal of Human Evolution*, *49*, 499–514.

Antón, S. C., & Josh Snodgrass, J. (2012). Origins and Evolution of Genus *Homo*: New Perspectives. *Current Anthropology*, *53 No. S6*(December), S479–S496.

Bailey, S. E., & Wood, B. A. (2007). Trends in postcanine occlusal morphology within the hominin clade: The case of *Paranthropus*. In S. E. Bailey & J.-J. Hublin (Eds.), *Dental Perspectives on Human Evolution* (pp. 33–52). Springer.

Benazzi, S., Viola, B., Kullmer, O., Fiorenze, L., Harvati, K., Paul, T., … Mallegni, F. (2011). A reassessment of the Neanderthal teeth from Taddeo cave (southern Italy). *Journal of Human Evolution*, *61*, 377–387.

Bernal, V. (2007). Size and shape analysis of human molars: Comparing traditional and geometric morphometric techniques. *HOMO- Journal of Comparative Human Biology*, *58*(4), 279–296.

Bookstein, F. L. (1991). *Morphometric tools for landmark data*. Cambridge University Press.

Bookstein, F. L. (1997). Landmark methods for forms without landmarks: morphometrics of group differences in outline shape. *Medical Image Analysis*, *1*(3), 225–243.

Brace, C. L. (1972). Sexual dimorphism in human evolution. *Yearbook of Physical Anthropology*, *16*, 31–39.

Brace, C. L. (1973). Tooth measurements and the rejection of the taxon "*Homo habilis*". *Yearbook of Physical Anthropology*, *16*, 50–68.

Brace, C. L. (1979). Krapina, "Classic" Neanderthals, and the evolution of the European face. *Journal of Human Evolution*.

Brace, C. L., & Mahler, P. E. (1971). Post-Pleistocene changes in the human dentition. *American Journal of Physical Anthropology*, *34*(2), 191–203.

Brace, C. L., Rosenberg, K. R., & Hunt, K. D. (1987). Gradual change in human tooth size in the late Pleistocene and post-Pleistocene. *Evolution*, *41*(4), 705–720.

Brace, C. L., Tracer, D. P., Yaroch, L. A., Robb, J., Brandt, K., & Nelson, A. R. (1993). Clines and clusters versus "race:" A test in ancient Egypt and the case of a death on the Nile. *American Journal of Physical Anthropology*, *92*(SUPPL. 17), 1–31.

Braga, J., & Thackeray, J. F. (2003). Early *Homo* at Kromdraai B: probabilistic and morphological analysis of the lower dentition. *Comptes Rendus Palevol*.

Braga, J., Thackeray, J. F., Subsol, G., Kahn, J. L., Maret, D., Treil, J., & Beck, A. (2010). The enamel-dentine junction in the postcanine dentition of *Australopithecus africanus*: intra-individual metameric and antimeric variation. *Journal of Anatomy*, *216*(1), 62–79.

Bräuer, G. (1984). A craniological approach to the origin of anatomically modern *Homo sapiens* in Africa and implications for the appearance of modern Europeans. In F. H. Smith & F. Spencer (Eds.), *The Origins of Modern Humans: A World Survey of the Fossil Evidence* (pp. 327–410). New York: Alan R. Liss.

Braun, S., Thackeray, J. F., & Loots, M. (2004). Scientific notes: A morphometric technique to assess probabilities of conspecificity in extant primates and Plio-Pleistocene hominids. *Annals of the Transvaal Museum*, *41*, 93–95.

Broom, R. (1938). The Pleistocene anthropoid apes of South Africa. *Nature*, *142*, 377–9.

Broom, R., & Robinson, J. T. (1952). *Swartkrans Ape Man: Paranthropus Crassidens*. Pretoria: Transvaal Museum.

Broom, R., Robinson, J. T., & Schepers, G. W. H. (1950). *Sterkfontein Ape-Man Plesianthropus*. Transvaal Museum.

Busch, D. D. (2006). *Mastering Digital Photography* (2nd ed.). Boston: Thomson Course Technology.

Campbell, T. D. (1925). *Dentition and Palate of the Australian Aboriginal*. Adelaide: Hassell Press.

Cerling, T. E., Mbua, E., Kirera, F. M., Manthi, F. K., Grine, F. E., Leakey, M. G., … Uno, K. T. (2011). Diet of *Paranthropus boisei* in the early Pleistocene of East Africa. *Proceedings of the National Academy of Sciences of the United States of America*, *108*(23), 9337–9341.

Clarke, R. J. (2008). Latest information on Sterkfontein's Australopithecus skeleton and a new look at Australopithecus. *South African Journal of Science*, *104*, 443–449.

Clarke, R. J. (2012). A Homo habilis maxilla and other newly-discovered hominid fossils from Olduvai Gorge, Tanzania. *Journal of Human Evolution*. doi:10.1016/j.jhevol.2011.11.007

Crevecoeur, I., Skinner, M. M., Bailey, S. E., Gunz, P., Bortoluzzi, S., & Al., E. (2014). First Early Hominin from Central Africa (Ishango, Democratic Republic of Congo. *PLoS ONE*, *9*(1), e84652.

Dahlberg, A. A. (1960). The dentition of the first agriculturalists (Jarmo, Iraq). *American Journal of Physical Anthropology*, *18*, 243–256.

Dart, R. A. (1925). *Australopithecus africanus*: the man-ape from South Africa. *Nature*, *115*, 195–199.

Dart, R. A. (1948). The Makapansgat proto-human *Australopithecus prometheus*. *American Journal of Physical Anthropology*, *6*(3), 259–84.

Darwin, C. R. (1869). *On the Origin of Species by Means of Natural Selection, or the Preservation of Favoured Races in the Struggle for Life* (p. 51).

Day, M. H., Leakey, R. E. F., Walker, A. C., & Wood, B. A. (1976). New hominids from East Turkana, Kenya. *American Journal of Physical Anthropology*, *45*, 369–435.

Dayal, M. R., Kegley, A. D. T., Strkalj, G., Bidmos, M. A., & Kuykendall, K. L. (2009). The history and composition of the Raymond A. Dart Collection of Human Skeletons at the University of the Witwatersrand, Johannesburg, South Africa. *American Journal of Physical Anthropology*, *140*(2), 324–335.

De Queiroz, K. (2007). Species concepts and species delimitation. *Systematic Biology*, *56*(6), 879–886.

Dempsey, P. J., & Townsend, G. C. (2001). Genetic and environmental contributions to variation in human tooth size. *Heredity*, *86*, 685–693.

Dobzhansky, T. (1950). Mendelian populations and their evolution. *American Naturalist*, *84*(819), 401–418.

Dryden, I. L., & Mardia, K. V. (1998). *Statistical Shape Analysis*. John Wiley & Sons.

Emes, Y., Aybar, B., & Yalcin, S. (2011). On the evolution of human jaws and teeth: a review. *Bulletin of the International Association of Paleodontology*, *5*(1), 37–47.

Estebaranz, F., Martinez, L. M., Galbany, J., Turbon, D., & Perez-Perez, A. (2009). Testing hypotheses of dietary reconstruction from buccal dental microwear in *Australopithecus afarensis*. *Journal of Human Evolution*, *57*, 739–750.

Ferguson, W. W. (1989). Critique of "*Australopithecus afarensis*" as a single species based on dental metrics and morphology. *Primates*.

Fisher, R. A. (1936). The use of multiple measurements in taxonomic problems. *Annals of Eugenics*, *7*(2), 179–188.

Fornai, C., Bookstein, F. L., & Weber, G. H. (2013). Second maxillary molars confirm a dimorphism of Australopithecus at Sterkfontein Member 4. In *European Society for the Study of Human Evolution Third Annual Meeting*.

Gómez-Robles, A., Bermúdez de Castro, J. M., Martinón-Torres, M., Prado-Simón, L., & Arsuaga, J. L. (2012). A geometric morphometric analysis of hominin upper second and

third molars, with particular emphasis on European Pleistocene populations. *Journal of Human Evolution*, *63*(3), 512–526.

Gómez-Robles, A., Martinón-Torres, M., Bermúdez de Castro, J. M., Margvelashvili, A., Bastir, M., Arsuaga, J. L., … Martínez, L. M. (2007). A geometric morphometric analysis of hominin upper first molar shape. *Journal of Human Evolution*, *53*(3), 272–285.

Gómez-Robles, A., Bermúdez de Castro, J. M., Arsuaga, J.-L. L., Carbonell, E., Polly, P. D., Gomez-Robles, A., … Polly, D. (2013). No known hominin species matches the expected dental morphology of the last common ancestor of Neanderthals and modern humans. *Proceedings of the National Academy of Sciences of the United States of America*, *110*(45), 18196–18201. doi:10.1073/pnas.1302653110

Gómez-Robles, A., Martinón-Torres, M., Bermudez de Castro, J. M., Prado, L., Sarmiento, S., & Arsuaga, J. L. (2008). Geometric morphometric analysis of the crown morphology of the lower first premolar of hominins, with speciall attention to Pleistocene Homo. *Journal of Human Evolution*, *55*, 627–638.

Gordon, A. D., Green, D. J., & Richmond, B. G. (2008). Strong postcranial size dimorphism in *Australopithecus afarensis*: results from two new resampling methods for multivariate data sets with missing data. *American Journal of Physical Anthropology*, *135*, 311–328.

Gordon, A. D., & Wood, B. A. (2013). Evaluating the use of pairwise dissimilarity metrics in paleoanthropology. *Journal of Human Evolution*, *65*, 465–477.

Grine, F. E. (Ed.). (2007). *Evolutionary History of the robust Australopithecines*. *Evolutionary History of the robust Australopithecines*. Transaction Publishers.

Grine, F. E., & Daegling, D. J. (1993). New mandible of *Paranthropus robustus* from Member 1, Swartkrans Formation, South Africa. *Journal of Human Evolution*, *24*, 319–333.

Grine, F. E., Jacobs, R. L., Reed, K. E., & Plavcan, J. M. (2012). The enigmatic molar from Gondolin, South Africa: Implications for *Paranthropus* paleobiology. *Journal of Human Evolution*, *63*, 597–609.

Grine, F. E., Spoonheimer, M., Ungar, P. S., Lee-Thorp, J., & Teaford, M. F. (2012). Dental Microwear and Stable Isotopes Inform the Paleoecology of Extinct Hominins. *American Journal of Physical Anthropology*, *148*, 285–317.

Grine, F. E., Ungar, P. S., Teaford, M. F., & El-Zaatari, S. (2006). Molar microwear in *Praeanthropus afarensis*: evidence for dietary stasis through time and under diverse paleoecological conditions. *Journal of Human Evolution*, *51*(3), 297–319.

Groves, C. P., & Mazak, V. (1975). An approach to the taxonomy of the Hominidae: Gracile Villafranchian hominidae of Africa. *Casopis pro Mineralogia Geologii*, *20*, 225–247.

Guatelli-Steinberg, D., & Irish, J. D. (2005). Brief communication: Early hominin variability in first molar dental trait frequencies. *American Journal of Physical Anthropology*, *128*(2), 477–484.

Harcourt-Smith, W. E. H., & Aiello, L. C. (2004). Fossils, feet and the evolution of human bipedal locomotion. *Journal of Anatomy*, *204*(5), 403–16.

Harris, E. F., & Lease, L. R. (2005). Mesiodistal tooth crown dimensions of the primary dentition: A worldwide survey. *American Journal of Physical Anthropology*, *128*(3), 593–607.

Hawks, J., Wang, E. T., Cochran, G. M., Harpending, H. C., & Moyzis, R. K. (2007). Recent acceleration of human adaptive evolution. *Proceedings of the National Academy of Sciences of the United States of America*, *104*(52), 20753–20758.

Henneberg, M., & de Miguel, C. (2004). Hominins are a single lineage: brain and body size variability does not reflect postulated taxonomic diversity of hominins. *HOMO- Journal of Comparative Human Biology*, *55*, 21–37.

Henneberg, M., & Thackeray, J. F. (1995). A single-lineage hypothesis of hominid evolution. *Evolutionary Theory*, *11*, 31–38.

Hillson, S. (1996). *Dental Anthropology*. Cambridge University Press.

Hlusko, L. J. (2004). Protostylid variation in Australopithecus. *Journal of Human Evolution*, *46*(5), 579–594.

Hublin, J. J. (2014). Paleoanthropology: Homo erectus and the limits of a paleontological species. *Current Biology*, *24*(2).

Hughes, A. R., & Tobias, P. V. (1977). A fossil skull probably of the genus *Homo* from Sterkfontein, Transvaal. *Nature*, *265*(5592), 310–312.

Irish, J., & Guatelli-Steinberg, D. (2003). Ancient teeth and modern human origins: an expanded comparison of African Plio-Pleistocene and recent world dental samples. *Journal of Human Evolution*, *45*, 113–144.

Johanson, D. C., & Edey, M. A. (1990). *Lucy - The Beginnings of Mankind*. London: Penguin Books.

Johanson, D. C., & Taieb, M. (1976). Plio-Pleistocene hominid discoveries in Hadar, Ethiopia. *Nature*, *260*, 293–297.

Kibii, J. M., Churchill, S. E., Schmid, P., Carlson, K. J., Reed, N. D., de Ruiter, D. J., & Berger, L. R. (2011). A partial pelvis of *Australopithecus sediba*. *Science (New York, N.Y.)*, *333*(6048), 1407–1411.

Kieser, J. A. (1990). *Human Adult Odontometrics: The study of variation in adult tooth size*. Cambridge University Press.

Kimbel, W. H. (1991). Species, species concepts and hominid evolution. *Journal of Human Evolution, 20*, 355–371.

Kimbel, W. H., & Delezene, L. K. (2009). "Lucy" redux: A review of research on *Australopithecus afarensis*. *American Journal of Physical Anthropology, 140*(SUPPL. 49), 2–48.

Kimbel, W. H., Johanson, D. C., & Coppens, Y. (1982). Pliocene Hominid Cranial Remains from the Hadar Formation, Ethiopia. *American Journal of Physical Anthropology*, *57*, 453–99.

Kimbel, W. H., & Martin, L. (Eds.). (1993). *Species, species concepts, and primate evolution*. New York: Plenum Press.

Kimbel, W. H., & Rak, Y. (1993). The importance of species taxa in paleoanthropology and an argument for the phylogenetic concept of the species category. In W. H. Kimbel & L. B. Martin (Eds.), *Species, Species Concepts, and Primate Evolution* (pp. 461–484).

Kimbel, W. H., Rak, Y., & Johanson, D. C. (2004). *The skull of Australopithecus afarensis*. Oxford University Press.

Kimbel, W. H., & White, T. D. (1988). Variation, sexual dimorphism and the taxonomy of *Australopithecus*. In F. E. Grine (Ed.), *Evolutionary History of the "Robust" Australopithecines* (pp. 259–268). New York: Aldine de Gruyter.

Kivell, T. L., Kibii, J. M., Churchill, S. E., Schmid, P., & Berger, L. R. (2011). *Australopithecus sediba* hand demonstrates mosaic evolution of locomotor and manipulative abilities. *Science (New York, N.Y.), 333*(6048), 1411–1417.

Larsen, C. S. (1995). Biological Changes in Human Populations with Agriculture. *Annual Review of Anthropology*, *24*, 185–213.

Leakey, L. S. B. (1960). Recent discoveries at Olduvai Gorge. *Nature*, *188*, 1050–52.

Leakey, L. S. B. (1961). The Juvenile mandible from Olduvai. *Nature*, *191*, 417–18.

Leakey, L. S., Tobias, P. V, Napier, J. R., & Leakey L.S.B. Tobias P.V. Napier J.R. (1964). A New Species of Genus *Homo* from Olduvai Gorge. *Nature*, *202*(4), 424–427.

Leakey, M. D., Hay, R. ., Curtis, G. H., Drake, R. E., Jackes, M. K., & White, T. D. (1976). Fossil Hominids from the Laetoli Beds. *Nature*, *262*, 460–466.

Leakey, M. G., Spoor, F., Dean, M. C., Feibel, C. S., Antón, S. C., Kiarie, C., & Leakey, L. N. (2012). New fossils from Koobi Fora in northern Kenya confirm taxonomic diversity in early *Homo*. *Nature*.

Leakey, R. E. F. (1972). Further evidence of Lower Pleistocene hominids from East Rudolf, North Kenya, 1971. *Nature*, *237*, 264–9.

Leakey, R. E. F., & Walker, A. C. (1988). New *Australopithecus boisei* specimens from East and West Lake Turkana, Kenya. *American Journal of Physical Anthropology*, *76*(1), 1–24.

Leakey, R. E. F., & Wood, B. A. (1973). New evidence of the genus *Homo* from East Rudolf, Kenya. II. *American Journal of Physical Anthropology*, *39*(3), 355–68.

Lee, S. H. (2005). Brief communication: Is variation in the cranial capacity of the Dmanisi sample too high to be from a single species? *American Journal of Physical Anthropology*, *127*(3), 263–266.

Lee, S.-H. (2005). Patterns of size sexual dimorphism in *Australopithecus afarensis*: another look. *Homo : Internationale Zeitschrift Fur Die Vergleichende Forschung Am Menschen*, *56*(3), 219–232. doi:10.1016/j.jchb.2005.07.001

Lee-Thorp, J. (2011). The demise of "Nutcracker Man. *Proceedings of the National Academy of Sciences of the United States of America*, *108*(23), 9319–9320.

Lele, S., & Cole, T. M. (1995). Euclidean distance matrix analysis: a statistical review. In K. V. Mardia & C. A. Gill (Eds.), *Current issues in Statistical Shape Analysis* (pp. 49–53). University of Leeds Press.

Lele, S., & Richtsmeier, J. L. (1991). Euclidian distance matrix analysis: a coordinate-free approach for comparing biological shapes using landmark data. *American Journal of Physical Anthropology*, *86*, 415–427.

Leonard, W. R. (1991). *Australopithecus afarensis* and the single species hypothesis. *Primates*, *32*(1), 125–130.

Leonard, W. R., & Hegmon, M. (1987). Evolution of P3 morphology in *Australopithecus afarensi*s. *American Journal of Physical Anthropology*, *73*(1), 41–63.

Lockwood, C. A. (1999). Sexual dimorphism in the face of *Australopithecus africanus*. *American Journal of Physical Anthropology*, *108*(1), 97–127.

Lockwood, C. A., Jungers, W. L., & Kimbel, W. H. (1996). Randomization procedures and sexual dimorphism in *Australopithecus afarensis*. *Journal of Human Evolution*, *31*, 537–548.

Lockwood, C. A., Kimbel, W. H., & Johanson, D. C. (2000). Temporal trends and metric variation in the mandibles and dentition of *Australopithecus afarensis*. *Journal of Human Evolution*, *39*(1), 23–55.

Lockwood, C. A., & Tobias, P. V. (2002). Morphology and affinities of new hominin cranial remains from Member 4 of the Sterkfontein Formation, Gauteng Province, South Africa. *Journal of Human Evolution*, *42*(4), 389–450.

Lordkipanidze, D., Jashashvili, T., Vekua, A., Ponce de León, M. S., Zollikofer, C. P. E. P. E., Rightmire, G. P. P., … Bukhsiandidze, M. (2007). Postcranial evidence from early *Homo* from Dmanisi, Georgia. *Nature*, *449*(7160), 305–310..

Lordkipanidze, D., Ponce de León, M. S., Margvelashvili, A., Rak, Y., Rightmire, G. P., Vekua, A., & Zollikofer, C. P. E. (2013). A complete skull from Dmanisi, Georgia, and the evolutionary biology of early *Homo*. *Science (New York, N.Y.)*, *342*(6156), 326–31.

Manly, B. F. J. (2005). *Multivariate Statistical Methods. A primer - 3rd Edition*. Chapman & Hall/CRC.

Martinón-Torres, M., Bermúdez de Castro, J. M., Gómez-Robles, A., Margvelashvili, A., Prado, L., Lordkipanidze, D., & Vekua, A. (2008). Dental remains from Dmanisi (Republic of Georgia): Morphological analysis and comparative study. *Journal of Human Evolution*, *55*(2), 249–273.

Martinón-Torres, M., Bastir, M., Bermúdez de Castro, J. M., Gomez-Robles, A., Sarmiento, S., Muela, A., & Arsuaga, J. L. (2006). Hominin lower second premolar morphology: evolutionary inferences through geometric morphometric analysis. *Journal of Human Evolution*, *50*, 523–533.

Mayr, E. (1942). *Systematics and the origin of species*. New York: Columbia University Press.

Mayr, E. (1970). Populations, Species and Evolution. *Evolution*, –.

McHenry, H. M. (1983). The capitate of *Australopithecus afarensis* and *A. africanus*. *American Journal of Physical Anthropology*, *62*(2), 187–198.

Mitteroecker, P., Gunz, P., Bernhard, M., Schaefer, K., & Bookstein, F. L. (2004). Comparison of cranial ontogenetic trajectories among great apes and humans. *Journal of Human Evolution*, *46*(6), 679–698.

Mitteroecker, P., Gunz, P., Windhager, S., & Schaefer, K. (2013). A brief review of shape, form, and allometry in geometric morphometrics, with applications to human facial morphology. *Hystrix, the Italian Journal of Mammalogy*.

Moggi-Cecchi, J. (2003). The elusive "second species" in Sterkfontein Member 4: the dental metrical evidence. *South African Journal of Science*, *99*, 268–270.

Moggi-Cecchi, J., Menter, C., Boccone, S., & Keyser, A. (2010). Early hominin dental remains from the Plio-Pleistocene site of Drimolen, South Africa. *Journal of Human Evolution*, *58*, 374–405.

Moorrees, C. F., & Reed, R. B. (1954). Correlations among crown diameters of human teeth. *Archives of Oral Biology*, *9*, 685–697.

Navsa, N., & Thackeray, J. F. (1998). Morphometric Analyses of the Dentition of type specimens of *Australopithecus boisei* (OH 5) and *Homo habilis* (OH 7), compared with the type specimen of *Paranthropus (Australopithecus) robustus* (TM 1517). In M. A. Raath, H. Soodyall, D. Barkhan, K. . Kuykendall, & P. V. Tobias (Eds.), *Abstracts of contributions to the Dual Congress* (p. 134).

Nichol, J. E. (1999). Geomorphological evidence and Pleistocene refugia in Africa. *The Geographical Journal*, *165*(1), 79–89.

O'Higgins, P., & Dryden, I. L. (1993). Sexual dimorphism in hominoids: further studies of craniofacial shape differences in *Pan, Gorilla* and *Pongo*. *J Hum Evol*, *24*, 183–205.

Partridge, T. C., Shaw, J., Heslop, D., & Clarke, R. J. (1999). The new hominid skeleton from Sterkfontein, South Africa: age and preliminary assessment. *Journal of Quaternary Science*, *14*(4), 293–298.

Paterson, H. E. H. (1985). The Recognition Concept of Species. In E. S. Vrba (Ed.), *Speciation and its consequences* (Transvaal ., pp. 21–29). Pretoria: Transvaal Museum.

Pickering, R., & Kramers, J. D. (2010). Re-appraisal of the stratigraphy and determination of new U-Pb dates for the Sterkfontein hominin site, South Africa. *Journal of Human Evolution*, *59*(1), 70–86.

Pinhasi, R., Eshed, V., & Shaw, P. (2008). Evolutionary changes in the masticatory complex following the transition to farming in the southern Levant. *American Journal of Physical Anthropology*, *135*(2), 136–148.

Poulsen, J., & French, A. (2013). Discriminant Function Analysis (DA). *Course notes, San Francisco State University*.

Prüfer, K., Munch, K., Hellmann, I., Akagi, K., Miller, J. R., Walenz, B., … Pääbo, S. (2012). The bonobo genome compared with the chimpanzee and human genomes. *Nature*.

Rabenold, D., & Pearson, O. M. (2011). Abrasive, silica phytoliths and the evolution of thick molar enamel in primates, with implications for the diet of *Paranthropus boisei*. *PLoS ONE*, *6*(12).

Rak, Y., Ginzburg, A., & Geffen, E. (2007). Gorilla-like anatomy on *Australopithecus* mandibles suggests *Au. afarensis* link to robust australopiths. *Proceedings of the National Academy of Sciences of the United States of America*, *104*(16), 6568–6572.

Reno, P. L., McCollum, M. A., Meindl, R. S., & Lovejoy, C. O. (2010). An enlarged postcranial sample confirms *Australopithecus afarensis* dimorphism was similar to modern humans. *Philosophical Transactions of the Royal Society (Biological Sciences)*, *365*, 3355–3363.

Reno, P. L., Meindl, R. S., McCollum, M. A., & Lovejoy, C. O. (2003). Sexual dimorphism in *Australopithecus afarensis* was similar to that of modern humans. *Proceedings of the National Academy of Sciences of the United States of America*, *100*(16), 9404–9409.

Richmond, B. G., & Jungers, W. L. (1995). Size Variation and Sexual Dimorphism in *Australopithecus afarensis* and Living Hominoids. *Journal of Human Evolution*, *29*(3), 229–245.

Rightmire, G. P. (1980). Middle Pleistocene hominids from Olduvai Gorge, northern Tanzania. *American Journal of Physical Anthropology*, *53*(2), 225–241.

Rightmire, G. P. (1993). Variation among early *Homo* crania from Olduvai Gorge and the Koobi Fora region. *American Journal of Physical Anthropology*, *90*(1), 1–33.

Rightmire, G. P. (1996). The human cranium from Bodo, Ethiopia: evidence for speciation in the Middle Pleistocene. *Journal of Human Evolution*, *31*, 21–39.

Rightmire, G. P. (1998). Human evolution in the Middle Pleistocene: the role of *Homo heidelbergensis*. *Evolutionary Anthropology*, *6*(6), 218–227.

Rightmire, G. P., Van Arsdale, A. P., & Lordkipanidze, D. (2008). Variation in the mandibles from Dmanisi, Georgia. *Journal of Human Evolution*, *54*(6), 904–908.

Robinson, J. T. (1956). The dentition of the Australopithecinae. In *Transvaal Museum Memoir no. 9* (Vol. 9). Pretoria: Transvaal Museum.

Robinson, J. T. (1965). *Homo habilis* and the australopithecines. *Nature*, *205*, 121–124.

Robinson, J. T. (1966). The distinctiveness of *Homo habilis*. *Nature*, *209*, 957–960.

Rohlf, F. J., & Slice, D. (1990). Extensions of the Procrustes method for the optimal superimposition of landmarks. *Systematic Zoology*, *39*, 40–59.

Ryan, A. S., & Johanson, D. C. (1989). Anterior dental microwear in *Australopithecus afarensis*: comparisons with human and nonhuman primates. *Journal of Human Evolution*.

Scally, A., Dutheil, J., & Hillier, L. (2012). Insights into hominid evolution from the gorilla genome sequence. *Nature*, *483*(7388), 169–175.

Schmid, P. (1989). How different is Lucy? In J. Book (Ed.), *Proceedings of the Milan 2nd International Congress of Human Paleontology* (pp. 109–114).

Schwartz, J. H. (2000). Taxonomy of the Dmanisi crania. *Science*, *289*(55-56).

Scott, G. R., & Turner, C. G. (1997). *The Anthropology of Modern Human Teeth: Dental Morphology and Its Variation*. Cambridge University Press.

Shea, B. T. (1983). Allometry and heterochrony in the African apes. *American Journal of Physical Anthropology*, *62*(3), 275–289.

Silverman, N., Richmond, B. G., & Wood, B. (2001). Testing the Taxonomic Integrity of *Paranthropus boisei* sensu stricto. *American Journal of Physical Anthropology*, *115*, 167–178.

Simpson, G. G. (1961). *Principles of Animal Taxonomy*. New York: Columbia University Press.

Singleton, M., Rosenberger, A. L., Robinson, C., & O'neill, R. (2011). Allometric and Metameric Shape Variation in *Pan* Mandibular Molars: A Digital Morphometric Analysis. *Anatomical Record*, *294*(2), 322–334.

Skinner, M. (2008). *Enamel-dentine junction morphology of extant hominoid and fossil hominin lower molars*. *ProQuest Dissertations and Theses*. The George Washington University.

Skinner, M. M., Gordon, A. D., & Collard, N. J. (2006). Mandibular size and shape variation in the hominins at Dmanisi, Republic of Georgia. *Journal of Human Evolution*, *51*(1), 36–49.

Skinner, M. M., Gunz, P., Wood, B. A., & Hublin, J.-J. (2009). How many landmarks? Assessing classification accuracy of *Pan* lower molars using geometric morphometric analysis of the occlusal basin as seen at the EDJ. In T. Koppe, G. Meyer, & K. Alt (Eds.), *Comparative dental morphology* (pp. 23–29). Basel: Karger.

Skinner, M. M., Gunz, P., Wood, B. A., & Hublin, J.-J. J. (2008). Enamel-dentine junction (EDJ) morphology distinguishes the lower molars of *Australopithecus africanus* and *Paranthropus robustus*. *Journal of Human Evolution*, *55*(6), 979–988.

Skinner, M. M., Wood, B. A., Boesch, C., Olejniczak, A. J., Rosas, A., Smith, T. M., & Hublin, J.-J. (2008). Dental trait expression at the enamel-dentine junction of lower molars in extant and fossil hominoids. *Journal of Human Evolution*, *54*, 173–186.

Smith, H. F., & Grine, F. E. (2008). Cladistic analysis of early *Homo* crania from Swartkrans and Sterkfontein, South Africa. *Journal of Human Evolution*, *54*(5), 684–704.

Spoonheimer, M. (2013). Some Ruminations on Australopith Diets. In K. E. Reed, J. G. Fleagle, & R. E. Leakey (Eds.), *The Paleobiology of Australopithecus (Vertebrate Paleobiology and Paleoanthropology)* (pp. 225–233). Dordrecht: Springer Science + Business Media.

Stockburger, D. W. (2013). Multivariate Statistics: Concepts, Models and Applications - Discriminant Function Analysis. *Course notes, Missouri State University*.

Suwa, G., Afsaw, B., Beyene, Y., White, T. D., Katoh, S., Nagaoka, S., … WoldeGabriel, G. (1997). The first skull of *australopithecus boisei*. *Nature*, *389*(6650), 489–492.

Suwa, G., Wood, B. A., & White, T. D. (1994). Further analysis of mandibular molar crown and cusp areas in Pliocene and early Pleistocene hominids. *American Journal of Physical Anthropology*, *93*, 407–426.

Tattersall, I. (1986). Species recognition in human paleontology. *Journal of Human Evolution*, *15*, 165–176.

Tattersall, I., & Schwartz, J. (2009). Evolution of the Genus *Homo*. *Annu. Rev. Earth Planet. Sci.*

Teaford, M. F., & Ungar, P. S. (2000). Diet and the evolution of the earliest human ancestors. *Proceedings of the National Academy of Sciences of the United States of America*, *97*(25), 13506–13511.

Thackeray, J. F. (1997). Probabilities of Conspecificity. *Nature*, *390*(6655), 30–31.

Thackeray, J. F. (1998). Comparisons between the type specimens of *Paranthropus robustus* (TM 1517) and *Homo habilis* (OH 7). In M. A. Raath, H. Soodyall, D. Barkhan, K. L. Kuykendall, & P. V. Tobias (Eds.), *Abstracts of contributions to the Dual Congress* (p. 134).

Thackeray, J. F. (1999). Alternative views on hominid diversity in the context of Darwin's assessment of barnacles. In J. M. Anderson (Ed.), *Towards Gondwana Alive. Promoting Biodiversity and Stemming the Sixth Extinction* (pp. 106–109). National Botanical Institute, Gondwana Alive Society, Pretoria.

Thackeray, J. F. (2003). Comparison of hominid fossils attributed to *Australopithecus* and *Homo*. *South African Journal of Science*, *99*, 241–242.

Thackeray, J. F. (2005). Probabilities of conspecificity: an application of a morphometric approach to extant and extinct hominoids. In G. Strkalj, N. Pather, & B. Kramer (Eds.), *Voyages in Science. Essays by South African Anatomists in Honour of Phillip V. Tobias's 80th Birthday* (pp. 85–97). Content Solutions, Pretoria.

Thackeray, J. F. (2006). Reconceptualization of African hominins dated between 1.5 and 2.5 Mya. *Annals of the Transvaal Museum*, *43*, 116–117.

Thackeray, J. F. (2007a). Approximation of a biological species constant? *South African Journal of Science*, *103*, 489.

Thackeray, J. F. (2007b). Sexual dimorphism in early *Homo*. *South African Journal of Science*, *103*(7-8), 265.

Thackeray, J. F., Bellamy, C. L., Bellars, D., Bronner, G., Bronner, L., Chimimba, C., … Whiting, M. J. (1997). Probabilities of conspecificity: Application of a morphometric technique to modern taxa and fossil specimens attributed to *Australopithecus* and *Homo*. *S. Afr. J. Sci.*, *93*(4), 195–196.

Thackeray, J. F., Botha, R. & L'Abbé, L. (2005). Comparison of lower molars attributed to early *Homo* and *Paranthropus robustus*. *South African Journal of Science*, *101*, 488.

Thackeray, J. F., & Dykes, S. J. (2014). A biological species constant and a probabilistic definition of a species, based on morphometric analyses. *(under Review)*.

Thackeray, J. F., & L'Abbé, L. (2005). Comparison of lower molars attributed to early *Homo* and *Paranthropus robustus*. *South African Journal of Science, 101*, 488.

Thackeray, J. F., Mdaka, S., Navsa, N., Moshau, R., & Singo, S. (2000). Morphometric analyses of conspecific males and females: an exploratory study of extant primate and extinct hominid taxa. *South African Journal of Science, 96*, 534–536.

Thackeray, J. F., & Odes, E. (2013). Morphometric analysis of Early Pleistocene African hominin crania in the context of a statistical (probabilistic) definition of a species. *Antiquity*, *087*(335).

Thackeray, J. F., & Prat, S. (2009). Chimpanzee subspecies and "robust" australopithecine holotypes, in the context of comments by Darwin. *South African Journal of Science*, *105*(11-12), 463–464.

Tobias, P. V. (1964). The Olduvai Bed I hominine with special reference to its cranial capacity. *Nature*, *202*, 3–4. doi:10.1086/200627

Tobias, P. V. (1965). The early *Australopithecus* and *Homo* from Tanzania. *Anthropologie*, *3*, 43–48.

Tobias, P. V. (1973). Implications of the new age estimates of the early South African hominids. *Nature*, *246*(5428), 79–83.

Tobias, P. V. (1978). South African australopithecines in time and hominid phylogeny, with special reference to dating and affinities of the Taung skull. In C. J. Jolly (Ed.), *Early hominids of Africa* (pp. 45–84). London: Duckworth.

Tobias, P. V. (1967). *The cranium and maxillary dentition of Australopithecus (Zinjanthropus) boisei*. Cambridge: Cambridge University Press.

Ungar, P. (2004). Dental topography and diets of *Australopithecus afarensis* and early *Homo*. *Journal of Human Evolution*, *46*(5), 605–622.

Van Arsdale, A. P., & Lordkipanidze, D. (2012). A quantitative assessment of mandibular variation in the Dmanisi hominins. *PaleoAnthropology*, *2012*(134-144).

Van Arsdale, A. P., & Wolpoff, M. H. (2013). A single lineage in early Pleistocene *Homo*: size variation continuity in early Pleistocene *Homo* crania from East Africa and Georgia. *Evolution; International Journal of Organic Evolution*, *67*(3), 841–50.

Van Gerven, D. P. (1972). The contribution of size and shape variation to patterns of sexual dimorphism of the human femur. *American Journal of Physical Anthropology*, *37*(1), 49–60.

Vervaecke, H., Jeroen Stevens, & Elsacker, L. Van. (2004). *Pan* Continuity: Bonobo-Chimpanzee Hybrids . *Folia Primatol*, *75*, 59.

White, T. D. (1977). New fossil hominids from Laetolil, Tanzania. *American Journal of Physical Anthropology*, *46*(2), 197–229.

White, T. D., & Johanson, D. C. (1982). Pliocene hominid mandibles from the Hadar Formation, Ethiopia: 1974-77 collections. *American Journal of Physical Anthropology*, *57*, 501–544.

Williamson, S. H., Hubisz, M. J., Clark, A. G., Payseur, B. A., Bustamante, C. D., & Nielsen, R. (2007). Localizing recent adaptive evolution in the human genome. *PLoS Genetics*, *3*(6), 0901–0915.

Wolpoff, M. H. (1971). Competitive exclusion among lower Pleistocene hominids: the single species hypothesis. *Man*, *6*(4), 601–14.

Wolpoff, M. H. (1973). Posterior tooth size, body size, and diet in South African gracile Australopithecines. *American Journal of Physical Anthropology*, *39*(3), 375–393.

Wolpoff, M. H. (1996). *Human Evolution (1996 Edition)* (1996th ed.). New York: McGraw-Hill.

Wolpoff, M. H., & Lee, S.-H. (2001). The late Pleistocene human species of Israel. *Bulletins et Memoirs de La Societe d'Anthroplogie de Paris*, *13*, 291–310.

Wood, B. (1991). *Koobi Fora Research Project, Volume 4, Hominid Cranial Remains.* Clarendon Press, Oxford.

Wood, B. (1992). Origin and evolution of the genus *Homo*. *Nature*, *355*(6363), 783–790.

Wood, B. (1996). Human evolution. *Bioessays*, *18*(12), 945–954.

Wood, B. (Ed.). (2011). *Wiley-Blackwell Encyclopedia of Human Evolution*. Blackwell Publishing Ltd.

Wood, B. A., & Abbott, S. A. (1983). Analysis of the dental morphology of Plio-pleistocene hominids. I. Mandibular molars: crown area measurements and morphological traits. *Journal of Anatomy*, *136*(Pt 1), 197–219.

Wood, B. A., Abbott, S. A., & Graham, S. H. (1983). Analysis of the dental morphology of Plio-Pleistocene hominids. II. Mandibular molars--study of cusp areas, fissure pattern and cross sectional shape of the crown. *Journal of Anatomy*, *137 (Pt 2)*, 287–314.

Wood, B. A., & Engleman, C. A. (1988). Analysis of the dental morphology of Plio-Pleistocene hominids. V. Maxillary postcanine tooth morphology. *Journal of Anatomy*, *161*, 1–35.

Wood, B. A., & Gordon, A. D. (n.d.). Human Origins Database. *www.humanoriginsdatabase.org*.

Wood, B. A., Li, Y., & Willoughby, C. (1991). Intraspecific variation and sexual dimorphism in cranial and dental variables among higher primates and their bearing on the hominid fossil record. *Journal of Anatomy*, *174*, 185–205.

Wood, B. A., & Uytterschaut, H. (1987). Analysis of the dental morphology of Plio-Pleistocene hominids. III. Mandibular premolar crowns. *Journal of Anatomy*, *154*, 121–156.

Wood, B., & Baker, J. (2011). Evolution in the Genus *Homo*. *Annual Review of Ecology Evolution and Systematics*, *42*(1), 47–69.

Wood, B., & Collard, M. (1999). The human genus. *Science (New York, N.Y.)*, *284*(5411), 65–71.

Wright, S. (1940). The statistical consequences of Mendelian heredity in relation to speciation. In J. Huxley (Ed.), *The New Systematics* (pp. 161–183). Oxford University Press.

Zelditch, M. L., Swiderski, D. L., Sheets, H. D., & Fink, W. L. (2004). *Geometric Morphometrics for Biologists : A Primer.* San Diego: Elsevier Academic Press.

APPENDICES

Appendix 1 Reference size data for fossil hominin mandibular first molars

Average mesiodistal and buccolingual diameters of *Australopithecus afarensis* lower first molar specimens

	Mesiodistal diameter	Buccolingual diameter	Source
Mean diameter	13.0 mm	12.3 mm	Alemseged et al., 2005
Minimum	10.1 mm	11.0 mm	Alemseged et al., 2005
Maximum	14.8 mm	14.8 mm	Alemseged et al., 2005

Mesiodistal and buccolingual diameters of *Australopithecus africanus* M_1 specimens

Specimen N°, side	Mesiodistal diameter	Buccolingual diameter	Source
Taung 1, left	13.3 mm	13.3 mm	Human Origins Database
Taung 1, right	13.4 mm	13.0 mm	Human Origins Database
Sts 52b, right	13.8 mm	13.2 mm	Human Origins Database
MLD 2, left	14.8 mm	14.1 mm	Human Origins Database
MLD 2, right	14.7 mm	13.9 mm	Human Origins Database

Mesiodistal and buccolingual diameters of *Homo habilis* and *Homo rudolfensis* M_1 specimens

Specimen N°, side	Mesiodistal diameter	Buccolingual diameter	Source
OH 7, left	14.1 mm	12.5 mm	Human Origins Database
OH 7, right	14.3 mm	12.6 mm	Human Origins Database
OH 16, right	14.6 mm	12.8 mm	Human Origins Database
KNM-ER 1802, left	14.9 mm	13.2 mm	Human Origins Database
KNM-ER 1802, right	14.8 mm	13.0 mm	Human Origins Database

Mesiodistal and buccolingual diameters of *Homo erectus* M_1 specimens

Specimen N°, side	Mesiodistal diameter	Buccolingual diameter	Source
KNM-ER 992, left	12.7 mm	10.9 mm	Human Origins Database
KNM-ER 992, right	12.5 mm	10.9 mm	Human Origins Database

OH 22, right	13.4 mm	12.0 mm	Human Origins Database
KNM-ER 820, left	12.5 mm	10.6 mm	Human Origins Database
KNM-ER 820, right	12.5 mm	10.7 mm	Human Origins Database
KNM-ER 806c, left	14.2 mm	12.5 mm	Human Origins Database

Mesiodistal and buccolingual diameters of *Paranthropus robustus* and *boisei* M_1 specimens

Specimen N°, side	Mesiodistal diameter	Buccolingual diameter	Source
Peninj 1, left	16.6 mm	15.4 mm	Human Origins Database
Peninj 1, right	16.4 mm	15.5 mm	Human Origins Database
KNM-ER 15930, left	14.6 mm	12.8 mm	Human Origins Database
SK 6, left	16.7 mm	15.5 mm	Human Origins Database
SK 6, right	16.7 mm	14.8 mm	Human Origins Database
SK 23, left	15.2 mm	14.8 mm	Human Origins Database
SK 23, right	15.0 mm	14.7 mm	Human Origins Database
TM 1517, right	14.8 mm	13.2 mm	Human Origins Database
SKW 5, right	13.6 mm	13.2 mm	Grine & Daegling 1993

Appendix 2 Photographic protocols

The tripod used the facility of allowing the camera to be mounted beneath its apex, between the legs of the tripod, with the lens oriented vertically downwards towards the specimen. The verticality of the lens could be checked via two spirit levels built into the tripod camera mounting apparatus. The tripod was devoid of any side struts that could hinder the placement of specimens beneath it and the angle of the legs was adjustable to allow for larger or smaller specimens to fit beneath the lens of the camera. Where an adjustable camera stand was available, a choice was made as to which option provided the most flexibility (ease of focus, ease of positioning of specimens (especially of delicate fossil specimens), stability, etc.). In both cases (tripod or purpose-built adjustable camera stand), the length of the optical axis of the camera from the lens to the surface of the specimen below it was measured at about 12cm, and from this distance, individual minute focussing changes could be made for each shot. All shots were taken with both focus and aperture set manually.

The scale bar was mounted on a custom-designed small platform attached via a firm flexi-wire arm to an adjustable bracket on an upright cylinder. The bracket allowed for general height adjustments while the flexi-wire platform allowed for minute adjustments of height, angle and position relative to the specimen. The scale bar was always levelled according to the occlusal surface level of the molar being photographed and this was squared, where possible, with the mesiodistal axis of the tooth.

Lighting was provided using two adjustable halogen lamps. Photographs of each specimen were taken using different exposure settings on the camera (exposure

compensation settings of 0, -0.3, -0.7, -1.0, -1.3, -1.7, -2.0) in both ambient light and artificial light. Variable lighting ensured that any diagnostic traits visible on the tooth would be observably maximised in at least one of the shots taken. "Normal exposure to under-exposure" was chosen for the range of light settings, since an under-exposed photograph can be manipulated digitally using Photoshop or another photographic editing programme to enhance the features required for analysis, whereas any photograph that is over-exposed will have those features "whited out" and no amount of editing after the event will restore those features to view.

Photographs were shot using an infrared remote control device to ensure minimisation of camera shake and noise from table vibrations related to any manual operation of the camera.

All teeth were positioned in such a way that the cervical line of the tooth (the cemento-enamel junction – where the crown meets root of the tooth) was horizontal and thus directly perpendicular to the axis of the focus of the lens (oriented vertically downwards).

Appendix 3 Principal Components Analyses: output data

PCA – Fossil specimens

PC	Eigenvalue	% variance	% cumulative	Brief description of variance
PC 1	0.011	72.500	72.500	Size; C_6 cusp absence/presence
PC 2	0.002	10.800	83.300	Cusp skewness
PC 3	0.001	4.040	87.340	Tooth width; buccal/lingual cusps

PC1: Centroid size regression – Correlation coefficient

R Square	0.982521

PCA – Fossil specimens plus bonobo outgroup

PC	Eigenvalue	% variance	% cumulative	Brief description of variance
PC 1	0.036	90.400	90.400	Size; C_6 cusp absence/presence
PC 2	0.043	4.340	94.800	Cusp skewness
PC 3	0.000	1.200	96.000	Tooth width; buccal/lingual cusps

PC1: Centroid size regression – Correlation coefficient

R Square	0.994428

PCA – Fossil specimens plus chimpanzee outgroup

PC	Eigenvalue	% variance	% cumulative	Brief description of variance
PC 1	0.0178	81.9	81.9	Size; C_6 cusp absence/presence
PC 2	0.00182	8.4	90.3	Cusp skewness
PC 3	0.000499	2.3	92.6	Tooth width; buccal/lingual cusps

PC1: Centroid size regression – Correlation coefficient

R Square	0.996023

PCA – Fossil specimens plus gorilla outgroup

PC	Eigenvalue	% variance	% cumulative	Brief description of variance
PC 1	0.010	67.000	67.000	Size; C_6 cusp absence/presence
PC 2	0.002	14.200	81.200	Tooth width; buccal/lingual cusps
PC 3	0.001	0.069	81.269	Cusp skewness

PC1: Centroid size regression – Correlation coefficient

R Square	0.991945

PCA – Fossil specimens plus modern human outgroup

PC	Eigenvalue	% variance	% cumulative	Brief description of variance
PC 1	0.015	77.900	77.900	Size; C_6 cusp absence/presence
PC 2	0.002	8.070	85.970	Cusp skewness
PC 3	0.001	3.250	89.220	Tooth width; buccal/lingual cusps

PC1: Centroid size regression – Correlation coefficient

R Square	0.995467

PCA – Fossil specimens plus four extant species

PC	Eigenvalue	% variance	% cumulative	Brief description of variance
PC 1	0.026	87.000	87.000	Size; C_6 cusp absence/presence
PC 2	0.001	4.020	91.020	Cusp skewness
PC 3	0.001	3.410	94.430	Tooth width; buccal/lingual cusps

PC1: Centroid size regression – Correlation coefficient

R Square	0.993224

Appendix 4 Procrustes Distance Matrix – 36 fossil specimens

Procrustes distance matrix	AL145-35L	AL228-23R	AL266-1L	AL266-1R	AL288-1R	AL333-W6L	LH2R	LH4L	LH4R	MLD2L	MLD2R	Sts52iR	Taung1L	Taung1R	OH22R	KNM-ER806	KNM-ER806	KNM-ER892	KNM-ER892	OH7L	OH7R	OH16R	KNM-ER1813	KNM-ER1813	PeninJ1L	PeninJ1R	SK6L	SK6R	SK23L	SK23R	SK63L	SK63R	SKW5R	TM1517R
AL145-35L	0.09970	0.13502	0.14016	0.16290	0.14062	0.10104	0.10164	0.11570	0.16710	0.14987	0.12830	0.12960	0.13657	0.12903	0.14315	0.17646	0.13657	0.12862	0.11530	0.12276	0.14444	0.12697	0.12621	0.12506	0.10392	0.10542	0.12463	0.11382	0.09069	0.07600	0.10654	0.10267	0.10990	0.10284
AL228-23R	0.09970	0.08792	0.13310	0.14429	0.11906	0.07490	0.08345	0.08551	0.12833	0.12647	0.08079	0.09198	0.07693	0.11052	0.09272	0.13570	0.10220	0.09215	0.11005	0.10855	0.13651	0.08903	0.09732	0.09464	0.08823	0.07710	0.09494	0.10250	0.09291	0.09154	0.11716	0.10652	0.10520	0.07859
AL266-1L	0.13502	0.08792	0.07574	0.08385	0.06662	0.06393	0.10726	0.06430	0.07401	0.06826	0.05211	0.08537	0.09754	0.07898	0.06825	0.06922	0.07126	0.05320	0.05289	0.08398	0.07522	0.08791	0.05758	0.08460	0.15072	0.11623	0.08656	0.11292	0.11403	0.12435	0.11217	0.12275	0.14257	0.11183
AL266-1R	0.14016	0.13310	0.07574	0.08063	0.06013	0.09517	0.13028	0.07345	0.08640	0.04974	0.07499	0.12104	0.13659	0.10504	0.09694	0.09883	0.09189	0.09034	0.08927	0.10599	0.09391	0.07858	0.13087	0.09009	0.11425	0.18327	0.15140	0.11182	0.14121	0.13143	0.13854	0.11802	0.15088	0.17581	0.14837
AL288-1R	0.16290	0.14429	0.08185	0.08063	0.07583	0.09011	0.13801	0.10412	0.06675	0.05612	0.08028	0.10926	0.13099	0.07688	0.10334	0.07630	0.08451	0.08446	0.07065	0.04527	0.12022	0.07876	0.08278	0.18338	0.14702	0.10661	0.12617	0.13590	0.15127	0.11517	0.13856	0.16921	0.14524
AL333-W6DL	0.14062	0.11806	0.06662	0.06013	0.07583	0.09266	0.10712	0.06384	0.04581	0.06665	0.10388	0.12259	0.08791	0.09903	0.09936	0.08297	0.08968	0.08853	0.11045	0.09413	0.07058	0.12362	0.08579	0.08808	0.17505	0.13414	0.09697	0.13078	0.12518	0.12956	0.12065	0.14534	0.15883	0.14122
LH2R	0.10104	0.07490	0.06393	0.09517	0.09011	0.09266	0.07571	0.09758	0.08546	0.06653	0.08435	0.08018	0.06637	0.07785	0.06146	0.09434	0.05601	0.05352	0.05352	0.04646	0.07692	0.07171	0.05510	0.06624	0.11481	0.09163	0.07190	0.08105	0.07944	0.09200	0.07564	0.07993	0.10932	0.08098
LH4L	0.10164	0.08345	0.10726	0.13028	0.13801	0.10712	0.08866	0.08426	0.12097	0.12186	0.10276	0.10057	0.09685	0.10266	0.11206	0.12278	0.14111	0.11086	0.10775	0.10562	0.10635	0.12624	0.09999	0.10663	0.09078	0.11863	0.08965	0.09930	0.10553	0.09260	0.09084	0.11174	0.10696	0.09709	0.09835
LH4R	0.11570	0.08551	0.06430	0.07245	0.10412	0.06384	0.07571	0.08426	0.08542	0.06961	0.05620	0.10045	0.10988	0.08710	0.07744	0.09307	0.09745	0.07688	0.07093	0.09669	0.08935	0.09438	0.09609	0.07712	0.09679	0.14842	0.11538	0.09702	0.12469	0.10710	0.10946	0.11238	0.12960	0.14114	0.11477
MLD2L	0.16710	0.12833	0.07401	0.08640	0.06675	0.06242	0.09758	0.12097	0.08542	0.04845	0.06866	0.10593	0.12537	0.07180	0.10555	0.09129	0.05705	0.07730	0.08713	0.10528	0.08266	0.07842	0.11070	0.08302	0.09405	0.18748	0.14537	0.10449	0.13642	0.14047	0.15276	0.13380	0.15147	0.16742	0.14855
MLD2R	0.14987	0.12647	0.06826	0.04974	0.05612	0.04581	0.08546	0.12186	0.06961	0.04845	0.06121	0.10949	0.12850	0.07588	0.09629	0.08258	0.06044	0.07419	0.07706	0.09610	0.07622	0.05901	0.11682	0.07785	0.09365	0.18143	0.14441	0.10051	0.13336	0.12986	0.13969	0.11645	0.14429	0.16778	0.14397
Sts52iR	0.12830	0.08879	0.05211	0.07499	0.08028	0.06665	0.06653	0.10276	0.05620	0.06866	0.06121	0.08295	0.09716	0.07203	0.06799	0.07864	0.07646	0.06374	0.08543	0.07095	0.08287	0.08796	0.05498	0.08559	0.14928	0.11145	0.08292	0.11355	0.10795	0.11597	0.11002	0.12571	0.14592	0.11217
Taung1L	0.12860	0.09198	0.08537	0.12104	0.10926	0.10388	0.08435	0.10057	0.10593	0.10949	0.08295	0.04641	0.10409	0.08548	0.10936	0.11693	0.09521	0.09905	0.10377	0.09396	0.10691	0.10717	0.09330	0.07592	0.11008	0.07019	0.04983	0.06548	0.08131	0.09588	0.08654	0.09054	0.10192	0.08045
Taung1R	0.13657	0.07693	0.08791	0.13099	0.12159	0.08018	0.09685	0.10988	0.12537	0.12850	0.09716	0.04641	0.11074	0.08979	0.11706	0.13604	0.10580	0.10607	0.10533	0.09992	0.12398	0.10224	0.10054	0.09485	0.08667	0.05279	0.05470	0.05136	0.06319	0.07611	0.08047	0.07127	0.07973	0.06142
OH22R	0.13657	0.11052	0.07898	0.10504	0.07688	0.08791	0.06637	0.10266	0.08710	0.07180	0.07588	0.07203	0.10409	0.11074	0.09205	0.05501	0.06567	0.06292	0.05505	0.06075	0.05122	0.07243	0.06509	0.04900	0.07723	0.15217	0.11917	0.08693	0.11285	0.11670	0.12397	0.10796	0.11243	0.13594	0.11362
KNM-ER806cL	0.12993	0.09272	0.06825	0.09694	0.11039	0.09503	0.07785	0.11206	0.07744	0.10555	0.09629	0.06799	0.08548	0.08979	0.09205	0.05501	0.07551	0.06796	0.06867	0.08614	0.10708	0.08467	0.06582	0.10491	0.13053	0.09729	0.08408	0.10315	0.09539	0.10226	0.10011	0.11013	0.13654	0.08990
KNM-ER820L	0.14315	0.11053	0.06922	0.09883	0.07455	0.09936	0.06146	0.12278	0.09307	0.09129	0.08258	0.07864	0.10936	0.11706	0.05501	0.08418	0.06191	0.04301	0.03699	0.07242	0.06237	0.05910	0.07242	0.04682	0.08002	0.15086	0.12369	0.10090	0.11432	0.12199	0.13368	0.10783	0.11410	0.14618	0.11067
KNM-ER820R	0.17646	0.13770	0.07126	0.09188	0.05644	0.08297	0.09434	0.14111	0.09745	0.05705	0.06044	0.07646	0.11693	0.13604	0.06567	0.09750	0.06191	0.04301	0.06020	0.06878	0.09475	0.07717	0.06486	0.10370	0.06870	0.09794	0.18830	0.15155	0.11461	0.14151	0.14875	0.16205	0.13406	0.14983	0.17612	0.14659
KNM-ER992L	0.13657	0.10220	0.05520	0.09034	0.07630	0.08968	0.05601	0.11086	0.07688	0.10777	0.07419	0.06374	0.09521	0.10580	0.05292	0.07551	0.04301	0.06020	0.02956	0.05699	0.04613	0.07321	0.06131	0.03552	0.08523	0.14757	0.12020	0.09734	0.11057	0.11652	0.12880	0.10324	0.11182	0.13677	0.11427
KNM-ER992R	0.12862	0.09215	0.05289	0.08927	0.08451	0.08853	0.05352	0.10775	0.07093	0.08713	0.07706	0.06024	0.09905	0.10607	0.05505	0.06796	0.03699	0.06878	0.02956	0.06140	0.05810	0.08098	0.05867	0.03258	0.08515	0.14170	0.11489	0.09776	0.11152	0.11384	0.12135	0.10513	0.11183	0.13724	0.09959
OH7L	0.11530	0.10005	0.08338	0.10599	0.08846	0.11045	0.05352	0.10562	0.09669	0.10528	0.09610	0.08543	0.10377	0.10533	0.06075	0.08867	0.06237	0.09475	0.05699	0.06140	0.03333	0.08227	0.06446	0.05356	0.08562	0.12933	0.11112	0.09836	0.09476	0.09834	0.11006	0.08193	0.08647	0.12105	0.09294
OH7R	0.12376	0.10855	0.07522	0.09391	0.07065	0.09413	0.04646	0.10635	0.08935	0.08266	0.07622	0.07095	0.09396	0.09992	0.05122	0.08614	0.05910	0.07717	0.04613	0.05810	0.03333	0.06539	0.07287	0.04867	0.07772	0.13952	0.11424	0.08755	0.09450	0.09990	0.11514	0.08283	0.09405	0.12677	0.10171
OH16R	0.14444	0.13261	0.07927	0.07858	0.04527	0.07058	0.07692	0.12624	0.09438	0.07842	0.05901	0.08287	0.10691	0.12398	0.07243	0.10708	0.07242	0.06486	0.07321	0.08098	0.08227	0.06539	0.11728	0.07619	0.07369	0.16706	0.13547	0.09639	0.11848	0.12276	0.13419	0.10045	0.12346	0.15283	0.13378
KNM-ER1802L	0.12697	0.08903	0.08791	0.13087	0.12022	0.12362	0.07171	0.09999	0.09609	0.11070	0.11682	0.08796	0.10717	0.10224	0.06509	0.08467	0.07287	0.10370	0.06131	0.05867	0.06446	0.07287	0.11728	0.05592	0.10001	0.12599	0.10515	0.11354	0.11111	0.11430	0.11923	0.11697	0.10525	0.12049	0.08710
KNM-ER1802R	0.12621	0.09732	0.05758	0.09009	0.07876	0.08579	0.05510	0.10663	0.07712	0.08302	0.07785	0.05498	0.09330	0.10054	0.04900	0.06382	0.04682	0.06870	0.03552	0.03258	0.05356	0.04967	0.07619	0.05592	0.08174	0.13974	0.10916	0.09324	0.10461	0.10866	0.11604	0.10083	0.10829	0.13449	0.09744
KNM-ER1590L	0.12506	0.09464	0.08460	0.11425	0.08278	0.08808	0.06624	0.09078	0.09679	0.09405	0.09365	0.08559	0.07592	0.08485	0.07723	0.10491	0.08002	0.09794	0.08523	0.08515	0.08562	0.07772	0.07369	0.10001	0.08174	0.12251	0.08542	0.06715	0.07954	0.09418	0.10584	0.09241	0.09517	0.10975	0.09624
PeninJ1L	0.10392	0.09823	0.15072	0.18327	0.18338	0.17505	0.11481	0.18634	0.14942	0.18748	0.18143	0.14928	0.11008	0.08667	0.15217	0.13053	0.15086	0.18330	0.14757	0.14170	0.12933	0.13952	0.14706	0.13974	0.12599	0.13974	0.12251	0.08542	0.06715	0.09418	0.08323	0.07363	0.04453	0.07202	0.06835	0.07400	0.06835	0.05507
PeninJ1R	0.10542	0.09464	0.08460	0.11425	0.08278	0.08808	0.06624	0.09078	0.09679	0.09405	0.09365	0.08559	0.07592	0.08485	0.07723	0.10491	0.08002	0.09794	0.08523	0.08515	0.08562	0.07772	0.07369	0.10001	0.08174	0.12251	0.08542	0.06715	0.07954	0.09418	0.10584	0.09241	0.09517	0.10975	0.09624	0.07400	0.06835	0.05507
SK6L	0.12463	0.10250	0.11292	0.14121	0.12617	0.13078	0.08105	0.10553	0.12469	0.13642	0.13336	0.11355	0.06548	0.05136	0.11285	0.10155	0.11432	0.14151	0.11057	0.11152	0.09476	0.09450	0.11848	0.11111	0.10461	0.07954	0.08282	0.05917	0.07268	0.06336	0.06150	0.05478	0.07363	0.05717	0.04669	0.07288	0.06185	0.05672
SK6R	0.11382	0.10250	0.11292	0.14121	0.12617	0.13078	0.08105	0.10553	0.12469	0.13642	0.13336	0.11355	0.06548	0.05136	0.11285	0.10155	0.11432	0.14151	0.11057	0.11152	0.09476	0.09450	0.11848	0.11111	0.10461	0.07954	0.08282	0.05917	0.07268	0.06336	0.06150	0.05478	0.07363	0.05717	0.04669	0.07288	0.06185	0.05672
SK23L	0.09069	0.09291	0.11403	0.13143	0.13590	0.12518	0.07944	0.09260	0.10710	0.14047	0.12986	0.10795	0.08131	0.06359	0.12199	0.14875	0.11652	0.11384	0.09834	0.12276	0.11430	0.10866	0.09418	0.08393	0.05818	0.06150	0.05478	0.04453	0.05671	0.05808	0.07939	0.06672	0.06672	0.07868	0.06868	0.06699	0.07288	0.06612
SK23R	0.07600	0.09154	0.12435	0.13854	0.15127	0.12956	0.09200	0.09084	0.10946	0.15276	0.13969	0.11597	0.09588	0.07611	0.12397	0.10226	0.13968	0.16205	0.12880	0.12135	0.11006	0.11514	0.13419	0.11923	0.11604	0.10584	0.07820	0.06185	0.08323	0.07363	0.04453	0.07102	0.07067	0.08005	0.06868	0.07288	0.06185	0.05672
SK63L	0.10654	0.11716	0.11217	0.11802	0.11517	0.12065	0.07564	0.11174	0.11238	0.13380	0.11645	0.11002	0.08654	0.08347	0.10796	0.10011	0.10783	0.13406	0.10324	0.10513	0.08193	0.08283	0.10045	0.11697	0.10083	0.09241	0.10486	0.08920	0.06761	0.05717	0.05671	0.07102	0.05512	0.09221	0.07868	0.06178	0.05692	0.06612
SK63R	0.10267	0.10652	0.12275	0.15088	0.13856	0.14534	0.07993	0.10696	0.12960	0.15147	0.14429	0.12571	0.09054	0.07127	0.11243	0.11013	0.11410	0.14983	0.11183	0.08647	0.09405	0.12346	0.10525	0.10829	0.09517	0.07400	0.07104	0.08001	0.04669	0.05808	0.07067	0.05512	0.06178	0.05692	0.06612
SKW5R	0.10990	0.10520	0.14257	0.17581	0.16921	0.15883	0.10932	0.09709	0.14114	0.16742	0.16778	0.14592	0.10192	0.07973	0.13534	0.13654	0.14618	0.17612	0.13677	0.13724	0.12105	0.12677	0.15283	0.12049	0.13449	0.10975	0.06835	0.06997	0.10358	0.07288	0.07939	0.08005	0.09221	0.06178	0.06612
TM1517R	0.10284	0.07859	0.11183	0.14837	0.14524	0.14122	0.08098	0.08835	0.11477	0.14855	0.14397	0.11217	0.08045	0.06142	0.11362	0.08990	0.11067	0.14659	0.10427	0.09959	0.09294	0.10171	0.13378	0.08710	0.09744	0.09624	0.05507	0.04872	0.08482	0.06099	0.06672	0.06868	0.07868	0.05692	0.06612

Appendix 5 Log se_m matrices for four extant species

Bonobo-bonobo pairwise comparisons – 20 x 20 log se_m matrix

	11354_M_L	11354_M_R	13201_F_L	13201_F_R	29026_F_L	29026_F_R	29027_F_L	29027_F_R	29028_M_L	29028_M_R	29050_M_L	29050_M_R	29053_M_L	29053_M_R	29055_F_L	29055_F_R	84036M03_M_L	84036M03_M_R	84036M11_F_L	84036M11_F_R
11354_M_L		-1,534	-1,692	-1,427	-1,647	-1,775	-1,640	-1,507	-1,499	-1,602	-1,712	-1,561	-1,570	-1,608	-1,648	-1,767	-1,576	-1,545	-1,572	-1,582
11354_M_R	-1,516		-1,643	-1,536	-1,451	-1,516	-1,472	-1,572	-1,617	-1,550	-1,521	-1,597	-1,518	-1,511	-1,559	-1,520	-1,629	-1,732	-1,468	-1,426
13201_F_L	-1,704	-1,673		-1,538	-1,648	-1,738	-1,662	-1,683	-1,578	-1,613	-1,707	-1,722	-1,624	-1,757	-1,678	-1,731	-1,849	-1,801	-1,531	-1,527
13201_F_R	-1,439	-1,567	-1,539		-1,412	-1,407	-1,395	-1,442	-1,439	-1,393	-1,475	-1,520	-1,566	-1,515	-1,421	-1,388	-1,598	-1,487	-1,311	-1,364
29026_F_L	-1,687	-1,509	-1,676	-1,440		-1,755	-1,679	-1,651	-1,555	-1,605	-1,706	-1,531	-1,601	-1,644	-1,689	-1,781	-1,583	-1,559	-1,541	-1,492
29026_F_R	-1,848	-1,607	-1,799	-1,468	-1,788		-1,736	-1,643	-1,626	-1,756	-1,726	-1,662	-1,640	-1,749	-1,795	-1,909	-1,678	-1,655	-1,608	-1,554
29027_F_L	-1,749	-1,598	-1,758	-1,491	-1,747	-1,771		-1,592	-1,539	-1,637	-1,716	-1,642	-1,605	-1,637	-1,610	-1,734	-1,641	-1,654	-1,595	-1,520
29027_F_R	-1,612	-1,695	-1,777	-1,535	-1,717	-1,675	-1,589		-1,750	-1,679	-1,721	-1,604	-1,609	-1,710	-1,742	-1,705	-1,699	-1,692	-1,531	-1,490
29028_M_L	-1,599	-1,735	-1,666	-1,526	-1,615	-1,653	-1,531	-1,745		-1,795	-1,610	-1,527	-1,588	-1,609	-1,713	-1,615	-1,606	-1,640	-1,493	-1,451
29028_M_R	-1,726	-1,693	-1,725	-1,505	-1,689	-1,808	-1,654	-1,698	-1,820		-1,683	-1,572	-1,619	-1,654	-1,821	-1,751	-1,631	-1,681	-1,590	-1,528
29050_M_L	-1,801	-1,628	-1,783	-1,552	-1,755	-1,742	-1,696	-1,705	-1,598	-1,648		-1,662	-1,668	-1,715	-1,767	-1,780	-1,685	-1,643	-1,589	-1,581
29050_M_R	-1,640	-1,693	-1,788	-1,586	-1,570	-1,668	-1,612	-1,578	-1,506	-1,526	-1,652		-1,667	-1,665	-1,629	-1,644	-1,798	-1,737	-1,551	-1,555
29053_M_L	-1,673	-1,639	-1,715	-1,657	-1,664	-1,670	-1,600	-1,607	-1,591	-1,598	-1,683	-1,692		-1,760	-1,660	-1,650	-1,697	-1,603	-1,494	-1,555
29053_M_R	-1,683	-1,604	-1,820	-1,578	-1,679	-1,751	-1,604	-1,680	-1,584	-1,604	-1,702	-1,661	-1,731		-1,709	-1,742	-1,738	-1,617	-1,482	-1,535
29055_F_L	-1,739	-1,668	-1,757	-1,500	-1,740	-1,814	-1,593	-1,728	-1,705	-1,788	-1,770	-1,641	-1,648	-1,725		-1,896	-1,647	-1,669	-1,669	-1,633
29055_F_R	-1,850	-1,622	-1,802	-1,460	-1,825	-1,920	-1,710	-1,684	-1,599	-1,710	-1,775	-1,649	-1,630	-1,751	-1,888		-1,656	-1,661	-1,678	-1,621
84036M03_M_L	-1,680	-1,751	-1,941	-1,689	-1,647	-1,709	-1,637	-1,698	-1,610	-1,611	-1,700	-1,823	-1,698	-1,767	-1,660	-1,677		-1,873	-1,515	-1,532
84036M03_M_R	-1,646	-1,851	-1,890	-1,576	-1,621	-1,683	-1,647	-1,688	-1,642	-1,658	-1,655	-1,760	-1,601	-1,643	-1,679	-1,678	-1,871		-1,582	-1,517
84036M11_F_L	-1,734	-1,648	-1,681	-1,461	-1,663	-1,698	-1,649	-1,589	-1,556	-1,628	-1,662	-1,634	-1,553	-1,569	-1,740	-1,757	-1,574	-1,643		-1,829
84036M11_F_R	-1,756	-1,618	-1,690	-1,526	-1,627	-1,656	-1,586	-1,560	-1,526	-1,578	-1,666	-1,651	-1,626	-1,634	-1,717	-1,712	-1,602	-1,591	-1,841	

Chimpanzee-chimpanzee pairwise comparisons – 20 x 20 log se_m matrix

	83006M15_M_L	83006M15_M_R	83006M17_M_L	83006M17_M_R	83006M21_M_L	83006M21_M_R	83006M22_M_L	83006M22_M_R	83006M32_F_L	83006M32_F_R	83006M37_F_L	83006M37_F_R	91060M406_F_L	91060M406_F_R	91060M410_F_L	91060M410_F_R	91060M414_M_L	91060M414_M_R	91060M422_F_L	91060M422_F_R
83006M15_M_L		-1,609	-1,564	-1,587	-1,765	-1,638	-1,604	-1,701	-1,637	-1,588	-1,653	-1,661	-1,610	-1,596	-1,537	-1,610	-1,736	-1,653	-1,651	-1,430
83006M15_M_R	-1,607		-1,630	-1,647	-1,690	-1,700	-1,607	-1,568	-1,697	-1,673	-1,616	-1,639	-1,614	-1,574	-1,662	-1,621	-1,621	-1,669	-1,722	-1,552
83006M17_M_L	-1,591	-1,659		-1,949	-1,710	-1,660	-1,506	-1,540	-1,609	-1,596	-1,569	-1,591	-1,603	-1,570	-1,674	-1,726	-1,752	-1,736	-1,623	-1,428
83006M17_M_R	-1,575	-1,638	-1,910		-1,695	-1,621	-1,506	-1,515	-1,564	-1,593	-1,560	-1,577	-1,572	-1,622	-1,691	-1,687	-1,681	-1,675	-1,663	-1,397
83006M21_M_L	-1,665	-1,592	-1,583	-1,607		-1,766	-1,640	-1,686	-1,559	-1,696	-1,739	-1,796	-1,563	-1,612	-1,679	-1,656	-1,735	-1,704	-1,748	-1,408
83006M21_M_R	-1,589	-1,652	-1,584	-1,584	-1,816		-1,695	-1,728	-1,685	-1,676	-1,612	-1,749	-1,680	-1,660	-1,677	-1,705	-1,677	-1,709	-1,750	-1,584
83006M22_M_L	-1,550	-1,555	-1,425	-1,464	-1,686	-1,691		-1,813	-1,540	-1,604	-1,582	-1,611	-1,514	-1,601	-1,591	-1,538	-1,520	-1,531	-1,676	-1,493
83006M22_M_R	-1,650	-1,519	-1,462	-1,476	-1,735	-1,726	-1,816		-1,599	-1,591	-1,611	-1,657	-1,554	-1,572	-1,531	-1,578	-1,600	-1,617	-1,622	-1,499
83006M32_F_L	-1,619	-1,681	-1,563	-1,558	-1,641	-1,716	-1,576	-1,632		-1,728	-1,547	-1,644	-1,742	-1,614	-1,573	-1,662	-1,663	-1,718	-1,629	-1,669
83006M32_F_R	-1,573	-1,660	-1,554	-1,590	-1,781	-1,711	-1,643	-1,627	-1,731		-1,642	-1,735	-1,628	-1,698	-1,732	-1,642	-1,656	-1,694	-1,774	-1,535
83006M37_F_L	-1,649	-1,614	-1,538	-1,568	-1,835	-1,658	-1,632	-1,658	-1,561	-1,653		-1,885	-1,578	-1,623	-1,600	-1,639	-1,754	-1,754	-1,666	-1,447
83006M37_F_R	-1,630	-1,610	-1,533	-1,559	-1,866	-1,768	-1,634	-1,677	-1,632	-1,719	-1,859		-1,607	-1,650	-1,618	-1,644	-1,738	-1,750	-1,679	-1,489
91060M406_F_L	-1,690	-1,696	-1,656	-1,664	-1,743	-1,810	-1,648	-1,685	-1,840	-1,723	-1,662	-1,718		-1,854	-1,711	-1,872	-1,852	-1,855	-1,776	-1,672
91060M406_F_R	-1,630	-1,610	-1,576	-1,668	-1,746	-1,743	-1,689	-1,657	-1,666	-1,746	-1,661	-1,714	-1,807		-1,767	-1,771	-1,734	-1,715	-1,858	-1,538
91060M410_F_L	-1,574	-1,701	-1,683	-1,740	-1,815	-1,763	-1,681	-1,619	-1,628	-1,784	-1,641	-1,685	-1,667	-1,770		-1,829	-1,680	-1,723	-1,829	-1,519
91060M410_F_R	-1,644	-1,657	-1,732	-1,733	-1,790	-1,788	-1,626	-1,663	-1,714	-1,691	-1,677	-1,708	-1,826	-1,771	-1,827		-1,861	-1,885	-1,731	-1,549
91060M414_M_L	-1,688	-1,575	-1,676	-1,644	-1,787	-1,678	-1,525	-1,603	-1,632	-1,622	-1,710	-1,719	-1,723	-1,651	-1,595	-1,779		-1,909	-1,644	-1,435
91060M414_M_R	-1,629	-1,647	-1,686	-1,663	-1,781	-1,734	-1,561	-1,645	-1,712	-1,685	-1,734	-1,757	-1,751	-1,658	-1,663	-1,827	-1,933		-1,658	-1,534
91060M422_F_L	-1,666	-1,739	-1,610	-1,690	-1,862	-1,814	-1,745	-1,687	-1,662	-1,804	-1,684	-1,724	-1,710	-1,839	-1,807	-1,712	-1,707	-1,696		-1,539
91060M422_F_R	-1,466	-1,590	-1,436	-1,445	-1,544	-1,670	-1,583	-1,586	-1,723	-1,585	-1,487	-1,555	-1,627	-1,541	-1,518	-1,551	-1,519	-1,594	-1,560	

Modern human-modern human pairwise comparisons – 20 x 20 log se_m matrix

	A27Bush_F_L	A27Bush_F_R	A84FING_F_L	A84FING_F_R	A173BUSH_M_L	A173BUSH_M_R	A281SOTHO_M_L	A281SOTHO_M_R	A861FING_M_L	A861FING_M_R	A1263SOTHO_F_L	A1263SOTHO_F_R	A1264TSWA_M_L	A1264TSWA_M_R	A1483TSWA_F_L	A1483TSWA_F_R	A3421_MIXED_M_L	A3421_MIXED_M_R	A3607MIXED_F_L	A3607MIXED_F_R
A27Bush_F_L		-1,827	-1,324	-1,406	-1,480	-1,591	-1,486	-1,486	-1,401	-1,441	-1,363	-1,339	-1,283	-1,332	-1,523	-1,596	-1,608	-1,522	-1,355	-1,421
A27Bush_F_R	-1,762		-1,352	-1,444	-1,509	-1,570	-1,539	-1,545	-1,445	-1,481	-1,422	-1,368	-1,296	-1,339	-1,586	-1,629	-1,595	-1,547	-1,358	-1,456
A84FING_F_L	-1,284	-1,376		-1,896	-1,386	-1,279	-1,536	-1,454	-1,540	-1,527	-1,700	-1,678	-1,341	-1,415	-1,446	-1,527	-1,326	-1,439	-1,549	-1,529
A84FING_F_R	-1,371	-1,473	-1,901		-1,482	-1,362	-1,659	-1,548	-1,636	-1,610	-1,728	-1,680	-1,411	-1,512	-1,566	-1,690	-1,426	-1,551	-1,617	-1,675
A173BUSH_M_L	-1,485	-1,578	-1,432	-1,521		-1,719	-1,499	-1,461	-1,488	-1,632	-1,415	-1,350	-1,481	-1,496	-1,602	-1,621	-1,640	-1,894	-1,385	-1,566
A173BUSH_M_R	-1,584	-1,627	-1,313	-1,389	-1,707		-1,431	-1,419	-1,387	-1,476	-1,329	-1,282	-1,385	-1,398	-1,536	-1,537	-1,610	-1,630	-1,304	-1,435
A281SOTHO_M_L	-1,513	-1,630	-1,604	-1,720	-1,521	-1,464		-1,911	-1,772	-1,712	-1,664	-1,614	-1,431	-1,505	-1,769	-1,927	-1,499	-1,549	-1,615	-1,669
A281SOTHO_M_R	-1,497	-1,620	-1,506	-1,594	-1,467	-1,437	-1,896		-1,709	-1,660	-1,622	-1,544	-1,383	-1,436	-1,682	-1,756	-1,482	-1,493	-1,591	-1,643
A861FING_M_L	-1,409	-1,517	-1,589	-1,679	-1,491	-1,403	-1,754	-1,707		-1,751	-1,653	-1,540	-1,478	-1,496	-1,668	-1,698	-1,482	-1,517	-1,599	-1,673
A861FING_M_R	-1,443	-1,547	-1,570	-1,647	-1,630	-1,486	-1,687	-1,651	-1,744		-1,571	-1,469	-1,485	-1,506	-1,627	-1,720	-1,506	-1,639	-1,530	-1,675
A1263SOTHO_F_L	-1,344	-1,467	-1,721	-1,744	-1,390	-1,317	-1,618	-1,591	-1,625	-1,549		-1,738	-1,338	-1,398	-1,497	-1,569	-1,381	-1,443	-1,554	-1,548
A1263SOTHO_F_R	-1,339	-1,433	-1,718	-1,715	-1,346	-1,289	-1,588	-1,533	-1,532	-1,467	-1,758		-1,295	-1,389	-1,448	-1,537	-1,357	-1,405	-1,544	-1,486
A1264TSWA_M_L	-1,404	-1,481	-1,502	-1,566	-1,597	-1,513	-1,525	-1,493	-1,590	-1,603	-1,478	-1,415		-1,851	-1,642	-1,575	-1,508	-1,641	-1,423	-1,597
A1264TSWA_M_R	-1,411	-1,482	-1,535	-1,626	-1,570	-1,485	-1,558	-1,504	-1,567	-1,583	-1,496	-1,468	-1,809		-1,635	-1,619	-1,509	-1,666	-1,459	-1,642
A1483TSWA_F_L	-1,508	-1,636	-1,472	-1,586	-1,583	-1,528	-1,728	-1,656	-1,645	-1,609	-1,501	-1,433	-1,506	-1,541		-1,862	-1,554	-1,606	-1,478	-1,634
A1483TSWA_F_R	-1,565	-1,664	-1,537	-1,695	-1,586	-1,514	-1,870	-1,715	-1,660	-1,688	-1,559	-1,506	-1,425	-1,510	-1,847		-1,555	-1,631	-1,573	-1,689
A3421_MIXED_M_L	-1,551	-1,603	-1,310	-1,404	-1,579	-1,560	-1,416	-1,415	-1,417	-1,447	-1,344	-1,301	-1,331	-1,373	-1,513	-1,528		-1,641	-1,331	-1,463
A3421_MIXED_M_R	-1,474	-1,563	-1,432	-1,538	-1,840	-1,589	-1,474	-1,433	-1,461	-1,588	-1,414	-1,357	-1,472	-1,539	-1,573	-1,613	-1,649		-1,375	-1,590
A3607MIXED_F_L	-1,354	-1,421	-1,589	-1,652	-1,379	-1,310	-1,588	-1,579	-1,590	-1,527	-1,573	-1,543	-1,302	-1,379	-1,492	-1,602	-1,387	-1,423		-1,635
A3607MIXED_F_R	-1,444	-1,544	-1,592	-1,734	-1,584	-1,465	-1,666	-1,655	-1,688	-1,696	-1,591	-1,509	-1,500	-1,586	-1,672	-1,743	-1,543	-1,661	-1,659	

Gorilla-Gorilla pairwise comparisons – 20 x 20 log se_m matrix

	7318M3_F_L	7318M3_F_R	7556M2_F_L	7556M2_F_R	7732M1_M_L	7732M1_M_R	7732M2_M_L	7732M2_M_R	7732M3_F_L	7732M3_F_R	7732M5_M_L	7732M5_M_R	7732M6_M_L	7732M6_M_R	7732M7_M_L	7732M7_M_R	7732M8_F_L	7732M8_F_R	732M15_F_L	732M15_F_R
7318M3_F_L		-1,824	-1,674	-1,663	-1,652	-1,648	-1,684	-1,575	-1,651	-1,734	-1,328	-1,571	-1,643	-1,672	-1,554	-1,466	-1,726	-1,600	-1,752	-1,759
7318M3_F_R	-1,796		-1,775	-1,742	-1,628	-1,626	-1,642	-1,671	-1,657	-1,677	-1,351	-1,606	-1,674	-1,726	-1,514	-1,489	-1,813	-1,808	-1,771	-1,795
7556M2_F_L	-1,673	-1,803		-1,913	-1,587	-1,649	-1,635	-1,656	-1,656	-1,666	-1,330	-1,537	-1,654	-1,650	-1,558	-1,516	-1,776	-1,769	-1,716	-1,733
7556M2_F_R	-1,680	-1,787	-1,930		-1,547	-1,606	-1,674	-1,587	-1,609	-1,689	-1,315	-1,499	-1,594	-1,616	-1,522	-1,496	-1,835	-1,699	-1,764	-1,776
7732M1_M_L	-1,687	-1,691	-1,623	-1,566		-1,714	-1,592	-1,621	-1,619	-1,576	-1,494	-1,575	-1,596	-1,576	-1,544	-1,360	-1,680	-1,597	-1,710	-1,719
7732M1_M_R	-1,695	-1,701	-1,697	-1,636	-1,726		-1,736	-1,722	-1,817	-1,785	-1,366	-1,532	-1,801	-1,755	-1,791	-1,479	-1,674	-1,614	-1,807	-1,870
7732M2_M_L	-1,790	-1,777	-1,742	-1,764	-1,663	-1,795		-1,777	-1,706	-1,778	-1,418	-1,565	-1,705	-1,704	-1,711	-1,507	-1,802	-1,667	-2,041	-2,042
7732M2_M_R	-1,655	-1,779	-1,736	-1,651	-1,665	-1,755	-1,750		-1,694	-1,634	-1,420	-1,579	-1,748	-1,700	-1,706	-1,524	-1,709	-1,746	-1,782	-1,836
7732M3_F_L	-1,649	-1,684	-1,654	-1,590	-1,582	-1,769	-1,598	-1,613		-1,889	-1,300	-1,498	-1,711	-1,784	-1,664	-1,481	-1,619	-1,617	-1,665	-1,708
7732M3_F_R	-1,758	-1,730	-1,691	-1,697	-1,565	-1,762	-1,696	-1,579	-1,915		-1,295	-1,516	-1,736	-1,839	-1,644	-1,518	-1,682	-1,598	-1,747	-1,786
7732M5_M_L	-1,434	-1,486	-1,437	-1,404	-1,564	-1,424	-1,417	-1,446	-1,407	-1,376		-1,489	-1,366	-1,365	-1,340	-1,237	-1,515	-1,489	-1,528	-1,499
7732M5_M_R	-1,664	-1,729	-1,631	-1,576	-1,633	-1,579	-1,552	-1,593	-1,594	-1,585	-1,477		-1,573	-1,629	-1,486	-1,451	-1,693	-1,691	-1,632	-1,613
7732M6_M_L	-1,732	-1,791	-1,743	-1,667	-1,649	-1,843	-1,687	-1,758	-1,802	-1,800	-1,349	-1,568		-2,010	-1,724	-1,578	-1,672	-1,662	-1,753	-1,813
7732M6_M_R	-1,740	-1,823	-1,718	-1,667	-1,609	-1,776	-1,665	-1,688	-1,854	-1,882	-1,327	-1,603	-1,989		-1,669	-1,611	-1,665	-1,671	-1,742	-1,777
7732M7_M_L	-1,654	-1,642	-1,658	-1,606	-1,608	-1,844	-1,704	-1,726	-1,765	-1,719	-1,334	-1,492	-1,735	-1,701		-1,595	-1,621	-1,591	-1,760	-1,797
7732M7_M_R	-1,569	-1,620	-1,619	-1,583	-1,427	-1,535	-1,503	-1,547	-1,585	-1,596	-1,234	-1,460	-1,592	-1,646	-1,598		-1,536	-1,585	-1,603	-1,615
7732M8_F_L	-1,727	-1,842	-1,777	-1,819	-1,645	-1,628	-1,696	-1,630	-1,621	-1,658	-1,410	-1,600	-1,583	-1,598	-1,522	-1,433		-1,840	-1,801	-1,769
7732M8_F_R	-1,605	-1,841	-1,774	-1,687	-1,567	-1,571	-1,565	-1,671	-1,624	-1,578	-1,388	-1,602	-1,578	-1,608	-1,496	-1,487	-1,844		-1,684	-1,675
732M15_F_L	-1,654	-1,702	-1,619	-1,650	-1,577	-1,662	-1,837	-1,604	-1,569	-1,624	-1,324	-1,441	-1,566	-1,576	-1,562	-1,402	-1,703	-1,581		-2,113
732M15_F_R	-1,662	-1,727	-1,637	-1,663	-1,587	-1,726	-1,838	-1,659	-1,613	-1,665	-1,297	-1,423	-1,628	-1,612	-1,600	-1,416	-1,672	-1,574	-2,114	

Appendix 6 Log se_m matrix for fossil specimens 36 x 36 log se_m pairwise comparisons

	AL145-35L	AL128-23R	AL266-1L	AL266-1R	AL288-1R	AL333-W6DL	LH2R	LH4L	LH4R	MLD2L	MLD2R	StS26bR	Taung1L	Taung1R	OH22R	KNM-ER806L	KNM-ER820L	KNM-ER820R	KNM-ER992L	KNM-ER992R	OH7L	OH7R	OH16R	KNM-ER1802L	KNM-ER1802F	KNM-ER1593C	Peninj1L	Peninj1R	SK6L	SK6R	SK23L	SK23R	SK6GL	SK6GR	SKW5R	TM1517R
AL145-35L		-1,526	-1,428	-1,407	-1,369	-1,421	-1,400	-1,247	-1,423	-1,303	-1,363	-1,415	-1,309	-1,356	-1,349	-1,308	-1,345	-1,376	-1,397	-1,302	-1,341	-1,325	-1,308	-1,348	-1,276	-1,263	-1,268	-1,240	-1,318	-1,365	-1,292	-1,281	-1,333	-1,286
AL128-23R	-1,402		-1,510	-1,401	-1,333	-1,479	-1,463	-1,291	-1,540	-1,363	-1,414	-1,486	-1,291	-1,334	-1,354	-1,339	-1,313	-1,368	-1,392	-1,436	-1,266	-1,317	-1,295	-1,290	-1,308	-1,394	-1,274	-1,316	-1,210	-1,309	-1,333	-1,246	-1,218	-1,366	-1,307
AL266-1L	-1,397	-1,602		-1,592	-1,514	-1,570	-1,582	-1,267	-1,490	-1,457	-1,542	-1,534	-1,374	-1,410	-1,454	-1,459	-1,452	-1,553	-1,587	-1,622	-1,427	-1,476	-1,478	-1,430	-1,521	-1,438	-1,313	-1,327	-1,345	-1,309	-1,343	-1,354	-1,368	-1,333	-1,418	-1,409
AL266-1R	-1,342	-1,459	-1,558	-1,492	-1,609	-1,609	-1,390	-1,223	-1,451	-1,505	-1,638	-1,493	-1,323	-1,318	-1,369	-1,408	-1,359	-1,442	-1,433	-1,455	-1,340	-1,371	-1,369	-1,299	-1,373	-1,399	-1,219	-1,256	-1,301	-1,248	-1,265	-1,297	-1,305	-1,210	-1,279	-1,288
AL288-1R	-1,240	-1,328	-1,417	-1,429	-1,325	-1,439	-1,135	-1,278	-1,435	-1,458	-1,457	-1,307	-1,308	-1,552	-1,524	-1,634	-1,562	-1,549	-1,657	-1,619	-1,504	-1,463	-1,596	-1,522	-1,251	-1,270	-1,311	-1,240	-1,232	-1,351	-1,276	-1,262	-1,343
AL333-W6DL	-1,436	-1,617	-1,616	-1,689	-1,468		-1,450	-1,350	-1,669	-1,546	-1,657	-1,580	-1,378	-1,368	-1,420	-1,425	-1,359	-1,458	-1,463	-1,486	-1,355	-1,398	-1,419	-1,336	-1,404	-1,467	-1,279	-1,330	-1,346	-1,275	-1,333	-1,334	-1,255	-1,382	-1,342
LH2R	-1,447	-1,634	-1,660	-1,503	-1,615	-1,483		-1,308	-1,486	-1,494	-1,583	-1,589	-1,395	-1,462	-1,688	-1,493	-1,615	-1,680	-1,740	-1,778	-1,594	-1,717	-1,629	-1,590	-1,668	-1,586	-1,427	-1,412	-1,433	-1,415	-1,442	-1,420	-1,471	-1,464	-1,474	-1,497
LH4L	-1,237	-1,404	-1,288	-1,279	-1,253	-1,325	-1,251		-1,472	-1,272	-1,252	-1,291	-1,237	-1,203	-1,283	-1,272	-1,224	-1,278	-1,288	-1,293	-1,201	-1,216	-1,186	-1,216	-1,184	-1,285	-1,143	-1,222	-1,192	-1,135	-1,217	-1,210	-1,163	-1,144	-1,286	-1,195
LH4R	-1,383	-1,623	-1,481	-1,477	-1,366	-1,614	-1,399	-1,442		-1,432	-1,483	-1,476	-1,321	-1,304	-1,381	-1,369	-1,320	-1,399	-1,420	-1,442	-1,294	-1,323	-1,328	-1,310	-1,310	-1,411	-1,258	-1,316	-1,296	-1,211	-1,305	-1,340	-1,273	-1,223	-1,389	-1,309
MLD2L	-1,379	-1,564	-1,565	-1,647	-1,640	-1,608	-1,523	-1,359	-1,549		-1,744	-1,675	-1,459	-1,432	-1,600	-1,507	-1,475	-1,619	-1,590	-1,576	-1,522	-1,570	-1,485	-1,514	-1,534	-1,614	-1,323	-1,403	-1,407	-1,370	-1,368	-1,388	-1,311	-1,407	-1,411
MLD2R	-1,428	-1,603	-1,638	-1,769	-1,651	-1,707	-1,601	-1,328	-1,588	-1,733		-1,688	-1,426	-1,422	-1,586	-1,498	-1,506	-1,636	-1,613	-1,651	-1,506	-1,572	-1,555	-1,470	-1,550	-1,599	-1,351	-1,384	-1,414	-1,363	-1,436	-1,339	-1,412	-1,426
StS26bR	-1,403	-1,597	-1,554	-1,547	-1,574	-1,554	-1,530	-1,289	-1,505	-1,587	-1,611		-1,463	-1,459	-1,513	-1,460	-1,408	-1,528	-1,508	-1,532	-1,440	-1,502	-1,438	-1,413	-1,505	-1,540	-1,344	-1,417	-1,445	-1,350	-1,386	-1,405	-1,376	-1,305	-1,386	-1,405
Taung1L	-1,316	-1,422	-1,413	-1,397	-1,443	-1,371	-1,356	-1,255	-1,369	-1,391	-1,368	-1,483		-1,667	-1,379	-1,498	-1,310	-1,410	-1,425	-1,400	-1,362	-1,401	-1,332	-1,335	-1,365	-1,386	-1,457	-1,526	-1,511	-1,483	-1,443	-1,420	-1,468	-1,382	-1,484	-1,516
Taung1R	-1,349	-1,451	-1,434	-1,377	-1,430	-1,347	-1,408	-1,207	-1,337	-1,349	-1,351	-1,464	-1,653		-1,370	-1,510	-1,316	-1,399	-1,413	-1,401	-1,356	-1,411	-1,328	-1,329	-1,372	-1,362	-1,511	-1,522	-1,632	-1,610	-1,579	-1,541	-1,556	-1,487	-1,527	-1,573
OH22R	-1,299	-1,427	-1,436	-1,385	-1,630	-1,355	-1,590	-1,243	-1,371	-1,474	-1,471	-1,474	-1,321	-1,326		-1,402	-1,653	-1,761	-1,695	-1,693	-1,686	-1,686	-1,570	-1,722	-1,642	-1,576	-1,301	-1,328	-1,301	-1,310	-1,305	-1,291	-1,366	-1,349	-1,360	-1,399
KNM-ER806L	-1,281	-1,436	-1,464	-1,447	-1,465	-1,384	-1,420	-1,256	-1,383	-1,403	-1,406	-1,445	-1,464	-1,490	-1,425		-1,401	-1,498	-1,462	-1,468	-1,423	-1,437	-1,360	-1,388	-1,426	-1,410	-1,420	-1,513	-1,525	-1,489	-1,482	-1,440	-1,486	-1,391	-1,431	-1,559
KNM-ER820L	-1,237	-1,365	-1,412	-1,353	-1,582	-1,273	-1,497	-1,163	-1,289	-1,327	-1,370	-1,348	-1,231	-1,252	-1,632	-1,357		-1,755	-1,673	-1,751	-1,572	-1,524	-1,491	-1,575	-1,578	-1,469	-1,253	-1,246	-1,228	-1,253	-1,229	-1,213	-1,316	-1,309	-1,287	-1,359
KNM-ER820R	-1,227	-1,374	-1,467	-1,390	-1,645	-1,326	-1,516	-1,171	-1,321	-1,425	-1,454	-1,422	-1,285	-1,288	-1,693	-1,407	-1,709		-1,751	-1,729	-1,630	-1,617	-1,608	-1,611	-1,681	-1,516	-1,266	-1,274	-1,255	-1,277	-1,242	-1,233	-1,344	-1,303	-1,316	-1,389
KNM-ER992L	-1,284	-1,423	-1,527	-1,406	-1,599	-1,356	-1,601	-1,206	-1,368	-1,421	-1,456	-1,427	-1,325	-1,327	-1,653	-1,396	-1,653	-1,776	-1,910	-1,623	-1,670	-1,578	-1,688	-1,726	-1,474	-1,304	-1,289	-1,270	-1,302	-1,271	-1,250	-1,380	-1,354	-1,392	-1,449
KNM-ER992R	-1,305	-1,468	-1,562	-1,430	-1,586	-1,380	-1,640	-1,212	-1,391	-1,408	-1,495	-1,453	-1,301	-1,316	-1,651	-1,403	-1,731	-1,755	-1,911	-1,569	-1,586	-1,528	-1,636	-1,695	-1,489	-1,309	-1,294	-1,281	-1,292	-1,278	-1,273	-1,366	-1,345	-1,377	-1,440
OH7L	-1,310	-1,399	-1,467	-1,414	-1,794	-1,349	-1,555	-1,220	-1,343	-1,454	-1,450	-1,460	-1,362	-1,372	-1,745	-1,458	-1,652	-1,756	-1,724	-1,669	-1,870	-1,581	-1,696	-1,716	-1,550	-1,337	-1,339	-1,325	-1,393	-1,333	-1,300	-1,435	-1,409	-1,367	-1,445
OH7R	-1,343	-1,443	-1,510	-1,438	-1,749	-1,386	-1,672	-1,229	-1,365	-1,495	-1,509	-1,516	-1,395	-1,420	-1,739	-1,466	-1,597	-1,736	-1,765	-1,679	-1,863	-1,645	-1,635	-1,764	-1,541	-1,366	-1,360	-1,366	-1,425	-1,367	-1,333	-1,477	-1,440	-1,397	-1,469
OH16R	-1,383	-1,477	-1,568	-1,493	-1,692	-1,463	-1,641	-1,255	-1,427	-1,468	-1,549	-1,509	-1,383	-1,394	-1,679	-1,446	-1,621	-1,784	-1,729	-1,678	-1,631	-1,701	-1,521	-1,673	-1,615	-1,375	-1,361	-1,352	-1,364	-1,355	-1,367	-1,468	-1,423	-1,417	-1,452
KNM-ER1802L	-1,336	-1,480	-1,528	-1,431	-1,658	-1,388	-1,609	-1,292	-1,416	-1,503	-1,471	-1,491	-1,393	-1,402	-1,838	-1,481	-1,713	-1,795	-1,847	-1,793	-1,753	-1,699	-1,529	-1,742	-1,561	-1,364	-1,384	-1,345	-1,379	-1,352	-1,323	-1,416	-1,414	-1,443	-1,503
KNM-ER1802F	-1,371	-1,494	-1,615	-1,501	-1,787	-1,452	-1,684	-1,257	-1,412	-1,521	-1,548	-1,580	-1,420	-1,442	-1,755	-1,516	-1,712	-1,862	-1,881	-1,849	-1,770	-1,824	-1,677	-1,738	-1,583	-1,389	-1,392	-1,389	-1,424	-1,369	-1,361	-1,476	-1,440	-1,433	-1,528
KNM-ER1593C	-1,358	-1,528	-1,480	-1,475	-1,661	-1,463	-1,549	-1,306	-1,461	-1,548	-1,544	-1,562	-1,389	-1,379	-1,636	-1,448	-1,551	-1,644	-1,576	-1,591	-1,552	-1,549	-1,567	-1,505	-1,530	-1,367	-1,438	-1,377	-1,363	-1,353	-1,375	-1,328	-1,397	-1,423
Peninj1L	-1,402	-1,533	-1,479	-1,419	-1,496	-1,400	-1,515	-1,289	-1,433	-1,382	-1,421	-1,490	-1,585	-1,653	-1,487	-1,582	-1,459	-1,518	-1,531	-1,536	-1,463	-1,499	-1,451	-1,433	-1,461	-1,492	-1,730	-1,626	-1,624	-1,665	-1,600	-1,695	-1,638	-1,651	-1,791
Peninj1R	-1,382	-1,559	-1,478	-1,441	-1,499	-1,435	-1,485	-1,352	-1,475	-1,446	-1,439	-1,548	-1,638	-1,648	-1,498	-1,659	-1,436	-1,511	-1,500	-1,505	-1,450	-1,477	-1,422	-1,438	-1,449	-1,547	-1,714	-1,728	-1,596	-1,728	-1,606	-1,565	-1,510	-1,628	-1,682
SK6L	-1,391	-1,535	-1,492	-1,483	-1,515	-1,447	-1,502	-1,318	-1,452	-1,447	-1,464	-1,573	-1,619	-1,754	-1,467	-1,667	-1,415	-1,488	-1,478	-1,488	-1,432	-1,479	-1,409	-1,394	-1,442	-1,482	-1,607	-1,724	-1,709	-1,802	-1,676	-1,640	-1,537	-1,572	-1,625
SK6R	-1,350	-1,444	-1,451	-1,424	-1,550	-1,370	-1,478	-1,256	-1,362	-1,404	-1,408	-1,472	-1,585	-1,727	-1,471	-1,626	-1,435	-1,504	-1,504	-1,494	-1,494	-1,533	-1,415	-1,423	-1,471	-1,462	-1,599	-1,586	-1,704	-1,639	-1,523	-1,727	-1,629	-1,543	-1,678
SK23L	-1,386	-1,501	-1,443	-1,399	-1,437	-1,387	-1,463	-1,296	-1,413	-1,362	-1,383	-1,466	-1,504	-1,654	-1,424	-1,578	-1,368	-1,428	-1,432	-1,438	-1,393	-1,433	-1,365	-1,354	-1,374	-1,421	-1,598	-1,677	-1,755	-1,598	-1,710	-1,597	-1,571	-1,599	-1,575
SK23R	-1,413	-1,505	-1,434	-1,411	-1,409	-1,430	-1,422	-1,269	-1,428	-1,340	-1,397	-1,465	-1,461	-1,596	-1,389	-1,515	-1,332	-1,398	-1,391	-1,413	-1,339	-1,379	-1,356	-1,305	-1,347	-1,391	-1,513	-1,535	-1,608	-1,461	-1,690	-1,559	-1,469	-1,522	-1,512
SK6GL	-1,308	-1,385	-1,415	-1,386	-1,495	-1,335	-1,440	-1,188	-1,329	-1,327	-1,386	-1,403	-1,475	-1,578	-1,432	-1,528	-1,403	-1,477	-1,487	-1,473	-1,442	-1,491	-1,425	-1,365	-1,429	-1,380	-1,576	-1,462	-1,540	-1,632	-1,544	-1,526	-1,656	-1,521	-1,687
SK6GR	-1,338	-1,399	-1,422	-1,333	-1,462	-1,297	-1,475	-1,212	-1,320	-1,292	-1,331	-1,374	-1,431	-1,551	-1,457	-1,475	-1,438	-1,478	-1,503	-1,494	-1,457	-1,495	-1,421	-1,405	-1,435	-1,375	-1,560	-1,448	-1,479	-1,576	-1,560	-1,478	-1,697	-1,568	-1,633
SKW5R	-1,326	-1,482	-1,442	-1,337	-1,383	-1,360	-1,420	-1,289	-1,421	-1,323	-1,340	-1,390	-1,469	-1,527	-1,403	-1,450	-1,351	-1,426	-1,477	-1,461	-1,351	-1,387	-1,351	-1,369	-1,362	-1,379	-1,509	-1,501	-1,449	-1,426	-1,523	-1,466	-1,498	-1,503	-1,635
TM1517R	-1,329	-1,475	-1,484	-1,397	-1,515	-1,371	-1,493	-1,249	-1,393	-1,378	-1,405	-1,461	-1,552	-1,624	-1,493	-1,609	-1,474	-1,551	-1,585	-1,575	-1,480	-1,511	-1,437	-1,480	-1,509	-1,456	-1,700	-1,607	-1,553	-1,611	-1,551	-1,508	-1,715	-1,619	-1,686